

2014

## 1,2,3-triazoles as X-factor in gold(I) activation of challenging C-C triple bond transformations

Qiaoyi Wang  
*West Virginia University*

Follow this and additional works at: <https://researchrepository.wvu.edu/etd>

---

### Recommended Citation

Wang, Qiaoyi, "1,2,3-triazoles as X-factor in gold(I) activation of challenging C-C triple bond transformations" (2014). *Graduate Theses, Dissertations, and Problem Reports*. 357.  
<https://researchrepository.wvu.edu/etd/357>

This Dissertation is protected by copyright and/or related rights. It has been brought to you by the The Research Repository @ WVU with permission from the rights-holder(s). You are free to use this Dissertation in any way that is permitted by the copyright and related rights legislation that applies to your use. For other uses you must obtain permission from the rights-holder(s) directly, unless additional rights are indicated by a Creative Commons license in the record and/ or on the work itself. This Dissertation has been accepted for inclusion in WVU Graduate Theses, Dissertations, and Problem Reports collection by an authorized administrator of The Research Repository @ WVU. For more information, please contact [researchrepository@mail.wvu.edu](mailto:researchrepository@mail.wvu.edu).

**1,2,3-triazoles as X-factor in gold(I) activation  
of challenging C-C triple bond transformations**

**Qiaoyi Wang**

**Dissertation submitted to the  
Eberly College of Arts and Sciences  
at West Virginia University  
in partial fulfillment of the requirements  
for the degree of**

**Doctor of Philosophy  
in  
Organic Chemistry**

**Xiaodong Shi, Ph.D., Chair  
Peter Gannett, Ph.D.  
Jeffrey L. Petersen, Ph.D.  
Björn Söderberg, Ph.D.  
Kung K. Wang, Ph.D.**

**C. Eugene Bennett Department of Chemistry**

**Morgantown, West Virginia  
2014**

**Keywords: Functional 1,2,3-Triazoles, Transition Metal Catalysis ,  
Iron Chemistry, Allene, BN heterocycle, Triazole-gold complexes**

**Copyright 2014 Qiaoyi Wang**

# Abstract

The 'click chemistry' which provides 1,4-disubstituted 1,2,3-triazoles has been reported in 2001. New method for highly functionalized 1,2,3-triazole synthesis becomes very desirable along with the discovery of unique properties of this heterocyclic structure. Our group focused on the synthesis of functional 1,2,3-triazole for several years and new methodologies have been developed such as arylation, vinylation, propargylation and allenation. Besides the new methods are benefiting the field related to triazole functionalization, new reactivity of ligand-metal complexes was revealed.

A series of 1,2,3-triazole gold complexes were synthesized/characterized. This dissertation presents the results of research effort to explore the unique chemoselectivity and improved thermal stability that arises when triazole is introduced as a X-factor or secondary ligand. This effort successfully led to the efficient synthesis of traditionally challenging compounds. The benzotriazole modified gold(I) complex showed high reactivity toward propargyl ester/vinyl ether. Through a simple 3,3-rearrangement, allene derivatives, which were usually considered as intermediate in the gold(I) chemistry, were isolated as a major product. The treatment of allene derivatives with triazole gold complex showed no apparent decomposition of allene and confirmed the triazole-gold complex could selectively perform the  $\pi$ -acidity toward C-C triple bond over allene. With this triazole modification, the thermal stability of the corresponding gold(I) complexes is significantly improved. Triazole-gold(I) facilitated alkyne hydroboration was accomplished at 80 °C, which is a temperature leads to serious complex decomposition of previous cationic gold(I) species. Moreover,  $^{31}\text{P}$  NMR proved the stability of triazole-gold complex toward the highly reductive reaction precursor (such as boronhydride). This new strategy enabled an efficient method for amine borane heterocyclic structures synthesis, which has been considerable investigated recently as a potential hydrogen storage material.

*Dedicated to*  
*My amazing parents*  
*My loving wife*  
*And my heartfelt friends*

## Acknowledgements

I would like to express my deepest gratitude to my supervisor, Dr. Xiaodong Michael Shi, I have been so fortunate to have an advisor who gave me the freedom to explore on my own in the science of organic chemistry and at the same time the guidance to recover when I failed. Michael taught me how to become a real and better organic chemist. His patience and support helped me overcome many crisis situations. Without his help, this dissertation would truly not have been possible. I would like to give my sincere appreciation to Dr. Kung K. Wang, Dr. Björn Söderberg, Dr Brian Popp, and Dr Jessica Hoover in my academic development. Their invaluable advice and suggestion throughout my years here in WVU are appreciated and acknowledged.

I would also like to thank Dr. Jeffrey L. Petersen for his countless number of X-ray crystallographic analyses and guidance during my graduate studies. Moreover, I am deeply grateful to the above mentioned and Dr. Peter Gannett for their roles on my Doctoral Research Committee.

I would like to acknowledge my colleagues who I've had the pleasure of working with, Dr. Dawei Wang, Dr. Yijin Su, Dr. Haihui Peng, Dr. Chen Zhong, Dr. Sujata Sengupta, Dr. Wuming Yan, Dr. Lekn Nath Gautam, Tao Liao, Xiaohan Ye, Rong Cai, Yanwei Zhang, Sraven Kumar, Siddhita Aparaj, Seyedmorteza Hosseyni, Boliang Dong, Stephen Motika, and Yumeng Xi for all the assistance they have given me in the last five years. I would also like to thank Dr. Novruz Akhmedov for his kind and friendly help during NMR experiments. Though only my name appears on the cover of this dissertation, a great many people have contributed to its production. I would like to express my heart-felt gratitude to my family for their unconditional love, support and guidance throughout my life. My parents and my wife have been a constant source of love, concern, support and strength all these years. Without their understanding, encouragement and support, I could not have finished this thesis.

Financial supports from the C. Eugene Bennett Department of Chemistry at West Virginia University (particularly for a John R. Conard Fellowship) and the National Science Foundation are also gratefully acknowledged.

# TABLE OF CONTENTS

1,2,3-triazoles as X-factor in gold(I) activation .....	i
Abstract .....	ii
Acknowledgements .....	ii
TABLE OF CONTENTS .....	iii
LIFT OF FIGURES .....	v
LIST OF SCHEMES .....	vii
LIST OF TABLES .....	ix
Chapter One: Iron catalyzed C-O bond activation for the synthesis of propargyl-1,2,3-triazoles and 1,1-bis-triazoles .....	1
1.1 Introduction .....	1
1.2 Research Objective and Results .....	6
1.3 Conclusion .....	15
1.4 Contribution .....	16
Chapter Two: 1,2,3-triazoles work as X-factor to promote gold(I) complex in challenging chemical transformations - part I .....	17
2.1 Introduction .....	17
2.1.1 Background information about homogeneous gold catalysis .....	17
2.1.2 'Silver effect' in homogeneous gold(I) catalysis .....	21
2.2 Efforts toward the synthesis of different 1,2,3-triazole gold(I) complexes .....	29
2.3 Quantitative kinetic investigation of triazole-gold(I) complex catalyzed [3,3]-rearrangement of propargyl ester .....	36
2.4 Conclusion .....	42
2.5 Contribution .....	42
Chapter Three: 1,2,3-triazoles work as X-factor to promote gold(I) complex in challenging chemical transformations - part II .....	43
3.1 Introduction .....	43
3.2 Result and discussion .....	48
3.3 Conclusion .....	58
3.4 Contribution .....	59
Chapter Four: 1,2,3-triazoles work as X-factor to promote gold(I) complex in challenging chemical transformations - part III .....	60

4.1 Introduction.....	60
4.2 Result and discussion.....	69
4.3 Conclusion .....	82
4.4 Contribution .....	83
References.....	84
Appendix.....	97
Supporting Information.....	98
Chapter One: Iron catalyzed C-O bond activation for the synthesis of propargyl-1,2,3-triazoles and 1,1-bis-triazoles .....	98
Chapter Two: 1,2,3-triazoles work as X-factor to promote gold(I) complex in challenging chemical transformations - part I.....	117
Chapter Three: 1,2,3-triazoles work as X-factor to promote gold(I) complex in challenging chemical transformations - part II .....	127
Chapter Four: 1,2,3-triazoles work as X-factor to promote gold(I) complex in challenging chemical transformations - part III.....	139

# LIFT OF FIGURES

Figure 1. Proposed reaction mechanism of 'Click chemistry' .....	2
Figure 2. Mechanism for synthesis of 4,5-disubstituted <i>NH</i> -1,2,3-triazoles.....	4
Figure 3. Reaction substrate scope.....	11
Figure 4. Perspective view of the structure of C <sub>23</sub> H <sub>17</sub> N <sub>3</sub> (compound <b>1.3f</b> ).....	12
Figure 5. Synthesis of unsymmetrical N-C type bis-triazoles.....	14
Figure 6. Perspective view of the structure of C <sub>22</sub> H <sub>24</sub> N <sub>6</sub> O <sub>3</sub> (compound <b>1.5g</b> ).....	15
Figure 7. Classic homogeneous gold(I) catalysis cycle-circle.....	20
Figure 8. IPrAuCl and XPhosAuCl complexes with improved Au cation stability.....	21
Figure 9. Gold(I) complex resting states.....	24
Figure 10. XPS Spectra of (PPh <sub>3</sub> )AuCl/AgSbF <sub>6</sub> .....	27
Figure 11. <sup>31</sup> P NMR Spectra of Different Au(I) Samples.....	28
Figure 12. Different 1,2,3-triazole metal complexes obtained by Prof. Shi's group.....	29
Figure 13. Different post-triazole functionalization discovered by Prof. Shi's group.....	30
Figure 14. 1,2,3-triazole as structural isomer of NHC ligand: N σ-donor and better π-receptor .....	31
Figure 15. A library of 1,2,3-triazole gold(I) complexes with ligand and triazole orthogonal.....	34
Figure 16. Dependence of the initial rates on catalyst for rearrangement of <b>2.17</b> .....	38
Figure 17. Dependence of the initial rates on starting material for rearrangement of <b>2.17</b> .....	39
Figure 18. Kinetics profile using various TA–Au catalysts.....	40
Figure 19. Hammett plot of various TA–Au catalysts.....	41
Figure 20. Perspective view of the structure of C <sub>32</sub> H <sub>26</sub> SO <sub>3</sub> (compound <b>3.24a</b> ).....	54
Figure 21. Substrate scope of TA-Au catalyzed Schmitt cyclization.....	56
Figure 22. Reaction process profile .....	61



Figure 23. Isoelectronic relationship between CC and BN, and molecular consequences of BN/CC isosterism. ....	63
Figure 24. Illustration of benzene, 1,2-dihydro-1,2-azaborine, and borazine. ....	64
Figure 25. Structures reported by Liu's group with BN unit substituted CC unit. ....	67
Figure 26. Substrate scope of boranecarbonitrile <b>4.39</b> . ....	74
Figure 27. Perspective view of the structure of C <sub>10</sub> H <sub>11</sub> BN <sub>2</sub> (compound <b>4.39a</b> ). ....	75
Figure 28. Perspective view of the structure of C <sub>12</sub> H <sub>15</sub> BN <sub>2</sub> (compound <b>4.40b</b> ). ....	77
Figure 29. Monitoring the gold decomposition by <sup>31</sup> P NMR. ....	78
Figure 30. Reaction substrate scope. ....	80
Figure 31. Perspective view of the structure of C <sub>16</sub> H <sub>15</sub> BN <sub>2</sub> (compound <b>4.42</b> ). ....	82

# LIST OF SCHEMES

Scheme 1. The synthesis of 1,4-disubstituted 1,2,3-triazoles by Click Chemistry. ....	1
Scheme 2. Example of CuAAC reported by Sharpless. ....	1
Scheme 3. Synthesis of NH-1,2,3-triazoles through CuAAC. ....	3
Scheme 4. Thermal condensation of nitroalkene and sodium azide (Zard's method). ....	3
Scheme 5. Shi's approach: Lewis base-catalyzed cascade nitroalkene-aldehyde-azide condensation. ....	4
Scheme 6. Shi's Approach: N-2 alkyl/aryl substituted 1,2,3-triazole synthesis. ....	5
Scheme 7. Three different types of bis-triazole compounds. ....	7
Scheme 8. Challenges in triazole propargylation. ....	8
Scheme 9. Unexpected decomposition of terminal alkyne substrates. ....	13
Scheme 10. Recent gold(I) catalyzed transformations. ....	18
Scheme 11. Different resting states in the gold(I) catalysis when silver is presented. ....	23
Scheme 12. Synthesis of [IPrAuNTf <sub>2</sub> ] and its application in enyne cycloisomerization. ....	25
Scheme 13. Synthesis of triazole-gold(I) complexes reported by Nomiya. ....	31
Scheme 14. Synthesis of triazole-gold(I) complexes reported by Prof. Shi. ....	32
Scheme 15. Silver free conversion from <b>2.11</b> to <b>2.13a</b> . ....	33
Scheme 16. X-factor: an alternative strategy in tuning gold catalyst reactivity. ....	36
Scheme 17. TA–Au as a chemo-selective catalyst for alkyne activation. ....	37
Scheme 18. Selection of TA-Au <b>2.13b</b> as catalyst for alkyne activation. ....	38
Scheme 19. Proposed mechanism for TA–Au catalyzed 3,3-rearrangement. ....	40
Scheme 20. $\alpha$ -haloenone through gold(I) activated propargyl ester gave Z/E isomers. ....	44
Scheme 21. TA-Au catalyzed allene formation with chirality retention. ....	45
Scheme 22. Cyclization of enediyne derivative through diradical intermediate. ....	46
Scheme 23. Cyclization of enyne-allene derivative through diradical intermediate. ....	47

Scheme 24. Diradical intermediate generated in vivo and cleaved DNA. ....	47
Scheme 25. Myers-Saito reaction under thermal and photo activation conditions. ....	49
Scheme 26. TA-Au catalyzed allene formation fused with enyne to access enyne-allene. ....	50
Scheme 27. Propargyl ester/vinyl ether substrates treated with TA-Au. ....	51
Scheme 28. Proposed reaction process for the TA-Au catalyzed cyclization. ....	52
Scheme 29. Schmitt cyclization reported by Prof. Wang with excellent efficiency. ....	53
Scheme 30. Mechanism investigations. ....	58
Scheme 31. MeCN as 'X-Factor' in gold(I) catalysis. ....	60
Scheme 32. Early stage synthetic route of 1,2-azaborines. ....	65
Scheme 33. Attempt to synthesize parent 1,2-dihydro-1,2-azaborinen. ....	65
Scheme 34. BH 1,2-azaborine synthesis reported by Prof. Goubeau. ....	66
Scheme 35. 1,2-azaborine synthesis based on ring-closing metathesis strategy. ....	67
Scheme 36. Regio-selective hydroboration reported by Vedejs. ....	68
Scheme 37. Intramolecular hydroboration of alkyne: efficient but no precedence. ....	69
Scheme 38. Iodine activated alkyne hydroboration reaction. ....	69
Scheme 39. Possible transition metal catalyzed intramolecular alkyne hydroboration reaction patterns. ...	70
Scheme 40. Attempt to synthesize amine borane with lower B-H reductivity. ....	73
Scheme 41. Conditions for synthesis of amine boranecarbonitrile <b>4.39</b> . ....	74
Scheme 42. Introducing functional groups at boron position. ....	81

## LIST OF TABLES

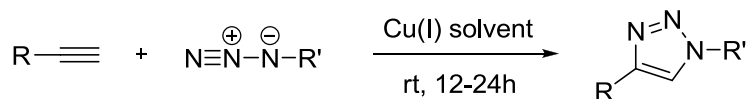
Table 1. Catalyst screening for Lewis acid C-O bond activation. ....	9
Table 2. Silver effect in alkyne hydration. ....	26
Table 3. <sup>31</sup> P NMR data of substituted TA-Au complexes. ....	35
Table 4. Screening of the reaction condition. ....	55
Table 5. Screening of the gold catalyst for amine directed alkyne hydroboration. ....	72
Table 6. Condition screening of alkyne hydroboration. ....	75

# Chapter One: Iron catalyzed C-O bond activation for the synthesis of propargyl-1,2,3-triazoles and 1,1-bis-triazoles

## 1.1 Introduction

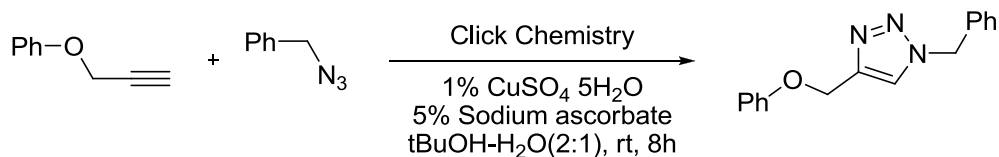
The 1,2,3-triazole molecular system, as an interesting heterocyclic structure, has gained a lot of attention recently.<sup>1</sup> The 'click chemistry' developed by Sharpless in 2001 provided an efficient method to access 1,4-disubstituted 1,2,3-triazoles (**Scheme 1**).<sup>2</sup>

**Scheme 1.** The synthesis of 1,4-disubstituted 1,2,3-triazoles by 'click chemistry'.



Although Cu(I) sources are active in this process, such as copper(I) bromide (CuBr) or copper(I) iodide (CuI), the catalyst performs better when it is prepared *in situ* by the reduction of Cu(II) salts (e.g. CuSO<sub>4</sub>) with reducing reagent such as sodium ascorbate or ascorbic acid (**Scheme 2**). This transformation tolerated a broad substrate scope and produced the 1,4-disubstituted 1,2,3-triazoles in good to excellent yields with perfect regioselectivity.

**Scheme 2.** Example of 'click chemistry' reported by Sharpless.



Density functional theory calculations (DFT) were subsequently used to investigate the reaction mechanism. In the presence of a base, the acidic terminal hydrogen is deprotonated first to give a Cu(I) acetylide complex intermediate. Studies have also shown that in the transition state, two copper centers were involved. One copper atom is bound to the acetylide, while the other Cu atom serves as Lewis acid to activate the azide by coordinating with the nitrogen atom. The azide and the acetylide are then linked together through bridging ligands which are labile and weakly coordinating. The azide displaces one ligand (L) to generate a copper-azide-acetylide complex (CuAAC). At this point, cyclization occurs and followed by protonation. The product is formed by elimination of copper to give the copper complex and the catalytically active copper-ligand complex is regenerated for maintaining catalytic reaction cycles (**Figure 1**).

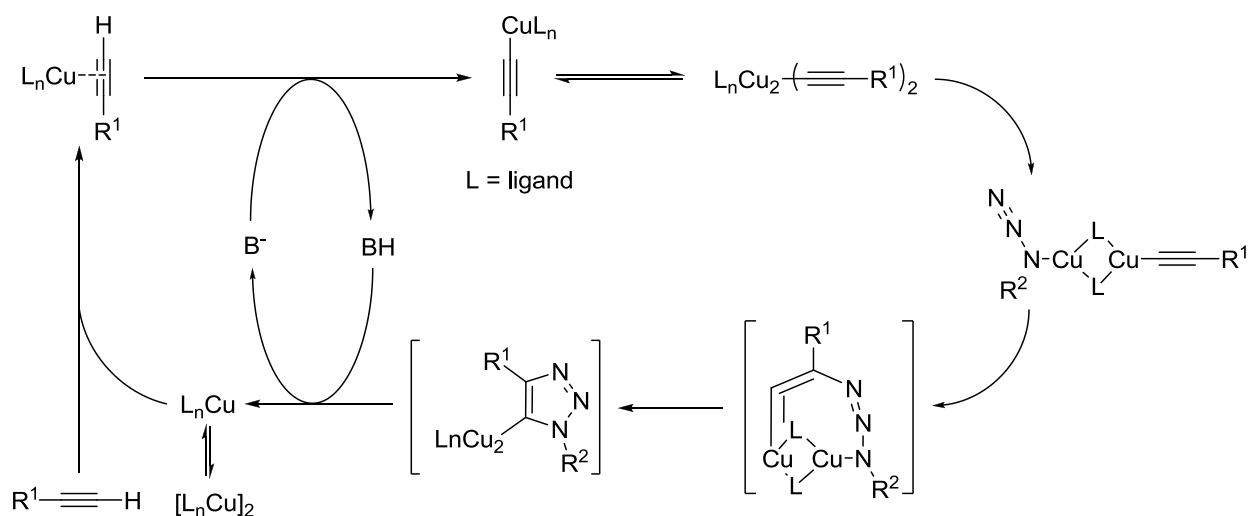
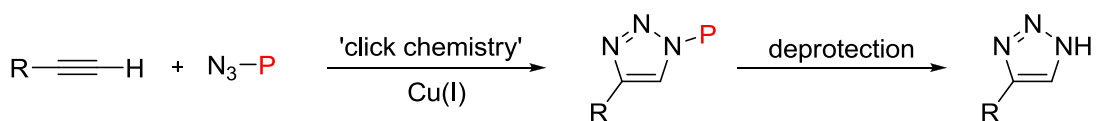


**Figure 1.** Proposed reaction mechanism of 'Click chemistry'.

Investigations of the application of 1,2,3-triazole as a ligand system was initiated during the past decade.<sup>3</sup> A series of new 1,2,3-triazole metal complexes were synthesized and characterized.<sup>4</sup> To better evaluate this unique heterocyclic structure as a ligand in the transition

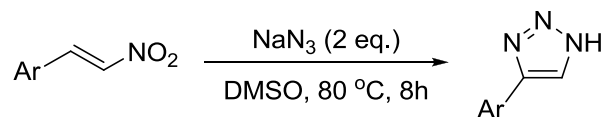
metal catalysis for new reactivity, it became apparent that new, efficient synthetic methods were needed to prepare a wide range of functionalized triazoles. The initial effort was devoted to the preparation of *NH*-1,2,3-triazoles based on the modification of 'click chemistry' which does not permit the use of unsubstituted azides such as NaN<sub>3</sub> and HN<sub>3</sub>. By substituting the azide with removable N-protecting groups, the *NH*-1,2,3-triazoles was first reported through the CuAAC intermediate and subsequent deprotection of N in 2005 (**Scheme 3**).<sup>5</sup>

**Scheme 3.** Synthesis of *NH*-1,2,3-triazoles through CuAAC.



Meanwhile, the 1,3-dipolar cycloaddition between nitroalkene and sodium azide was considered as another efficient methodology for the synthesis of *NH*-1,2,3-triazoles. Because the original conditions<sup>6</sup> could not be reproduced, Zard in 2005 eventually developed the optimal conditions, as indicated in **Scheme 4**, obtained good to excellent yields with minimal formation of presumable by-product (such as 1,3,5-triarylbenzene).<sup>7</sup>

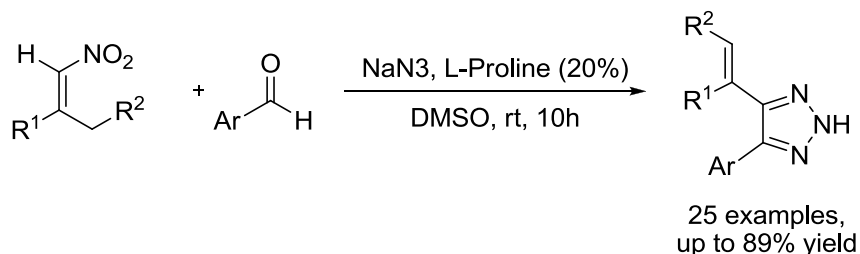
**Scheme 4.** Thermal condensation of nitroalkene and sodium azide (Zard's method).



The base-catalyzed cascade nitroalkene-aldehyde-azide condensation for the synthesis of 4,5-disubstituted *NH*-1,2,3-triazoles was developed and reported in 2008 by Shi and co-workers.<sup>8</sup> A series of new *NH*-1,2,3-triazoles was prepared in good to excellent yields under mild conditions

(Scheme 5). The alkene substituent could be easily converted into other functional groups such as carbonyl and alkanes.

**Scheme 5.** Shi's approach: Lewis base-catalyzed cascade nitroalkene-aldehyde-azide condensation.



Through the investigation of the reaction mechanism, a Henry reaction between nitroalkene and aldehyde was considered as the initiation step. Subsequently, the azide addition to the nitroalkene intermediate and elimination of the nitro group, formed the desired triazoles as major products. The mechanism was indicated in **Figure 2**.

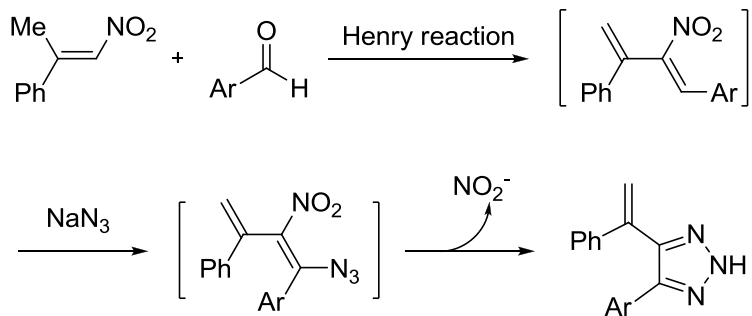


**Figure 2.** Mechanism for synthesis of 4,5-disubstituted *NH*-1,2,3-triazoles.

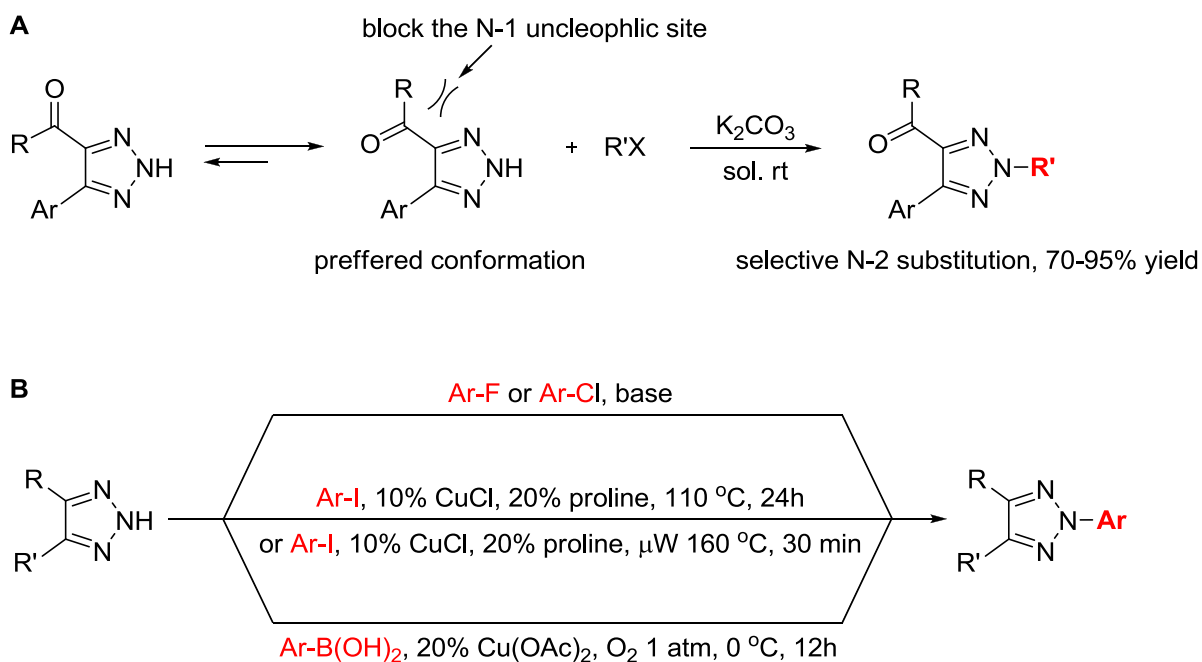
All the methodologies above provide the access to N-1 and C-4,5 substituted triazoles effectively. The N-2 substituted 1,2,3-triazoles have never been reported in the literature before 2008. Both CuAAC strategy ('click chemistry') and 1,3-dipolar cycloaddition will not provide the



N-2 substituted derivatives mechanistically. On another side, the nature of the triazole ring maintains a strong dipole moment and high electron density on the nitrogens. Therefore, the *NH*-1,2,3-triazole could be a good nucleophile, which reacts with electrophiles under suitable conditions to achieve the N-2 substituted derivatives. This strategy resulted a major concern of N-1/N-2 selectivity. All reported cases give N-1 substituted derivatives as predominate products through nucleophilic substitution reactions.<sup>9</sup>

The Shi group focused the effort toward the N-2 regioselective synthesis of 1,2,3-triazoles. Because the cascade condensation reaction gives an efficient access to 4,5-disubstitued derivatives, the increased steric hindrance from the two substituents is expected to influence the regioselectivity which is needed to achieve N-2 substituted derivatives through  $S_N2$  addition.<sup>10</sup> In the same year, N-2 aryl substituted derivatives were also achieved through three different approaches (**Scheme 6**).<sup>11</sup>

**Scheme 6.** Shi's Approach: N-2 alkyl/aryl substituted 1,2,3-triazole synthesis.

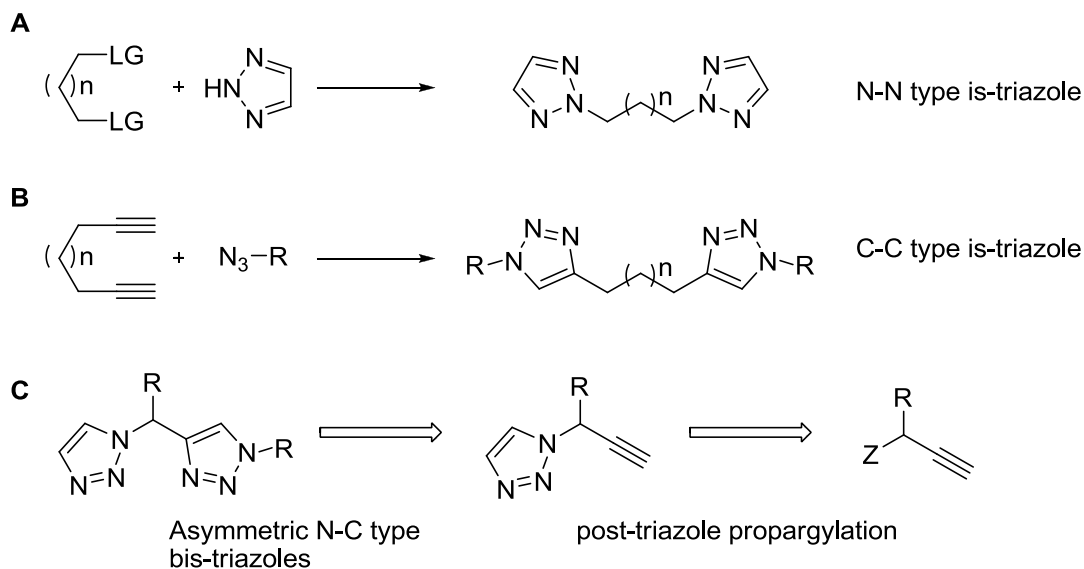


## 1.2 Research Objective and Results

The examples highlighted in the previous section completed the synthesis or functionalization of substituted 1,2,3-triazoles. With the synthetic 'kit box' to reach different functionalized triazoles, investigation of the potential application of 1,2,3-triazole as a ligand system in transition metal chemistry was initiated. Some interesting results have been reported in literatures regarding metal catalysis with simple 1,2,3-triazoles as ligands.<sup>12</sup> The fast growing research applications of this heterocycle necessitate the development of effective methods for the preparation of diverse 1,2,3-triazole derivatives, which can behave as classic bidentate or chelating ligand systems.

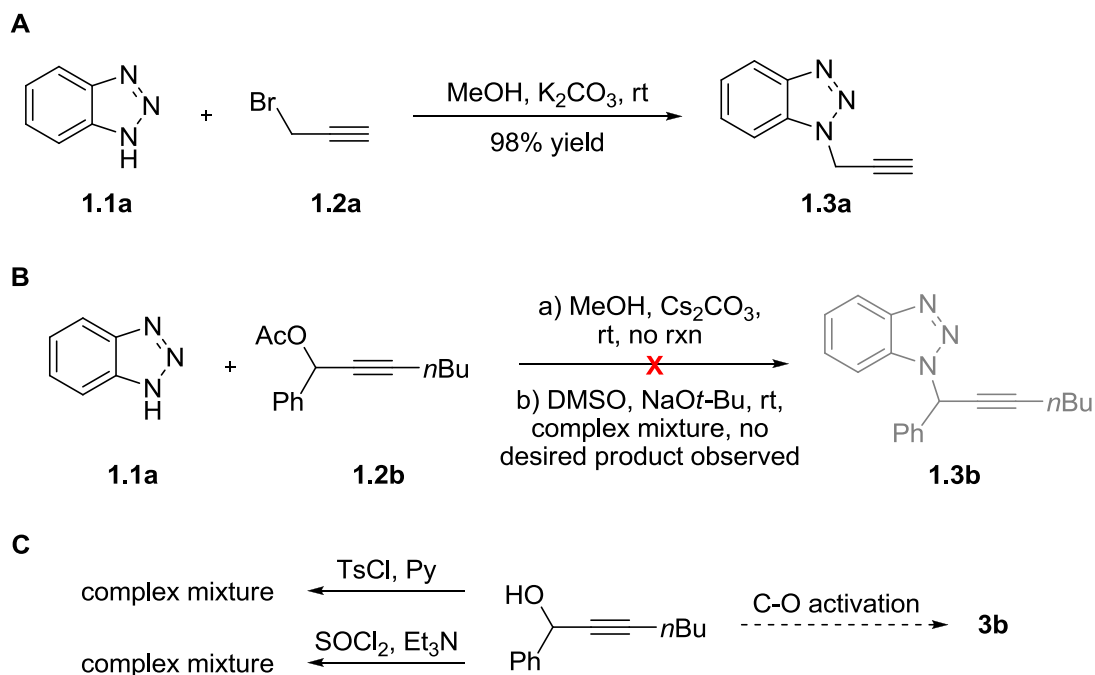
Bis-triazole compounds which behave as bidentate ligands could be synthesized through nucleophilic addition between *NH*-1,2,3-triazoles and linking moieties (N-N type bis-triazole), or 'click chemistry' between bis-alkynes and azide compounds (C-C type bis-triazole). Although, these synthetic strategies could effectively prepare bis-triazole compounds, (N-N type<sup>13</sup>, and C-C type<sup>14</sup>) all the products are symmetric (**Scheme 7A, B**).<sup>15</sup> The asymmetric bis-triazole retro-synthetic design indicated in **Scheme 7C** involved a post-triazole propargylation as the key step that could achieve a product with reasonable linking distance, based on Baldwin's Rule (5-member-ring or 6-member-ring are the favored ring sizes when metal atoms are involved after coordination). The synthetic designs are shown in **Scheme 7**.

**Scheme 7.** Three different types of bis-triazole compounds.



Although the retro-synthetic design appears straightforward, the actual preparation was much more challenging than expected, especially the post-triazole propargylation. In general, the propargylation can be challenging since the nucleophiles could potentially attack the triple bonds instead of the propargyl position, give corresponding allene intermediates that further convert into undesired products (such as Meyer-Schuster rearrangement products). As a consequence, the performance of this transformation usually depends on the nature of the substrates (i.e., the stability of leaving groups and steric hindrance of alkynes).<sup>16, 17</sup> Several tested reaction results are summarized in **Scheme 8**.

**Scheme 8.** Challenges in triazole propargylation.

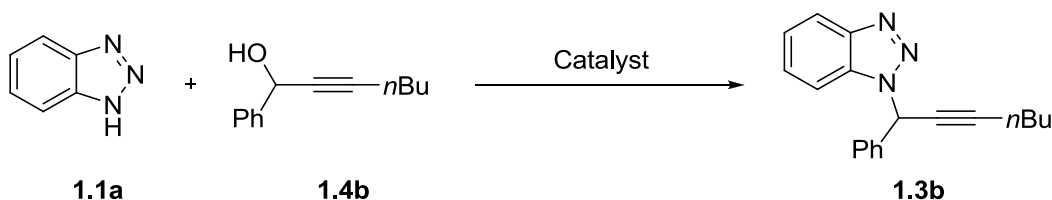


Though simple propargyl bromide **1.2a**, triazole propargylation could be achieved in excellent yields (**Scheme 8A**), the non-substituted methylene group eliminated the possibility of chirality or enantio-enriched moiety introduction. It is an important potential position to introduce the enantio-enriched environment other than chiral functionalized triazoles during ligand chirality control. The direct  $S_N2$  addition strategy to propargyl substituted alkynes failed. For example, reaction between triazole **1.1a** and propargyl acetate **1.2b** gave no reaction with  $\text{Cs}_2\text{CO}_3$  as the base. Treating the substrates under harsher conditions (DMSO and stronger base  $\text{NaOt-Bu}$ ) led to the formation of complex reaction mixtures with no desired propargyl triazole **1.3b** isolated (**Scheme 8B**). Moreover, attempts to convert propargyl alcohol **1.4a** into propargyl tosylate or halide also failed when classic conditions were applied. This was likely caused by the undesired side reactions associated with propargyl-allene decomposition as mentioned previously. When appropriate leaving/electron deficient substituted group presented under basic

conditions, the possible deprotonation procedure lead to the formation of corresponding allene derivatives and then gave undesired decomposition.

We therefore deduced that one alternative synthesis of propargyl triazoles could be the C-O bond activation of a propargyl alcohol with appropriate Lewis acid presented and followed by triazole addition (**Scheme 8C**). A series of different commonly used Lewis acid catalysts were then investigated to evaluate the ability to promote the propargylation of triazole **1.1a** and propargyl alcohol **1.4a**. The results are summarized in **Table 1**.

**Table 1.** Catalyst screening for Lewis acid C-O bond activation.<sup>a</sup>

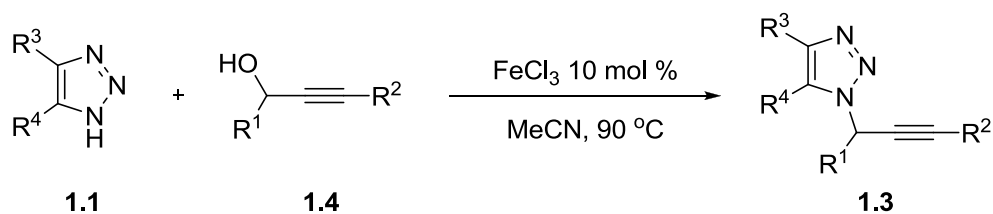


Entry	Catalyst	Loading(%)	Solv.	T(°C)	t(h)	Conv.(%) <sup>b</sup>	Yield(%) <sup>c</sup>	N1:N2
1	FeCl <sub>3</sub>	20	DCE	60	17	100	90	8:1
2	Cu(OAc) <sub>2</sub>	20	DCE	60	17	57	<5	n.d.
3	CuI	20	DCE	60	17	22	<5	n.d.
4	PdCl <sub>2</sub>	20	DCE	60	17	13	<5	n.d.
5	RuCl <sub>3</sub>	20	DCE	60	17	69	49	1.1:1
6	IrCl <sub>3</sub>	20	DCE	60	17	96	65	2:1
7	Co(OAc) <sub>2</sub>	20	DCE	60	17	28	<5	n.d.
8	LaCl <sub>3</sub>	20	DCE	60	17	21	<5	n.d.
9	CeCl <sub>3</sub>	20	DCE	60	17	30	<5	n.d.
10	Ti(O- <i>i</i> Pr)	20	DCE	60	17	52	<5	n.d.
11	AlCl <sub>3</sub>	20	DCE	60	17	26	<5	n.d.
12	TfOH	20	DCE	60	17	100	35	1.5:1
13	H <sub>3</sub> PO <sub>4</sub>	20	DCE	60	17	73	9	1:1

14	FeCl <sub>3</sub>	20	THF	60	7	90	70	6:1
15	FeCl <sub>3</sub>	20	Toluene	60	7	100	40	2:1
16	FeCl <sub>3</sub>	20	MeOH	60	7	60	44	7:1
17	FeCl <sub>3</sub>	20	MeNO <sub>2</sub>	60	7	90	<5	n.d.
18	FeCl <sub>3</sub>	20	DMF	60	7	<5	<5	n.d.
19	FeCl <sub>3</sub>	20	DMSO	60	7	<5	<5	n.d.
20	FeCl <sub>3</sub>	20	MeCN	60	7	91	85	10:1
21	FeCl <sub>3</sub>	20	MeCN	rt	12	62	50	9:1
22	FeCl <sub>3</sub>	20	MeCN	90	5	<b>100</b>	<b>93</b>	<b>11:1</b>
23	FeCl <sub>3</sub>	10	MeCN	90	10	100	90	10:1
24	FeCl <sub>3</sub>	5	MeCN	90	12	90	82	9:1

<sup>a</sup> Standard reaction condition: 1 equiv of propargyl alcohols, 1.2 equiv of triazoles, and indicated equiv of catalyst were added in order to corresponding solvents. <sup>b</sup> Conversions were determined based on the consumption of **1.4a**. <sup>c</sup> Yields determined by NMR with 1,3,5-trimethoxybenzene as the internal standard, and ratios determined by NMR of crude reaction mixtures.

Although significant decomposition of **1.4a** occurred with most of the Lewis acid catalysts (i.e. Entry 2, 10, 12, 13, 17), we observed that FeCl<sub>3</sub> was an effective catalyst for promoting this transformation and the desired product **1.3b** was obtained in good yield (entry 1). Further screening revealed MeCN as the optimal solvent (entries 14-20). Comparable yields were obtained even with decreased catalyst loading (entries 23 and 24), which is likely due to the decreased rate of possible carbon cation decomposition process. With the optimal conditions in hand, different triazoles and propargyl alcohols were evaluated to investigate the reaction substrate scope. The results are shown in **Figure 3**.



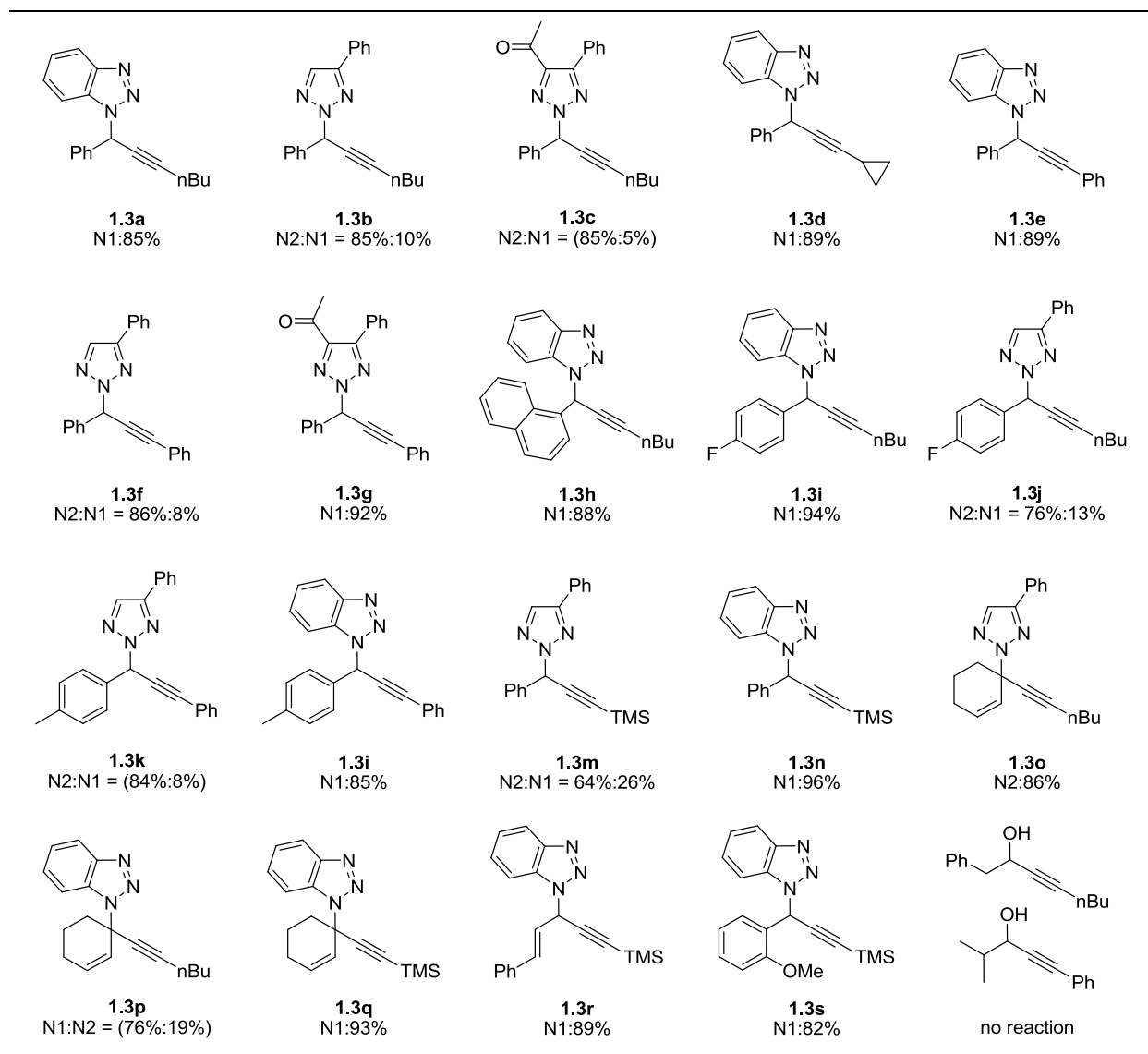


**Figure 3.** Reaction substrate scope. Yields were determined by NMR with 1,3,5-trimethoxybenzene as the internal standard, and ratios determined by NMR of crude reaction mixtures. The N-2 **1.3f** structure was confirmed by X-ray crystallography.

As showed in **Figure 3**, this Fe(III)-catalyzed propargylation was suitable for various different internal alkyne propargyl alcohols, which provided another available methods for effective post-triazole functionalization. Similar result was observed comparing to our previously reported strategy, the regioselectivity of 1,2,3-triazole strongly depends on the nature of the triazole substrate. For example, the benzotriazole gave N-1 regioselectivity, whereas,

predominantly N-2 isomers were obtained when more sterically hindered keto-modified 4,5-disubstituted triazoles were employed (i.e., **3c**, **3g**). Meanwhile, when C-4 phenyl triazole was treated under the same conditions, a mixture of both N-1 and N-2 regio-isomers in a 1:4 ratio, respectively, was obtained. The N-2 substituted derivative **3f** was structurally characterized by X-ray crystallography (**Figure 4**).

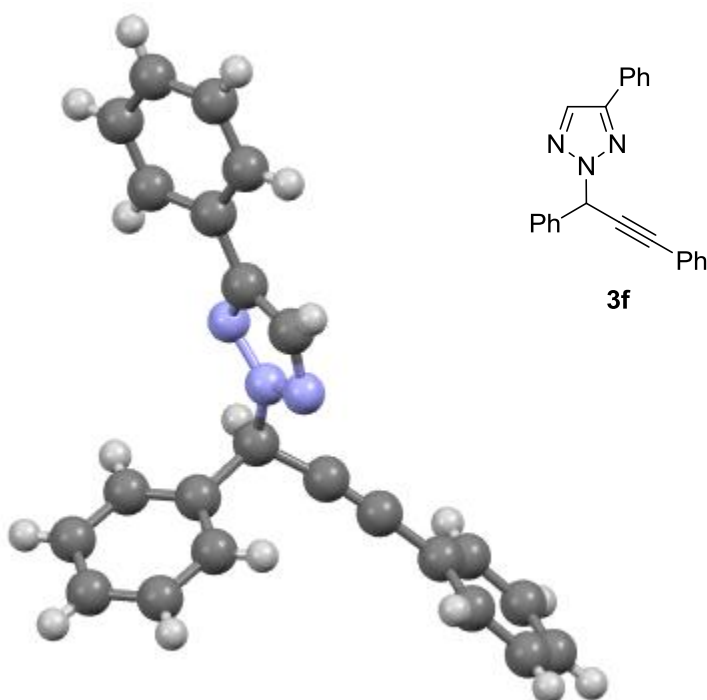


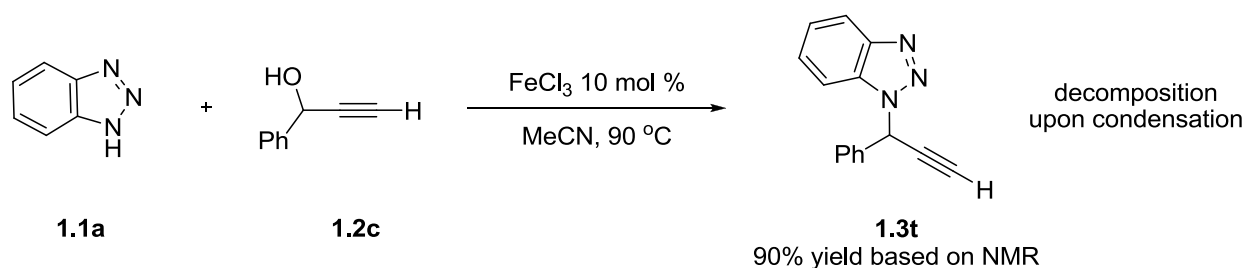
**Figure 4.** Perspective view of the structure of  $C_{23}H_{17}N_3$  (compound **1.3f**). The ball and stick drawing. CCDC number: 775267

The substituted groups on the propargyl position were critical for this transformation. The reaction generally worked well with aromatic substituted propargyl alcohols, except substrates with strong electron withdrawing groups (the *p*-nitrobenzene gave no reaction). No reactions were observed with aliphatic substituted propargyl alcohols. Impressively, the reaction proceeds smoothly with vinyl substituted substrate (such as **1.3r**), giving the corresponding triazole substituted enynes in excellent yields. Notably, Nazarov cyclization products were not observed



in these reactions, which highlighted the rather mild conditions of the reported method. Excellent yields were generally received for internal alkynes with different substituted groups, including alkyl, aryl, TMS, and cyclopropyl. The reaction was also suitable for terminal alkyne and gave the corresponding propargyl triazoles in good yields based on NMR (**Scheme 9**). Surprisingly, substrate **1.3t** was not stable upon concentration and gave complex reaction mixtures. This interesting transformation is currently under investigation.

**Scheme 9.** Unexpected decomposition of terminal alkyne substrates.



The unexpected decomposition of terminal alkyne **1.3t** raised serious concerns regarding the designated 'click chemistry' for the introduction of the second triazole rings. The 'click chemistry' is theoretically active only toward terminal alkynes since the copper-azide-acetylide complex plays key intermediate in the catalytic cycle. We therefore, tested the TMS derivatives which feature a relatively weaker C-Si  $\sigma$ -bond.

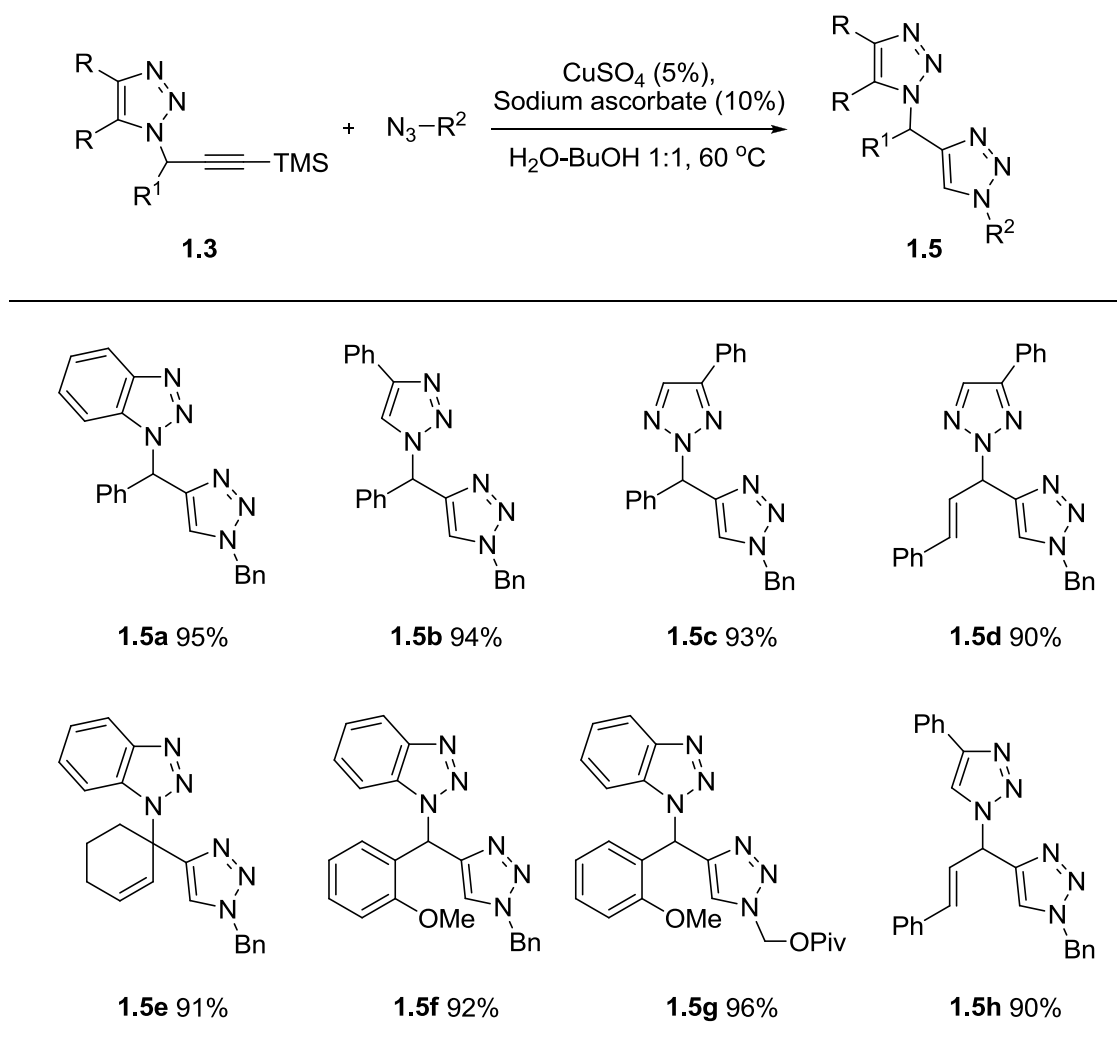


**Figure 5.** Synthesis of unsymmetrical N-C type bis-triazoles. Isolated yields for all cases. Condition: 0.05 equiv of CuSO<sub>4</sub>, 0.1 equiv of sodium ascorbate, BuOH-H<sub>2</sub>O (1:1), 60 °C, 12 h. Structure **1.5g** was confirmed by X-ray crystallography.

Fortunately, reactions between TMS-alkynes and corresponding azides gave the desired bis-triazoles (**1.5a-1.5h**) in excellent yields under standard 'click chemistry' condition (**Figure 5**).<sup>18</sup>

The molecular structure of compound **1.5g** was confirmed by X-ray crystallography (**Figure 6**).

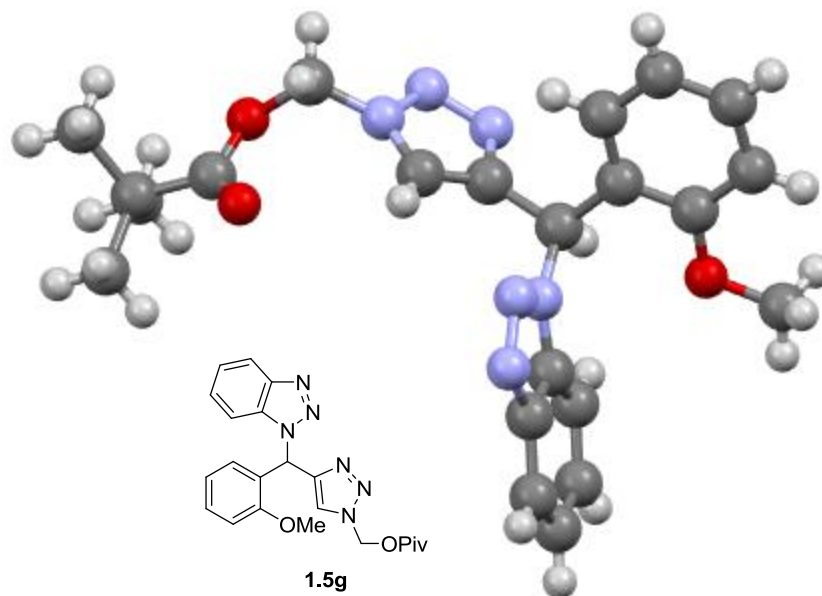


**Figure 6.** Perspective view of the structure of  $C_{22}H_{24}N_6O_3$  (compound **1.5g**). The ball and stick drawing. CCDC number: 775268

### 1.3 Conclusion

In conclusion, a  $FeCl_3$  catalyzed post-triazole propargylation was developed, giving the desired propargyl triazole in excellent yields which is a challenging synthesis when using N-2 nucleophilic substitution or 'click chemistry'. This method presents high efficiency. Application of this strategy led to the synthesis of unsymmetrical 1,1-bistriazoles. This study not only affords an efficient post-triazole functionalization strategy for the preparation of diverse triazole analogues, but also provides entry to a new class of bis-triazole compounds as a bidentate ligand system. Application of this type of bis-triazole ligands in transition metal coordination and reactivity tuning is currently under investigation in our group now.

## 1.4 Contribution

Dr. Wuming Yan and Dr. Yunfeng Chen were the researchers who had first investigated the reaction. Together Dr. Yan and Qiaoyi Wang were responsible for the substrate scope evaluation, ratio of N-1/N-2 regio-isomers determination and manuscript completion for successful submission to Organic Letters. Detailed X-ray crystallographic data analysis of compound **1.3f** and **1.5g** was done by Prof. Jeffrey L. Petersen, C. Eugene Bennett Department of Chemistry, West Virginia University.

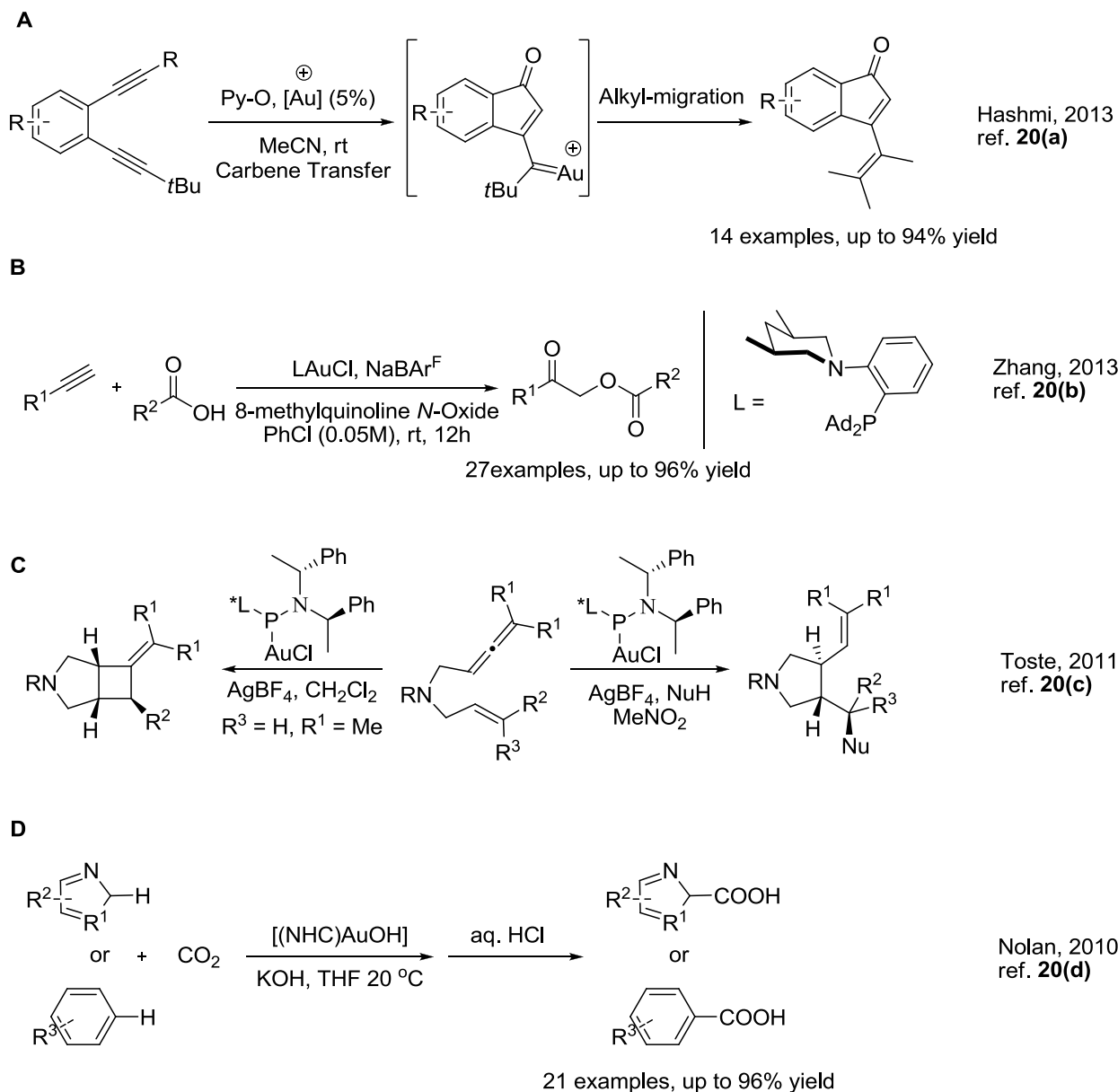
# **Chapter Two: 1,2,3-triazoles work as X-factor to promote gold(I) complex in challenging chemical transformations - part I**

## **2.1 Introduction**

### **2.1.1 Background information about homogeneous gold catalysis**

Homogeneous catalysis with gold complexes emerged as one of the most rapidly developing fields in this new century, which is called the 'gold rush'.<sup>19</sup> Newly discovered transformations have furnished numerous synthetic applications in the organic field.<sup>20</sup> In comparison to the traditional transition metal catalysis, gold chemistry presents several advantages: 1) high reactivity enables the reactions to occur under mild conditions; 2) high efficiency provides low catalyst loading (lower than 1 mol % in some cases); 3) multiple revealed reaction mechanisms involved in different reaction patterns increases the product diversity significantly with simple reaction precursors. Several representative examples regarding gold catalysis are shown in **Scheme 10**.

**Scheme 10.** Recent gold(I) catalyzed transformations.



Besides all the improvement and progress we have achieved, these exciting results revealed more questions regarding the process of homogeneous gold catalysis. At the beginning of the 21th century, gold(III) complexes were assumed to behave as a simple Lewis acid in the reported transformations.<sup>21</sup> Meanwhile, the  $\pi$ -acid activation by gold(I) catalysis was also straightforward.<sup>22</sup> Gold(I) complexes prepared for the chemical transformations are usually

bonded with strong coordinating ligands such as phosphines or NHC carbenes with chloride as the counter anion. The key functions for these ancillary ligands are: 1) increasing the solubility of the inorganic salt and tuning the reactivity or product selectivity; 2) improving the stability of gold(I) complexes during the reaction period toward moisture/air or other effects which could cause catalyst decomposition. The later function was considered to be very crucial in the gold(I) chemistry since the stability issue was one of the major drawbacks that limited the application of this promising metal catalytic system.

To access the reactivity of gold(I) complex as an efficient soft carbophilic  $\pi$ -acid toward the C-C multiple bonds, removal of chloride counter anion was required to generate the corresponding cationic gold(I) species. Most of the reported methods for homogeneous cationic gold(I) species generation adopted mixing the gold chlorides with silver salts to introduce the new anion such as  $\text{TfO}^-$ ,  $\text{BF}_4^-$ ,  $\text{ClO}_4^-$ ,  $\text{PF}_6^-$ ,  $\text{SbF}_6^-$ , and  $\text{B}(\text{C}_6\text{F}_5)_4^-$ .

With the activating species present, a general mechanism involved in most of the gold(I) homogeneous catalysis is showed in **Figure 7**. The opened coordination site complexation occurs with C-C multiple bond (C-C triple bond is used for example in **Figure 7**) in the substrate. Then the addition of nucleophile to the activated  $\pi$ -bond occurred and followed by proto deauration regenerated the Au cation and finished the catalytic cycle.

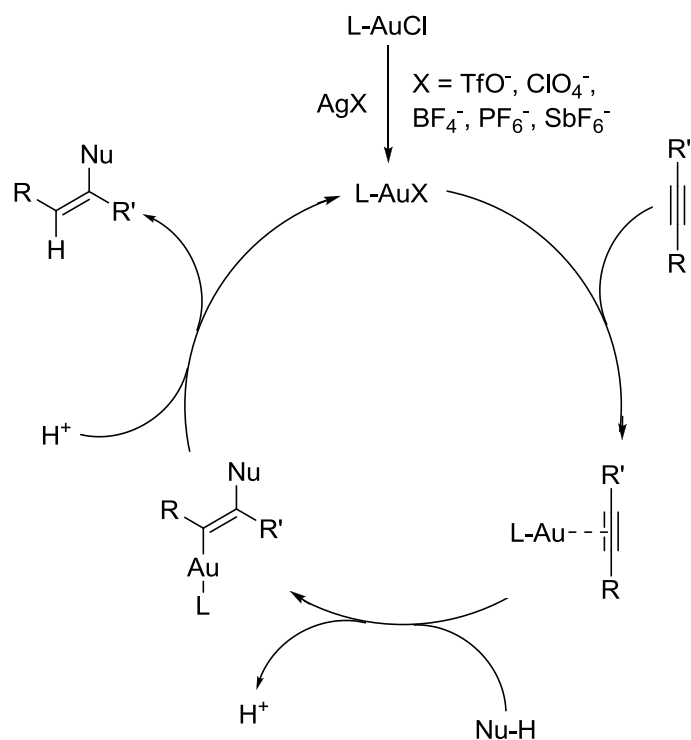


**Figure 7.** Classic homogeneous gold(I) catalytic cycle.

Despite the remarkable reactivity of the cationic gold(I) species, practical disadvantage does exist, most notably, a lack of stability under harsh conditions such as an elevated reaction temperature or the presence of a reductive nucleophile. These harsh conditions will cause serious catalyst decomposition indicated by the formation of gold mirror or gold nanoparticles. As a consequence, the gold(I) chemistry needs to be performed under mild conditions with careful substrate considerations.

Efforts have been devoted towards improving the stability of the gold(I) complexes. Preliminary results have demonstrated that the stability of the cationic gold(I) species can be improved through two general modifications: 1) different coordinating ligands and 2) counter ions with better coordination ability.



Among the reported systems, the N-heterocyclic carbenes (NHC's) and phos type ligands are representative examples in the early stage to improve the gold cation stability through different strategies. The NHC's have been applied as ligands in transition metal catalysis for decades<sup>23</sup> and are commonly described as excellent  $\sigma$ -donors which provide them distinctive affinity toward metals. Also, the vacant p-orbital provides the possibility of d-electron  $p$ -orbital back bonding, which improved the ligand coordination and the stability of the metal center. On the other hand, phos type phosphine ligands also showed excellent stabilizing ability to gold(I) complexes with their unique spatial confirmation.<sup>24</sup> The steric hindrance introduced after coordinating with Au cation blocks one open side along the axis of this linear L-Au-Cl moiety (**Figure 8**).

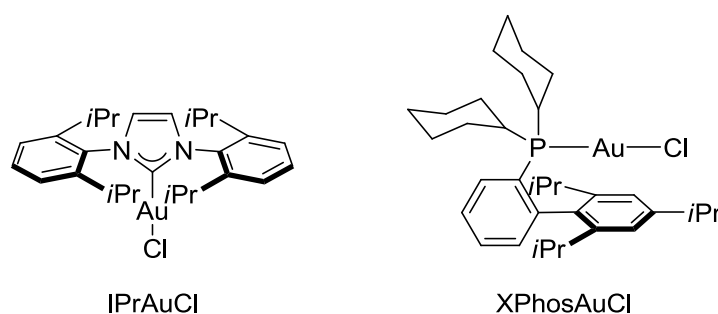


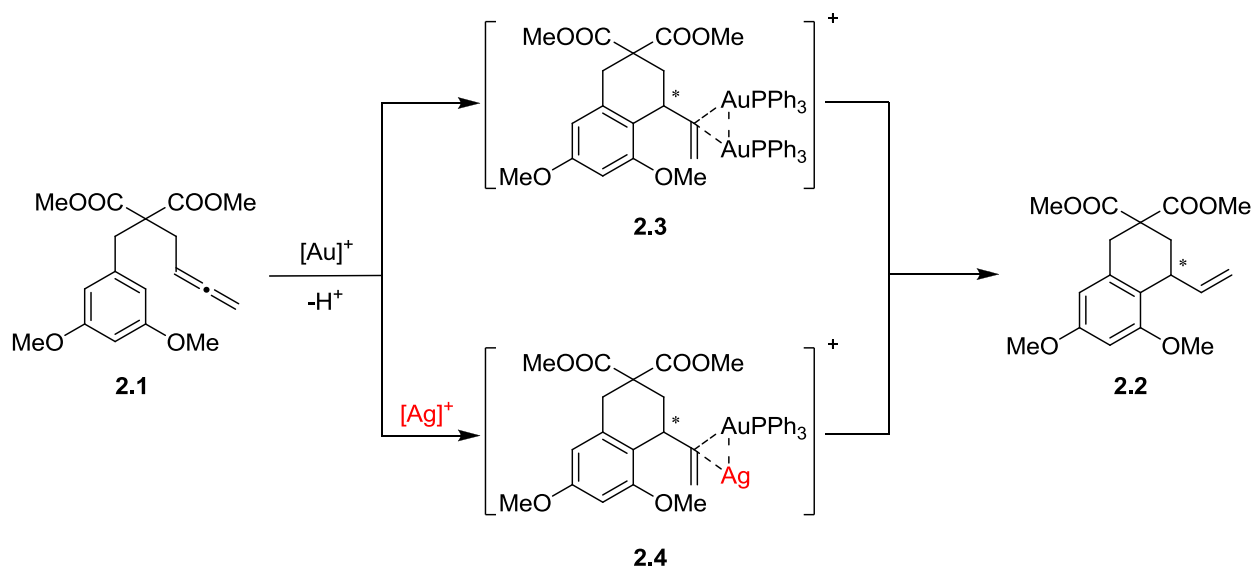
**Figure 8.** IPrAuCl and XPhosAuCl complexes with improved Au cation stability.

### 2.1.2 'Silver effect' in homogeneous gold(I) catalysis

With different primary ligands, the more stable Au cation complexes enabled the activation of some less reactive substrates such as internal alkynes, which usually required a harsher condition to reach efficient conversion. New Au complexes that expanded the temperature range for gold(I) catalysis could help researchers to overcome the dilemma of reactivity versus stability to achieve more desirable substrate tolerance.

While the breakthrough has been achieved by innovative primary ligands, a practical issue regarding the traditional gold catalysis still remained and limited the improvements for this promising metal catalyst, specifically the silver salt. The LAuCl complex is unreactive toward most of the substrates such as C-C triple bonds, due to the strong coordination between Au and Cl atoms which blocked the ligand exchange process. To remove the chloride, the most common method adopted by researchers is the addition of silver salt to form silver chloride precipitation and generated the cationic gold species. This method introduced less coordinating counter ion for gold which is more suitable for the activation process. It is agreed that the activated gold(I) cation - counter ion species are not very stable and need to be prepared before the reaction setup or generated *in situ*. The silver salts are highly hygroscopic and the chemical weighting should be taken under a humidity free environment, which usually requires operation in a glovebox. Moreover, a very recent result has shown that the newly introduced silver salt to the reaction mixture might not form the silver chloride precipitation and be removed very efficiently by passing the gold-silver mixture through a cotton plug or filter paper (which is a common method that has been applied in recent researches).<sup>25</sup> The trace amount of silver metal left in the reaction mixture together with the substrate is right now been demonstrated to functionalizing as gold-silver di-metal system in the resting state recently in 2009.<sup>26</sup> For the first time, this result revealed that silver plays a more important role in the reaction pathway other than a simple unreactive precipitation.

**Scheme 11.** Different resting states in the gold(I) catalysis when silver is presented.



In Prof. Gagne's result, the resting states of the gold(I) activated Friedel-Crafts reaction showed two convertible intermediates **2.3** and **2.4** due to different ratio of gold to silver cations (**Figure 9A**). Although the two intermediates did not affect the overall reaction and gave the same product in this very first case, it indeed changes the reaction rate.

Silver salt involved in the formation of intermediate **2.4**, and the excess amount of  $\text{AgNTf}_2$  added contributed in quenching the reaction rate (**Figure 9B**).

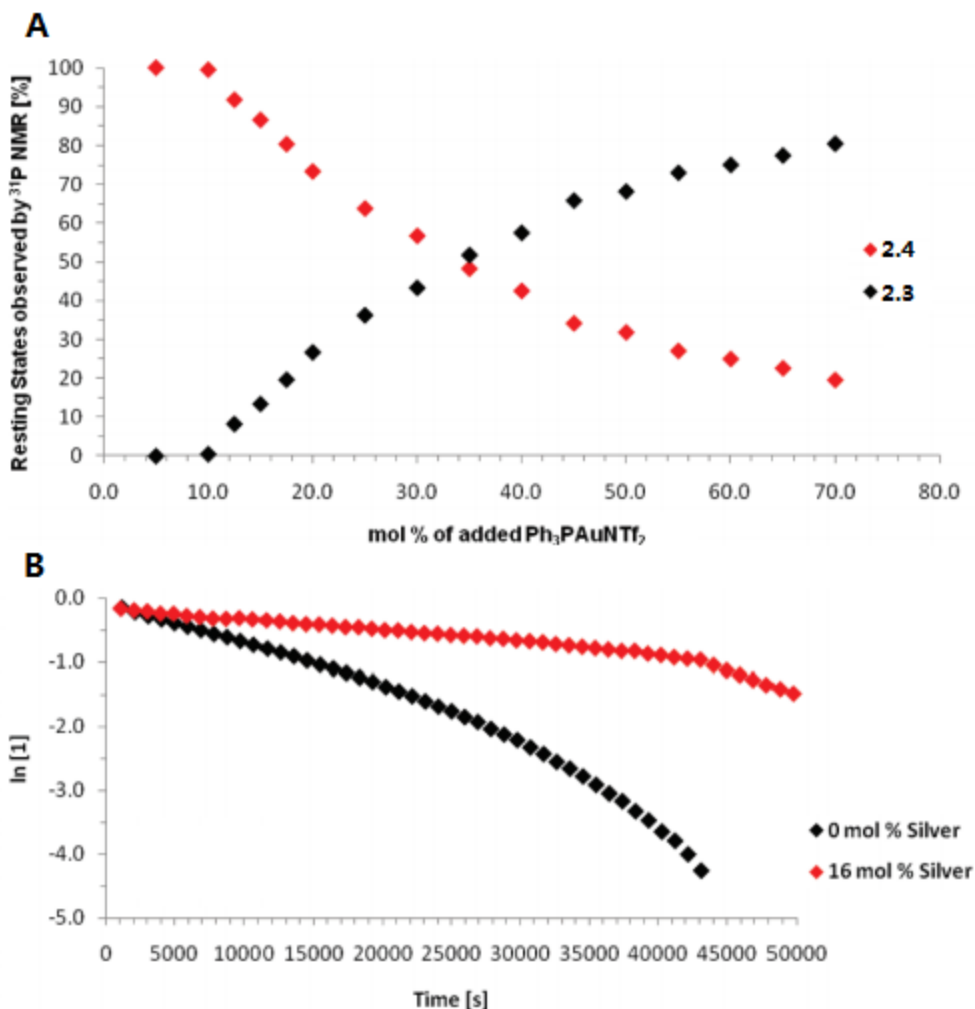
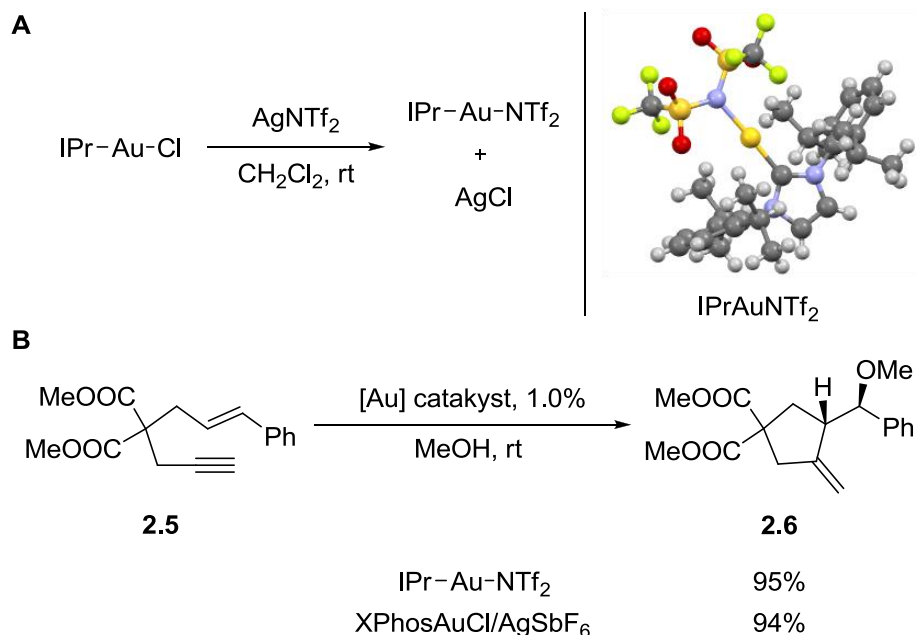


**Figure 9.** **A**, Change in catalyst resting state from **2.4** (Au-Ag) to **2.3** (Au-Au) upon additions of Ph<sub>3</sub>PAuNTf<sub>2</sub> to a solution of 0.1 mmol **1** and 15.5 mol % AgNTf<sub>2</sub> in CD<sub>2</sub>Cl<sub>2</sub>; **B**, ln **2.1** versus time [s] for the conversion to **2.2** by <sup>1</sup>H NMR; 0.1 mmol **2.1**, 5 mol % Ph<sub>3</sub>PAuNTf<sub>2</sub>, and 0.05 mmol hexamethylbenzene (internal standard) in 0.5 mL CD<sub>2</sub>Cl<sub>2</sub>; 6.2 mg (16 mol %) AgNTf<sub>2</sub> was added as a solid.

One of the gold(I) complexes that has been prepared which could be considered as 'silver free' was reported by Prof. Gagosz and co-workers in 2007 with bis(trifluoromethanesulfonyl)imide moiety (Tf<sub>2</sub>N<sup>-</sup>) as counter ion for gold(I) (**Scheme 12A**). Tf<sub>2</sub>N<sup>-</sup> is a weakly coordinating anion which could serve to stabilize gold(I) complex in both the solid and solution state.<sup>27</sup> This more stable property enabled people to perform recrystallization and remove the possible trace amount silver residue. Besides, weak coordination property did not

affect the ligand exchange process and helped maintaining the reactivity of this complex toward substrates in comparison with the classic ligand-Au/Ag salt system (**Scheme 12B**).<sup>28</sup>

**Scheme 12.** Synthesis of [IPrAuNTf<sub>2</sub>] and its application in enyne cycloisomerization.

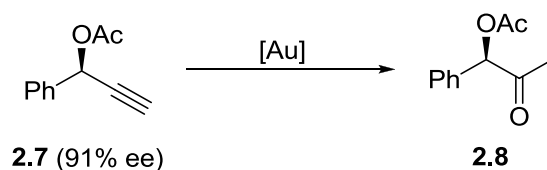


These types of weakly coordinating moieties are described as the 'X-factor' in gold catalysis along with OH, MeCN, and triazoles, which will be discussed in greater detail later.

In TA-Au complex, triazole played the same role as 'X-factor'. It provided us an opportunity to investigate not only the reactivity, but also the silver effect in gold(I) catalysis. A breakthrough result discovered in our group revealed a significant difference between Au-Ag and Au only activation. It has been reported before that adding the silver in some cases improved reactivity and reached better conversion and yield. To be worthy of attention, the silver promoted reactions showed the opposite result for the 'silver effect' comparing with Gagne's result (**Figure 9B**).<sup>29</sup> This comparison gained our interest and suggested that silver may function differently

than previously hypothesized. A TA-Au activated alkyne hydration initiated the investigation of difference between the pure Au and Au/Ag mixture.

**Table 2.** Silver effect in alkyne hydration.<sup>a</sup>



Entry	Catalyst	Conditions	Yield(%) <sup>b</sup>	ee(%)
1	1% TA-Au	5h	87	90
2	<b>10% AgA<sup>c</sup></b>	<b>12h</b>	<b>0</b>	<b>-</b>
3	<b>2% [PPh<sub>3</sub>Au]<sup>+</sup>A<sup>-c</sup></b>	<b>12h</b>	<b>0</b>	<b>-</b>
4	2% PPh <sub>3</sub> AuCl/AgOTf	12h	90	0
5	2% PPh <sub>3</sub> AuCl/AgSbF <sub>6</sub>	8h	97	0
6	2% PPh <sub>3</sub> AuCl/AgOTf	5h (N <sub>2</sub> )	92	90
7	2% [PPh <sub>3</sub> Au] <sup>+</sup> SbF <sub>6</sub> <sup>-</sup> + AgSbF <sub>6</sub>	12h	91	-

<sup>a</sup> General reaction conditions: **2.7** (1.0 equiv) and catalyst in 2.5 mL of dioxane/water (H<sub>2</sub>O, 3.0 equiv) at rt. Reactions were monitored by TLC. <sup>b</sup> NMR yields. <sup>c</sup> A<sup>-</sup> = TfO<sup>-</sup>, SbF<sub>6</sub><sup>-</sup>, BF<sub>4</sub><sup>-</sup>.

A direct comparison of different gold catalysts, with or without the presence of AgCl, was preformed (**Table 2**). As indicated in entry 2, under the optimal conditions reported by Sahoo (dioxane as solvent, 3 equiv. of H<sub>2</sub>O), none of the tested silver salts could catalyze the reaction, and a majority of **2.7** was recovered. The catalysts [(PPh<sub>3</sub>)Au]<sup>+</sup>A<sup>-</sup>, which were prepared from celite filtration of the PPh<sub>3</sub>AuCl/Ag<sup>+</sup>A<sup>-</sup> mixtures also could not promote this reaction (entry 3). However, when mixtures of PPh<sub>3</sub>AuCl and Ag<sup>+</sup>A<sup>-</sup> were used directly (without filtration of AgCl), the reaction worked as reported, though with complete stereochemical racemization (entries 4 and 5). Careful degassing and N<sub>2</sub> protection helped to avoid the racemization (entry 6).

Interestingly, a mixture of  $[(PPh_3)Au]^+TfO^-$  (the inactive complex obtained from filtration through celite) and  $AgSbF_6$  promoted this reaction effectively (entry 7), which suggested that the combination of gold and silver made the catalysis possible.

The difference here is obvious. The filtering procedure differs between using a regular filter paper or a celite pipette. The celite pipette gravity filtration was proven to be an efficient method to reach a complete removal of silver salts, as indicated by X-ray photoelectron spectroscopy (XPS).

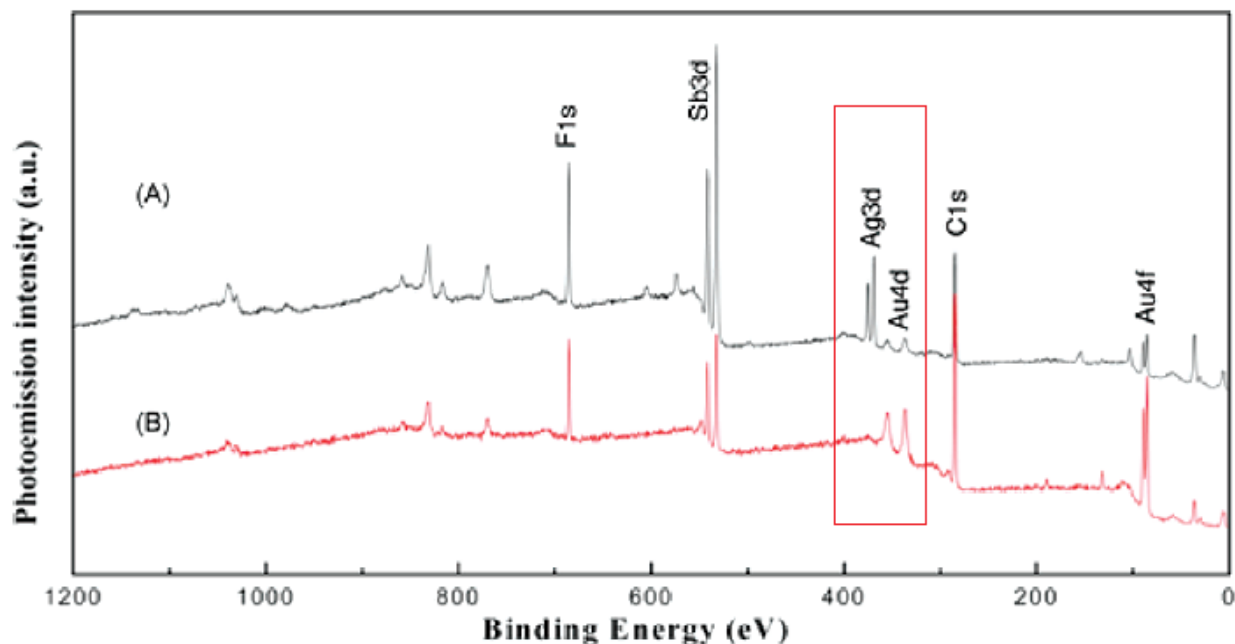


**Figure 10.** XPS Spectra of  $(PPh_3)AuCl/AgSbF_6$  Mixtures  $[(PPh_3)AuCl:AgSbF_6 = 1:1.5]$  after filtration through (A) Regular Filter Paper and (B) Celite

As showed in **Figure 10**, Au signals were observed in both spectra which presents at the binding energy Au  $4f_{7/2}$ , 85.5 eV; Au  $4f_{5/2}$ , 89.2 eV. The silver signal appears in the spectrum following the filtration by filter paper at **7A**: Ag  $3d_{5/2}$ , 368.7 eV; Ag  $3d_{3/2}$ , 374.7 eV. Whereas, the same signal was not found in the spectrum following celite gravity filtration. This result

unambiguously showed that the celite could serve to remove the silver effectively even when the silver is in relative excess ( $1.5/1.0 = \text{Ag}/\text{Au}$ ).

The LAuX (X indicates counter ion or X-factor in here) presents a linear spatial configuration, as a consequence, enables us to utilize  $^{31}\text{P}$  NMR spectroscopy to monitor the electronic nature of gold cations in solution. Different gold(I) species were tested and the corresponding  $^{31}\text{P}$  NMR spectra were compared in **Figure 11**.

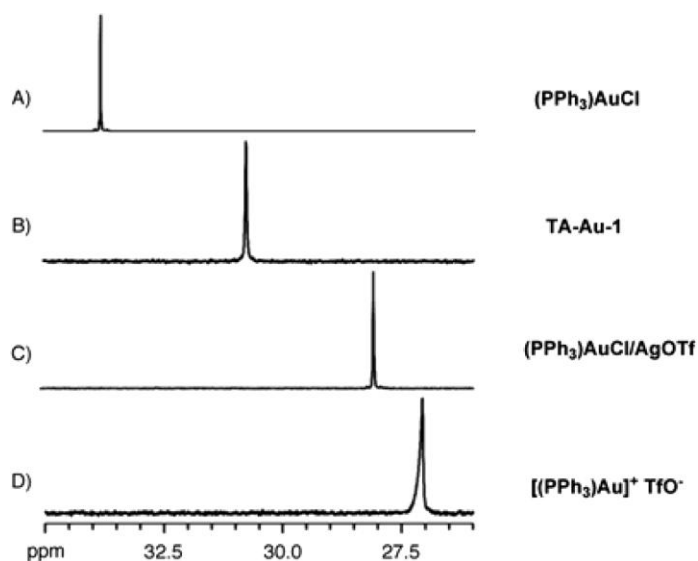


**Figure 11.**  $^{31}\text{P}$  NMR Spectra of Different Au(I) Samples. General conditions :The chemical shifts were calibrated using 85%  $\text{H}_3\text{PO}_4$  as an internal reference in a sealed capillary. The samples were prepared with 0.05 M gold in  $\text{CDCl}_3$ .

For the most cationic Au complex  $[(\text{PPh}_3)\text{Au}]^+\text{TfO}^-$  which was prepared by celite filtration,  $^{31}\text{P}$  resonance signal appeared at the most upfield with a chemical shift of 27.1 ppm (**8D**). However, the  $(\text{PPh}_3)\text{AuCl}/\text{AgOTf}$  mixture without any filtration exhibited a signal at 28.1 ppm (**8C**). This comparison clearly revealed the influence of silver through the trans-effect in gold(I) complexes.



As a result, the development of methodologies that could provide easy access to stable and 'silver free' gold(I) complexes are highly desirable.

## 2.2 Efforts toward the synthesis of different 1,2,3-triazole gold(I) complexes

Our group has focused on application of 1,2,3-triazole as a ligand system for years and several triazole based ligand-metal complexes were synthesized and characterized. The successful synthesis of complexes including Rh,<sup>30</sup> B,<sup>31</sup> and Au<sup>32</sup> proved that, 1,2,3-triazole is not, as previously assumed, an electron deficient heterocyclic structure lacking coordination ability.

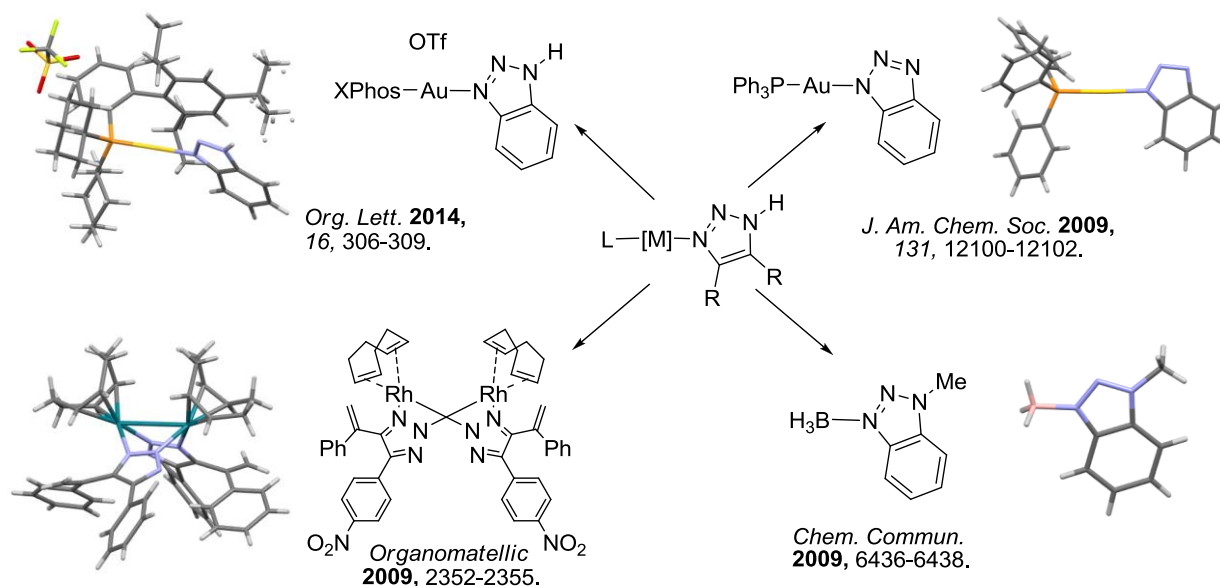


**Figure 12.** Different 1,2,3-triazole metal complexes obtained by Prof. Shi's group.

In all cases, the triazole coordinated complexes showed improved stability toward moisture and air together with interesting reactivity. Among these results, the triazole-gold(I) (TA-Au) complexes gained the most attention from us through comparison with traditional gold catalysis. The new complexes synthesized displayed significantly improved reaction diversity and stability. Our group has discovered a series of methodologies of post-triazole functionalization (**Figure**

13). With these methods in hand, we could easily gain access to modified 1,2,3-triazoles and test their coordinating ability.

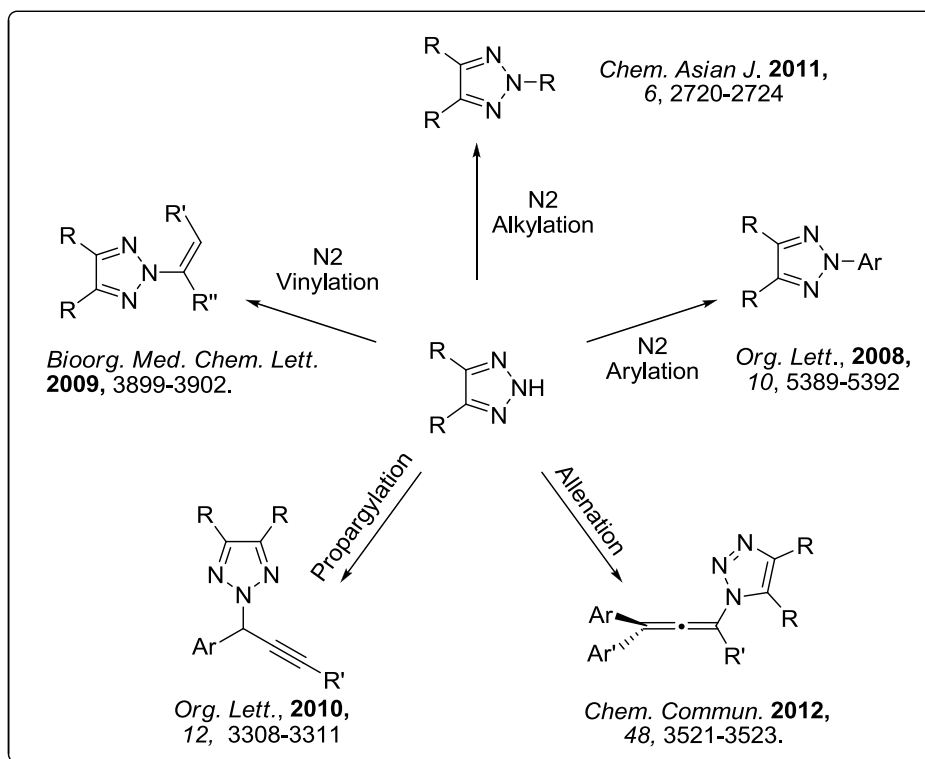
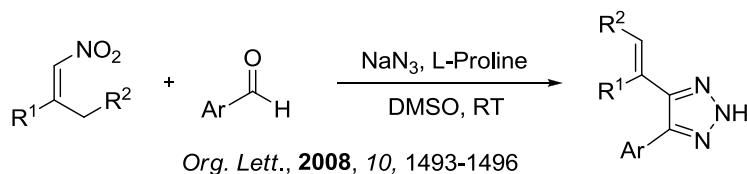


**Figure 13.** Different post-triazole functionalization discovered by Prof. Shi's group.

1,2,3-triazoles are structural isomers of the N-heterocyclic carbenes, with the ability to function as a good nitrogen  $\sigma$ -donor. Moreover, the electron deficient property of the triazole ring will theoretically promote the *d*-electron back-bonding more efficiently (**Figure 14**).

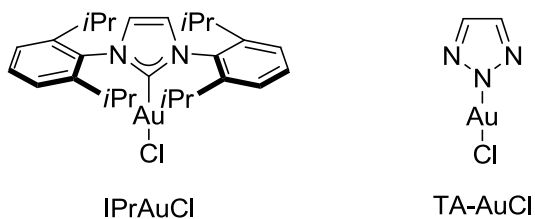
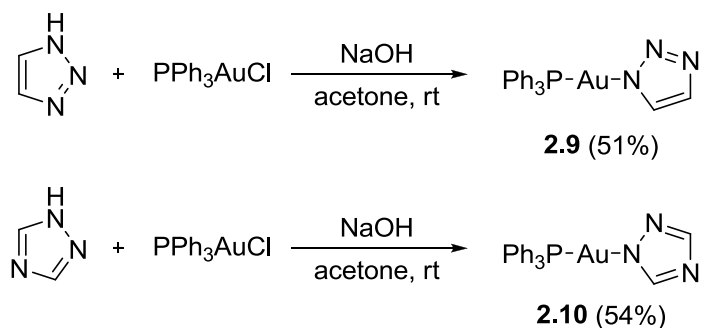


**Figure 14.** 1,2,3-triazole as structural isomer of NHC ligand: N  $\sigma$ -donor and better  $\pi$ -receptor

Based on the prior publications by Nomiya and co-workers, triazole-gold(I) complexes have been achieved from a basic condition resulted in neutral complexes in 1998 (**Scheme 13**). Stoichiometric amounts of  $\text{PPh}_3\text{AuCl}$  and respective triazole in the presence of the NaOH gave **2.9** in moderate yield (51%). Isolation of the colorless crystal was performed by a vapor diffusion between benzene and hexane as internal and external solvents.<sup>33</sup>

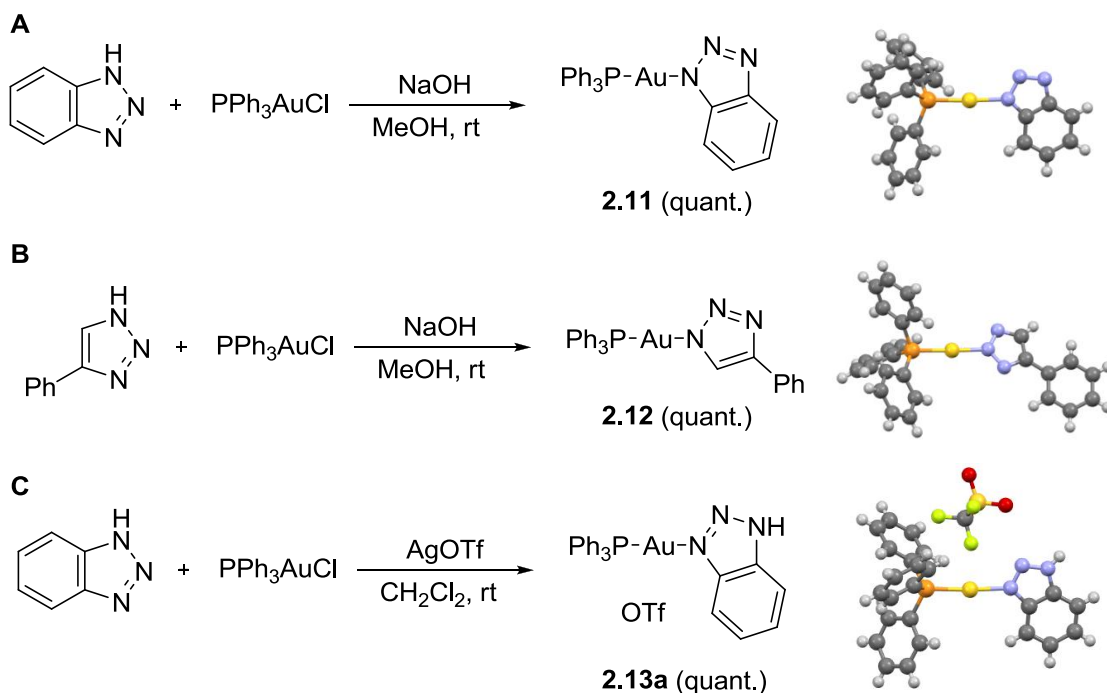
**Scheme 13.** Synthesis of triazole-gold(I) complexes reported by Nomiya.



Follow the similar reaction condition, we prepared the two neutral 1,2,3-triazole gold(I) complexes with  $\text{PPh}_3\text{AuCl}$  and benzotriazole/phenyltriazole as precursors in the presence of NaOH in MeOH.<sup>34</sup> The product was isolated by recrystallization from  $\text{CH}_2\text{Cl}_2$  and hexane, giving the pure product as white solids in quantitative yields. Cationic gold center neutral triazole complexes were also prepared by treating a mixture of benzotriazole/phenyltriazole and

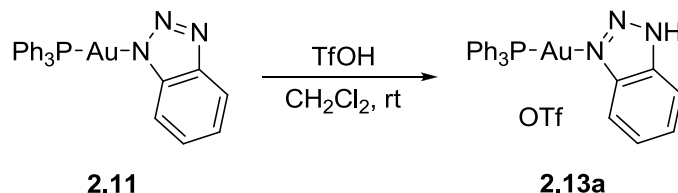
PPh<sub>3</sub>AuCl with silver salt AgOTf. Removal of the AgCl precipitate through celite filtration gave a clear solution and upon condensation under vacuum, a white solid was obtained and recrystallized from CH<sub>2</sub>Cl<sub>2</sub> and hexane to give colorless crystals in almost quantitative yield. Results are presented in **Scheme 14**.

**Scheme 14.** Synthesis of triazole-gold(I) complexes reported by Prof. Shi.



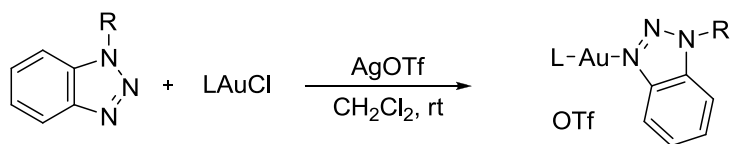
The complexes **2.11** and **2.12** in which the ligand is introduced as an anion are inert toward most of the tested substrates. The corresponding neutral triazole complex, **2.13a**, could be generated *in situ* via the addition of TfOH (**Scheme 15**).

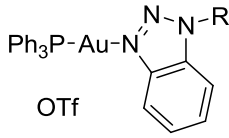
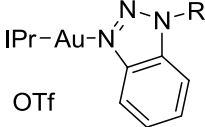
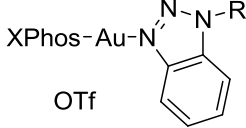
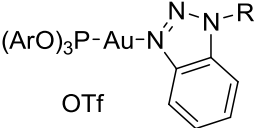
**Scheme 15.** Silver free conversion from **2.11** to **2.13a**.



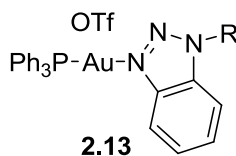
The arylation strategy works as an effective method for us to prepare functionalized triazoles with different electronic properties. To better investigate the modification ability of triazoles as ligands, a series of different N1-substituted benzotriazoles were prepared and treated with  $\text{PPh}_3\text{AuCl}$  and  $\text{AgOTf}$  under the identical conditions as described in **Scheme 14C**. Orthogonal of primary ligand and triazoles was carried out to build a library of 1,2,3-triazole gold(I) complexes with different electronic properties. The result is summarized in **Figure 15**.

The small library of triazole-gold(I) (TA-Au) complexes allowed us to investigate the reactivity of the catalysts with different electronic properties. A  $^{31}\text{P}$  NMR study was first conducted to evaluate the relative reactivity. The gold(I) chloride complex was considered unreactive, whereas, the cationic gold(I) with non-coordinating counter ion was considered as the most reactive species, the different substituted TA-Au complexes were assumed to show signals with chemical shifts between these two extreme cases. A series of TA-Au complexes was tested with triphenylphosphine ( $\text{PPh}_3$ ) as the primary ligand (**2.13a-2.13h**). The results are showed in **Table 3**.



L = PPh <sub>3</sub>	 <b>2.13</b>	R = H <b>2.13a</b>	R = Me <b>2.13b</b>	R = Ph <b>2.13c</b>	R = <i>p</i> -F-Ph <b>2.13d</b>
		R = <i>p</i> -Me-Ph <b>2.13e</b>		R = <i>p</i> -OMe-Ph <b>2.13f</b>	
		R = 2,4-dinitro-Ph <b>2.13g</b>		R = <i>p</i> -nitro-Ph <b>2.13h</b>	
L = IPr	 <b>2.14</b>	R = H <b>2.14a</b>	R = Me <b>2.14b</b>		
L = XPhos	 <b>2.15</b>	R = H <b>2.15a</b>	R = Me <b>2.15b</b>	R = <i>p</i> -nitro-Ph <b>2.15c</b>	
L = P(OAr) <sub>3</sub> Ar = 2,4-ditert butylphenyl	 <b>2.16</b>	R = H <b>2.16a</b>	R = Me <b>2.16b</b>	R = Ph <b>2.16c</b>	
		R = 2,4-dinitro-Ph <b>2.16d</b>			

**Figure 15.** A library of gold(I) complexes with different primary ligands and triazoles.

**Table 3.**  $^{31}\text{P}$  NMR data of substituted TA-Au complexes.<sup>a</sup>

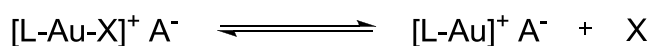
complex	$\text{PPh}_3\text{AuCl}$	R = <i>p</i> -OMe-Ph <b>2.13f</b>	R = <i>p</i> -Me-Ph <b>2.13e</b>	R = Me <b>2.13b</b>	R = H <b>2.13a</b>
chemical shift (ppm)	34.31	31.89	30.67	30.65	30.59
complex	R = Ph <b>2.13c</b>	R = <i>p</i> -F-Ph <b>2.13d</b>	R = <i>p</i> -nitro-Ph <b>2.13h</b>	R = 2,4-dinitro-Ph <b>2.13g</b>	$\text{PPh}_3\text{Au}^+\text{OTf}^-$
chemical shift (ppm)	30.44	30.28	30.19	29.80	28.80

<sup>a</sup>  $^{31}\text{P}$  NMR spectra of different Au(I) samples. General conditions: the chemical shifts were calibrated using 85%  $\text{H}_3\text{PO}_4$  as an internal reference in a sealed capillary. The samples were prepared with 0.05 M gold in  $\text{CDCl}_3$ .

As shown, the electronic properties could be easily tuned with different substituents on the triazole ring and a clear trend was observed. The substrate with the highest electron density **2.13f** gave the most downfield chemical shift at 31.89 ppm, which is still very reactive when compared with the inert  $\text{PPh}_3\text{AuCl}$  complex at 34.31 ppm. On the other end of the table, the very electron deficient substrate **2.13g** presented the extreme case of less coordination and gave the signal at 29.80 ppm, which is close to the 'pure' cationic gold(I) salt. All the other substrates lay between these two complexes providing an average distribution which means we might be able to tune the reactivity within a very small range and push the conversion with the most efficient model. To evaluate the electronic nature of these complexes, one model reaction was chosen to identify the difference through the kinetic investigation. The TA-Au catalyzed 3,3-rearrangement of propargyl ester to give an allene as the final product has been published before by our group.

The triazoles as second coordinating partner usually were known as secondary ligand (versus P ligand as the primary ligand) or 'X-factor' along with others such as MeCN, NTf<sub>2</sub><sup>-</sup>, and pyridine. The 'X-factor' usually promoted the stability of the gold(I) cation toward moisture and air, meanwhile, adjusting the reactivity through an equilibrium ligand exchange process (**Scheme 16**).

**Scheme 16.** X-factor: an alternative strategy in tuning gold catalyst reactivity.



L: ligand; X: coordinating factor; A<sup>-</sup>: counter ion

Moreover, based on the recent observation of Au-Cl-Au or Au-Cl-Ag complexes, making the reaction mechanism more complicated, the catalytic cycle has been proposed by others (**Figure 7**) needs to be revised.

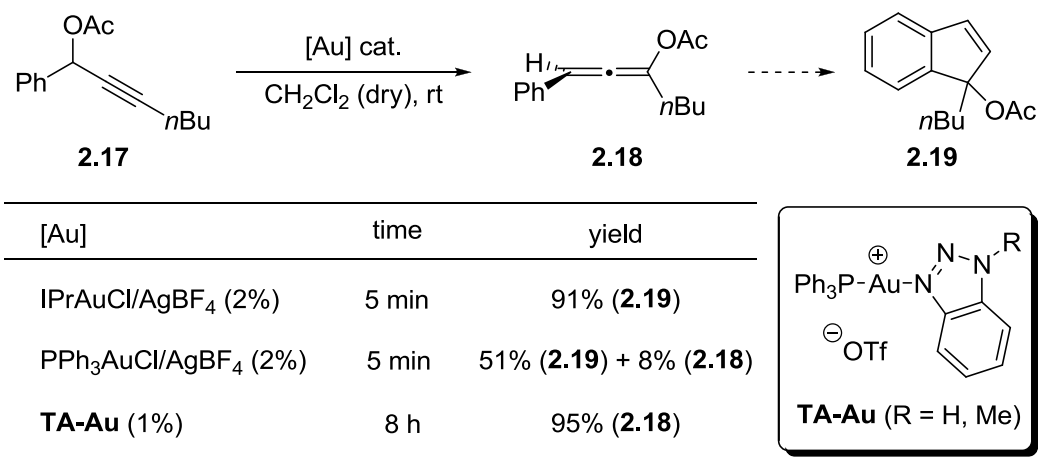
### 2.3 Quantitative kinetic investigation of triazole-gold(I) complex catalyzed [3,3]-rearrangement of propargyl ester

The TA-Au complex could preferentially activate alkyne over allene in propargyl ester 3,3-rearrangement, where indene was synthesized using 2 mol % IPrAuCl/AgBF<sub>4</sub>.<sup>35</sup> However, in our case, no indene was detected after 12 h with the presence of 1 mol % TA-Au.<sup>36</sup> We view this as a good opportunity for the mechanistic study. The simplified system may allow for the collection of quantitative kinetic information associated with TA-Au. In addition, it is also very important to understand the reason of the chemoselectivity offered by TA-Au, while other [L-Au]<sup>+</sup>



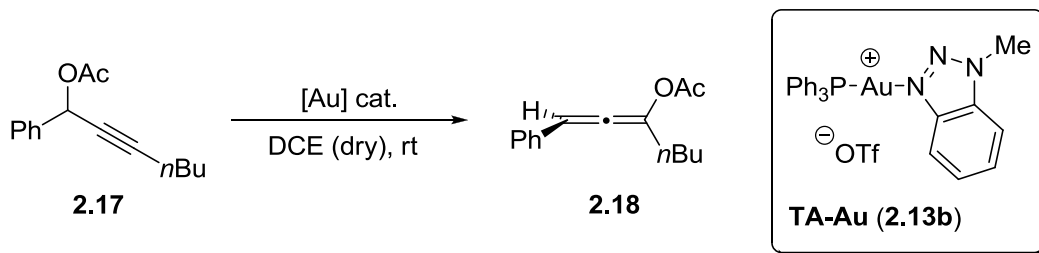
complexes led to rapid racemization at the propargyl position and resulted in poor chemoselectivity (activation of both alkyne and allene). The quantitative kinetic investigation of TA-Au catalyzed propargyl ester 3,3-rearrangement using *in situ* IR spectroscopy from a ‘live’ catalytic reaction was performed.<sup>37</sup>

**Scheme 17.** TA–Au as a chemoselective catalyst for alkyne activation.



To acquire meaningful kinetic data for a catalytic reaction, the turnover-limiting step needs to be established. This is a challenging task for the LAuCl/AgX system, leading to the rapid catalyst decomposition over time. A unique advantage of the TA-Au catalyst is its improved stability, which allows relatively steady concentration of the catalyst for the kinetic study. Thus, we set out to evaluate the kinetic dependence of concentration of the substrate and TA-Au. The standard reaction was chosen as the model reaction for the detailed investigation.

**Scheme 18.** Selection of TA-Au **2.13b** as catalyst for alkyne activation.



To avoid the potential influence of acid (formation of HOTf), the N-Me-benzotriazole (instead of N-H) coordinated TA-Au **2.13b** was selected (**Scheme 18**). The dependence of the initial rates on the concentration of TA-Au catalyst **2.13b** was studied with varying concentrations from 0.002–0.008 M. The initial rates in different runs were calculated based on the kinetic profiles monitored by in situ IR. A linear relationship is established as depicted in **Figure 16**. The reaction therefore shows first-order dependence on **[2.13b]**, suggesting the involvement of **2.13b** in the turnover-limiting step.

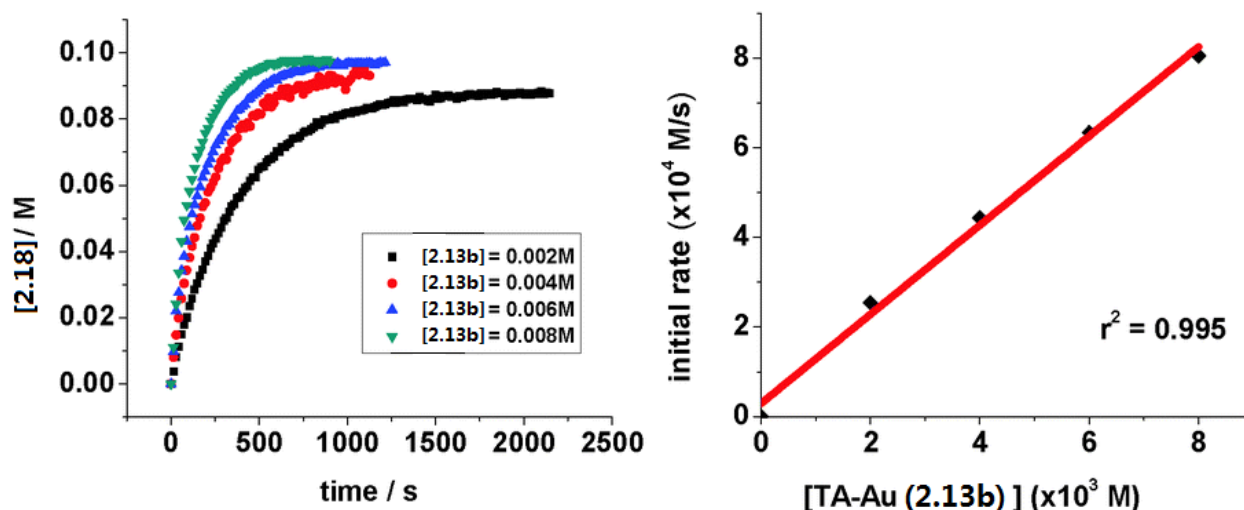


**Figure 16.** Dependence of the initial rates on catalyst concentrations for rearrangement of **2.17**. Reaction conditions: **2.18** (0.10 M in DCE, 1.2 mL), **2.13b** (0.002–0.008 M in DCE), 30 °C.

A subsequent experiment was performed to determine the kinetic order of **[2.17]**. Similarly, the initial rates were plotted against **[2.17]** varied from 0.10–0.20 M. Again, a first-order dependence was observed, as showed in **Figure 17**. Combining the two experiments, we were able to derive the rate law for this reaction:  $r = k_{\text{obs}}[\mathbf{2.17}]^1[\mathbf{2.13b}]^1$ . According to the rate law, both the catalyst **2.13b** and substrate **2.17** were involved, revealing the electronic activation of alkyne (*i.e.* ligand exchange) as the turnover-limiting step.

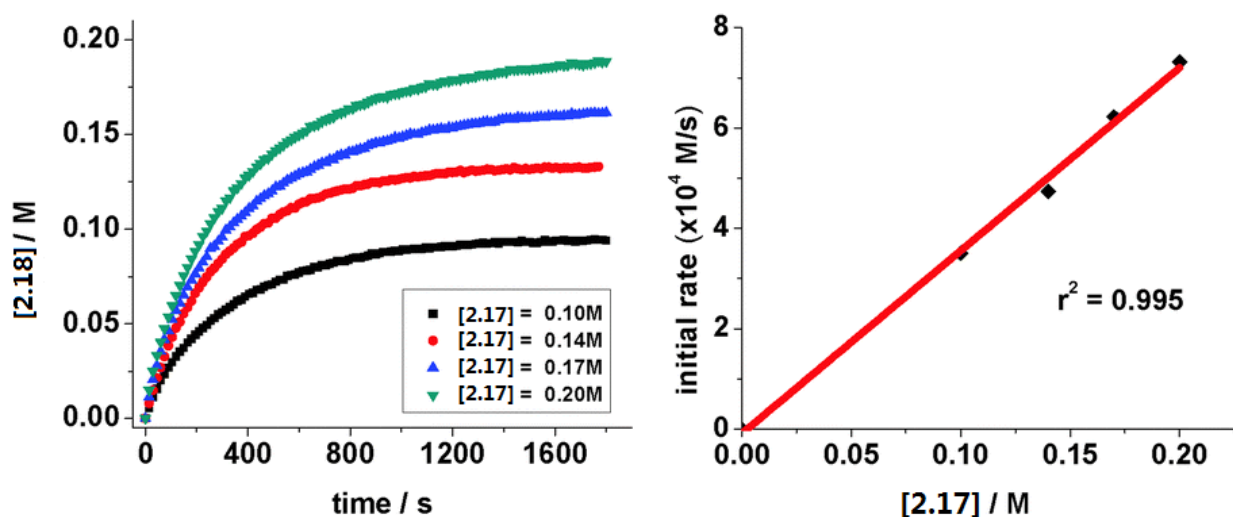
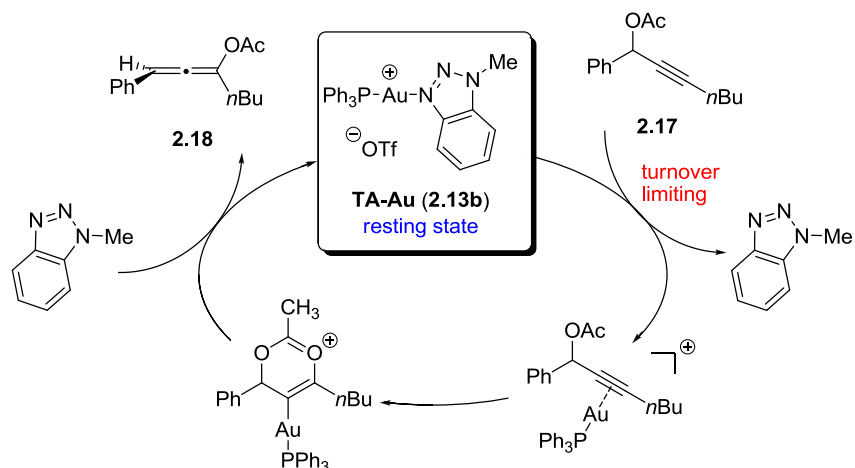


**Figure 17.** Dependence of the initial rates on starting material concentrations for rearrangement of **2.17**. Reaction conditions: **2.18** (0.10–0.20 M in DCE, 1.2 mL), **2.13b** (0.003 M in DCE), 30 °C.

With this kinetic data, a tentatively proposed mechanism of TA–Au catalyzed propargyl ester 3,3-rearrangement is shown in **Scheme 19**. First, the TA–Au complex undergoes the turnover-limiting ligand exchange with the substrate to form the cationic gold(I) alkyne  $\pi$ -complex. This complex then rapidly converts the propargyl ester to the corresponding allene. It is clearly seen that the ligand exchange step significantly slows the reaction rate compared to the use of free cationic gold(I) (**Scheme 16**), which is consistent with the fact that the same reaction catalyzed by  $\text{IPrAu(L)}^+$  ( $\text{L} = \text{Et}_3\text{N}, \text{py}$ ) was also slower.<sup>38</sup>

**Scheme 19.** Proposed mechanism for TA–Au catalyzed 3,3-rearrangement.



Finally, we prepared various TA–Au catalysts with different substituted benzotriazoles in order to investigate the impact of the electronic nature of the TA–Au catalysts. The reaction kinetics are illustrated in **Figure 18**. Combining the  $^{31}\text{P}$  NMR peaks corresponding to TA–Au catalysts directly provides information regarding the electronic nature of the gold center.

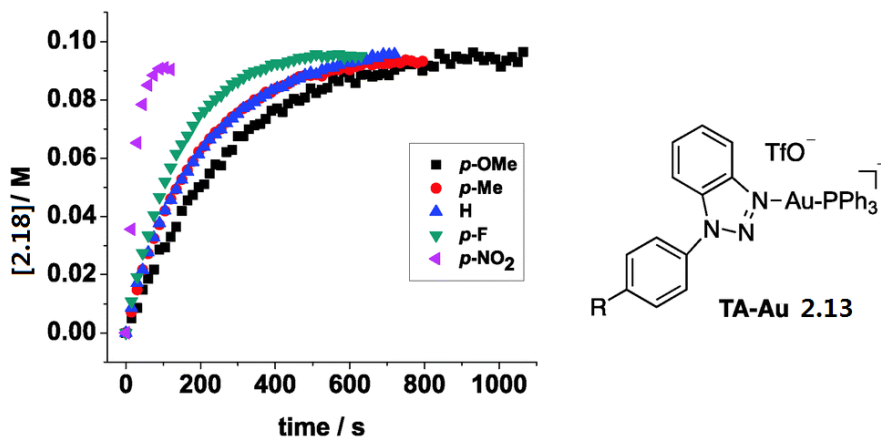


**Figure 18.** Kinetics profile using various TA–Au catalysts. Reaction conditions: **2.18** (0.10 M in DCE, 1.2 mL), TA–Au (0.003 M in DCE), 26 °C.

Clearly, the more cationic gold(I) species led to faster reaction rates. The slowest reaction was observed with the 4-methoxyphenyl substituted TA–Au catalyst. However, this reaction is

still faster than the reaction catalyzed by **2.13b**, suggesting the inherent electron-withdrawing nature of the phenyl group attached to benzotriazole. The linear free energy relationship was established by plotting  $\log(k/k_0)$  vs.  $\sigma_{para}$ , giving a  $\rho$  value of 0.74 (**Figure 19**).

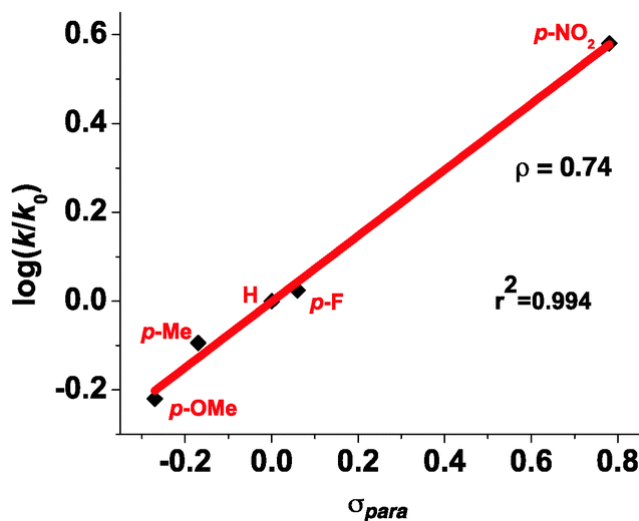


**Figure 19.** Hammett plot of various TA–Au catalysts.

The positive  $\rho$  value suggested partial positive charge building up during the reaction, which is consistent with the associative ligand substitution being the turnover-limiting step. The more electron-deficient triazole undergoes ligand exchange more rapidly, which is due to the faster reaction rate. This result also highlights the tunability of the TA-Au catalyst. Based on the different cases, the more electron-deficient TA-Au will give a shorter reaction time, while the more electron-rich TA-Au has a longer catalyst lifetime.

The chemoselectivity of the TA-Au catalysts (activation of alkyne over allene) can also be explained by this ligand–substrate exchange mechanism. The DFT calculation revealed that the HOMO of propargyl ester **2.17** is 20 kcal mol<sup>-1</sup> higher than the HOMO of allene **2.19**.<sup>39</sup> Thus, the ligand exchange is much slower between allene and TA–Au, which supports the observed selective alkyne activation.<sup>40</sup>

## 2.4 Conclusion

In summary, a series of triazole-gold(I) complex (TA-Au) has been prepared and propargyl ester 3,3-rearrangement catalyzed by TA-Au complexes has been quantitatively investigated. Considering that few physical organic studies have been reported regarding gold catalyzed alkyne activation due to the poor catalyst stability and complex reaction nature, this work provided direct experimental evidence for understanding the elementary step in the TA-Au catalyzed alkyne activation. The discovery of associative ligand exchange between TA-Au and alkyne as the turnover-limiting step provided mechanistic insight, which will benefit future investigations.

## 2.5 Contribution

Qiaoyi Wang was the researcher who had first investigated the reaction kinetic profile. Yumeng Xi was responsible for the kinetic profile determination. Together Qiaoyi Wang, Yumeng Xi, Dr Jijin Su, and Dr Dawei Wang were responsible for the functional triazole complexes synthesis, NMR spectrum investigation and manuscript completion for successful submission to Chemical Communications. The DFT calculation was done by Prof. Minyong Li, at Department of Medicinal Chemistry, School of Pharmacy, Shandong University. The detailed X-ray crystallographic data analysis of compound **2.11**, **2.12**, **2.13a** was done by Prof. Jeffrey L. Petersen, C. Eugene Bennett Department of Chemistry, West Virginia University.

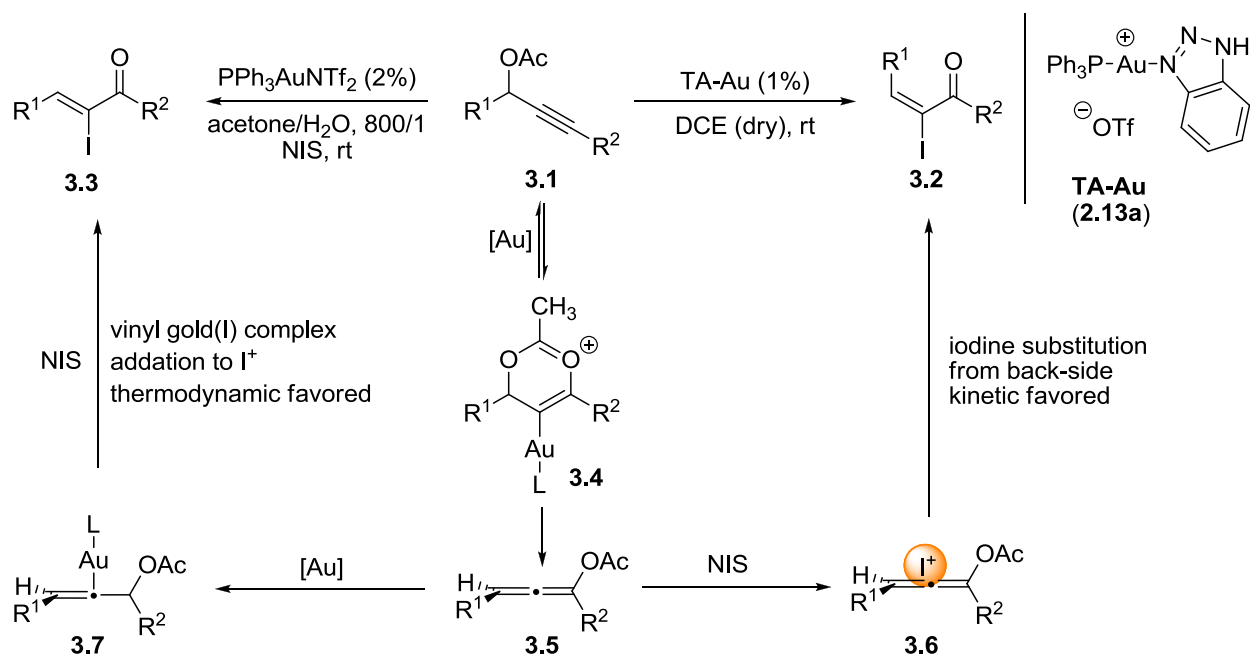
## Chapter Three: 1,2,3-triazoles work as X-factor to promote gold(I) complex in challenging chemical transformations - part II

### 3.1 Introduction

As discussed in the previous section, we have built a small library of triazole-gold (TA-Au) complexes. This type of unique complex did not only as we expected, show pronounced stability compared to simple cationic gold(I), but also brought new reactivity. The fact that TA-Au only activates C-C triple bond over allene indeed offered an effective synthetic method of allene synthesis from more readily available commercial starting material - propargyl alcohol.

The first evidence for TA-Au complex activated C-C triple bond over allene was reported in the synthesis of E- $\alpha$ -haloenones as a kinetic favored product, whereas the corresponding thermodynamic favored Z-isomer has been separated as major product which has been published before (**Scheme 20**).<sup>41</sup> According to the mechanistic investigation, the allene compound was widely adopted by researchers as the initiation intermediate after 3,3-rearrangement. However, the gold(I) species utilized as catalyst showed a lack of chemoselectivity and proceeded to activate allene sp carbon giving corresponding products. This investigation revealed that the E-isomer observed in our publication was a direct substitution product in which the  $\pi$ -acid catalyst was not involved.

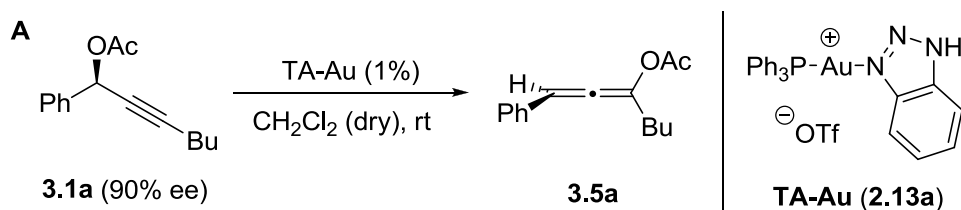
**Scheme 20.**  $\alpha$ -haloenone through gold(I) activated propargyl ester gave Z/E isomers.



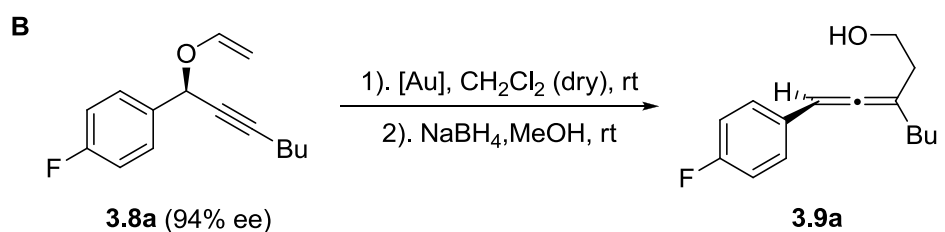
Inspired by this discovery, a follow up discussion concerning the direct synthesis of allene through TA-Au catalyzed 3,3-rearrangement was reported later. In this research, effort was devoted to reach asymmetric synthesis of allenes through chirality transfer from an asymmetric reaction precursor.<sup>42</sup> Both enantioenriched propargyl ester and propargyl vinyl ether were treated with TA-Au **2.13b**, the allene products were isolated in high yields in both cases. Though, the allene ester product gave no ee value (**Scheme 21A**) likely due to the low energetic barrier of allene ester racemization process ( $\Delta G = 5.7$  kcal/mol,  $t_{1/2} < 0.5$  h),<sup>43</sup> the allene aldehyde from propargyl vinyl ether had a chirality retention from starting material (**Scheme 21B**).



**Scheme 21.** TA-Au catalyzed allene formation with chirality retention.



[Au]	time	percentage	
<b>TA-Au (1%)</b>	30 min	59% ( <b>3.1a</b> ) 90% ee	41% ( <b>3.5a</b> ) 0% ee
<b>TA-Au (1%)</b>	4 h	17% ( <b>3.1a</b> ) 90% ee	83% ( <b>3.5a</b> ) 0% ee



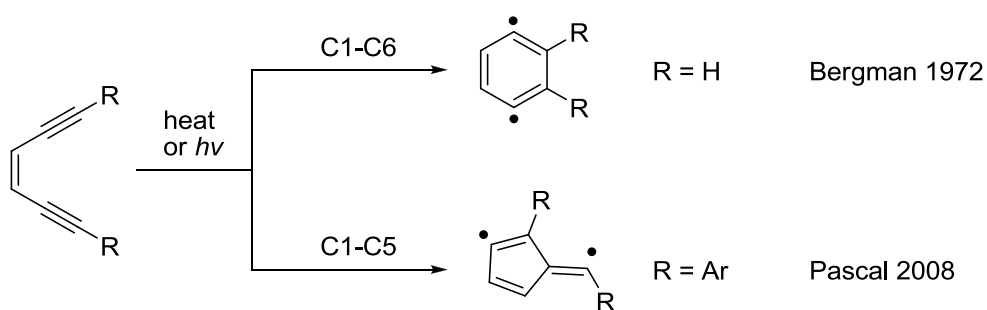
[Au]	time	yield	ee
$\text{PPh}_3\text{AuCl/AgBF}_4$	30 min	82%	5%
$[(\text{PPh}_3\text{Au})_3\text{O}]\text{BF}_4$	4 h	87%	73%
<b>TA-Au</b>	8 h	91%	90%

Based on these breakthrough results, our group attempted to apply this unique transformation in more challenging chemical reactions. One of the examples is the schmittel cyclization promoted by TA-Au catalyst at room temperature.<sup>44</sup>

Over the past several decades, thermal cycloaromatizations of enediyne (Bergman and Pascal)<sup>45</sup> and enyne–allene (Myers-Saito and Schmittel)<sup>46</sup> have attracted considerable attention due to their fundamentally intriguing mechanisms and the crucial biological applications.<sup>47</sup> Prof. Bergman initiated the investigation of the cycloaromatization (C1-C6) of enediyne system in

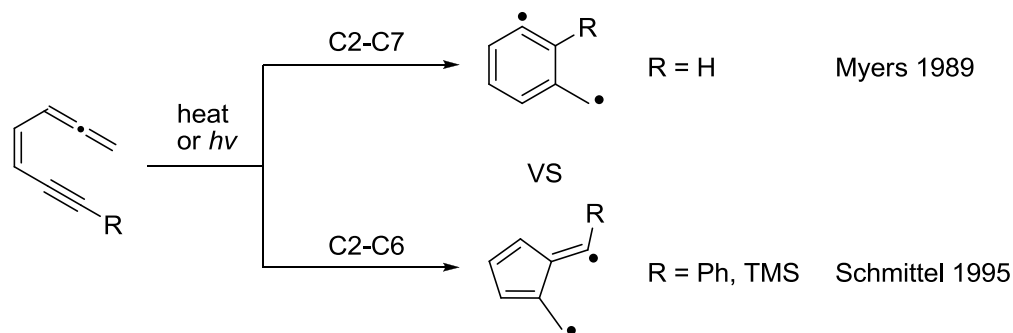
1972. The following efforts have been devoted to this field demonstrated this type of transformation involved in a diradical intermediate.<sup>48</sup> A possible competitive product of this reaction could be indene derivative from C1-C5 cycloaromatization. In 2008, Prof Pascal first discussed through computational and experimental data that, with diaryl substituent on the termini of alkyne positions could achieve C1-C5 indene derivatives as major products (**Scheme 22**).<sup>49</sup>

**Scheme 22.** Cyclization of enediyne derivative through diradical intermediate.



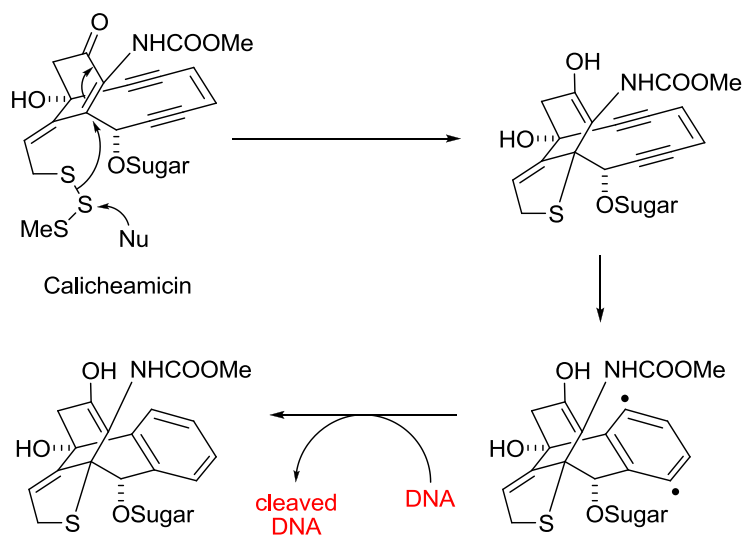
An alternative process similar to this transformation has been discovered by Prof. Myers (named as Myers-Saito cyclization)<sup>50</sup> for the first time in 1989 with enyne-allene as precursor followed the similar diradical intermediate to form cyclization (C2-C7) products. In contrast to the Bergman cyclization, this reaction exhibits a much lower activation barrier likely due to the higher reactivity of the allene moiety. Because of this higher reactivity, the reaction could perform at a lower temperature compared to the Bergman cyclization. Also, the alternative pathway (C2-C6) forms the indene derivative with the same enyne-allene precursor reported by Prof Schmittel<sup>51</sup> and Prof. Wang<sup>52</sup> independently in 1996 by the identical strategy of introducing steric hindrance moieties to the terminus of the substrates (**Scheme 23**).

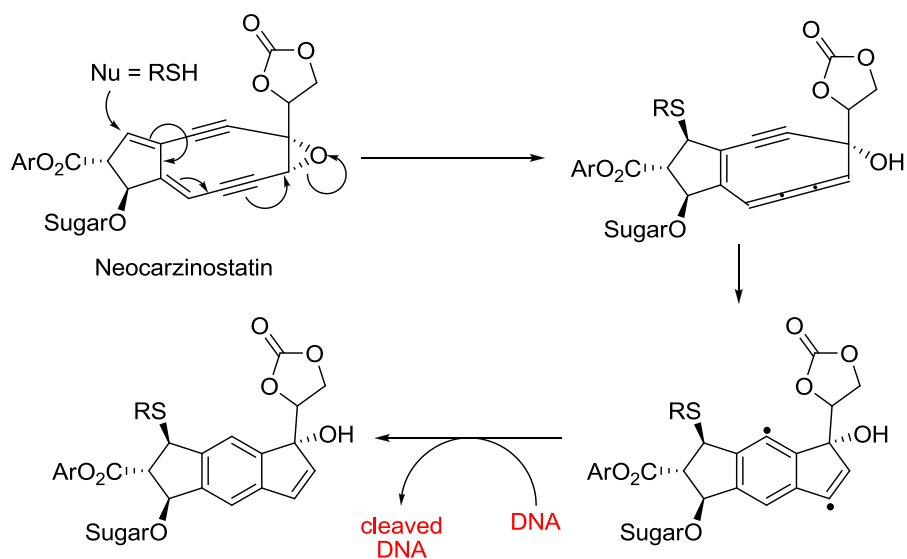
**Scheme 23.** Cyclization of enyne-allene derivative through diradical intermediate.



This type of reaction attracted attention due to the discovery of nature products containing endiynes moiety several years before.<sup>53</sup> Calicheamicin exhibits high cytotoxic activity due to its ability to form the reactive diradical species even under physiological conditions.<sup>54</sup> Here, the Bergman cyclization is activated by a triggering reaction. A distinguishing property of this diradical species is that it can effect a dual-strand cleavage of DNA. Neocarzinostatin<sup>55</sup> is a bacterial antibiotic that also shows similar reactivity toward dual-strand DNA (**Scheme 24**).

**Scheme 24.** Diradical intermediate generated in vivo and cleaved DNA.

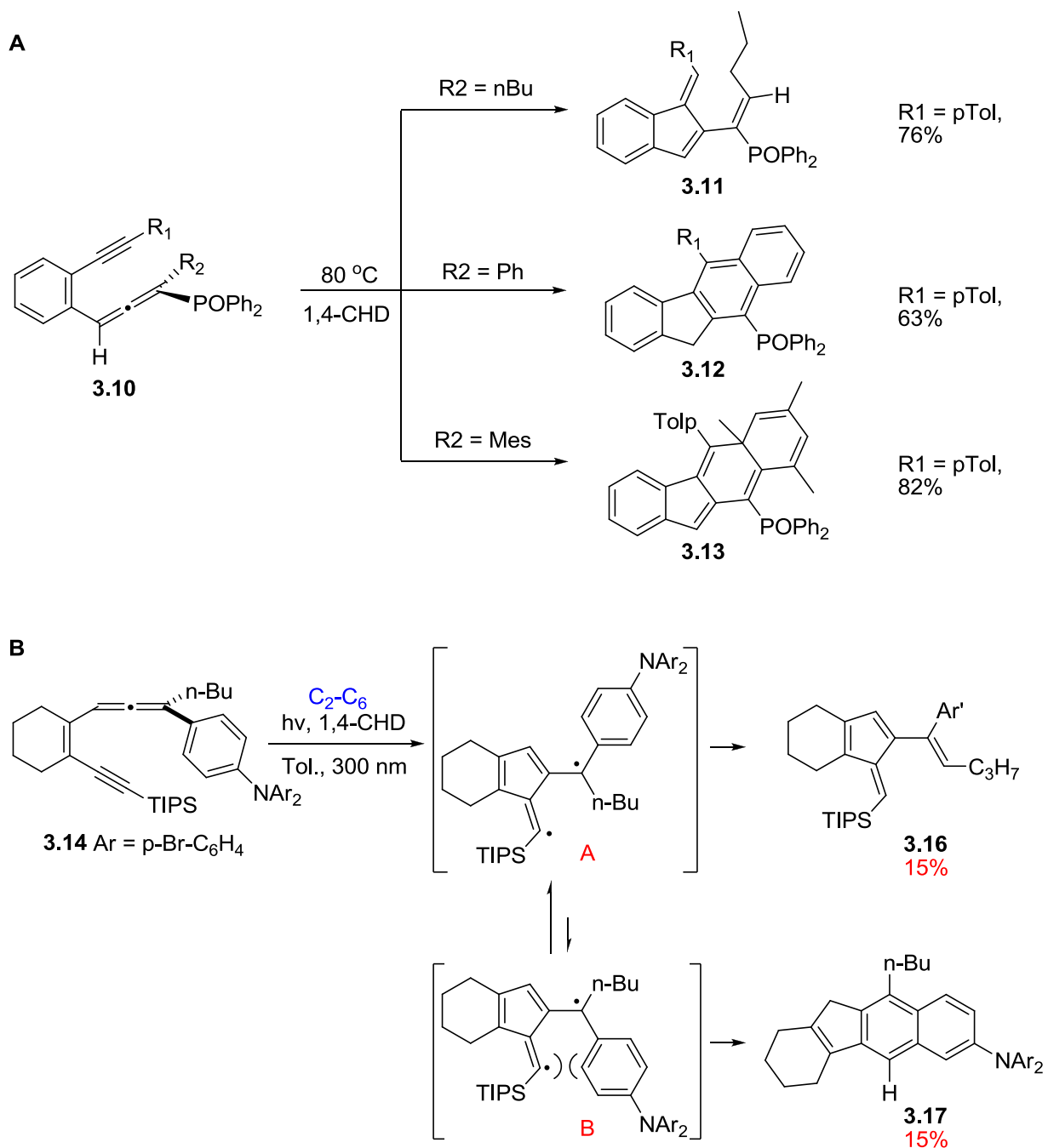




### 3.2 Result and discussion

All this reactivity promotes this diradical precursor as a very attractive anticancer drug candidate. Development of an appropriate molecule which could generate similar diradical intermediate under mild conditions became a hot topic in recent research. The results concerning diradical cyclization reactions are well documented.<sup>56</sup> More specifically, the Bergman/Pascal cyclization with endiynes as precursors usually required high temperature to overcome the activation barrier. Whereas, enyne-allene precursor (Myers-Saito/Schmittel cyclization) exhibits a lower activation barrier, which made it a good candidate for further investigation.<sup>57</sup> Usually reported temperature regarding enyne-allene system initiation, though much lower than endiynes activation temperature (around 200 °C), still need to be elevated (higher than human body temperature, e.g. 80 °C) (**Scheme 25A**).<sup>58</sup> Photo-activation also promoted the enyne-allene cyclization, however, only moderate yield was achieved (**Scheme 25B**).<sup>59</sup>

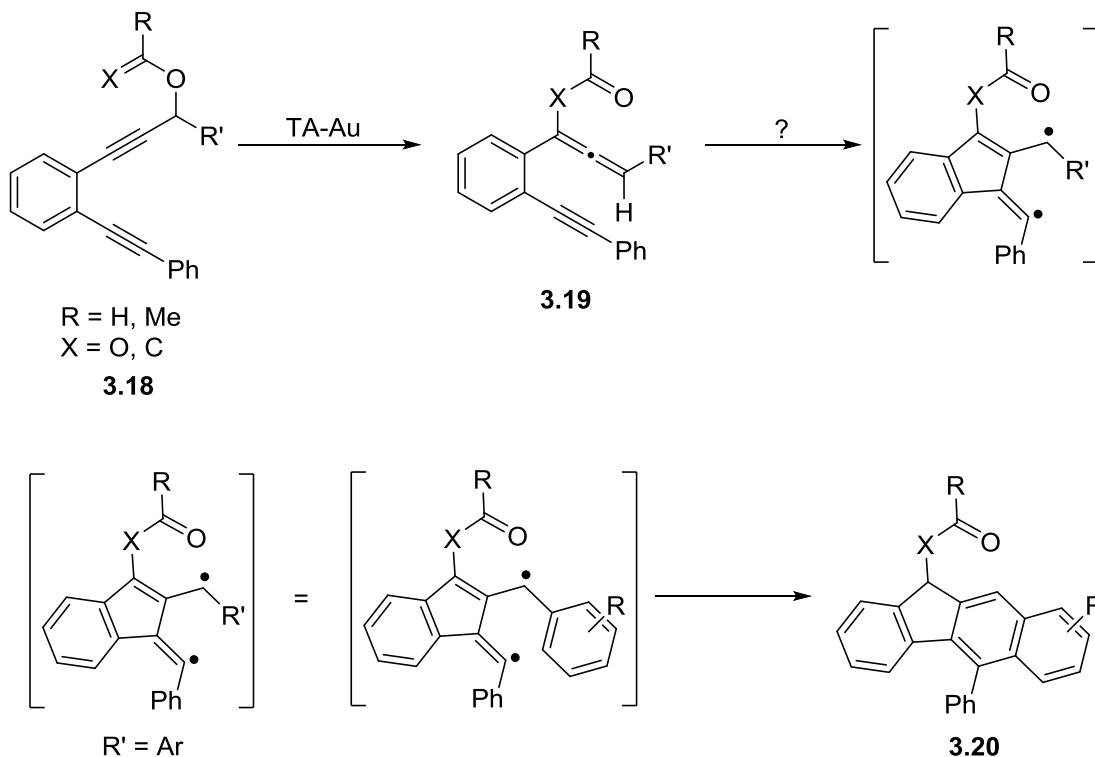
**Scheme 25.** Myers-Saito reaction under thermal and photo activation conditions.



To the best of our knowledge, no reported efficient conversion has been documented under mild conditions. Part of the reason is due to the lack of diversity of synthetic methodology towards enyne-allene synthesis, especially when the allene moiety was usually considered as

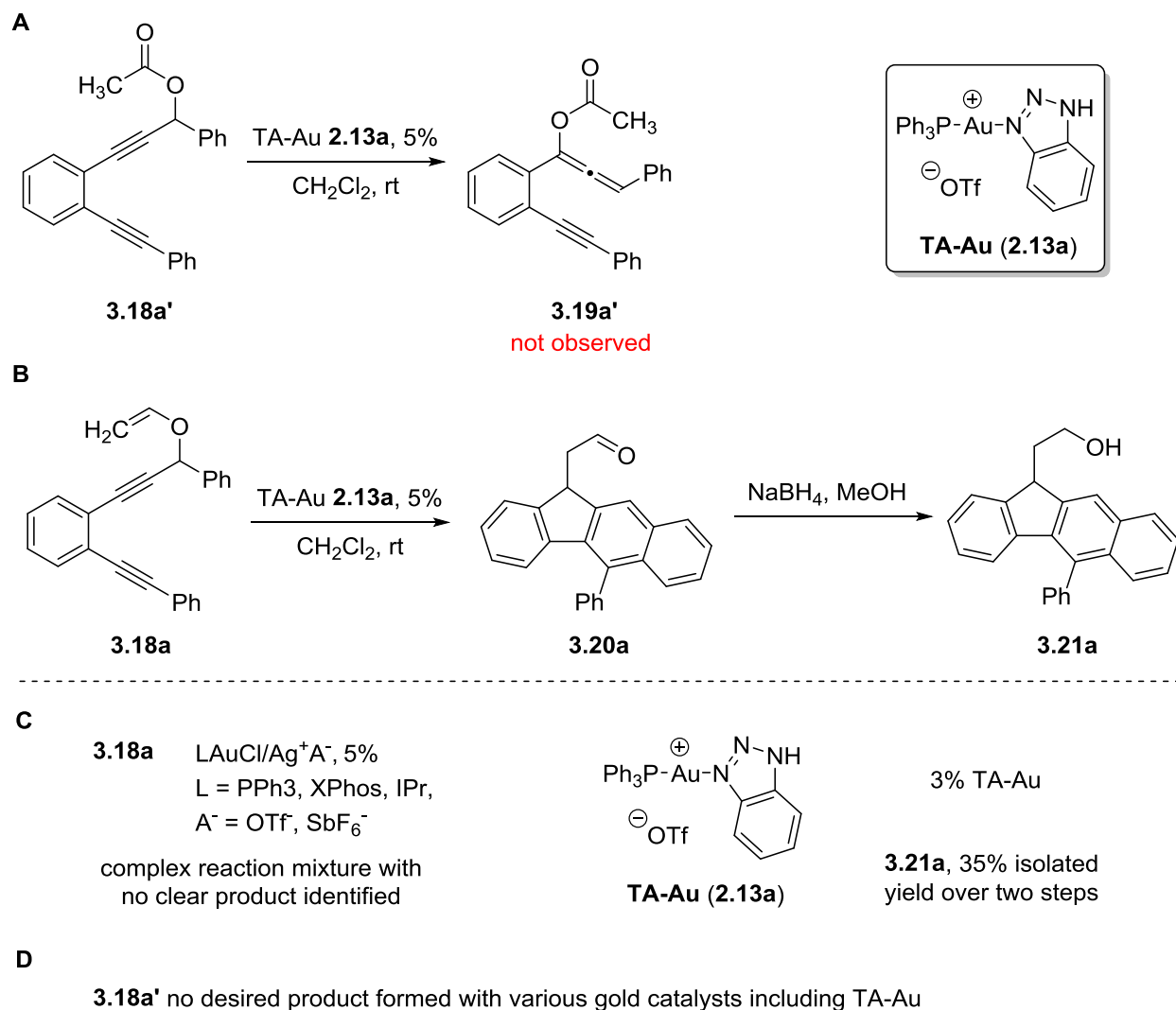
unstable.<sup>60</sup> Our TA-Au catalyzed 3,3-rearrangement chemoselectively gave allene derivatives as a final product which provides a route to synthesize the enyne-allene system efficiently, which will finally allow an easy access to the diradical species (**Scheme 26**).

**Scheme 26.** TA-Au catalyzed allene formation fused with enyne to access enyne-allene.



The key aspects of this work are: (a) the use of TA-Au catalysts offered excellent chemoselectivity for selective formation of allene product **3.19** with no further activation; (b) the ability to form the cyclization with enyne-allene precursor effectively; (c) optimal conditions the enyne-allene activation towards the diradical cyclization. To test our hypothesis, two types of starting materials were synthesized and treated with TA-Au complex **2.13a**, the reaction result was showed in **Scheme 27**.

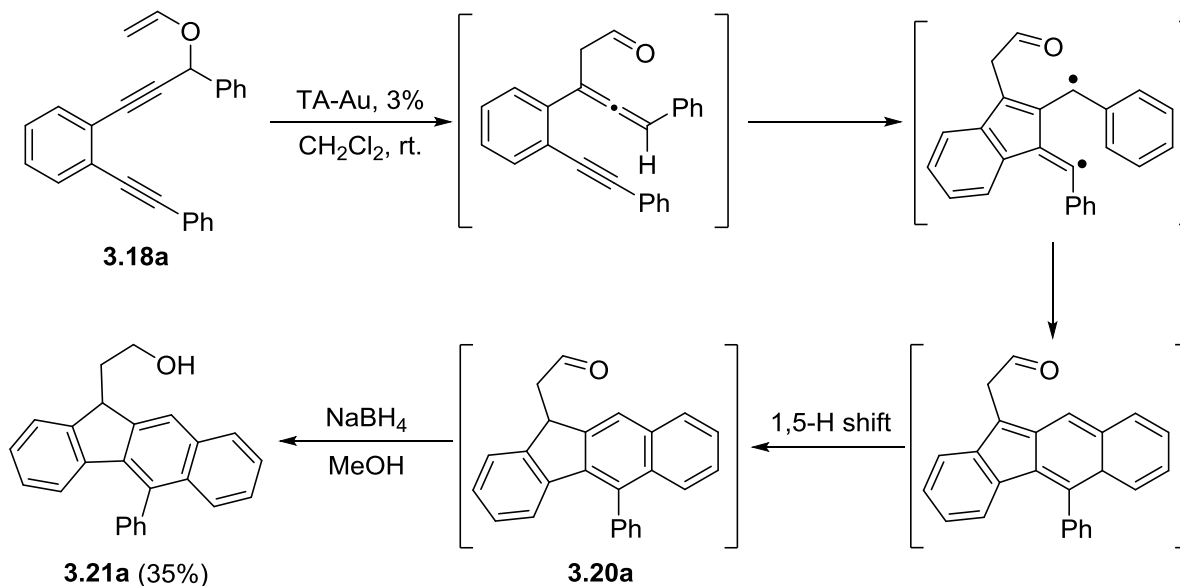
**Scheme 27.** Propargyl ester/vinyl ether substrates treated with TA-Au.



The propargyl ester **3.18a'** was treated with the TA-Au complex and no desired allene product was observed after 48 hours at room temperature. All the starting material was recovered with no conversion at all. To our delight, the propargyl vinyl ether was activated by the gold catalyst and gave the Schmittel cyclization product **3.20a** and after subsequent reduction for easy isolation, alcohol **3.21a** was separated with 35% isolated yields over two steps. This result was shocking, since the proposed allene product was not observed. Based on all the allene formation examples we have achieved before, we proposed that the enyne-allene derivative was

successfully formed by the TA-Au activation. After the formation of enyne-allene, the designed substrate exhibited high reactivity and performed the consequential Schmittel cyclization to form **3.20a**.

**Scheme 28.** Proposed reaction process for the TA-Au catalyzed cyclization.



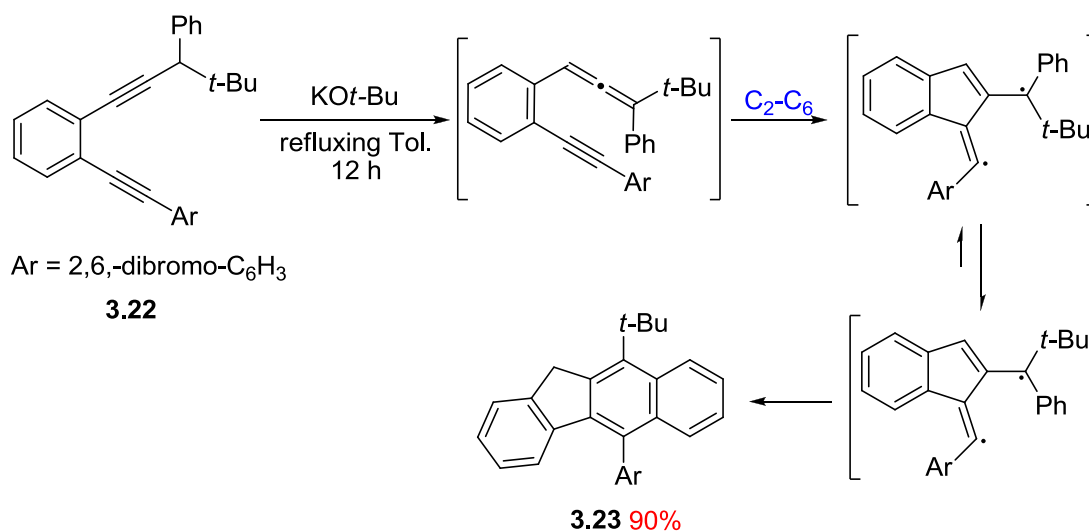
Notably, the reaction with TA-Au catalyst was ‘clean’ and the only cyclization product observed was **3.21a**. The major side competition process was the polymerization. No C2-C7 or other cyclization products were identified. The overall yield, though modest, was significantly higher than photoinitiation (**Scheme 25B**). The structure of **3.21a** was confirmed by X-ray diffraction of the corresponding tosyl derivatives **3.24a** as shown in **Figure 20**.

The same type of reaction was reported by Prof. Wang and co-workers with very similar substrate and excellent yield (90%).<sup>61</sup> Besides the efficient rearrangement forming enyne-allene intermediate, the steric hindrance group (such as *t*Bu) was also proposed promoting the aromatic quenching process by pushing the aromatic substituent toward the  $\text{sp}^2$  radical (**Scheme 29**).

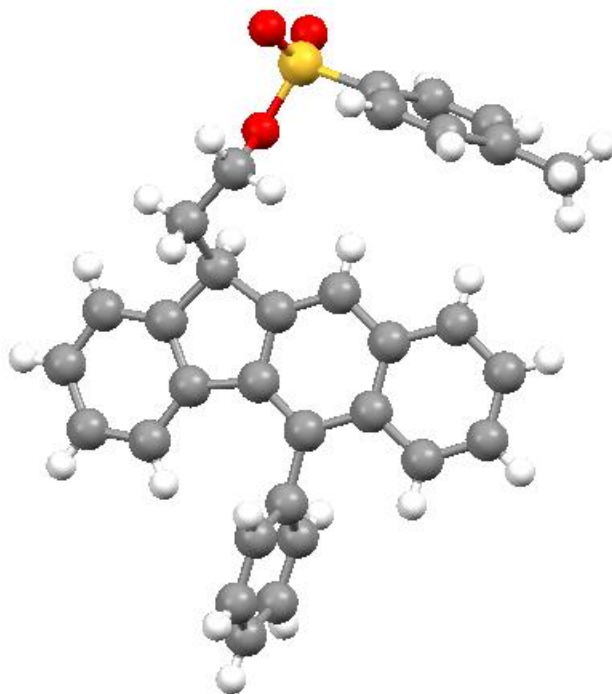


Combining both advances, the reaction was promoted to a level of efficiency that never had been achieved before. However, the *in situ* formation of enyne-allene required harsh conditions (treated with strong base and high temperature).

**Scheme 29.** Schmittel cyclization reported by Prof. Wang with excellent efficiency.

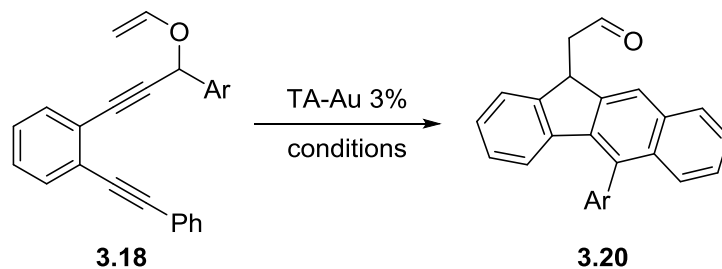


Overall, this result supported our hypothesis that (A) enyne-allene cyclization was energetically favored and could occur at room temperature, and (B) TA-Au catalyst could selectively activate the propargyl ether, generating the allene intermediates that allowed the subsequent aromatization. To the best of our knowledge, this is the first example of an enyne-allene C2-C6 cyclization at room temperature without the aid from bulky substituents.



**Figure 20.** Perspective view of the structure of  $C_{32}H_{26}SO_3$  (compound **3.24a**). The ball and stick drawing. CCDC number: 864331

Screening of solvents revealed dichloromethane as the optimal solvent. Considering that polymerization was the major side reaction, different concentrations and reaction temperatures were evaluated (**Table 4**). The TA-Au catalyst lost reactivity at  $-10\text{ }^{\circ}\text{C}$ . Raising the reaction temperature to  $0\text{ }^{\circ}\text{C}$  improved the overall reaction yield to 48% (**Table 4**, Entry 9). Whereas, the electron deficient substituent such as Br and  $\text{NO}_2$  provides better yield likely due to the stability of diradical species.

**Table 4.** Screening of the reaction condition.<sup>a</sup>

Entry <sup>b</sup>	Solvent	Conc. (M)	T (°C)	Conv (%)	Yield(%) <sup>c</sup>
1	CH <sub>2</sub> Cl <sub>2</sub>	0.075	-78	0 (4 h)	N.D.
2	CH <sub>2</sub> Cl <sub>2</sub>	0.075	-41	0 (4 h)	N.D.
3	CH <sub>2</sub> Cl <sub>2</sub>	0.075	-10	0 (4 h)	N.D.
4	CH <sub>2</sub> Cl <sub>2</sub>	0.075	0	>99 (6 h)	44
5	CH <sub>2</sub> Cl <sub>2</sub>	0.075	rt	>99 (15min)	35
6	CH <sub>2</sub> Cl <sub>2</sub>	0.0025	0	>99 (48 h)	11
7	CH <sub>2</sub> Cl <sub>2</sub>	0.005	0	>99 (48 h)	12
8	CH <sub>2</sub> Cl <sub>2</sub>	0.01	0	>99 (48 h)	20
9	CH <sub>2</sub> Cl <sub>2</sub>	0.1	0	>99 (48 h)	48
10	CH <sub>2</sub> Cl <sub>2</sub>	0.1	0	>99 (48 h)	65
11	MeCN	0.1	0	>99 (48 h)	47
12	MeNO <sub>2</sub>	0.1	0	>99 (48 h)	26
13	THF	0.1	0	>99 (48 h)	21
14	acetone	0.1	0	>99 (48 h)	32
15	MeOH	0.1	0	>99 (48 h)	15
16	toluene	0.1	0	>99 (48 h)	41

17	DMF	0.1	0	>99 (48 h)	0
18	DMSO	0.1	0	>99 (48 h)	0

<sup>a</sup> General reaction condition: **3.18a** (0.2 mmol), catalyst (3 mol %) in solvent, the reactions were monitored by TLC, 0 °C to rt. <sup>b</sup> entry 1-10 was tested with **3.18a**, entry 11-19 was tested with **3.18c**. <sup>c</sup> Conversion and yields were determined by NMR with 1,3,5-trimethoxybenzene as internal standard.

Some representative aromatic substituents at the allene termini were prepared to evaluate the reaction substrate scope. The results are summarized in **Figure 21**.

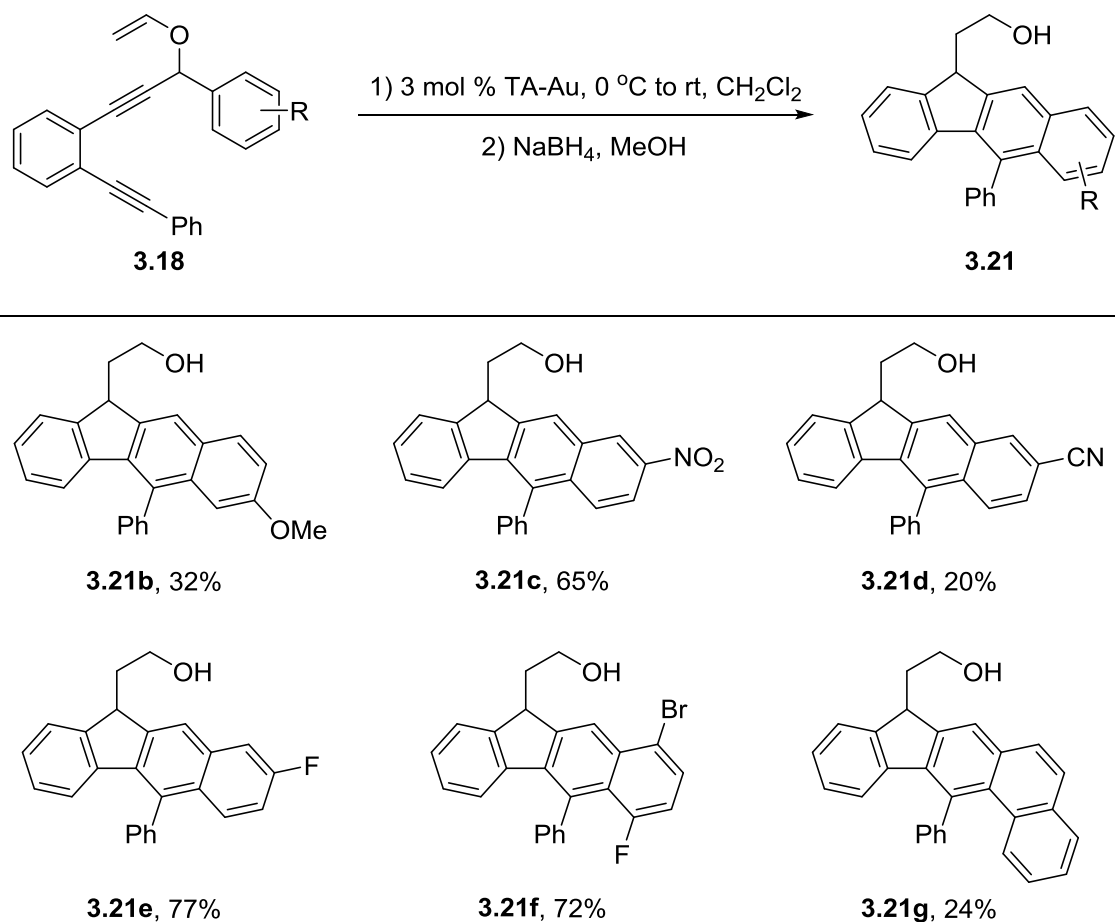
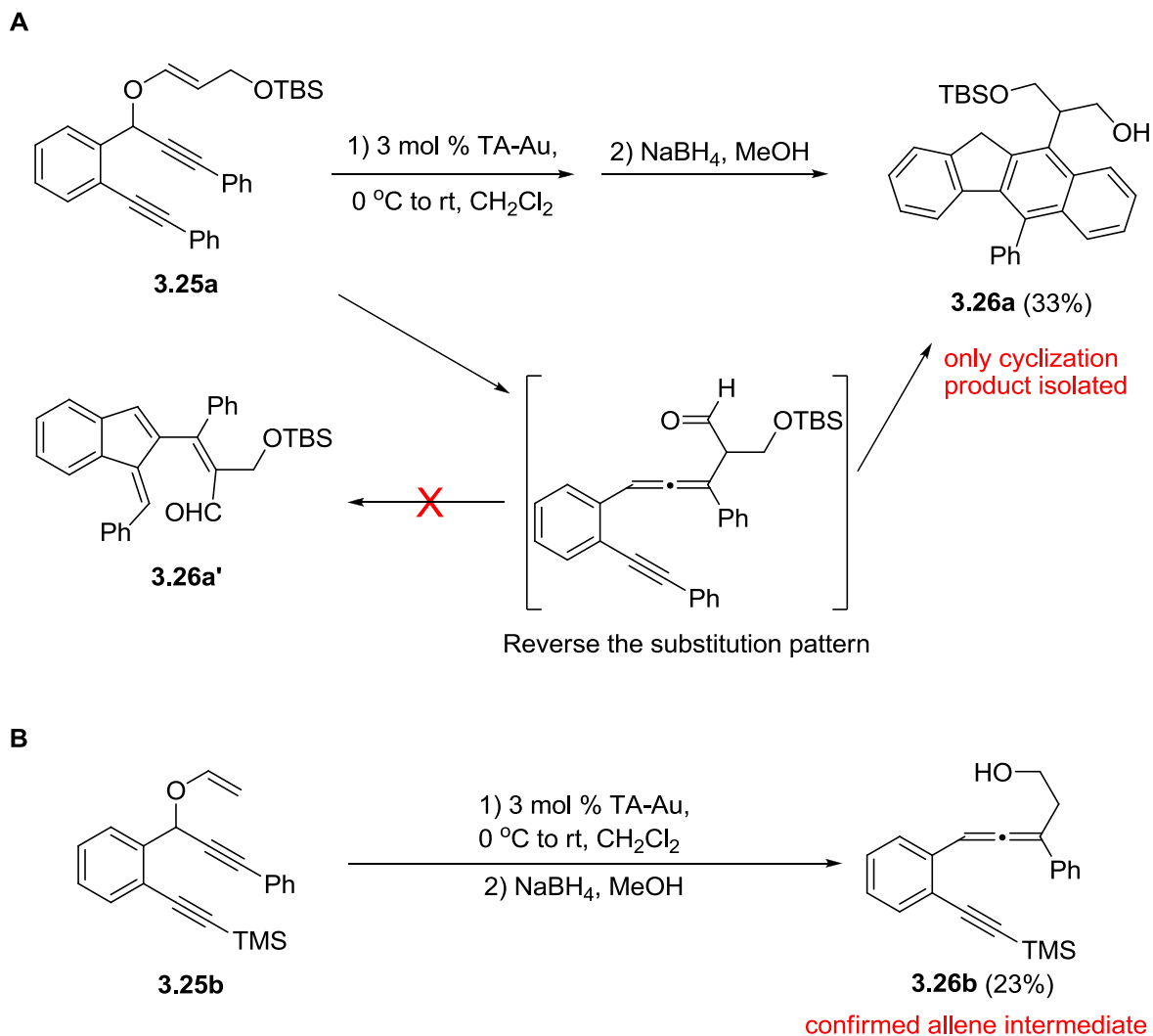


**Figure 21.** Substrate scope of TA-Au catalyzed Schmitt cyclization.

As illustrated in **Figure 21**, the C2-C6 cyclization could occur for both electron donating and electron withdrawing substituents on the aromatic rings. Electron withdrawing groups gave

significantly improved yields by reducing the undesired diradical polymerization.<sup>62</sup> Conjugation did not show significant influence on the cyclization, which was consistent with the proposed mechanism that involved a highly reactive diradical intermediate. To further evaluate the reaction mechanism, propargyl vinyl ether with “reversed” substitution pattern (**3.25a**) and TMS-substituted alkyne (**3.25b**) were prepared and reacted with TA-Au catalyst. As showed in **Scheme 30A**, propargyl ether **3.25a** 3,3-rearrangement would produce the trisubstituted allene. Under the photocyclization condition shown in **Scheme 25B**, the diradical intermediates proceeded through two different reaction paths, which should lead to the formation of **3.26a** and **3.26a'**. Interestingly, the TA-Au catalyzed conditions gave exclusively **3.26a** as the cyclization product. This might be explained by the mild reaction conditions that favored the aromatic cyclization instead of the elimination (formation of **3.26a'**), which highlighted the significantly improved selectivity of this method over thermal and photo conditions. Switching the alkyne termini substituents from Ph to TMS helped to successfully isolate the proposed allene intermediate **3.26b** (**Scheme 30B**, decreasing cyclization reaction rates), which provided another piece of solid evidence for the proposed mechanism and the unique reactivity of TA-Au (activate alkyne over allene).

### Scheme 30. Mechanism investigations.



### 3.3 Conclusion.

In conclusion, reported herein is a new catalytic version of the Schmittel cyclization. The TA-Au catalyst offered impressive chemoselectivity, activating the specific alkynes only, which allowed the sequential cyclization to occur at much milder conditions. Both the allene intermediate and the final products were unambiguously confirmed. As a result, an effective new

strategy was uncovered under much milder conditions and enhanced substrate scope (substrates that could not be achieved with previously reported thermal or photo conditions). As consequence, this new method opens the possibility for mechanistic investigation and new diradical based drug discovery by this interesting enyne-allene cyclization process.

### **3.4 Contribution.**

Qiaoyi Wang was the researcher who had first investigated the reaction condition and mechanism investigation. Together, Qiaoyi Wang and Siddhita Aparaj were responsible for substrate scope, NMR spectrum, and manuscript completion for successful submission to Organic Letters. The detailed X-ray crystallographic data analysis of compound **3.24a** was done by Prof. Jeffrey L. Petersen, C. Eugene Bennett Department of Chemistry, West Virginia University.

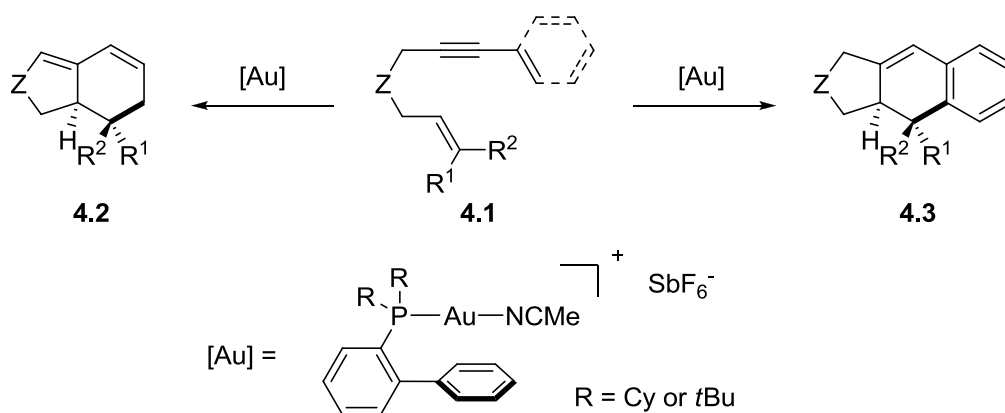
## Chapter Four: 1,2,3-triazoles work as X-factor to promote gold(I)

### complex in challenging chemical transformations - part III

#### 4.1 Introduction

'X-factor' assisted improvement of the gold(I) stability has been reported in several examples during the last decade. Along with the  $\text{Tf}_2\text{N}^-$  as special counter ion (introduced in Chapter 2), MeCN exhibiting coordinating ability toward gold(I) complexes has been reported by Prof. Echavarren and co-workers as a neutral 'X-factor' in crystalline gold complex based on the Buchwald ligand in the year 2005 (Scheme 31).<sup>63</sup>

**Scheme 31.** MeCN as 'X-Factor' in gold(I) catalysis.



1,2,3-triazole which plays the same role like acetonitrile in gold(I) complexes as a neutral coordinating moiety, has been reported by Prof. Shi's group in 2009.<sup>64</sup> This strategy was applied in a hydroamination reaction of internal alkyne which usually requires harsh conditions such as an elevated reaction temperature. Both neutral and ionic triazole gold(I) complexes were tested





complex **2.13a** exhibited significantly improved thermal stability at the raised temperature which was required in this reaction and reached an improved yield (**Figure 22, f**). When 5% of free benzotriazole was presented in the reaction port, a slower reaction rate was observed, which suggested a competitive ligand exchange process between triazole and the reaction substrate **4.4** (**Figure 22, e**). The reaction was further promoted by the *in situ* generated activating gold(I) species with **2.11** by the addition of  $\text{H}_3\text{PO}_4\cdot 12\text{WO}_3$ , reaching a yield of 91% with only 1% catalyst loading (**Figure 22, g**).

This result was significantly encouraging in that the series of TA-Au complexes stabilized the gold(I) cation to a higher level which has not been previously reported. And with this innovative catalyst, our group were focused on exploring more challenging chemical transformations. The following case exhibited one example.

The C=C moiety is one of the most common building block in organic molecules, and the aromatic groups accumulated by multiple C=C bonds play extremely important role in the science of chemistry. This important moiety could be substituted by two other atoms (N and B) to give the isoteric and isoelectronic structure of B-N. This isoelectronic relationship between CC and BN bond could be extended to all the other hybridisation stages. Though the isoelectronic bonds look similar, there are differences between these two structures. The most significant one is that, the BN unit is polarized whereas the CC unit is non-polar. Use C=C/B-N as an example, the polarity of BN unit was most contributed by the unequally distributed  $\pi$  electrons (or the p electrons on the N atom overlapping with the empty orbital on the B atom) other than the  $\sigma$  bond (**Figure 23**).<sup>65</sup>

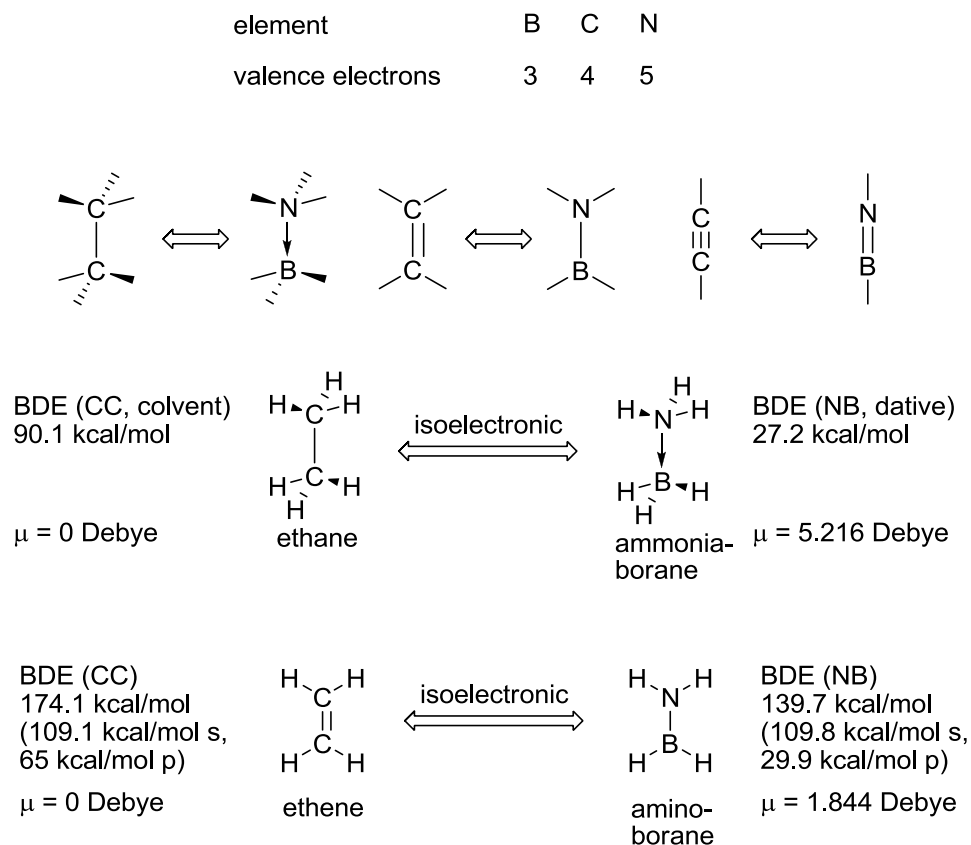


**Figure 23.** Isoelectronic relationship between CC and BN, and molecular consequences of BN/CC isosterism.

This interesting property initiated people's interest to substitute the CC unit with BN in the molecules with the expectation of different properties or reactivity that has been introduced by the BN polar bond. Efforts have been devoted to this area nearly a century ago (1926) since Prof. Stock and Pohland first reported the synthesis of borazine which was usually known as inorganic benzene.<sup>66</sup> The word 'inorganic' precisely described the borazine property. The utility of this heterocyclic structure has been involved in serving as a precursor for BN based ceramic material synthesis<sup>67</sup> and chemical hydrogen storage material<sup>68</sup> more recently. The properties of both benzene and borazine have been thoroughly investigated since these two molecules have been

known for a relatively long time. However, another type of the isostructural compound corresponding to them has far eluded characterization, 1,2-dihydro-1,2-azaborine.<sup>69</sup>

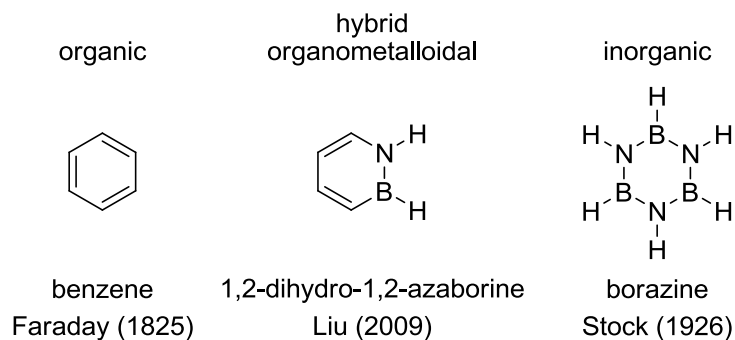
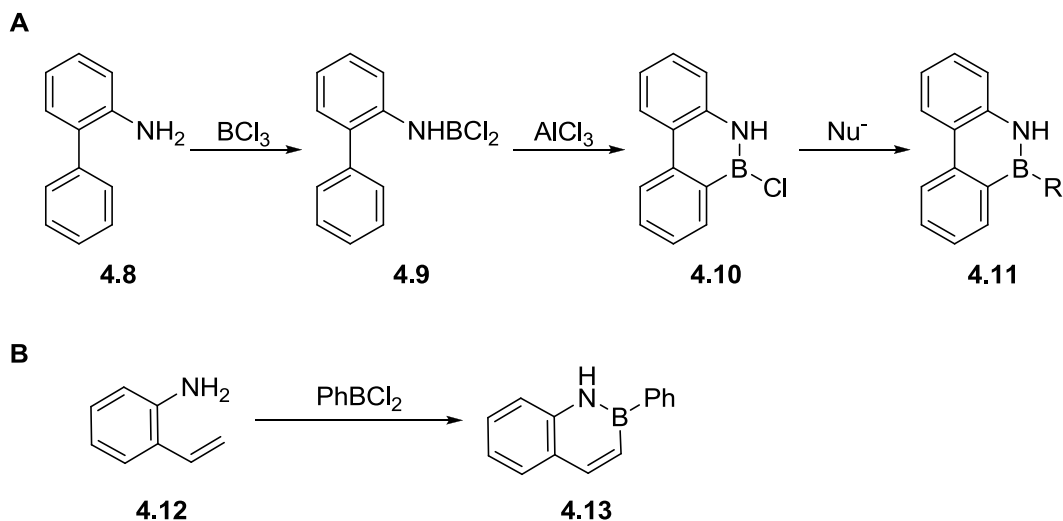


**Figure 24.** Illustration of benzene, 1,2-dihydro-1,2-azaborine, and borazine.

One of the major reasons for a lack of investigation of this 1,2-dihydro-1,2-azaborine is the lack of efficient synthetic method for the preparation. The benzene has been discovered by Faraday almost two hundred years ago,<sup>70</sup> and one century later followed the borazine.<sup>71</sup> However, the semi-substituted derivative 1,2-dihydro-1,2-azaborine has been very recently reported by Prof. Liu (in 2009).<sup>72</sup> When comparing with the fast growing synthetic chemistry, this relatively late improvement explains the challenge in synthetic design and all other practical issue such as product stability.

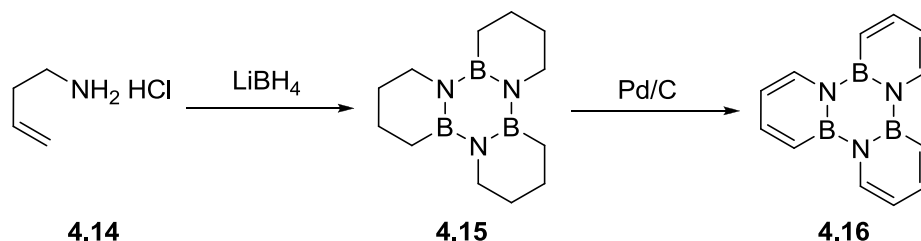
Similar substrate synthesis can be traced back to late 1950's by Prof. Dewar and co-workers. Their first attempt to synthesis the 9,10-azaboraphenanthrene<sup>73</sup> and 2-phenyl-1,2-azaboranaphthalene<sup>74</sup> based on the Friedel–Crafts cyclization was illustrated in **Scheme 32**.

**Scheme 32.** Early stage synthetic route of 1,2-azaborines.



Encouraged by these results, the same group has devoted their efforts to synthesize the parent 1,2-dihydro-1,2-azaborinen through the hydroboration–oxidation strategy. Instead of the desired product, a trimerized product of BN-triphenylene was obtained. After the failed attempt to isolate the parent 1,2-dihydro-1,2-azaborinen,<sup>75</sup> Dewar's group conclude that '*borazarene [1,2-dihydro-1,2-azaborine] therefore seems to be a very reactive and chemically unstable system, prone to polymerization and other reactions...*'

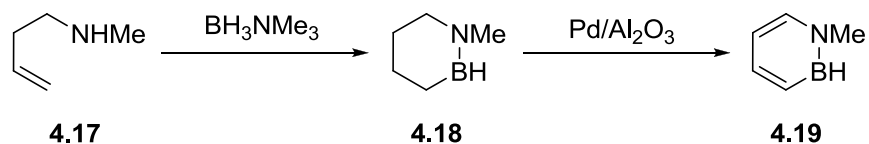
**Scheme 33.** Attempt to synthesize parent 1,2-dihydro-1,2-azaborinen.



Other pioneer work efforts toward the synthesis of 1,2-azaborine using secondary butenyl amine has been reported by Prof. Goubeau and co-workers (1972) through a cyclohexene

analogue **4.18**.<sup>76</sup> The following dehydrogenation with Pd/Al<sub>2</sub>O<sub>3</sub> provided the BH substrate **4.19** which was later characterized by mass spectrometry.<sup>77</sup>

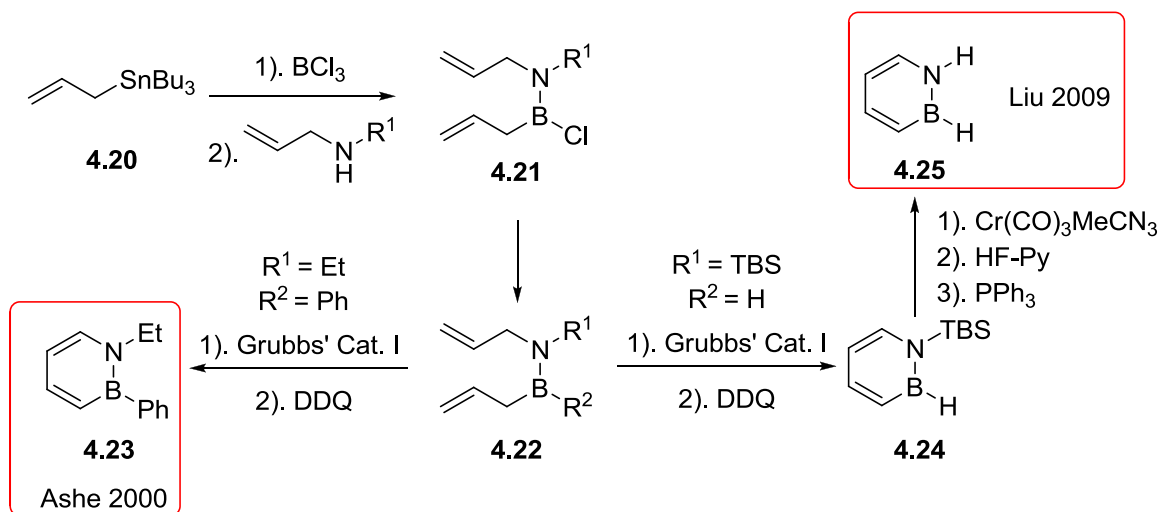
**Scheme 34.** BH 1,2-azaborine synthesis reported by Prof. Goubeau.



These innovations along with other efforts such as desulfurization of BN-benzothiophenes with Raney nickel reported by Dewar and Gronowitz independently in 1960's hinted the potential arene mimics of the azaborine containing compounds.<sup>78</sup> However, the early developments have been limited by the synthetic methodology and characterization technologies during that period.

Modern synthetic methods and instrumentation have enabled a new generation of chemists to pick up where pioneering researchers left off, taking azaborine chemistry into uncharted and exciting territory. Prof. Ashe's group reached a breakthrough in the year 2000 based on the ring-closing metathesis chemistry under mild conditions. Through this strategy, the 1,2-azaborine **4.23** was achieved on a gram scale.<sup>79</sup> In 2009, Prof. Liu's group reported a work following the same strategy by reducing the B-Cl bond with superhydride LiHBET<sub>3</sub>, a similar BH substrate as reported before has been isolated.<sup>80</sup> The TBS as a protecting group on N atom could be removed after a Cr  $\pi$ -complex formation (protection) with the treatment of HF-Py to give the parent 1,2-dihydro-1,2-azaborinen **4.25** for the first time (**Scheme 35**).

**Scheme 35.** 1,2-azaborine synthesis based on ring-closing metathesis strategy.



Similar strategy enabled Prof. Liu's group to synthesize a series of BN unit substituted structures with full characterization in the following years (**Figure 25**). The investigation of more applicable field as hydrogen storage materials is also reported by the same group.<sup>81</sup>

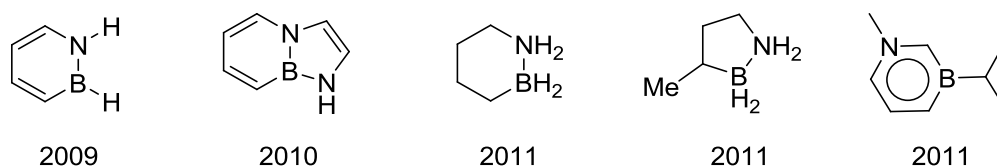
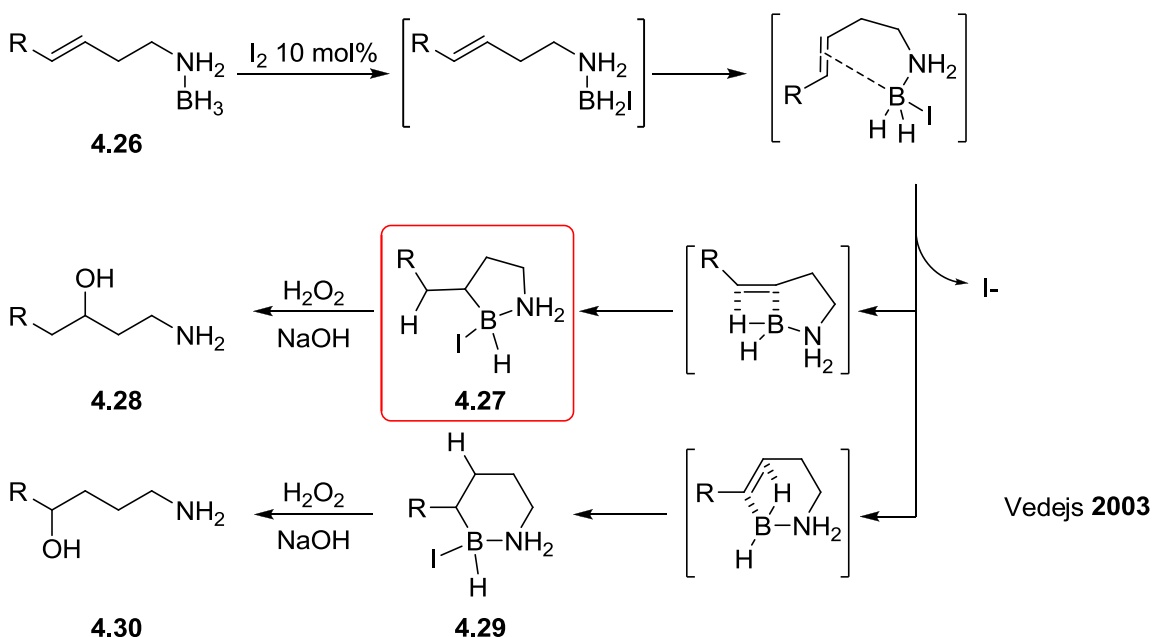


**Figure 25.** Structures reported by Liu's group with BN unit substituted CC unit.

Among all the reported methods, one with high efficiency to access BN heterocyclic structure is the amine directed hydroboration of CC multiple bond reported by Goubeau and Dewar.<sup>82</sup> Although Dewar failed on the primary amine substrate, this strategy still exhibits a very outstanding advantage: short synthetic route (only two steps). In contrast, Prof. Ashe and Liu's methods involved multi-step synthesis (which will decrease the overall product yield) and unstable intermediate such as aminoborane **4.21**, required air and moisture free reaction

condition. The similar hydroboration strategy has been reported by Prof. Vedejs and co-workers in 2003 (**Scheme 36**).<sup>83</sup> Their original focus is the amine directed hydroboration to reach a regioselective product **4.28** over the undesired product **4.30** from internal alkene precursors. The catalytic amount iodine introduced in the reaction mixture functionalized as a promoter which oxidized the less reactive amine-borane **4.26** to a more reactive intermediate with B-I bond presented. And the B-I bond in compound **4.27** was proposed to oxidize other unactivated **4.26** to achieve full conversion. It is worth noting that the BN including intermediate **4.27** was successfully isolated in two cases among the substrates with moderate yields (<50% for both).

**Scheme 36.** Regioselective hydroboration reported by Vedejs.



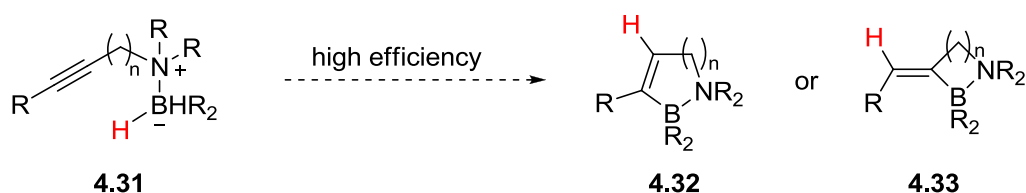
The moderate yield observed for this result compared to the excellent yields of the final products **4.28**, suggested that, the BN cyclic structure is less stable. This is probably due to the less stable  $sp^3$  hybridized C-B bond. If the hybridization could be switched to  $sp^2$  (vinyl borane as product), the stability of these types of compounds could be improved significantly.<sup>84</sup>



Therefore, our group initiated the investigation of alkyne hydroboration reaction to form the BN heterocyclic structure more effectively.

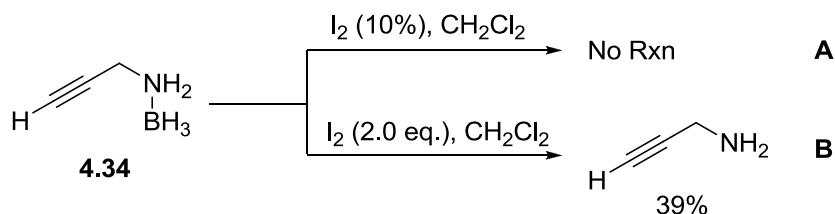
## 4.2 Result and discussion

**Scheme 37.** Intramolecular hydroboration of alkyne: efficient but no precedence.



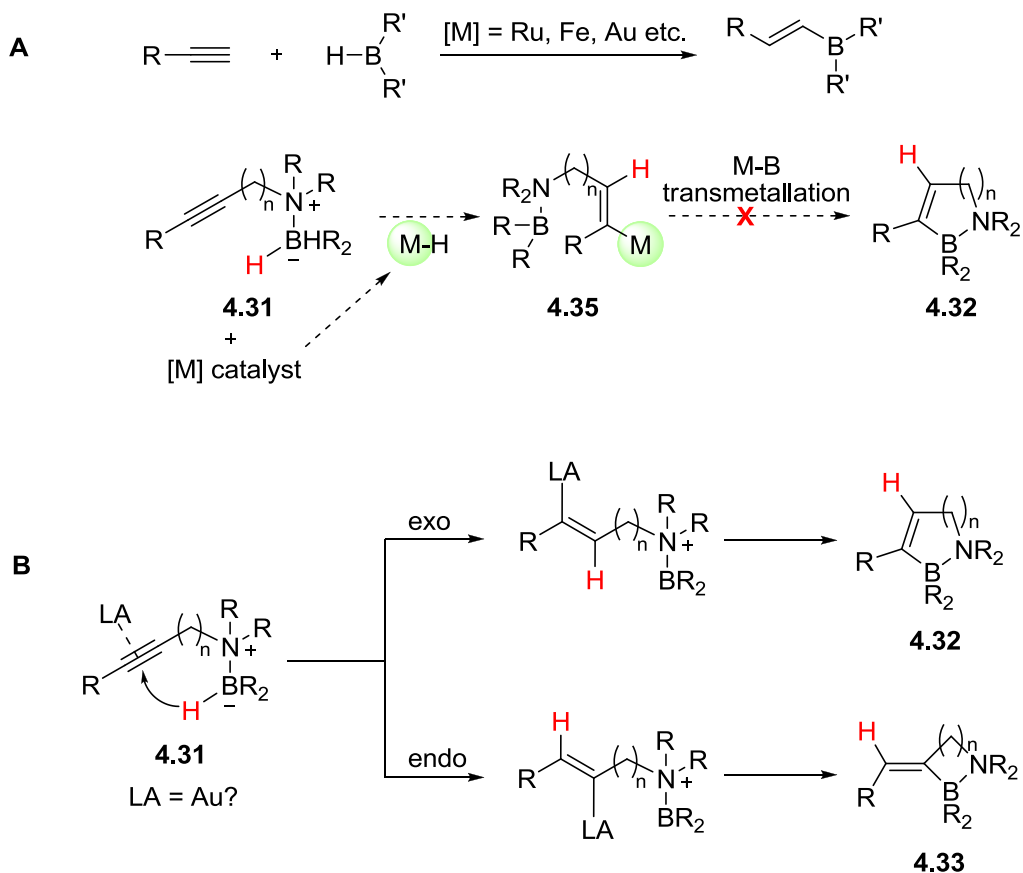
As indicated in **Scheme 37**, the amine directed alkyne hydroboration could provide an efficient approach to cyclic amine-borane compounds through either endo or exo transition state. The reaction has not previously been reported so far, likely due to the less reactive CC triple bond and the reduced reactivity of amine-borane. The iodine activation strategy adopted by Vedejs successfully solved the amine-borane reactivity issue.<sup>85</sup> Therefore, the same strategy has been applied to the propargyl amine-borane complex to evaluate the performance of this reaction pattern on alkyne.

**Scheme 38.** Iodine activated alkyne hydroboration reaction.



The catalytic amount of iodine could not promote the substrate **4.34** under identical reaction conditions as reported in alkene hydroboration by Vedejs (**Scheme 38A**). Meanwhile, the excess amount of iodine caused a serious decomposition of **4.34** and gave a complex mixture with 39% propargyl amine recovered. Although I<sup>-</sup> served as a good leaving group, the very reluctant CC triple bond still had not been activated yet. Two alternative strategies intuitively came out are: 1) transition metal catalyzed hydroboration through more active M-H intermediate; 2)  $\pi$ -acid activation of CC triple bond induced hydroboration. These two activation models are indicated in **Scheme 39**.

**Scheme 39.** Possible transition metal catalyzed intramolecular alkyne hydroboration reaction patterns.



These two strategies presumably will help to overcome the major challenges associated with this transformation: 1) the low reactivity of alkyne; 2) the possibility of double addition rather than desired mono-hydroboration.

Although transition metal catalyzed hydroboration suffered from catalyst decomposition, successful examples have been reported.<sup>86</sup> To avoid the undesired catalyst decomposition (caused by boron hydride reduction), almost all of the reported cases used metal cations or nanoparticles that were able to form a metal hydride (M-H) bond. Meanwhile, a close inspection of the mechanism revealed that the very available M-H promoted hydride addition is not suitable for the N-B bond cyclization product formation (through M-B transmetallation, **Scheme 39A**). The *cis*-addition of alkyne led to the formation of trans-isomer based on the structure confirmation and resulted to the boron atom and metal locating on different sides of the C=C. The proposed transmetallation process will then be blocked and could not form the desired product efficiently. Thus, transition metal catalyzed alkyne hydroboration for the synthesis of cyclic amine borane has not been achieved in the past.

Metal hydride strategy has been ruled out, the only hypothesis left is the Lewis acid activated alkyne hydroboration. Based on this activation mode, we hypothesized that a cyclic amine borane could be synthesized through the intramolecular alkyne hydroboration as showed in **Scheme 39B**. An appropriate acidic transition metal catalyst that tolerates boron hydride substrates and an amine borane precursor could be identified. Two practical concerns are: 1) the stability of active metal catalysts to survive the reductive conditions and 2) the feasibility of the proposed M-B transmetallation. The efficient  $\pi$ -acid catalysts for CC triple bond activation has been identified to be gold and platinum so far.

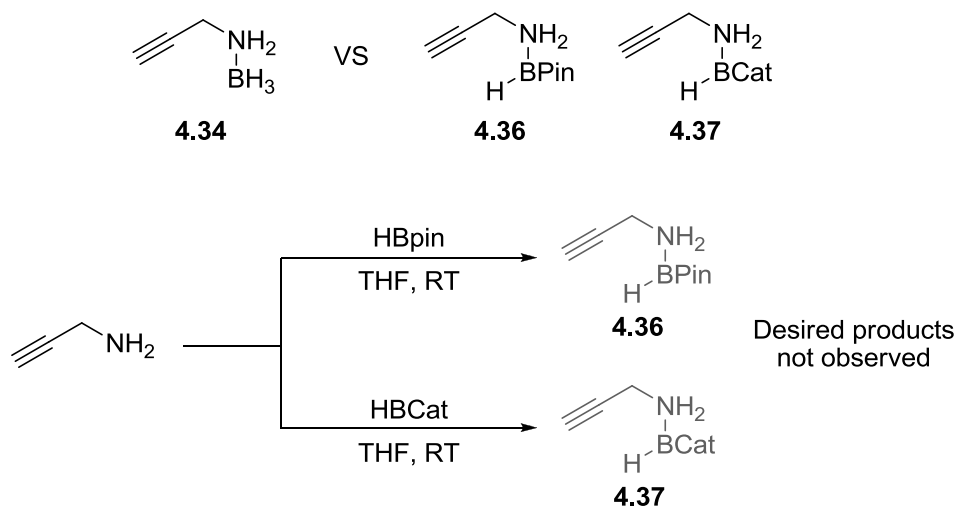


4	P(OMe) <sub>3</sub> AuCl/AgOTf	1 hr or 24 hr	<5	n.d.
5	[PPh <sub>3</sub> Au] <sup>+</sup> Tf <sub>2</sub> N <sup>-</sup>	1 hr or 24 hr	<5	n.d.
6	[XPhosAu] <sup>+</sup> Tf <sub>2</sub> N <sup>-</sup>	1 hr or 24 hr	<5	n.d.
7	[PPh <sub>3</sub> Au-TA] <sup>+</sup> TfO <sup>-</sup>	1 hr or 24 hr	<5	n.d.
8	[PPh <sub>3</sub> Au-TA] <sup>+</sup> F <sub>6</sub> Sb <sup>-</sup>	1 hr or 24 hr	<5	n.d.
9	[IPrAu-TA] <sup>+</sup> TfO <sup>-</sup>	1 hr or 24 hr	<5	n.d.
10	[IPrAu-TA] <sup>+</sup> F <sub>6</sub> Sb <sup>-</sup>	1 hr or 24 hr	<5	n.d.
11	[XPhosAu-TA] <sup>+</sup> TfO <sup>-</sup>	1 hr or 24 hr	<5	n.d.
12	[XPhosAu-TA] <sup>+</sup> F <sub>6</sub> Sb <sup>-</sup>	1 hr or 24 hr	<5	n.d.

General reaction condition: **4.34** (0.2 mmol), catalyst (5 mol %) in solvent (1 ml), the reactions were monitored by TLC, 0 °C to RT. Conversion and yields were determined by NMR with 1,3,5-trimethoxybenzene as the internal standard.

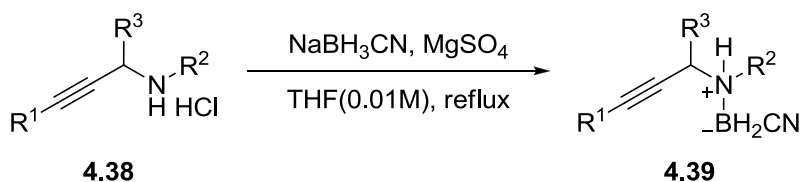
This problem may be a consequence of boron hydride reduction. To overcome this problem, we developed the “less reactive” amine borane that would slow down the decomposition of our gold catalysts. The pinacolborane and catecholborane were treated with propargyl amine to form the desired product with B-O bond substituent to lower the B-H reductivity. However, these two boron sources did not form the amine borane complexes very efficiently.

**Scheme 40.** Attempt to synthesize amine borane with lower B-H reductivity.



After extensive screening of various substrates, the cyano-substituted amine borane **4.38** was prepared by the general synthetic route shown in **Scheme 41**.

**Scheme 41.** Conditions for synthesis of amine boranecarbonitrile **4.39**.



Propargyl amine hydrochloride salt **4.38**, was treated with  $\text{NaBH}_3\text{CN}$  and  $\text{MgSO}_4$  in THF. The reaction mixture was maintained at reflux and provide the desired product **4.39** with high efficiency (generally yield > 85%), with both primary and secondary amine substrates being tolerated. A Series of **4.39** with different substrates was prepared and summarized in **Figure 26**.

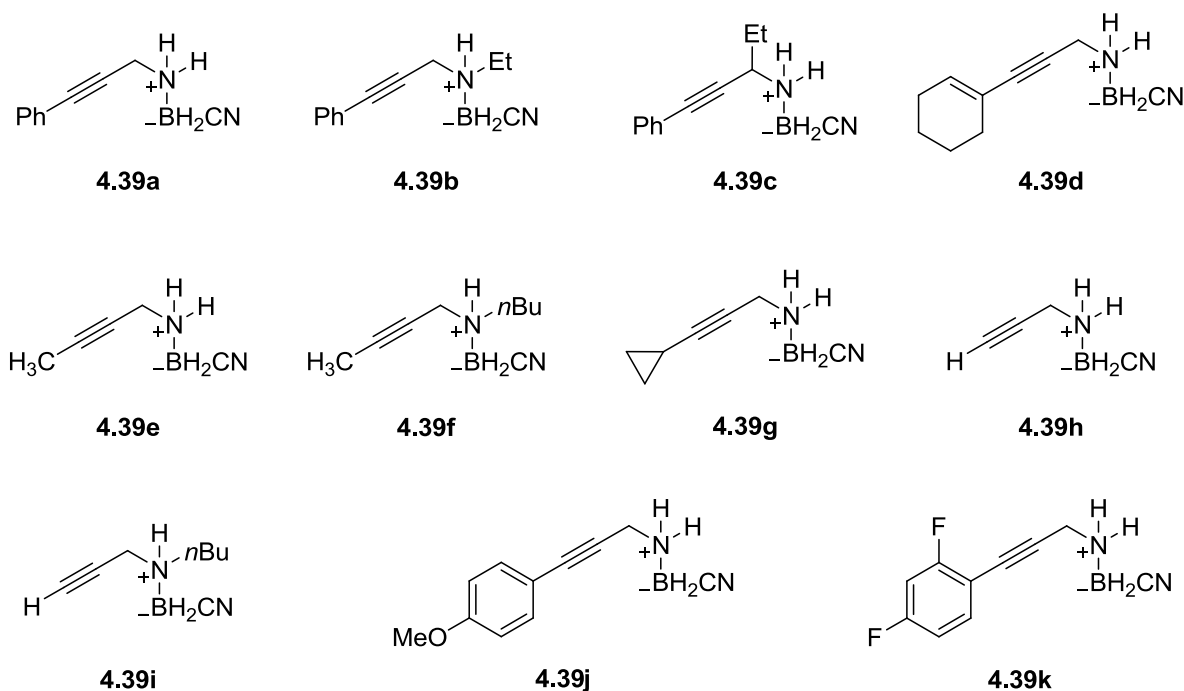


**Figure 26.** Substrate scope of boranecarbonitrile **4.39**.

An X-ray structure analysis of **4.39a** confirmed the proposed structure.

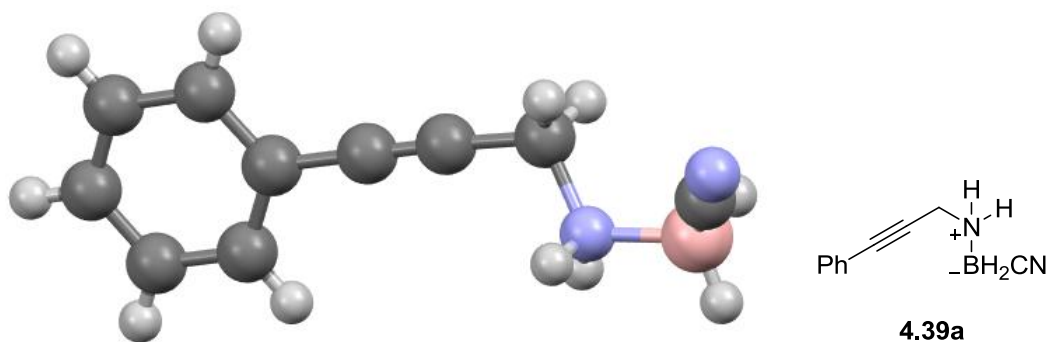
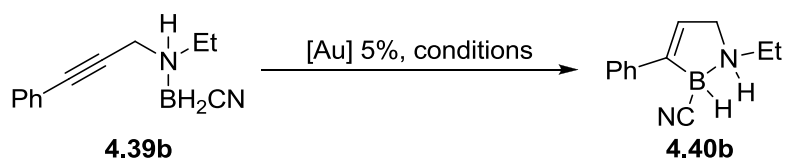


**Figure 27.** Perspective view of the structure of  $C_{10}H_{11}BN_2$  (**4.39a**). The ball and stick drawing. CCDC number: 954118

This method tolerated various substitute groups at the alkyne terminus. Both the primary and aliphatic substituted secondary propargyl amine worked well for the B-N complex formation. The aromatic substituted propargyl amine ( $R_2 = Ar$ ) did not give the corresponding complex **4.39** under the optimal conditions, which is likely a consequence of the decreased basicity of the nitrogen. Nevertheless, this method allowed the general access to the cyano-stabilized amine borane, containing the less reactive borohydride (B-H).

With this new amine borane **4.39** in hand, we investigated its reactivity toward gold catalysts. Notably, compared to the terminal alkyne, the internal alkyne is usually much less reactive toward  $\pi$ -acid catalysts. Therefore, to better validate the feasibility of this gold catalyzed intramolecular hydroboration, complex **4.39b** (containing internal alkyne) was selected for our initial screening. The results are summarized in **Table 6**.

**Table 6.** Condition Screening of alkyne hydroboration.



Entry	Catalyst	Solvent	<i>t</i> [h]	T [ °C]	Conv.	Yield
1	PPh <sub>3</sub> AuCl	CH <sub>2</sub> Cl <sub>2</sub>	rt	72 hr	<5 %	n.d.
2	PPh <sub>3</sub> AuCl/AgOTf	CH <sub>2</sub> Cl <sub>2</sub>	rt	30 min or 72 hr	19 %	17 %
3	IPrAuCl/AgOTf	CH <sub>2</sub> Cl <sub>2</sub>	rt	30 min or 72 hr	15 %	11 %
4	XPhosAuCl/AgOTf	CH <sub>2</sub> Cl <sub>2</sub>	rt	30 min or 72 hr	<5 %	n.d.
5	P(OMe) <sub>3</sub> AuCl/AgOTf	CH <sub>2</sub> Cl <sub>2</sub>	rt	30 min or 72 hr	<5 %	n.d.
6	[PPh <sub>3</sub> Au-TA] <sup>+</sup> TfO <sup>-</sup>	CH <sub>2</sub> Cl <sub>2</sub>	rt	72 hr	<5 %	n.d.
7	[PPh <sub>3</sub> Au] <sup>+</sup> Tf <sub>2</sub> N <sup>-</sup>	CH <sub>2</sub> Cl <sub>2</sub>	rt	72 hr	32 %	21 %
8	[XPhosAu] <sup>+</sup> Tf <sub>2</sub> N <sup>-</sup>	CH <sub>2</sub> Cl <sub>2</sub>	rt	72 hr	>99 %	71 %
9	[XPhosAu-NCMe] <sup>+</sup> F <sub>6</sub> Sb <sup>-</sup>	CH <sub>2</sub> Cl <sub>2</sub>	rt	30 min or 72 hr	16 %	2 %
10	PPh <sub>3</sub> AuCl	DCE	80	72 hr	<5 %	n.d.
11	XPhosAuCl/AgOTf	DCE	80	30 min or 72 hr	10 %	5 %
12	IPrAuCl/AgOTf	DCE	80	30 min or 72 hr	<5 %	n.d.
13	[PPh <sub>3</sub> Au-TA] <sup>+</sup> TfO <sup>-</sup>	DCE	80	24 hr or 72hr	35 %	24 %
14	[PPh <sub>3</sub> Au] <sup>+</sup> Tf <sub>2</sub> N <sup>-</sup>	DCE	80	24 hr or 72 hr	47 %	34 %
15	[XPhosAu-TA] <sup>+</sup> TfO <sup>-</sup>	DCE	<b>80</b>	<b>72 hr</b>	<b>99 %</b>	<b>93 %</b>
16	[XPhosAu-TA] <sup>+</sup> F <sub>6</sub> Sb <sup>-</sup>	DCE	80	72 hr	73 %	59 %
17	[XPhosAu] <sup>+</sup> Tf <sub>2</sub> N <sup>-</sup>	DCE	80	72 hr	82 %	72 %
18	[XPhosAu-TA] <sup>+</sup> TfO <sup>-</sup>	THF	65	72 hr	85 %	73 %
19	[XPhosAu-TA] <sup>+</sup> TfO <sup>-</sup>	DMF	80	72 hr	84 %	63 %
20	[XPhosAu-TA] <sup>+</sup> TfO <sup>-</sup>	toluene	90	72 hr	39 %	36 %
21	[XPhosAu-TA] <sup>+</sup> TfO <sup>-</sup>	MeCN	80	72 hr	88 %	65 %

General reaction conditions: **4.39b** (39 mg, 0.2 mmol 1.0 eq.), solvent (5 mL) and [Au] catalyst (0.01 mmol, 5 mol %). was successively added into 20 mL reaction vial and stirred at cooresponding temprature. rt = room temperature, n.d. = not determined, TA = 1H-benzo[d][1,2,3]triazole. Conversion and yields were determined by NMR with *p*-xylene as internal standard.

Unlike amine borane **4.34** which caused rapid gold decomposition, the cyano-substituted amine borane **4.39b** gave the desired cyclic amine borane **4.40b** using the PPh<sub>3</sub>AuCl/AgOTf catalyst, though with very low yield (17%, entry 2). The structure of **4.40b** was confirmed by X-



ray crystallography (**Figure 28**). Notably, the reaction gave 3:1 (*cis:trans*) isomer mixture in solution. However, upon crystallization, all of the *trans*-isomer converted to *cis*-isomer. This process was confirmed by NMR: re-dissolving the *cis*-isomer indicated a slow equilibrium (up to 3 hours) to 3:1 *cis:trans* mixture, and slow evaporation the solvent gave the pure *cis*-isomer again. Overall, the success in obtaining the cyclic amine borane **4.40b** greatly supported our hypothesis that the  $\pi$ -acidic gold catalyzed alkyne activation is a feasible approach for the preparation of cyclic amine borane. To improve the reaction performance, we screened other gold catalysts. As showed in entries 1-5, although the cyano-modified amine borane **4.39b** was a weaker reductant, the reaction still suffered from gold decomposition. Interestingly, the TA-Au catalysts (entry 6), though giving no reaction, indicated better resistance toward **4.39b**, according to the decreased rate of gold mirror formation. To verify this result, we monitored the catalyst decomposition (upon treatment with cyano-substituted amine borane **4.39b**) using  $^{31}\text{P}$  NMR (**Figure 29**).

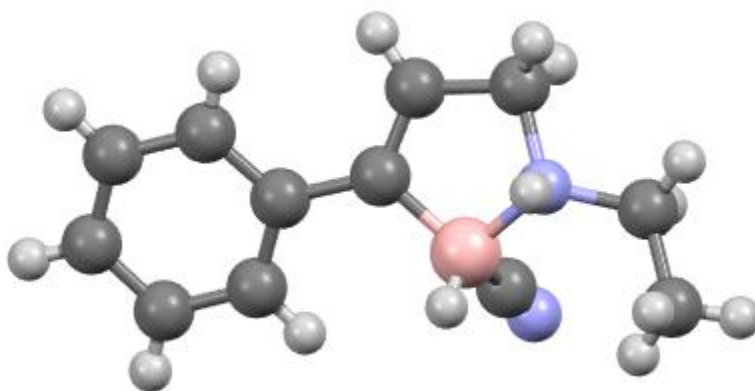


**Figure 28.** Perspective view of the structure of  $\text{C}_{12}\text{H}_{15}\text{BN}_2$  (compound **4.40b**). The ball and stick drawing. CCDC number: 954119

As shown, treating  $[\text{L-Au}]^+$  with **4.39b** caused immediate decomposition, even with XPhos as the primary ligand. Interestingly, with the 1,2,3-triazole modified gold complexes, much slower decomposition was observed. The bulky XPhos ligand further improved the gold cation

stability, giving little decomposition even after 20 hours at room temperature. With this improved catalyst stability, we further evaluated the reaction conditions at elevated temperature. To our great delight, with the XPhos-based TA-Au catalyst at 80 °C, **4.39b** was consumed and **4.40b** was isolated in excellent yield (93%, **Table 5**, entry 9). Solvent screening revealed DCE as the optimal choice. Other factors, such as the choice of the counter anions ( $\text{SbF}_6^-$  or  $\text{NTf}_2^-$ ) and MeCN-stabilized  $[\text{L-Au}]^+$ ,<sup>89</sup> were also evaluated. Triazole-gold complex gave the best result due to the superior stability under the applied reductive conditions (see detailed screening conditions and  $^{31}\text{P}$  NMR spectra in supporting information).

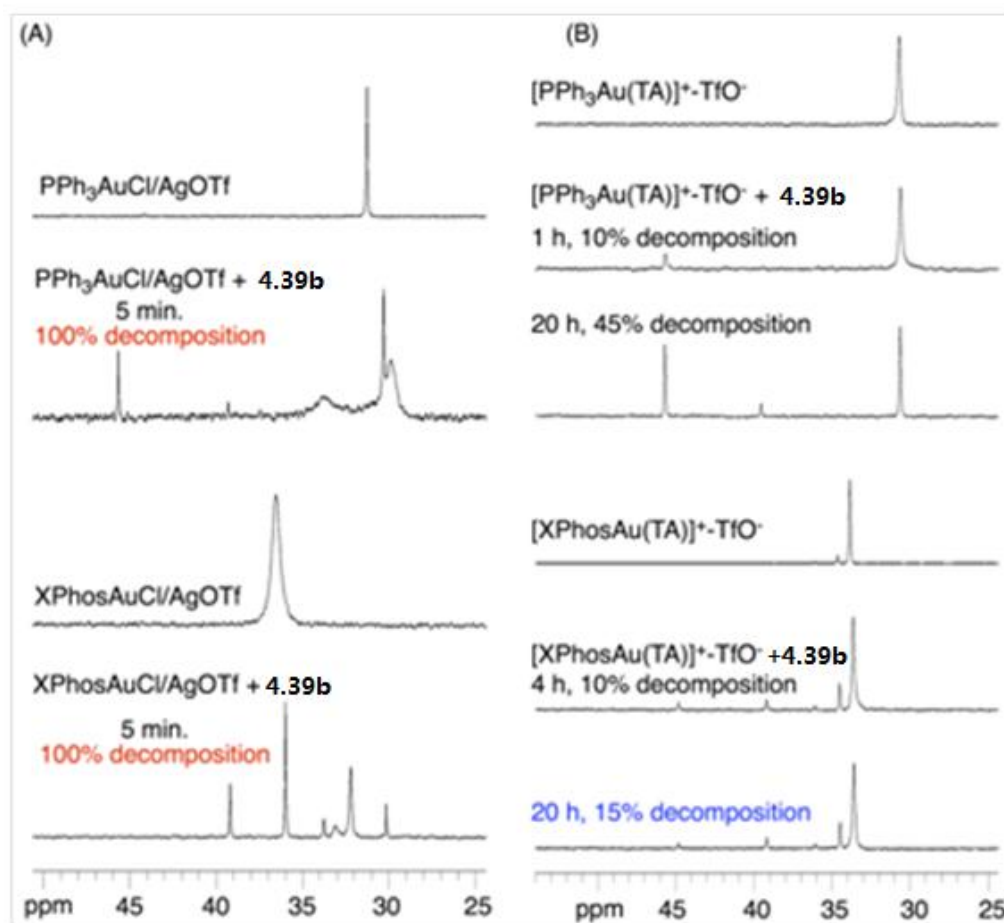


**Figure 29.** Monitoring the gold decomposition by  $^{31}\text{P}$  NMR. General conditions:  $^{31}\text{P}$  NMR was collected at room temperature in  $\text{CDCl}_3$  with a sealed capillary tube containing  $\text{H}_3\text{PO}_4/\text{D}_2\text{O}$  (1.0 M) solution as external standard for integration (100), and chemical shift ( $\delta = 0.00$  ppm).

With this optimized conditions in hand, we explored the reaction substrate scope. The results are summarized in **Figure 30**. As shown, this method tolerated large substrate scope. First, both terminal and internal alkynes were adapted for this transformation. The more reactive terminal alkynes gave excellent yields (**4.40h** and **4.40i**). Most of the tested internal alkynes also worked well under this condition. The alkyne terminal ( $R^1$ ) can be alkyl, aryl, cyclopropyl and even alkenyl (from enyne). The aliphatic internal alkynes were less reactive, giving slightly lower yields (**4.40e** and **4.40f**) compared to the aromatic internal alkynes. Electron donating group substituted alkyne (**4.39j** to **4.40j**) reacted slowly under the applied conditions (even with an extended reaction period, 4 days). The reaction was quenched upon the observed decomposition of starting material **4.39j**. The overall yield was moderate when compared with the electron deficient substrate **4.39k**. No ring-opening product was observed in the cyclopropane modified alkyne (**4.40g**), excluding a single electron mechanism in this transformation. Both primary and secondary propargyl amines were tolerated with the reaction conditions, giving cyclic amine borane product as a mixture of cis-trans isomers with different ratios (**4.40b**, **4.40f** and **4.40i**). The overall reactivity of these two types of amines was comparable. Substitution on the propargyl  $R^3$  position indicated little influence on the reactivity, giving **4.40c** in excellent yield. Overall, the good substrate tolerability at alkyne terminal ( $R^1$ ), the propargyl position ( $R^3$ ) and amine ( $R^2$ ) positions highlighted the great potential of this method for the preparation of azaborine with broad substrate scope.

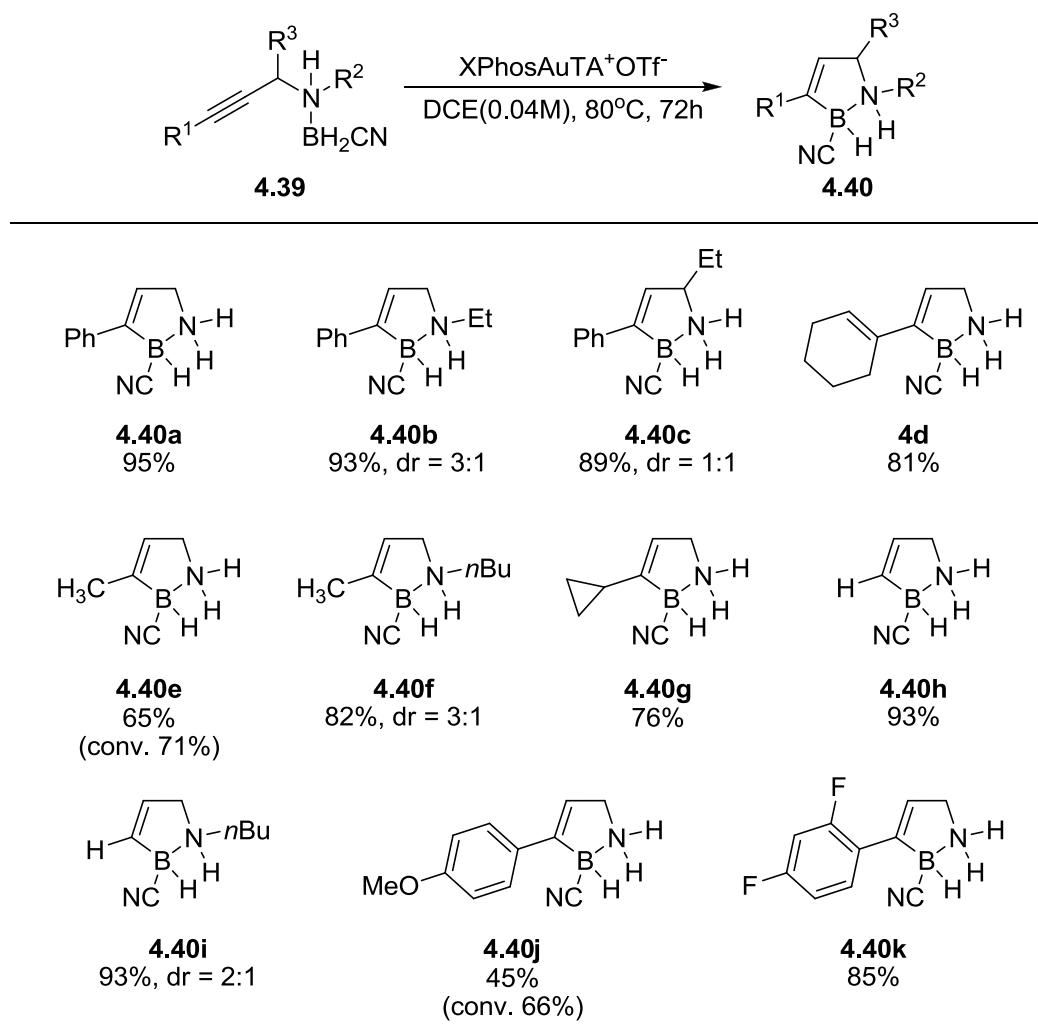
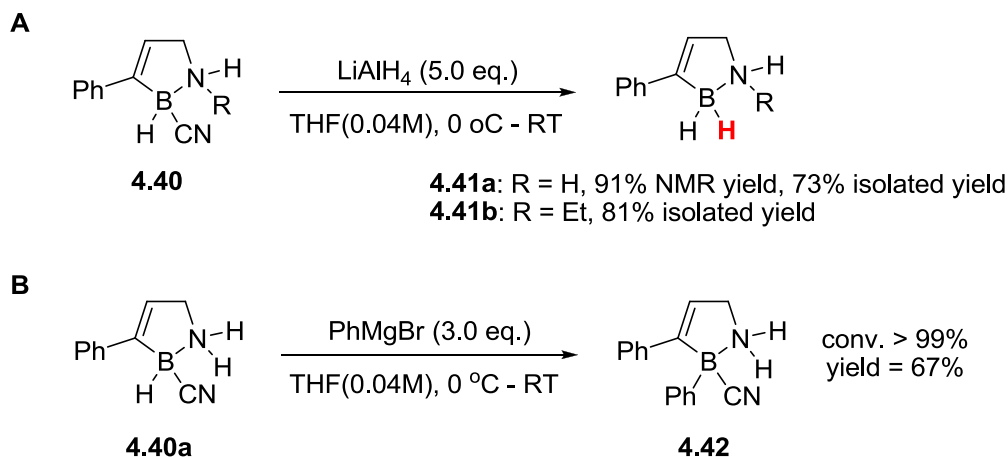


**Figure 30.** Reaction substrate scope. All conversion, yield and dr was determined after 72 hr (96 hr for **4.40j**) by NMR with p-xylene as internal standard.

To emphasize the practical utility of this method, a 5 mmol scale reaction of **4.39a** was performed under the identical conditions and **4.40a** was isolated as a white solid in 85% yield. The cyano group on boron was originally introduced to overcome the undesired gold catalyst decomposition. Thus, to further extend this methodology as a general protocol for potential azaborine synthesis, we investigated the post-cyclization derivatization with the expectation to

introduce diverse functional groups on the boron position. Two representative transformations on the B position are summarized in **Scheme 42**.

**Scheme 42.** Introducing functional groups at boron position.



First, treating the cyclic amine borane **4.40a/4.40b** with  $\text{LiAlH}_4$  gave the corresponding reduction product **4.41a/4.42b** in good to excellent yields (**Scheme 42A**).<sup>90</sup> Notably, the non-substituted amine borane **4.41a** was not stable toward air. Thus, although excellent NMR yield (91%) was observed, only 73% product was isolated. This was probably due to the loss of  $\text{H}_2$  gas and sequential decomposition. Nevertheless, considering the fact that the  $\text{BH}_3$  based amine borane **4.34** caused rapid gold decomposition and was not suitable for this transformation at all, this cyano borane modification provided an alternative solution to extend the reaction scope. Moreover, reaction of **4.40a** with 3 equiv.  $\text{PhMgBr}$  gave the corresponding phenyl substituted cyclic amine borane **4.42** with the structure confirmed by X-ray crystallography (**Figure 31**). Combining these two strategies in **Scheme 42**, functionalization of the boron position was readily achievable, and highlighted the large scope of cyclic amine borane synthesis that can be facilitated with the TA-Au catalysis.

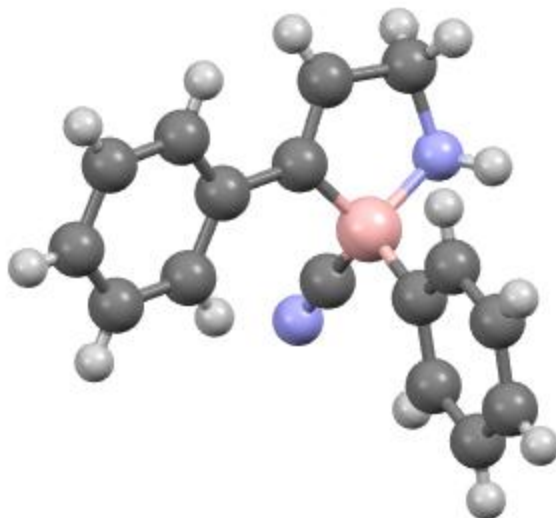


**Figure 31.** Perspective view of the structure of  $C_{16}H_{15}BN_2$  (compound **4.42**). The ball and stick drawing. CCDC number: 965653

### 4.3 Conclusion

Overall, we report herein a novel strategy for the highly efficient preparation of cyclic amine boranes. With the newly developed cyano-modified amine borane and stable XPhos-based TA-Au catalyst, the inherently challenging alkyne hydroboration was achieved successfully. The overall transformation operated under “open-flask” conditions. The excellent substrate tolerability and readily available derivatization methods warrant this transformation as a new efficient approach for cyclic amine borane synthesis in general. Preparation of other BN/CC isosteric derivatives (such as benzene and indole) and applications of the resulting compounds in  $H_2$  storage and catalysis are currently under investigation in our lab and will be reported in due course.

#### 4.4 Contribution

Qiaoyi Wang was the researcher who had first investigated the synthesis of compound **4.39**, gold(I) complexes and reaction condition. Together, Qiaoyi Wang and Stephen E. Motika were responsible for substrate scope, NMR spectrum, and manuscript completion. The manuscript was accepted by *Angewandte Communication International Edition*. The detailed X-ray crystallographic data analysis of compound **4.39a**, **4.40b** and **4.42** were done by Prof. Jeffrey L. Petersen, C. Eugene Bennett Department of Chemistry, West Virginia University.

## References

- 
- <sup>1</sup> (a) Chabre, Y. M.; Roy, R. *Curr. Top. Med. Chem.* **2008**, *8*, 1237;. (b) Colombo, M.; Peretto, I. *Drug Discovery Today* **2008**, *13*, 677; (c) Hanselmann, R.; Job, G. E.; Johnson, G.; Lou, R. L.; Martynow, J. G.; Reeve, M. M. *Org. Process Res. Dev.* **2010**, *14*, 152; (d) Moumne, R.; Larue, V.; Seijo, B.; Lecourt, T.; Micouin, L.; Tisne, C. *Org. Biomol. Chem.* **2010**, *8*, 1154–1159; (e) Li, H. M.; Cheng, F. O.; Duft, A. M.; Adronov, A. *J. Am. Chem. Soc.* **2005**, *127*, 14518; (f) Rozkiewicz, D. I.; Janczewski, D.; Verboom, W.; Ravoo, B. J.; Reinhoudt, D. N. *Angew. Chem., Int. Ed.* **2006**, *45*, 5292; (g) Wyszogrodzka, M.; Haag, R. *Chem. Eur. J.* **2008**, *14*, 9202; (h) Gadzikwa, T.; Farha, O. K.; Malliakas, C. D.; Kanatzidis, M. G.; Hupp, J. T.; Nguyen, S. T. *J. Am. Chem. Soc.* **2009**, *131*, 13613; (i) Golas, P. L.; Matyjaszewski, K. *Chem. Soc. Rev.* **2010**, *39*, 1338; (j) Hahn, M. E.; Muir, T. W. *Trends Biochem. Sci.* **2005**, *30*, 26; (k) Heal, W. P.; Wickramasinghe, S. R.; Leatherbarrow, R. J.; Tate, E. W. *Org. Biomol. Chem.* **2008**, *6*, 2308; (l) Ahsanullah, J.; Schmieder, P.; Kuhne, R.; Rademann, J. *Angew. Chem., Int. Ed.* **2009**, *48*, 5042; (m) Schneider, G. *Nat. Rev. Drug Discovery* **2010**, *9*, 273.
- <sup>2</sup> (a) Rostovtsev, V. V.; Green, L. G.; Fokin, V. V.; Sharpless, K. B. *Angew. Chem., Int. Ed.* **2002**, *41*, 2596; (b) Kolb, H. C.; Finn, M. G.; Sharpless, K. B. *Angew. Chem., Int. Ed.* **2001**, *40*, 2004; (c) Moses, J. E.; Moorhouse, A. D. *Chem. Soc. Rev.* **2007**, *36*, 1249. (d) Wu, P.; Fokin, V. V. *Aldrichim. Acta.* **2007**, *40*, 7.
- <sup>3</sup> (a) Wang, D.; Zhang, Y.; Harris, A.; Gautam, L. N. S.; Shi, X. *Adv. Syn. Catal.* **2011**, *353*, 2584;. (b) Wang, D.; Zhang, Y.; Cai, R.; Shi, X.; *Beilstein J. Org. Chem.* **2011**, *7*, 1014;. (c) Wang, D.; Gautam, L. N. S.; Bollinger, C.; Harris, A.; Li, M.; Shi, X. *Org. Lett.* **2011**, *13*, 2618; (d) Duan, H.; Sengupta, S.; Petersen, J. L.; Akhmedov, N.; Shi, X. *J. Am. Chem. Soc.*



- 
- 2009**, *131*, 12100; (e) Duan, H.; Yan, W.; Sengupta, S.; Shi, X. *Bioorg. Med. Chem. Lett.* **2009**, 3899.
- <sup>4</sup> (a) Aucagne, V.; Hanni, K. D.; Leigh, D. A.; Lusby, P. J.; Walker, D. B. *J. Am. Chem. Soc.* **2006**, *128*, 2186; (b) Suijkerbuijk, B. M. J. M.; Aerts, B. N. H.; Dijkstra, H. P.; Lutz, M.; Spek, A. L.; van Koten, G.; Gebbink, R. J. M. K. *Dalton. Trans.* **2007**, 1273; (c) Maeda, C.; Yamaguchi, S.; Ikeda, C.; Shinokubo, H.; Osuka, A. *Org. Lett.* **2008**, *10*, 549; (d) Mullen, K. M.; Gunter, M. J. *J. Org. Chem.* **2008**, *73*, 3336; (e) Detz, R. J.; Heras, S. A.; de Gelder, R.; van Leeuwen, P. W. N. M.; Hiemstra, H.; Reek, J. N. H.; van Maarseveen, J. H. *Org. Lett.* **2006**, *8*, 3227; (f) Monkowius, U.; Ritter, S.; König, B.; Zabel, M.; Yersin, H. *Eur. J. Inorg. Chem.* **2007**, 4597; (g) Fukuzawa, S.; Oki, H.; Hosaka, M.; Sugasawa, J.; Kikuchi, S. *Org. Lett.* **2007**, *9*, 5557; (h) Richardson, C.; Fitchett, C. M.; Keene, F. R.; Steel, P. J. *Dalton Trans.* **2008**, 2534; (i) Schweinfurth, D.; Hardcastle, K. I.; Bunz, U. H. F. *Chem. Commun.* **2008**, 2203; (j) Maisonia, A.; Serafin, P.; Traïkia, M.; Debiton, E.; Thery, V.; Aitken, D. J.; Lemoine, P.; Bernard, V.; Gautier, A. *Eur. J. Inorg. Chem.* **2008**, 298.
- <sup>5</sup> Loren, Jon C.; Krasinski, Antoni; Fokin, Valery V.; Sharpless, K. Barry *Synlett*, **18**, 2005, 2847.
- <sup>6</sup> Zefirov, N.S.; Chapovskaya, N.K.; Kolesnikov, V. V. *Chem. Commun.* **1971**, 1001.
- <sup>7</sup> Béatrice Quiclet-Sire; Samir Z. Zard. *Synthesis*. **2005**, *19*, 3319.
- <sup>8</sup> Sengupta, S.; Duan, H.; Lu, W.; Petersen, J. L.; Shi, X. *Org. Lett.* **2008**, *10*, 1493.
- <sup>9</sup> Wang, K.; Chen, M.; Wang, Q.; Shi, X.; Lee, J. K. *J. Org. Chem.* **2013**, *78*, 7249.
- <sup>10</sup> Yan, W.; Liao, T.; Tuguldur, O.; Zhong, C.; Petersen, J. L.; Shi, X. *Chem. Asian. J.* **2011**, *6*, 2720.

- 
- <sup>11</sup> (a) Chen, Y.; Liu, Y.; Petersen, J. L.; Shi, X. *Chem. Commun.* **2008**, 3254; (b) Liu, Y.; Yan, W.; Chen, Y.; Petersen, J. L.; Shi, X. *Org. Lett.* **2008**, *10*, 5389.
- <sup>12</sup> (a) Mindt, T. L.; Struthers, H.; Brans, L.; Anguelov, T.; Schweinsberg, C.; Maes, V.; Tourwe, D.; Schibli, R. *J. Am. Chem. Soc.* **2006**, *128*, 15096; (b) Li, Y.; Huffman, J. C.; Flood, A. H. *Chem. Commun.* **2007**, 2692; (c) Meudtner, R. M.; Ostermeier, M.; Goddard, R.; Limberg, C.; Hecht, S. *Chem. Eur. J.* **2007**, *13*, 9834; (d) Colasson, B.; Save, M.; Milko, P.; Roithova, J.; Schroder, D.; Reinaud, O. *Org. Lett.* **2007**, *9*, 4987; (e) van Assema, S. G. A.; Tazelaar, C. G. J.; de Jong, G. B.; van Maarseveen, J. H.; Schakel, M.; Lutz, M.; Spek, A. L.; Slootweg, J. C.; Lammertsma, K. *Organometallics* **2008**, *27*, 3210; (f) Mindt, T. L.; Müller, C.; Melis, M.; de Jong, M.; Schibli, R. *Bioconjugate Chem.* **2008**, *19*, 1689.
- <sup>13</sup> Hu, M. C.; Wang, Y.; Zhai, Q. G.; Li, S. N.; Jiang, Y. C.; Zhang, Y. *Inorg. Chem.* **2009**, *48*, 1449.
- <sup>14</sup> (a) Aucagne, V.; Leigh, D. A. *Org. Lett.* **2006**, *8*, 4505; (b) Fletcher, J. T.; Bumgarner, B.; Engels, N. D.; Skoglund, D. A. *Organometallics* **2008**, *27*, 5430; (c) Aizpurua, J. M.; Azcune, I.; Fratila, R. M.; Balentova, E.; Sagartzazu-Aizpurua, M.; Miranda, J. I. *Org. Lett.* **2010**, *12*, 1584.
- <sup>15</sup> (a) Banday, A.; Shameem, S.; Ganai, B. *Org. Med. Chem. Lett.* **2012**, *2*, 1; (b) Elamari, H.; Slimi, R.; Chabot, G. G.; Quentin, L.; Scherman, D.; Girard, C. *Eur. J. Med. Chem.* **2013**, *60*, 360. (c) Chemama, M.; Fonvielle, M.; Arthur, M.; Valery, J. M.; Etheve-Quellejeu, M. *Chem. Eur. J.* **2009**, *15*, 1929; (d) Nahrwold, M.; Bogner, T.; Eissler, S.; Verma, S.; Sewald, N. *Org. Lett.* **2010**, *12*, 1064; (e) Michaels, H. A.; Murphy, C. S.; Clark, R. J.; Davidson, M. W.; Zhu, L. *Inorg. Chem.* **2010**, *49*, 4278; (f) Mamidyala, S. K.; Finn, M. G. *Chem. Soc. Rev.* **2010**, *39*, 1252.

- 
- <sup>16</sup> For Lewis and Bronsted acid catalyzed propargylations, see: (a) Nishibayashi, Y.; Shinoda, A.; Miyake, Y.; Matsuzawa, H.; Sato, M. *Angew. Chem., Int. Ed.* **2006**, *45*, 4835; (b) Zhan, Z. P.; Yu, J. L.; Liu, H. J.; Cui, Y. Y.; Yang, R. F.; Yang, W. Z.; Li, J. P. *J. Org. Chem.* **2006**, *71*, 8298; (c) Sanz, R.; Miguel, D.; Martinez, A.; Alvarez-Gutierrez, J. M.; Rodriguez, F. *Org. Lett.* **2007**, *9*, 727; (d) Nishimoto, Y.; Kajioka, M.; Saito, T.; Yasuda, M.; Baba, A. *Chem. Commun.* **2008**, 6396.
- <sup>17</sup> For examples of the Meyer-Schuster reaction, see: (a) Georgy, M.; Boucard, V.; Campagne, J. M. *J. Am. Chem. Soc.* **2005**, *127*, 14180; (b) Engel, D. A.; Dudley, G. B. *Org. Lett.* **2006**, *8*, 4027; (c) Sun, C. X.; Lin, X. C.; Weinreb, S. M. *J. Org. Chem.* **2006**, *71*, 3159; (d) Trost, B. M.; Chung, C. K. *J. Am. Chem. Soc.* **2006**, *128*, 10358; (e) Matsuzawa, H.; Miyake, Y.; Nishibayashi, Y. *Angew. Chem., Int. Ed.* **2007**, *46*, 6488; (f) Sugawara, Y.; Yamada, W.; Yoshida, S.; Ikeno, T.; Yamada, T. *J. Am. Chem. Soc.* **2007**, *129*, 12902; (g) Dai, L. Z.; Shi, M. *Chem. Eur. J.* **2008**, *14*, 7011; (h) Bandini, M.; Eichholzer, A. *Angew. Chem., Int. Ed.* **2009**, *48*, 9533; (i) Wang, D.; Ye, X.; Shi, X. *Org. Lett.* **2010**, *12*, 2088.
- <sup>18</sup> (a) Thibault, R. J.; Takizawa, K.; Lowenheilm, P.; Helms, B.; Mynar, J. L.; Frechet, J. M. J.; Hawker, C. J. *J. Am. Chem. Soc.* **2006**, *128*, 12084; (b) Angell, Y.; Burgess, K. *Angew. Chem., Int. Ed.* **2007**, *46*, 3649; (c) Fletcher, J. T.; Bumgarner, B. J.; Engels, N. D.; Skoglund, D. A. *Organometallics* **2008**, *27*, 5430; (d) Jarowski, P. D.; Wu, Y. L.; Schweizer, W. B.; Diederich, F. *Org. Lett.* **2008**, *10*, 3347; (e) Schweinfurth, D.; Hardcastle, K. I.; Bunz, U. H. F. *Chem. Commun.* **2008**, 2203; (f) Ozcubukcu, S.; Ozkal, E.; Jimeno, C.; Pericas, M. A. *Org. Lett.* **2009**, *11*, 4680.
- <sup>19</sup> (a) A. S. K. Hashmi; F. D. Toste, *Modern Gold Catalyzed Synthesis*, Wiley-VCH, Weinheim, 2012; (b) A. S. K. Hashmi; M. Rudolph, *Chem. Soc. Rev.* **2012**, *41*, 2448; (c) D. J. Gorin, B.

- 
- D. Sherry; F. D. Toste, *Chem. Rev.* **2008**, *108*, 3351; (d) A. Arcadi, *Chem. Rev.* **2008**, *108*, 3266; (e) E. Jimenez-Nunez; A. M. Echavarren, *Chem. Rev.* **2008**, *108*, 3326; ( f) A. S. K. Hashmi, *Chem. Rev.* **2007**, *107*, 3180; (g) A. Furstner and P. W. Davies, *Angew. Chem., Int. Ed.* **2007**, *46*, 3410; (h) L. Zhang, J. Sunand S. A. Kozmin, *Adv. Synth. Catal.* **2006**, *348*, 2271; (i) A. S. K. Hashmi; G. J. Hutchings, *Angew. Chem. Int. Ed.* **2006**, *45*, 7896.
- <sup>20</sup> (a) Nösel, P.; dos Santos Comprido, L. N.; Lauterbach, T.; Rudolph, M.; Rominger, F.; Hashmi, A. S. K. *J. Am. Chem. Soc.* **2013**, *135*, 15662; (b) Ji, K.; Zhao, Y.; Zhang, L. *Angew. Chem. Int. Ed.* **2013**, *52*, 6508; (c) González, A. Z.; Benitez, D.; Tkatchouk, E.; Goddard, W. A.; Toste, F. D. *J. Am. Chem. Soc.* **2011**, *133*, 5500; (d) Boogaerts, I. I. F.; Nolan, S. P. *J. Am. Chem. Soc.* **2010**, *132*, 8858.
- <sup>21</sup> (a) A. S. K. Hashmi, J. P. Weyrauch, M. Rudolph; E. Kurpejovic, *Angew. Chem. Int. Ed.* **2004**, *43*, 6545; (b) A. S. K. Hashmi, M. Rudolph, J. P. Weyrauch, M. Wolfle, W. Frey; J. W. Bats, *Angew. Chem. Int. Ed.* **2005**, *44*, 2798; (c) N. Debono, M. Iglesias; F. Sanchez, *Adv. Synth. Catal.* **2007**, *349*, 2470; (d) A. S. K. Hashmi, M. Rudolph, H. U. Siehl, M. Tanaka, J. W. Bats; W. Frey, *Chem. Eur. J.* **2008**, *14*, 3703; (e) N. D. Shapiro, Y. Shi, F. D. Toste, *J. Am. Chem. Soc.* **2009**, *131*, 11654; (f) Y. Zhang, B. Feng; C. Zhu, *Org. Biomol. Chem.* **2012**, *10*, 9137; (g) J. A. O'Neill, G. M. Rosair, A. L. Lee, *Catal. Sci. Technol.* **2012**, *2*, 1818.
- <sup>22</sup> (a) A. S. K. Hashmi; F. D. Toste, *Modern Gold Catalyzed Synthesis*, Wiley-VCH, Weinheim, 2012; (b) A. S. K. Hashmi; M. Rudolph, *Chem. Soc. Rev.* **2012**, *41*, 2448; (c) D. J. Gorin, B. D. Sherry; F. D. Toste, *Chem. Rev.* **2008**, *108*, 3351; (d) A. Arcadi, *Chem. Rev.* **2008**, *108*, 3266; (e) E. Jimenez-Nunez; A. M. Echavarren, *Chem. Rev.* **2008**, *108*, 3326; ( f) A. S. K. Hashmi, *Chem. Rev.* **2007**, *107*, 3180; (g) A. Furstner; P. W. Davies, *Angew. Chem. Int. Ed.*

- 
- 2007**, *46*, 3410; (h) L. Zhang, J. Sun; S. A. Kozmin, *Adv. Synth. Catal.* **2006**, *348*, 2271; (i) A. S. K. Hashmi; G. J. Hutchings, *Angew. Chem. Int. Ed.* **2006**, *45*, 7896.
- <sup>23</sup> (a) Gaillard, S.; Cazin, C. S. J.; Nolan, S. P. *Acc. Chem. Res.* **2011**, *45*, 778; (b) Nolan, S. P. *Acc. Chem. Res.* **2010**, *44*, 91; (c) Marion, N.; Nolan, S. P. *Chem. Soc. Rev.* **2008**, *37*, 1776; (d) Marion, N.; Carlqvist, P.; Gealageas, R.; de Frémont, P.; Maseras, F.; Nolan, S. P. *Chem. Eur. J.* **2007**, *13*, 6437.
- <sup>24</sup> (a) Mauger, C. C.; Mignani, G. A. *Aldrichimica Acta.* **2006**, *39*, 17; (b) Schlummer, B.; Scholz, U. *Adv. Synth. Catal.* **2004**, *346*, 1599.
- <sup>25</sup> For recent reviews, see: (a) A. S. K. Hashmi, *Angew. Chem. Int. Ed.* **2010**, *49*, 5232; (b) L. Liu, G. B. Hammond, *Chem. Soc. Rev.* **2012**, *41*, 3129; (c) R. E. M. Brooner, R. A. Widenhofer, *Angew. Chem. Int. Ed.* **2013**, *52*, 11714.
- <sup>26</sup> (a) Weber, D.; Gagné, M. R. *Org. Lett.* **2009**, *11*, 4962; (b) Weber, D.; Tarselli, M. A.; Gagné, M. R. *Angew. Chem. Int. Ed.* **2009**, *48*, 5733.
- <sup>27</sup> de Frémont, P.; Scott, N. M.; Stevens, E. D.; Nolan, S. P. *Organometallics* **2005**, *24*, 2411.
- <sup>28</sup> Nieto-Oberhuber, C.; Muñoz, M. P.; López, S.; Jiménez-Núñez, E.; Nevado, C.; Herrero-Gómez, E.; Raducan, M.; Echavarren, A. M. *Chem. Eur. J.* **2006**, *12*, 1677.
- <sup>29</sup> Wang, D.; Cai, R.; Sharma, S.; Jirak, J.; Thummanapelli, S. K.; Akhmedov, N. G.; Zhang, H.; Liu, X.; Petersen, J. L.; Shi, X. *J. Am. Chem. Soc.* **2012**, *134*, 9012.
- <sup>30</sup> Duan, H.; Sengupta, S.; Petersen, J. L.; Shi, X. *Organometallics* **2009**, *28*, 2352.
- <sup>31</sup> Liao, W.; Chen, Y.; Liu, Y.; Duan, H.; Petersen, J. L.; Shi, X. *Chem. Commun.* **2009**, 6436.
- <sup>32</sup> (a) Duan, H.; Sengupta, S.; Petersen, J. L.; Akhmedov, N. G.; Shi, X. *J. Am. Chem. Soc.* **2009**, *131*, 12100; (b) Xi, Y.; Wang, D.; Ye, X.; Akhmedov, N. G.; Petersen, J. L.; Shi, X. *Org. Lett.* **2013**, *16*, 306.

- 
- <sup>33</sup> Nomiya, K.; Noguchi, R.; Ohsawa, K.; Tsuda, K. *J. Chem. Soc., Dalton Trans.* **1998**, 4101.
- <sup>34</sup> Duan, H.; Sengupta, S.; Petersen, J. L.; Akhmedov, N. G.; Shi, X. *J. Am. Chem. Soc.* **2009**, *131*, 12100.
- <sup>35</sup> (a) N. Marion, S. Diez-Gonzalez, P. Fremont, A. R. Noble; S. P. Nolan, *Angew. Chem. Int. Ed.* **2006**, *45*, 3647; and for an early example, see: (b) L. Zhang; S. Wang, *J. Am. Chem. Soc.* **2006**, *128*, 1442.
- <sup>36</sup> Wang, D.; Zhang, Y.; Cai, R.; Shi, X. *Beilstein J. Org. Chem.* **2011**, *7*, 1014.
- <sup>37</sup> (a) C. He, J. Ke, H. Xu; A. Lei, *Angew. Chem. Int. Ed.* **2013**, *52*, 1527; (b) Z. Huang, L. Jin, H. Han, A. Lei, *Org. Biomol. Chem.* **2013**, *11*, 1810; (c) J. Li, L. Jin, C. Liu; A. Lei, *Chem. Commun.* **2013**, *49*, 9615.
- <sup>38</sup> P. Nun, S. Gaillard, A. M. Z. Slawin; S. P. Nolan, *Chem. Commun.* **2010**, *46*, 9113.
- <sup>39</sup> DFT calculation was performed on Gaussian 03 program at the B3LYP/6-311G level of theory.
- <sup>40</sup> P. Nun, S. Gaillard, A. Poater, L. Cavallo; S. P. Nolan, *Org. Biomol. Chem.* **2011**, *9*, 101.
- <sup>41</sup> Wang, D.; Ye, X.; Shi, X. *Org. Lett.* **2010**, *12*, 2088.
- <sup>42</sup> Wang, D.; Gautam, L. N. S.; Bollinger, C.; Harris, A.; Li, M.; Shi, X. *Org. Lett.* **2011**, *13*, 2618.
- <sup>43</sup> The DFT computational studies were carried out by the Gaussian 03 program to a B3LYP/6-311G level.
- <sup>44</sup> Wang, Q.; Aparaj, S.; Akhmedov, N. G.; Petersen, J. L.; Shi, X. *Org. Lett.* **2012**, *14*, 1334.
- <sup>45</sup> (a) Jones, R. R.; Bergman, R. G. *J. Am. Chem. Soc.* **1972**, *94*, 660; (b) Bergman, R. G. *Acc. Chem. Res.* **1973**, *6*, 25; (c) Greer, E. M.; Lavinda, O. *J. Org. Chem.* **2010**, *75*, 8650; (d)

- 
- Vavilala, C.; Byrne, N.; Kraml, C. M.; Ho, D. M.; Pascal, R. A., Jr. *J. Am. Chem. Soc.* **2008**, *130*, 13549.
- <sup>46</sup> (a) Myers, A. G.; Kuo, E. Y.; Finney, N. S. *J. Am. Chem. Soc.* **1989**, *111*, 8057. (b) Myers, A. G.; Dragovich, P. S. *J. Am. Chem. Soc.* **1989**, *111*, 9130. (c) Nechab, M.; Campolo, D.; Maury, J.; Perfetti, P.; Vanthuynne, N.; Siri, D.; Bertrand, M. P. *J. Am. Chem. Soc.* **2010**, *132*, 14742; (d) Schmittel, M.; Strittmatter, M.; Kiau, S. *Tetrahedron Lett.* **1995**, *36*, 4975; (e) Schmittel, M.; Strittmatter, M.; Kiau, S. *Angew. Chem. Int. Ed.* **1996**, *35*, 1843; (f) Vavilala, C.; Bats, J. W.; Schmittel, M. *Synthesis* **2010**, *13*, 2213.
- <sup>47</sup> (a) Nicolaou, K. C.; Dai, W. M. *Angew. Chem. Int. Ed.* **1991**, *30*, 1387; (b) Choi, T. A.; Czerwonka, R.; Freohner, W.; Krahl, M. P.; Reddy, K. R.; Franzblau, S. G.; Kneolker, H. J. *Chem-Med Chem.* **2006**, *1*, 812; (c) Thevissen, K.; Marchand, A.; Chaltin, P.; Meert, E. M. K.; Cammue, B. P. *A Curr. Med. Chem.* **2009**, *16*, 2205.
- <sup>48</sup> (a) Alabugin, I. V.; Gilmore, K.; Patil, S.; Manoharan, M.; Kovalenko, S. V.; Clark, R. J.; Ghiviriga, I. *J. Am. Chem. Soc.* **2008**, *130*, 11535; (b) Sakai, S.; Nishitani, M. *J. Phys. Chem. A* **2010**, *114*, 11807; (c) Prall, M.; Wittkopp, A.; Schreiner, P. R. *J. Phys. Chem. A* **2001**, *105*, 9265; (d) Sakai, S.; Nishitani, M. *J. Phys. Chem. A* **2010**, *114*, 11807; (e) Chen, H. T.; Chen, H. L.; Ho, J. J. *J. Phys. Org. Chem.* **2010**, *23*, 134.
- <sup>49</sup> (a) Gillmann, T.; Isen, T. H.; Massa, W.; Wocadlo, S. *Synlett* **1995**, 1257; (b) Garcia, J. G.; Ramos, B.; Pratt, L. M.; Rodriguez, A. *Tetrahedron Lett.* **1995**, *36*, 7391.
- <sup>50</sup> Schmittel, M.; Mahajan, A. A.; Bucher, G. *J. Am. Chem. Soc.* **2005**, *127*, 5324.
- <sup>51</sup> Schmittel, M.; Strittmatter, M.; Kiau, S. *Angew. Chem.* **1996**, *108*, 1952.
- <sup>52</sup> Wang, K. K.; Wang, Z.; Tarli, A.; Gannett, P. *J. Am. Chem. Soc.* **1996**, *118*, 10783.

- 
- <sup>53</sup> (a) Nicolaou, K. C.; Maligres, P.; Shin, J.; de Leon, E.; Rideout, D. *J. Am. Chem. Soc.* **1990**, *112*, 7825; (b) Nicolaou, K. C.; Dai, W. M. *Angew. Chem.* **1991**, *103*, 1453; (c) Lee, S. H.; Goldberg, I. H. *Biochemistry* **1989**, *28*, 1019; (d) Goldberg, I. H. *Free Radicals Biol. Med.* **1987**, *3*, 41; (e) Povirk, L. F.; Dattagupta, N.; Warf, B. C.; Goldberg, I. H. *Biochemistry* **1981**, *20*, 4007.
- <sup>54</sup> Walker, S.; Landovitz, R.; Ding, W. D.; Ellestad, G. A.; Kahne, D. *Proc. Natl. Acad. Sci.* **1992**, *89*, 4608.
- <sup>55</sup> Kobayashi, S.; Hori, M.; Wang, G. X.; Hiramama, M. *J. Org. Chem.* **2005**, *71*, 636.
- <sup>56</sup> (a) Pandithavidana, D. R.; Poloukhtine, A.; Popik, V. V. *J. Am. Chem. Soc.* **2008**, *131*, 351; for recent reviews please see: (b) Peterson, P. W.; Mohamed, R. K.; Alabugin, I. V. *Eur. J. Org. Chem.* **2013**, 2505; (c) Bucher, G.; Mahajan, A. A.; Schmittel, M. *J. Org. Chem.* **2009**, *74*, 5850.
- <sup>57</sup> Schreiner, P. R.; Prall, M. *J. Am. Chem. Soc.* **1999**, *121*, 8615.
- <sup>58</sup> Schmittel, M.; Strittmatter, M.; Kiau, S. *Angew. Chem. Int. Ed.* **1996**, *35*, 1843.
- <sup>59</sup> Schmittel, M.; Mahajan, A. A.; Bucher, G. *J. Am. Chem. Soc.* **2005**, *127*, 5324.
- <sup>60</sup> (a) Tejedor, D.; Mendez-Abt, G.; Cotos, L.; Garcia-Tellado, F. *Chem. Soc. Rev.* **2013**, *42*, 458; (b) Hashmi, A. S. K. *In Modern Allene Chemistry*, Vol. 1; Krause, N., Hashmi, A. S. K., Eds.; Wiley-VCH Verlag: Weinheim, 2004; pp 3; (c) Myers, A. G.; Zheng, B. *J. Am. Chem. Soc.* **1996**, *118*, 4492; (d) Ready, J. M.; Pu, X. *J. Am. Chem. Soc.* **2008**, *130*, 10874; (e) Furstner, A.; Mendez, M. *Angew. Chem. Int. Ed.* **2003**, *115*, 5513. (f) Burton, B. S.; von Pechmann, H. *Ber. Dtsch. Chem. Ges* **1887**, *20*, 145.
- <sup>61</sup> (a) Wen, B.; Petersen, J. L.; Wang, K. K. *Chem. Commun.* **2010**, *46*, 1938; (b) Cui, H.; Akhmedov, N. G.; Petersen, J. L.; Wang, K. K. *J. Org. Chem.* **2010**, *75*, 2050.



- 
- <sup>62</sup> (a) Xiao, Y.; Hu, A. *Macromol. Rapid Commun.* **2011**, *32*, 1688; (b) Ma, J.; Ma, X.; Deng, S.; Li, F.; Hu, A. *J. Polym. Sci., Part A: Polym. Chem.* **2011**, *49*, 1368.
- <sup>63</sup> Nieto-Oberhuber, C.; López, S.; Echavarren, A. M. *J. Am. Chem. Soc.* **2005**, *127*, 6178.
- <sup>64</sup> Duan, H.; Sengupta, S.; Petersen, J. L.; Akhmedov, N. G.; Shi, X. *J. Am. Chem. Soc.* **2009**, *131*, 12100.
- <sup>65</sup> (a) R. H. Pritchard, C.W. Kern, *J. Am. Chem. Soc.* **1969**, *91*, 1631; (b) S. J. Blanksby, G. B. Ellison, *Acc. Chem. Res.* **2003**, *36*, 255; (c) L. R. Thorne, R. D. Suenram, F. J. Lovas, *J. Chem. Phys.* **1983**, *78*, 167; (d) D. J. Grant, D. A. Dixon, *J. Phys. Chem. A* **2006**, *110*, 12955.
- <sup>66</sup> (a) A. Stock, E. Pohland, *Ber. Dtsch. Chem. Ges.* **1926**, *59*, 2210; (b) D. F. Gaines, J. Borlin in *Boron Hydride Chemistry* (Ed. E. L. Muetterties), Academic Press, New York, 1975, pp. 241.
- <sup>67</sup> J.M. Carrapichanoa; J.R. Gomesb; R.F. Silvac, *Wear*, **2002**. 1070.
- <sup>68</sup> (a) Davis, B. L.; Dixon, D. A.; Garner, E. B.; Gordon, J. C.; Matus, M. H.; Scott, B.; Stephens, F. H. *Angewandte Chemie International Edition* **2009**, *48*, 6812; (b) F. H. Stephens, V. Pons, R. T. Baker, *Dalton Trans.* **2007**, 2613; (c) M. H. Matus, K. D. Anderson, D. M. Camaioni, S. T. Autrey, D. A. Dixon, *J. Phys. Chem. A* **2007**, *111*, 4411; (d) M. E. Bluhm, M. G. Bradley, R. Butterick III, U. Kusari, L. G. Sneddon, *J. Am. Chem. Soc.* **2006**, *128*, 7748; (e) M. C. Denney, V. Pons, T. J. Hebden, D. M. Heinekey, K. I. Goldberg, *J. Am. Chem. Soc.* **2006**, *128*, 12048.
- <sup>69</sup> (a) A. J. Fritsch, *Chem. Heterocycl. Compd.* **1977**, *30*, 381; (b) W. E. Piers, M. J. D. Bosdet, *Can. J. Chem.* **2009**, *87*, 8.
- <sup>70</sup> M. Faraday, *Phil. Trans. R. Soc.* **1825**. *115*. 440.
- <sup>71</sup> Please see reference 64.

- 
- <sup>72</sup> Marwitz, A. J. V.; Matus, M. H.; Zakharov, L. N.; Dixon, D. A.; Liu, S.-Y. *Angew. Chem. Int. Ed.* **2009**, *48*, 973.
- <sup>73</sup> M. J. S. Dewar, V. P. Kubba, R. Pettit, *J. Chem. Soc.* **1958**, 3073.
- <sup>74</sup> M. J. S. Dewar, R. Dietz, *J. Chem. Soc.* **1959**, 2728.
- <sup>75</sup> K. M. Davies, M. J. S. Dewar, P. Rona, *J. Am. Chem. Soc.* **1967**, *89*, 6294.
- <sup>76</sup> (a) M. Ferles, Z. Polivka, *Collect. Czech. Chem. Commun.* **1968**, *33*, 2121; (b) Z. Polivka, V. Kubelka, N. Holubova, M. Ferles, *Collect. Czech. Chem. Commun.* **1970**, *35*, 1131.
- <sup>77</sup> H. Wille, J. Goubeau, *Chem. Ber.* **1972**, *105*, 2156; (b) H. Wille, J. Goubeau, *Chem. Ber.* **1974**, *107*, 110.
- <sup>78</sup> M. J. S. Dewar, P. A. Marr, *J. Am. Chem. Soc.* **1962**, *84*, 3782; (b) S. Gronowitz, I. Ander, *Chem. Scr.* **1980**, *15*, 23; (c) S. Gronowitz, I. Ander, *Chem. Scr.* **1980**, *15*, 135; (d) S. Gronowitz, I. Ander, *Chem. Scr.* **1980**, *15*, 145.
- <sup>79</sup> (a) A. J. Ashe, X. D. Fang, *Org. Lett.* **2000**, *2*, 2089; (b) A. J. Ashe, X. Fang, X. Fang, J. Kampf, *Organometallics* **2001**, *20*, 5413; (c) J. Pan, J. W. Kampf, A. J. Ashe, *Organometallics* **2004**, *23*, 5626; (d) J. Pan, J. W. Kampf, A. J. Ashe, *Organometallics* **2008**, *27*, 1345; (e) X. Fang, H. Yang, J. Kampf, M. Holl, A. J. Ashe, *Organometallics* **2006**, *25*, 513; (f) J. Pan, J. W. Kampf, A. J. Ashe, *Org. Lett.* **2007**, *9*, 679; (g) J. Pan, J. W. Kampf, A. J. Ashe, *Organometallics* **2009**, *28*, 506; (h) J. Pan, J. W. Kampf, A. J. Ashe, *J. Organomet. Chem.* **2009**, *694*, 1036.
- <sup>80</sup> A. J. V. Marwitz, M. H. Matus, L. N. Zakharov, D. A. Dixon, S.-Y. Liu, *Angew. Chem.* **2009**, *121*, 991.
- <sup>81</sup> (a) E. R. Abbey, L. N. Zakharov, S.-Y. Liu, *J. Am. Chem. Soc.* **2010**, *132*, 16340; (b) Matus, M. H.; Liu, S.-Y.; Dixon, D. A. *J. Phys. Chem. A* **2010**, *114*, 2644; (c) Luo, W.; Campbell, P.

---

G.; Zakharov, L. N.; Liu, S.-Y. *J. Am. Chem. Soc.* **2011**, *133*, 19326; (d) Xu, S.; Zakharov, L. N.; Liu, S.-Y. *J. Am. Chem. Soc.* **2011**, *133*, 20152; (e) Xu, S.; Mikulas, T. C.; Zakharov, L. N.; Dixon, D. A.; Liu, S.-Y. *Angew. Chem. Int. Ed.* **2013**, *52*, 7527.

<sup>82</sup> Please see reference 72 and 75.

<sup>83</sup> (a) Scheideman, M.; Shapland, P.; Vedejs, E. *J. Am. Chem. Soc.* **2003**, *125*, 10502; (b) Zhang, L.; Peng, D.; Leng, X.; Huang Z. *Angew. Chem. Int. Ed.* **2013**, *52*, 3676; (c) Wang, G.; Vedejs, E. *Org. Lett.* **2009**, *11*, 1059; (d) Oyola, Y.; Singleton, D. A. *J. Am. Chem. Soc.* **2009**, *131*, 3130; (e) Scheideman, M.; Wang, G.; Vedejs, E. *J. Am. Chem. Soc.* **2008**, *130*, 8669.

<sup>84</sup> (a) Zhao, X.; Liang, L.; Stephan, D. W. *Chem. Commun.* **2012**, *48*, 10189; (b) Clary, J. W.; Rettenmaier, T. J.; Snelling, R.; Bryks, W.; Banwell, J.; Wipke, W. T.; Singaram, B. *J. Org. Chem.* **2011**, *76*, 9602.

<sup>85</sup> Please see reference 81.

<sup>86</sup> (a) Haberberger M.; Enthaler S. *Chem. Asian J.* **2013**, *8*, 50; (b) Neilson, B. M.; Bielawski, C. W. *Organometallics* **2013**, *32*, 3121; (c) Gunanathan, C.; Hölscher, M.; Pan, F.; Leitner, W. *J. Am. Chem. Soc.* **2012**, *134*, 14349; (d) Leyva, A.; Zhang X.; Corma A. *Chem. Commun.* **2009**, 4947; (e) He X.; Hartwig J. F. *J. Am. Chem. Soc.* **1996**, *118*, 1696.

<sup>87</sup> Please see reference 62.

<sup>88</sup> (a) Oliver-Meseguer, J.; Leyva-Perez, A.; Al-Resayes S. I.; Corma, A. *Chem. Commun.* **2013**, *49*, 7782; (b) Oliver-Meseguer, J.; Cabrero-Antonino, J. R.; Domínguez, I.; Leyva-Pérez, A.; Corma, A. *Science* **2012**, *338*, 1452.

<sup>89</sup> Please see reference 61.

<sup>90</sup> Schnurr, A.; Vitze, H.; Bolte, M.; Lerner, H.-W.; Wagner, M. *Organometallics* **2010**, *29*, 6012.



## Appendix

Publications during Ph.D. work at West Virginia University:

- 1). Wang, Q.; Motika, S. E.; Akhmedov, N. G.; Petersen, J. L.; Shi, X. *Angewandte Chemie International Edition* **2014** accepted.
- 2). Xi, Y.; Wang, Q.; Su, Y.; Li, M.; Shi, X. *Chemical Communications* **2014**, *50*, 2158.
- 3). Wang, K.; Chen, M.; Wang, Q.; Shi, X.; Lee, J. K. *The Journal of Organic Chemistry* **2013**, *78*, 7249.
- 4). Gautam, L. N.; Wang, Q.; Akhmedov, N. G.; Petersen, J. L.; Shi, X. *Organic & Biomolecular Chemistry* **2013**, *11*, 1917.
- 5). Wang, Q.; Aparaj, S.; Akhmedov, N. G.; Petersen, J. L.; Shi, X. *Organic Letters* **2012**, *14*, 1334.
- 6). Li, M.; Wang, Q.; Shi, X.; Hornak, L. A.; Wu, N. *Analytical Chemistry* **2011**, *83*, 7061.
- 7). Li, M.; Cushing, S. K.; Wang, Q.; Shi, X.; Hornak, L. A.; Hong, Z.; Wu, N. *The Journal of Physical Chemistry Letters* **2011**, *2*, 2125.
- 8). Yan, W.; Wang, Q.; Lin, Q.; Li, M.; Petersen, J. L.; Shi, X. *Chemistry – A European Journal* **2011**, *17*, 5011.
- 9). Yan, W.; Wang, Q.; Chen, Y.; Petersen, J. L.; Shi, X. *Organic Letters* **2010**, *12*, 3308.

## Supporting Information

### Chapter One: Iron catalyzed C-O bond activation for the synthesis of propargyl-1,2,3-triazoles and 1,1-bis-triazoles

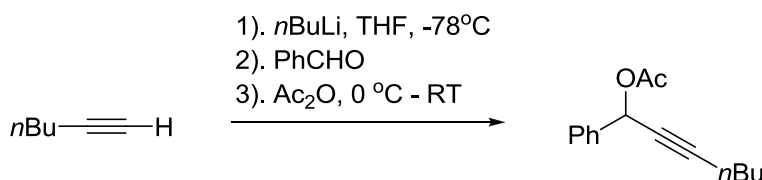
#### I. General Methods and materials

All of the reactions dealing with air and/or moisture-sensitive reactions were carried out under an atmosphere of nitrogen using oven/flame-dried glassware and standard syringe/septa techniques. Unless otherwise noted, all commercial reagents and solvents were obtained from the commercial provider and used without further purification.  $^1\text{H}$  NMR and  $^{13}\text{C}$  NMR spectra were recorded on Varian 600 MHz spectrometers. Chemical shifts were reported relative to internal tetramethylsilane ( $\delta$  0.00 ppm) or  $\text{CDCl}_3$  ( $\delta$  7.26 ppm) for  $^1\text{H}$  and  $\text{CDCl}_3$  ( $\delta$  77.0 ppm) for  $^{13}\text{C}$ . Flash column chromatography was performed on 230-430 mesh silica gel. Analytical thin layer chromatography was performed with precoated glass baked plates (250 $\mu$ ) and visualized by fluorescence and by charring after treatment with potassium permanganate stain. Melting points were measured on a Mel-Temp 1001D apparatus and uncorrected. HRMS were recorded on LTQ-FTUHRA spectrometer.

Substrates **1.2b**, **1.4** were synthesized according to the literatures as below:

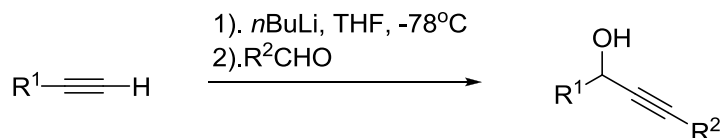
1. Yu, M.; Zhang, G.; Zhang, L. *Org. Lett.* **2007**, *9*, 2147-2150.
2. Marion, N.; Carlqvist, P.; Gealageas, R.; Fremont, P.; Maseras, F.; Nolan, S. P. *Chem. Eur. J.* **2007**, *13*, 6437-6451.
3. Wang, D.; Ye, X.; Shi, X. *Org. Lett.* **2010**, *12*, 2088-2091.

#### Representative procedure for the preparation of propargylic acetate **1.2a**



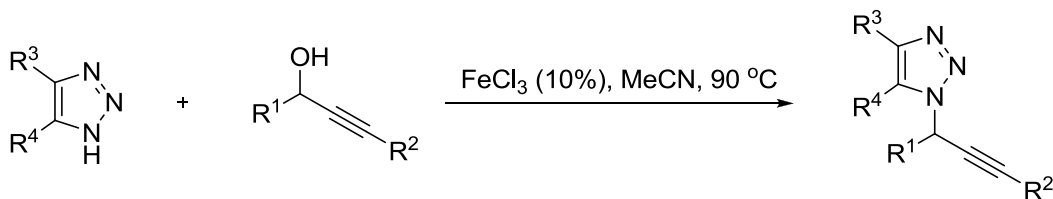
To a solution of hex-1-yne (39 mmol) in anhydrous THF (50 mL) at  $-78\text{ }^{\circ}\text{C}$  under  $\text{N}_2$  atmosphere was added *n*-BuLi (1.6 M solution in hexanes, 20.6 mL, 33 mmol). The reaction was stirred at this temperature for 20 min then at room temperature for 1h. After cooling to at  $-78\text{ }^{\circ}\text{C}$ , benzaldehyde (30 mmol) was added to the mixture and was allowed to warm to room temperature gradually and stirred for an additional hour. After addition of acetate anhydrous (60 mmol) at  $0\text{ }^{\circ}\text{C}$ , the reaction mixture was warmed to room temperature and stirred for 2h before quenched with aqueous  $\text{NH}_4\text{Cl}$ . The mixture was extracted with EtOAc (3 x 20 mL), and the combined organic phases were washed with water and brine, dried with anhydrous  $\text{MgSO}_4$ , and filtered. The filtrate was concentrated under reduced pressure and the residue was purified by flash chromatography on silica gel (hexanes/ethyl acetate, V/V, 20:1) to produce the desired acetate as yellow oil in quantitative yield.

#### Representative procedure for the preparation of propargylic alcohol 1.4



To a solution of alkyne (39 mmol) in anhydrous THF (50 mL) at  $-78\text{ }^{\circ}\text{C}$  under  $\text{N}_2$  atmosphere was added *n*-BuLi (1.6 M solution in hexanes, 20.6 mL, 33 mmol). The reaction was stirred at this temperature for 20 min then at room temperature for 1h. After cooling to at  $-78\text{ }^{\circ}\text{C}$ , aldehyde (30 mmol) was added to the mixture and was allowed to warm to room temperature gradually and stirred for an additional hour before quenched with aqueous  $\text{NH}_4\text{Cl}$ . The mixture was extracted with EtOAc (3 x 20 mL), and the combined organic phases were washed with water and brine, dried with anhydrous  $\text{MgSO}_4$ , and filtered. The filtrate was concentrated under reduced pressure and the residue was purified by flash chromatography on silica gel (hexanes/ethyl acetate, V/V, 15:1) to produce the desired alcohol as yellow oil in quantitative yield.

#### Representative procedure for propargylation of 1.4 with triazoles

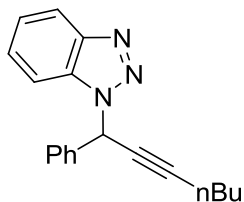


A solution of propargylic alcohol (1 mmol) and triazole (1.2 mmol) with catalyst iron(III) chloride (0.1 mmol) in acetonitrile (10 ml) was stirred at 90 degree in the presence of water

condensor for 5h. The reaction mixture was quenched with 10 ml distilled water and then extracted with EtOAc (3 x 10 mL). The combined organic phases were washed with water and brine, dried with anhydrous  $\text{MgSO}_4$ , and filtered. The filtrate was concentrated under reduced pressure and the residue was purified by flash chromatography on silica gel (hexanes/ethyl acetate, V/V, 15:1) to produce the desired product as yellow oil except for **1.3f**.

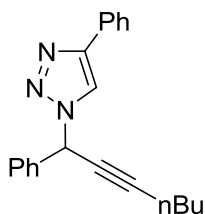


## II. Compounds Characterization



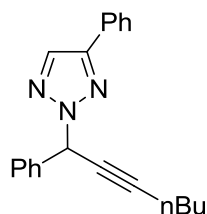
**1.3a (N1)**

**1-(1-phenylhept-2-ynyl)-1H-benzo[d][1,2,3]triazole (1.3a (N1)):**  $^1\text{H-NMR}$  (600 MHz,  $\text{CDCl}_3$ )  $\delta$  8.04 (d,  $J = 8.4$  Hz, 1H), 7.54-7.51 (m, 3H), 7.37-7.29 (m, 5H), 7.14 (s, 1H), 2.34 (dt,  $J = 7.2$  Hz, 2.4 Hz, 2H), 1.56 (quintet,  $J = 7.2$  Hz, 2H), 1.42 (hextet,  $J = 7.2$  Hz, 2H), 0.90 (t,  $J = 7.2$  Hz, 3H);  $^{13}\text{C-NMR}$  (150 MHz,  $\text{CDCl}_3$ )  $\delta$  146.7, 135.9, 131.3, 128.7, 128.6, 127.1, 123.9, 120.0, 111.1, 90.3, 73.6, 55.5, 30.4, 21.9, 18.4, 13.4; HRMS Calculated for  $\text{C}_{19}\text{H}_{20}\text{N}_3$   $[\text{M}+\text{H}]^+$ : 290.16572, Found: 290.16517.



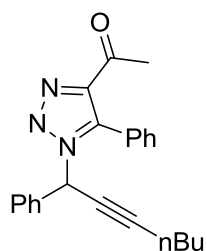
**1.3b (N1)**

**4-phenyl-1-(1-phenylhept-2-ynyl)-1H-1,2,3-triazole (1.3b (N1)):**  $^1\text{H-NMR}$  (600 MHz,  $\text{CDCl}_3$ )  $\delta$  7.89 (s, 1H), 7.82 (d,  $J = 7.8$  Hz, 2H), 7.52 (d,  $J = 7.2$  Hz, 2H), 7.41-7.30 (m, 6H), 6.73 (s, 1H), 2.37 (dt,  $J = 7.2$  Hz, 1.8 Hz, 2H), 1.60 (quintet,  $J = 7.2$  Hz, 2H), 1.47 (hextet,  $J = 7.2$  Hz, 2H), 0.95 (t,  $J = 7.2$  Hz, 3H);  $^{13}\text{C-NMR}$  (150 MHz,  $\text{CDCl}_3$ )  $\delta$  148.0, 136.7, 130.5, 129.0, 128.8, 128.7, 128.1, 127.1, 125.7, 118.0, 90.1, 74.4, 56.3, 30.4, 22.0, 18.5, 13.5; HRMS Calculated for  $\text{C}_{21}\text{H}_{22}\text{N}_3$   $[\text{M}+\text{H}]^+$ : 316.18137, Found: 316.18082.



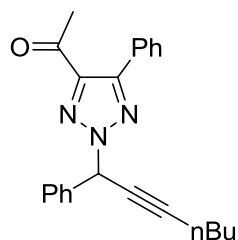
**1.3b (N2)**

**4-phenyl-2-(1-phenylhept-2-ynyl)-2H-1,2,3-triazole (1.3b (N2)):**  $^1\text{H-NMR}$  (600 MHz,  $\text{CDCl}_3$ )  $\delta$  7.89 (s, 1H), 7.81 (d,  $J = 7.2$  Hz, 2H), 7.59 (d,  $J = 7.2$  Hz, 2H), 7.42 (t,  $J = 7.2$  Hz, 2H), 7.39-7.32 (m, 5H), 2.37 (dt,  $J = 7.2$  Hz, 1.8 Hz, 2H), 1.59 (quintet,  $J = 7.2$  Hz, 2H), 1.47 (hextet,  $J = 7.2$  Hz, 2H), 0.94 (t,  $J = 7.2$  Hz, 3H);  $^{13}\text{C-NMR}$  (150 MHz,  $\text{CDCl}_3$ )  $\delta$  147.9, 137.0, 131.7, 130.3, 128.7, 128.6, 128.5, 128.4, 127.4, 126.0, 89.3, 74.7, 60.8, 30.4, 21.9, 18.6, 13.5; HRMS Calculated for  $\text{C}_{21}\text{H}_{22}\text{N}_3$   $[\text{M}+\text{H}]^+$ : 316.18137, Found: 316.18082.



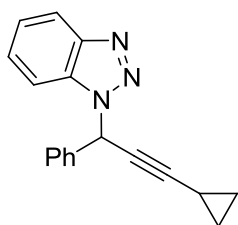
**1.3c (N1)**

**phenyl(5-phenyl-1-(1-phenylhept-2-ynyl)-1H-1,2,3-triazol-4-yl)methanone (1.3c (N1)):**  $^1\text{H-NMR}$  (600 MHz,  $\text{CDCl}_3$ )  $\delta$  8.26 (d,  $J = 7.2$  Hz, 2H), 7.56 (d,  $J = 7.2$  Hz, 1H), 7.47 (t,  $J = 7.2$  Hz, 2H), 7.38-7.29 (m, 4H), 7.25-7.23 (m, 4H), 7.05 (dd,  $J = 7.2$  Hz, 2.4 Hz, 2H), 6.27 (t,  $J = 3.6$  Hz, 1H), 2.71 (dt,  $J = 7.2$  Hz, 1.8 Hz, 2H), 1.54 (quintet,  $J = 7.2$  Hz, 2H), 1.28 (hextet,  $J = 7.2$  Hz, 2H), 0.89 (t,  $J = 7.2$  Hz, 3H);  $^{13}\text{C-NMR}$  (150 MHz,  $\text{CDCl}_3$ )  $\delta$  186.4, 141.9, 141.5, 137.1, 133.0, 131.9, 130.7, 129.8, 129.6, 128.7, 128.5, 128.4, 128.2, 127.8, 127.4, 126.8, 111.8, 103.4, 32.3, 28.7, 22.0, 13.7; HRMS Calculated for  $\text{C}_{28}\text{H}_{26}\text{N}_3\text{O}$   $[\text{M}+\text{H}]^+$ : 420.20759, Found: 420.20704.



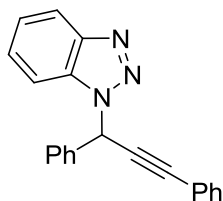
**1.3c (N2)**

**phenyl(5-phenyl-2-(1-phenylhept-2-ynyl)-2H-1,2,3-triazol-4-yl)methanone (1.3c (N2)):**  $^1\text{H-NMR}$  (600 MHz,  $\text{CDCl}_3$ )  $\delta$  8.08 (d,  $J = 8.4$  Hz, 2H), 7.83 (dd,  $J = 7.2$  Hz, 2.4 Hz, 2H), 7.63 (d,  $J = 7.2$  Hz, 2H), 7.59 (t,  $J = 7.8$  Hz, 1H), 7.46 (t,  $J = 7.8$  Hz, 2H), 7.41-7.37 (m, 6H), 6.69 (t,  $J = 2.4$  Hz, 1H), 2.37 (dt,  $J = 7.2$  Hz, 2.4 Hz, 2H), 1.60 (quintet,  $J = 7.2$  Hz, 2H), 1.48 (hextet,  $J = 7.8$  Hz, 2H), 0.94 (t,  $J = 7.2$  Hz, 3H);  $^{13}\text{C-NMR}$  (150 MHz,  $\text{CDCl}_3$ )  $\delta$  187.7, 149.9, 142.1, 137.2, 136.4, 133.2, 130.6, 129.7, 129.0, 128.9, 128.8, 128.7, 128.2, 128.1, 127.6, 90.0, 74.3, 61.5, 30.4, 21.9, 18.6, 13.5; HRMS Calculated for  $\text{C}_{28}\text{H}_{26}\text{N}_3\text{O}$   $[\text{M}+\text{H}]^+$ : 420.20759, Found: 420.20704.



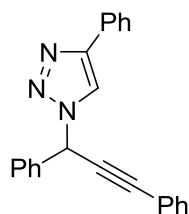
**1.3d (N1)**

**1-(3-cyclopropyl-1-phenylprop-2-ynyl)-1H-benzo[d][1,2,3]triazole (1.3d (N1)):**  $^1\text{H-NMR}$  (600 MHz,  $\text{CDCl}_3$ )  $\delta$  8.05 (d,  $J = 8.4$  Hz, 1H), 7.52 (d,  $J = 7.8$  Hz, 1H), 7.49 (d,  $J = 7.2$  Hz, 2H), 7.38-7.29 (m, 5H), 7.10 (s, 1H), 1.40-1.37 (m, 1H), 0.86-0.83 (m, 2H), 0.78-0.75 (m, 2H);  $^{13}\text{C-NMR}$  (150 MHz,  $\text{CDCl}_3$ )  $\delta$  143.4, 136.0, 134.6, 131.8, 128.8, 128.7, 127.2, 127.0, 123.9, 120.0, 111.1, 93.2, 68.7, 55.5, 8.4; HRMS Calculated for  $\text{C}_{18}\text{H}_{16}\text{N}_3$   $[\text{M}+\text{H}]^+$ : 274.13442, Found: 274.13423.



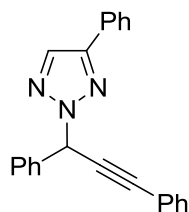
**1.3e (N1)**

**1-(1,3-diphenylprop-2-ynyl)-1H-benzo[d][1,2,3]triazole (1.3e (N1)):**  $^1\text{H-NMR}$  (600 MHz,  $\text{CDCl}_3$ )  $\delta$  8.08 (d,  $J = 7.2$  Hz, 1H), 7.60-7.64 (m, 3H), 7.52 (d,  $J = 7.8$  Hz, 2H), 7.40-7.33 (m, 9H);  $^{13}\text{C-NMR}$  (150 MHz,  $\text{CDCl}_3$ )  $\delta$  146.8, 135.4, 131.8, 131.4, 129.2, 128.9, 128.8, 128.4, 127.4, 127.0, 124.0, 121.5, 120.1, 111.0, 89.1, 82.4, 55.7; HRMS Calculated for  $\text{C}_{21}\text{H}_{16}\text{N}_3$   $[\text{M}+\text{H}]^+$ : 310.13442, Found: 310.13387.



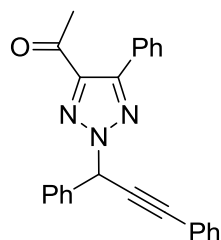
**1.3f (N1)**

**1-(1,3-diphenylprop-2-ynyl)-4-phenyl-1H-1,2,3-triazole (1.3f (N1)):**  $^1\text{H-NMR}$  (600 MHz,  $\text{CDCl}_3$ )  $\delta$  7.96 (s, 1H), 7.83 (d,  $J = 8.4$  Hz, 2H), 7.61 (d,  $J = 7.2$  Hz, 2H), 7.55 (d,  $J = 7.2$  Hz, 2H), 7.44-7.37 (m, 8H), 7.33-7.31 (m, 1H), 6.99 (s, 1H);  $^{13}\text{C-NMR}$  (150 MHz,  $\text{CDCl}_3$ )  $\delta$  148.3, 136.2, 131.9, 130.5, 129.3, 129.2, 129.1, 128.8, 128.5, 128.2, 127.2, 125.8, 121.4, 118.1, 88.8, 83.1, 56.7; HRMS Calculated for  $\text{C}_{23}\text{H}_{18}\text{N}_3$   $[\text{M}+\text{H}]^+$ : 336.15007, Found: 336.14992.



**1.3f (N2)**

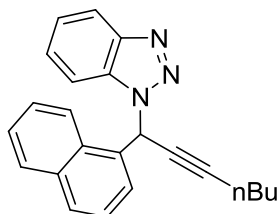
**2-(1,3-diphenylprop-2-ynyl)-4-phenyl-2H-1,2,3-triazole (1.3f (N2)):**  $^1\text{H-NMR}$  (600 MHz,  $\text{CDCl}_3$ )  $\delta$  7.95 (s, 1H), 7.86 (d,  $J = 7.2$  Hz, 2H), 7.72 (d,  $J = 7.2$  Hz, 2H), 7.59 (dd,  $J = 7.2$  Hz, 2.4 Hz, 2H), 7.45 (q,  $J = 7.8$  Hz, 4H), 7.40-7.35 (m, 5H), 6.94 (s, 1H);  $^{13}\text{C-NMR}$  (150 MHz,  $\text{CDCl}_3$ )  $\delta$  148.2, 136.4, 131.9, 131.8, 130.2, 128.9, 128.8, 128.7, 128.5, 128.2, 127.5, 126.0, 122.0, 88.0, 83.7, 61.0; HRMS Calculated for  $\text{C}_{23}\text{H}_{18}\text{N}_3$   $[\text{M}+\text{H}]^+$ : 336.15007, Found: 336.14992.



**1.3g (N2)**

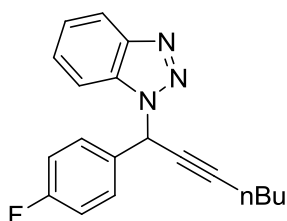
**(2-(1,3-diphenylprop-2-ynyl)-5-phenyl-2H-1,2,3-triazol-4-yl)(phenyl)methanone (1.3g (N2)):**  $^1\text{H-NMR}$  (600 MHz,  $\text{CDCl}_3$ )  $\delta$  8.10 (d,  $J = 8.4$  Hz, 2H), 7.86 (d,  $J = 7.8$  Hz, 2H), 7.72 (d,  $J = 7.2$  Hz, 2H), 7.60 (t,  $J = 7.8$  Hz, 1H), 7.56 (d,  $J = 7.8$  Hz, 2H), 7.47-7.34 (m, 11H), 6.94 (s, 1H);  $^{13}\text{C-NMR}$  (150 MHz,  $\text{CDCl}_3$ )  $\delta$  187.6, 150.1, 142.3, 137.2, 135.8, 133.3, 131.9, 130.6, 129.6,

129.2, 129.1, 129.0, 128.9, 128.8, 128.4, 128.3, 128.2, 127.8, 121.8, 88.7, 83.1, 61.8; HRMS Calculated for C<sub>30</sub>H<sub>22</sub>N<sub>3</sub>O [M+H]<sup>+</sup>: 440.17629, Found: 440.17679.



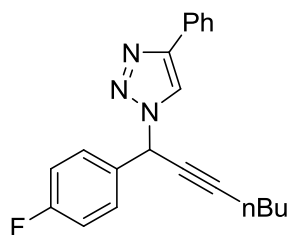
**1.3h (N1)**

**1-(1-(naphthalen-1-yl)hept-2-ynyl)-1H-benzo[d][1,2,3]triazole (1.3h (N1)):** <sup>1</sup>H-NMR (600 MHz, CDCl<sub>3</sub>) δ 8.25 (d, *J* = 9.0 Hz, 1H), 8.19 (d, *J* = 7.2 Hz, 1H), 7.99 (d, *J* = 8.4 Hz, 1H), 7.87 (d, *J* = 8.4 Hz, 1H), 7.82 (d, *J* = 9.0 Hz, 2H), 7.55 (t, *J* = 7.2 Hz, 1H), 7.48-7.41 (m, 3H), 7.30-7.23 (m, 2H), 2.32 (dt, *J* = 7.2 Hz, 2.4 Hz, 2H), 1.54 (quintet, *J* = 7.2 Hz, 2H), 1.39 (hextet, *J* = 7.2 Hz, 2H), 0.88 (t, *J* = 7.2 Hz, 3H); <sup>13</sup>C-NMR (150 MHz, CDCl<sub>3</sub>) δ 146.6, 134.0, 131.7, 130.6, 130.5, 130.3, 128.8, 127.1, 127.0, 126.5, 126.1, 124.8, 123.7, 122.9, 120.0, 111.1, 90.5, 74.3, 53.7, 30.4, 21.9, 18.5, 13.5; HRMS Calculated for C<sub>23</sub>H<sub>22</sub>N<sub>3</sub> [M+H]<sup>+</sup>: 340.18137, Found: 340.18082.



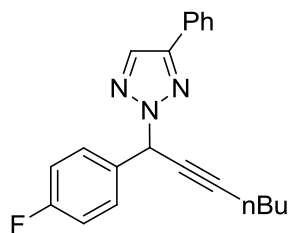
**1.3i (N1)**

**1-(1-(4-fluorophenyl)hept-2-ynyl)-1H-benzo[d][1,2,3]triazole (1.3i (N1)):** <sup>1</sup>H-NMR (600 MHz, CDCl<sub>3</sub>) δ 8.05 (d, *J* = 8.4 Hz, 1H), 7.53-7.49 (m, 3H), 7.37 (t, *J* = 7.2 Hz, 1H), 7.33 (t, *J* = 7.2 Hz, 1H), 7.11 (s, 1H), 7.02 (t, *J* = 8.4 Hz, 2H), 2.34 (dt, *J* = 7.2 Hz, 2.4 Hz, 2H), 1.56 (quintet, *J* = 7.2 Hz, 2H), 1.41 (hextet, *J* = 7.2 Hz, 2H), 0.90 (t, *J* = 7.2 Hz, 3H); <sup>13</sup>C-NMR (150 MHz, CDCl<sub>3</sub>) δ 163.6, 162.0, 146.8, 131.9, 131.8, 131.2, 129.0, 128.9, 127.2, 124.0, 120.1, 115.8, 115.6, 110.9, 90.6, 73.5, 54.8, 30.3, 21.9, 18.4, 13.4; HRMS Calculated for C<sub>19</sub>H<sub>19</sub>FN<sub>3</sub> [M+H]<sup>+</sup>: 308.15630, Found: 308.15588.



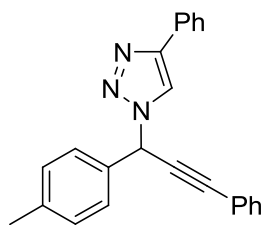
**1.3j (N1)**

**1-(1-(4-fluorophenyl)hept-2-ynyl)-4-phenyl-1H-1,2,3-triazole (1.3j (N1)):**  $^1\text{H-NMR}$  (600 MHz,  $\text{CDCl}_3$ )  $\delta$  7.89 (s, 1H), 7.82 (d,  $J = 7.2$  Hz, 2H), 7.51-7.49 (m, 2H), 7.38 (t,  $J = 7.8$  Hz, 2H), 7.30 (t,  $J = 7.2$  Hz, 1H), 7.04 (t,  $J = 7.8$  Hz, 2H), 6.68 (s, 1H), 2.35 (dt,  $J = 7.2$  Hz, 2.4 Hz, 2H), 1.58 (quintet,  $J = 7.2$  Hz, 2H), 1.45 (hextet,  $J = 7.2$  Hz, 2H), 0.93 (t,  $J = 7.2$  Hz, 3H);  $^{13}\text{C-NMR}$  (150 MHz,  $\text{CDCl}_3$ )  $\delta$  163.7, 162.1, 148.0, 132.6, 132.5, 130.3, 129.0, 128.9, 128.7, 128.2, 125.7, 117.9, 115.9, 115.7, 90.4, 74.2, 55.7, 30.3, 22.0, 18.4, 13.5; HRMS Calculated for  $\text{C}_{21}\text{H}_{21}\text{FN}_3$   $[\text{M}+\text{H}]^+$ : 334.17195, Found: 334.17140.



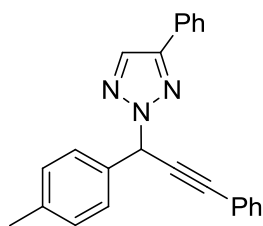
**1.3j (N2)**

**2-(1-(4-fluorophenyl)hept-2-ynyl)-4-phenyl-2H-1,2,3-triazole (1.3j (N2)):**  $^1\text{H-NMR}$  (600 MHz,  $\text{CDCl}_3$ )  $\delta$  7.88 (s, 1H), 7.79 (d,  $J = 7.2$  Hz, 2H), 7.57 (q,  $J = 4.8$  Hz, 2H), 7.42 (t,  $J = 7.8$  Hz, 2H), 7.36-7.33 (m, 1H), 7.05 (t,  $J = 7.8$  Hz, 2H), 6.64 (s, 1H), 2.36 (dt,  $J = 7.2$  Hz, 2.4 Hz, 2H), 1.58 (quintet,  $J = 7.2$  Hz, 2H), 1.47 (hextet,  $J = 7.2$  Hz, 2H), 0.93 (t,  $J = 7.2$  Hz, 3H);  $^{13}\text{C-NMR}$  (150 MHz,  $\text{CDCl}_3$ )  $\delta$  163.9, 162.3, 148.3, 133.1, 133.0, 132.0, 130.5, 129.7, 129.6, 129.0, 128.7, 126.3, 115.9, 115.7, 89.9, 74.9, 60.3, 30.7, 22.2, 18.8, 13.8; HRMS Calculated for  $\text{C}_{21}\text{H}_{21}\text{FN}_3$   $[\text{M}+\text{H}]^+$ : 334.17195, Found: 334.17140.



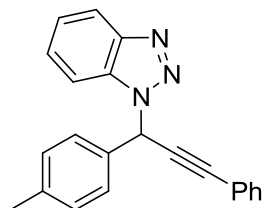
**1.3k (N1)**

**4-phenyl-1-(3-phenyl-1-p-tolylprop-2-ynyl)-1H-1,2,3-triazole (1.3k (N1)):**  $^1\text{H-NMR}$  (600 MHz,  $\text{CDCl}_3$ )  $\delta$  7.94 (s, 1H), 7.82 (d,  $J = 7.2$  Hz, 2H), 7.54 (d,  $J = 7.2$  Hz, 2H), 7.50 (d,  $J = 8.4$  Hz, 2H), 7.41-7.36 (m, 5H), 7.31 (t,  $J = 7.2$  Hz, 1H), 7.23 (d,  $J = 8.4$  Hz, 2H), 6.94 (s, 1H), 2.37 (s, 3H);  $^{13}\text{C-NMR}$  (150 MHz,  $\text{CDCl}_3$ )  $\delta$  148.2, 139.3, 133.2, 131.9, 130.5, 129.7, 129.3, 128.7, 128.5, 128.2, 127.2, 125.7, 121.5, 118.1, 88.6, 83.3, 56.5, 21.1; HRMS Calculated for  $\text{C}_{24}\text{H}_{20}\text{N}_3$   $[\text{M}+\text{H}]^+$ : 350.16572, Found: 350.16517.



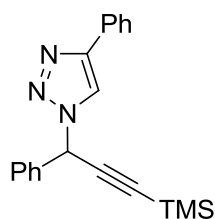
**1.3k (N2)**

**4-phenyl-2-(3-phenyl-1-p-tolylprop-2-ynyl)-2H-1,2,3-triazole (1.3k (N2)):**  $^1\text{H-NMR}$  (600 MHz,  $\text{CDCl}_3$ )  $\delta$  7.92 (s, 1H), 7.83 (d,  $J = 7.2$  Hz, 2H), 7.59-7.55 (m, 4H), 7.44 (t,  $J = 7.2$  Hz, 2H), 7.37-7.33 (m, 4H), 7.23 (d,  $J = 7.8$  Hz, 2H), 6.89 (s, 1H), 2.37 (s, 3H);  $^{13}\text{C-NMR}$  (150 MHz,  $\text{CDCl}_3$ )  $\delta$  148.1, 138.8, 133.5, 132.0, 131.8, 130.3, 129.4, 128.8, 128.7, 128.4, 128.2, 127.5, 126.0, 122.1, 87.8, 83.9, 60.8, 21.1; HRMS Calculated for  $\text{C}_{24}\text{H}_{20}\text{N}_3$   $[\text{M}+\text{H}]^+$ : 350.16572, Found: 350.16517.



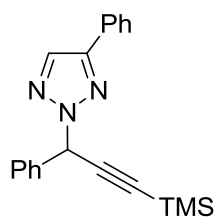
**1.3l (N1)**

**1-(3-phenyl-1-p-tolylprop-2-ynyl)-1H-benzo[d][1,2,3]triazole (1.3l (N1)):**  $^1\text{H-NMR}$  (600 MHz,  $\text{CDCl}_3$ )  $\delta$  8.07 (d,  $J = 8.4$  Hz, 1H), 7.62 (d,  $J = 8.4$  Hz, 1H), 7.51-7.48 (m, 4H), 7.40-7.32 (m, 6H), 7.18 (d,  $J = 7.8$  Hz, 2H), 2.33 (s, 3H);  $^{13}\text{C-NMR}$  (150 MHz,  $\text{CDCl}_3$ )  $\delta$  146.8, 138.9, 132.5, 131.9, 131.4, 129.6, 129.1, 128.4, 127.3, 127.0, 124.0, 121.7, 120.1, 111.1, 88.9, 82.7, 55.6, 21.1; HRMS Calculated for  $\text{C}_{22}\text{H}_{18}\text{N}_3$   $[\text{M}+\text{H}]^+$ : 324.15007, Found: 324.14952.



**1.3m (N1)**

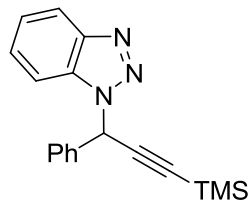
**4-phenyl-1-(1-phenyl-3-(trimethylsilyl)prop-2-ynyl)-1H-1,2,3-triazole (1.3m (N1)):**  $^1\text{H-NMR}$  (600 MHz,  $\text{CDCl}_3$ )  $\delta$  7.87 (s, 1H), 7.81 (d,  $J = 8.4$  Hz, 2H), 7.52 (d,  $J = 8.4$  Hz, 2H), 7.42-7.37 (m, 5H), 7.32 (t,  $J = 8.4$  Hz, 1H), 6.75 (s, 1H), 0.26 (s, 9H);  $^{13}\text{C-NMR}$  (150 MHz,  $\text{CDCl}_3$ )  $\delta$  148.2, 135.9, 130.5, 129.2, 129.0, 128.8, 128.2, 127.2, 125.7, 118.0, 98.8, 94.8, 56.6, -0.3; HRMS Calculated for  $\text{C}_{20}\text{H}_{22}\text{N}_3\text{Si}$   $[\text{M}+\text{H}]^+$ : 332.15830, Found: 332.15790.



**1.3m (N2)**

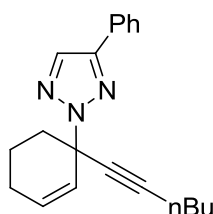
**4-phenyl-2-(1-phenyl-3-(trimethylsilyl)prop-2-ynyl)-2H-1,2,3-triazole (1.3m (N2)):**  $^1\text{H-NMR}$  (600 MHz,  $\text{CDCl}_3$ )  $\delta$  7.88 (s, 1H), 7.81 (d,  $J = 7.2$  Hz, 2H), 7.58 (d,  $J = 7.8$  Hz, 2H), 7.43-7.33 (m, 6H), 6.69 (s, 1H), 0.25 (s, 9H);  $^{13}\text{C-NMR}$  (150 MHz,  $\text{CDCl}_3$ )  $\delta$  148.1, 136.1, 131.9, 130.2, 128.8, 128.7, 128.6, 128.5, 127.5, 126.0, 99.1, 93.6, 61.0, -0.3; HRMS Calculated for  $\text{C}_{20}\text{H}_{22}\text{N}_3\text{Si}$   $[\text{M}+\text{H}]^+$ : 332.15830, Found: 332.15790.





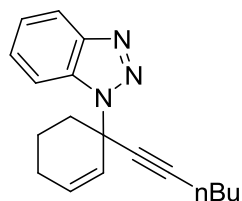
**1.3n (N1)**

**1-(1-phenyl-3-(trimethylsilyl)prop-2-ynyl)-1H-benzo[d][1,2,3]triazole (1.3n (N1)):**  $^1\text{H-NMR}$  (600 MHz,  $\text{CDCl}_3$ )  $\delta$  8.04 (d,  $J = 8.4$  Hz, 1H), 7.57 (d,  $J = 8.4$  Hz, 1H), 7.51 (d,  $J = 7.2$  Hz, 2H), 7.38-7.28 (m, 5H), 7.17 (s, 1H), 0.23 (s, 9H);  $^{13}\text{C-NMR}$  (150 MHz,  $\text{CDCl}_3$ )  $\delta$  146.7, 135.1, 131.3, 128.8, 128.7, 127.1, 126.9, 123.9, 120.0, 111.1, 98.0, 95.0, 55.7, -0.4; HRMS Calculated for  $\text{C}_{18}\text{H}_{20}\text{N}_3\text{Si}$   $[\text{M}+\text{H}]^+$ : 306.14265, Found: 306.14210.



**1.3o (N2)**

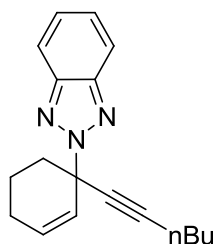
**2-(1-(hex-1-ynyl)cyclohex-2-enyl)-4-phenyl-2H-1,2,3-triazole (1.3o (N2)):**  $^1\text{H-NMR}$  (600 MHz,  $\text{CDCl}_3$ )  $\delta$  7.83 (s, 1H), 7.79 (d,  $J = 7.2$  Hz, 2H), 7.42 (t,  $J = 7.8$  Hz, 2H), 7.33 (t,  $J = 7.8$  Hz, 1H), 6.14 (s, 1H), 5.31-5.27 (m, 1H), 2.35-2.30 (m, 3H), 2.23-2.14 (m, 3H), 1.99-1.95 (m, 1H), 1.77-1.72 (m, 1H), 1.51 (quintet,  $J = 7.2$  Hz, 2H), 1.42 (sextet,  $J = 7.2$  Hz, 2H), 0.92 (t,  $J = 7.2$  Hz, 3H);  $^{13}\text{C-NMR}$  (150 MHz,  $\text{CDCl}_3$ )  $\delta$  147.7, 131.0, 130.8, 129.3, 129.0, 128.5, 126.2, 126.1, 90.8, 81.1, 61.0, 31.0, 29.7, 29.0, 22.2, 20.1, 19.2, 13.8; HRMS Calculated for  $\text{C}_{20}\text{H}_{24}\text{N}_3$   $[\text{M}+\text{H}]^+$ : 306.19702, Found: 306.19678.



**1.3p (N1)**

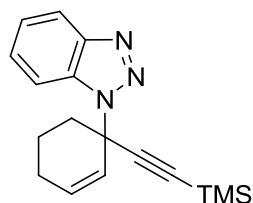
**1-(1-(hex-1-ynyl)cyclohex-2-enyl)-1H-benzo[d][1,2,3]triazole (1.3p (N1)):**  $^1\text{H-NMR}$  (600 MHz,  $\text{CDCl}_3$ )  $\delta$  8.06 (d,  $J = 7.8$  Hz, 1H), 7.57 (d,  $J = 8.4$  Hz, 1H), 7.45 (t,  $J = 7.2$  Hz, 1H), 7.35

(t, 7.2 Hz, 1H), 6.10 (s, 1H), 5.65-5.68 (m, 1H), 2.43-2.37 (m, 1H), 2.32 (t,  $J = 7.2$  Hz, 3H), 2.29-2.22 (m, 1H), 2.16-2.08 (m, 1H), 2.00-1.96 (m, 1H), 1.86-1.81 (m, 1H), 1.52 (quintet,  $J = 7.2$  Hz, 2H), 1.42 (sextet,  $J = 7.2$  Hz, 2H), 0.92 (t,  $J = 7.2$  Hz, 3H);  $^{13}\text{C-NMR}$  (150 MHz,  $\text{CDCl}_3$ )  $\delta$  146.5, 132.1, 128.8, 127.0, 126.9, 123.7, 120.1, 110.4, 91.3, 80.5, 56.4, 30.7, 29.5, 28.9, 21.9, 20.6, 19.0, 13.6; HRMS Calculated for  $\text{C}_{18}\text{H}_{22}\text{N}_3$   $[\text{M}+\text{H}]^+$ : 280.18137, Found: 280.18082.



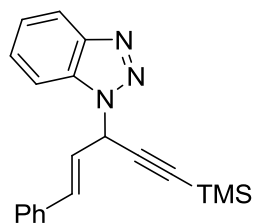
**1.3p (N2)**

**2-(1-(hex-1-ynyl)cyclohex-2-enyl)-2H-benzo[d][1,2,3]triazole (1.3p (N2)):**  $^1\text{H-NMR}$  (600 MHz,  $\text{CDCl}_3$ )  $\delta$  7.87 (dd,  $J = 6.6$  Hz, 3.0 Hz, 2H), 7.36 (dd,  $J = 6.6$  Hz, 3.0 Hz, 2H), , 6.19 (s, 1H), 5.55-5.58 (m, 1H), 2.39-2.21 (m, 6H), 2.02-1.97 (m, 1H), 1.80-1.76 (m, 1H), 1.50 (quintet,  $J = 7.2$  Hz, 2H), 1.41 (sextet,  $J = 7.2$  Hz, 2H), 0.90 (t,  $J = 7.2$  Hz, 3H);  $^{13}\text{C-NMR}$  (150 MHz,  $\text{CDCl}_3$ )  $\delta$  144.4, 128.8, 126.7, 126.4, 118.3, 91.3, 81.0, 62.7, 30.9, 29.7, 29.6, 22.1, 20.1, 19.2, 13.8; HRMS Calculated for  $\text{C}_{18}\text{H}_{22}\text{N}_3$   $[\text{M}+\text{H}]^+$ : 280.18137, Found: 280.18082.



**1.3q (N1)**

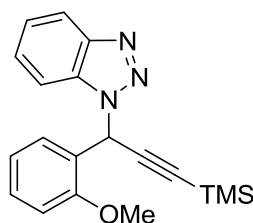
**1-(1-((trimethylsilyl)ethynyl)cyclohex-2-enyl)-1H-benzo[d][1,2,3]triazole (1.3q (N1)):**  $^1\text{H-NMR}$  (600 MHz,  $\text{CDCl}_3$ )  $\delta$  8.05 (d,  $J = 7.2$  Hz, 1H), 7.54 (d,  $J = 8.4$  Hz, 1H), 7.44 (t,  $J = 7.2$  Hz, 1H), 7.34 (t,  $J = 7.2$  Hz, 1H), 6.23 (s, 1H), 5.65-5.61 (m, 1H), 2.44-2.37 (m, 1H), 2.33-2.30 (m, 1H), 2.25-2.20 (m, 1H), 2.14-2.08 (m, 1H), 2.01-1.95 (m, 1H), 1.85-1.78 (m, 1H), 0.17 (s, 9H);  $^{13}\text{C-NMR}$  (150 MHz,  $\text{CDCl}_3$ )  $\delta$  146.4, 132.1, 131.4, 127.1, 126.3, 123.8, 120.1, 110.2, 104.7, 95.0, 56.1, 29.0, 28.7, 20.5, -0.2; HRMS Calculated for  $\text{C}_{17}\text{H}_{22}\text{N}_3\text{Si}$   $[\text{M}+\text{H}]^+$ : 290.15830, Found: 290.15786.



**1.3r (N1)**

**(E)-1-(1-phenyl-5-(trimethylsilyl)pent-1-en-4-yn-3-yl)-1H-benzo[d][1,2,3]triazole (1.3r (N1)):**

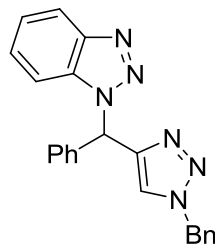
$^1\text{H-NMR}$  (600 MHz,  $\text{CDCl}_3$ )  $\delta$  8.07 (d,  $J = 7.8$  Hz, 1H), 7.36-7.32 (m, 5H), 7.27-7.24 (m, 3H), 6.92 (dd,  $J = 16.2$  Hz, 6.6 Hz, 1H), 6.63 (d,  $J = 7.2$  Hz, 1H), 5.65 (dd,  $J = 16.2$  Hz, 1.8 Hz, 1H), 0.18 (s, 9H);  $^{13}\text{C-NMR}$  (150 MHz,  $\text{CDCl}_3$ )  $\delta$  146.4, 139.0, 136.6, 132.2, 129.0, 128.8, 127.4, 127.3, 124.0, 120.2, 114.8, 110.2, 101.7, 97.8, 64.8, -0.3; HRMS Calculated for  $\text{C}_{20}\text{H}_{22}\text{N}_3\text{Si}$   $[\text{M}+\text{H}]^+$ : 332.15830, Found: 332.15883.



**1.3s (N1)**

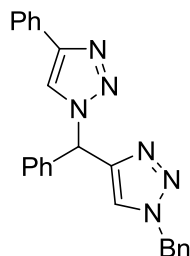
**1-(1-(2-methoxyphenyl)-3-(trimethylsilyl)prop-2-ynyl)-1H-benzo[d][1,2,3]triazole (1.3s (N1)):**

$^1\text{H-NMR}$  (600 MHz,  $\text{CDCl}_3$ )  $\delta$  8.02 (d,  $J = 8.4$  Hz, 1H), 7.97 (dd,  $J = 7.8$  Hz, 1.8 Hz, 1H), 7.60 (d,  $J = 8.4$  Hz, 1H), 7.39 (t,  $J = 7.2$  Hz, 1H), 7.34-7.28 (m, 3H), 7.05 (t,  $J = 7.8$  Hz, 1H), 6.80 (d,  $J = 8.4$  Hz, 1H), 3.66 (s, 3H), 0.19 (s, 9H);  $^{13}\text{C-NMR}$  (150 MHz,  $\text{CDCl}_3$ )  $\delta$  156.8, 146.0, 131.9, 130.6, 129.2, 126.8, 123.5, 123.4, 120.5, 119.8, 110.9, 110.7, 99.1, 93.3, 55.4, 50.3, -0.4; HRMS Calculated for  $\text{C}_{19}\text{H}_{22}\text{N}_3\text{OSi}$   $[\text{M}+\text{H}]^+$ : 336.15321, Found: 336.15266.



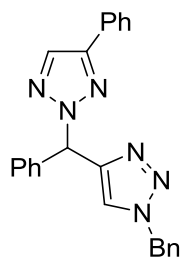
**1.5a**

**1-((1-benzyl-1H-1,2,3-triazol-4-yl)(phenyl)methyl)-1H-benzo[d][1,2,3]triazole (1.5a):**  $^1\text{H-NMR}$  (600 MHz,  $\text{CDCl}_3$ )  $\delta$  8.05 (d,  $J = 8.4$  Hz, 1H), 7.65 (s, 1H), 7.49 (d,  $J = 8.4$  Hz, 1H), 7.45 (s, 1H), 7.41 (t,  $J = 7.2$  Hz, 1H), 7.38-7.33 (m, 4H), 7.31-7.28 (m, 3H), 7.25-7.24 (m, 4H), 5.52 (s, 2H);  $^{13}\text{C-NMR}$  (150 MHz,  $\text{CDCl}_3$ )  $\delta$  146.1, 145.8, 137.3, 134.2, 132.7, 129.2, 128.9, 128.8, 128.6, 128.0, 127.6, 127.2, 124.1, 123.8, 120.0, 110.3, 59.5, 54.4; HRMS Calculated for  $\text{C}_{22}\text{H}_{19}\text{N}_6$   $[\text{M}+\text{H}]^+$ : 367.16712, Found: 367.16789.



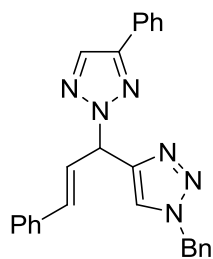
**1.5b**

**1-benzyl-4-(phenyl(4-phenyl-1H-1,2,3-triazol-1-yl)methyl)-1H-1,2,3-triazole (1.5b):**  $^1\text{H-NMR}$  (600 MHz,  $\text{CDCl}_3$ )  $\delta$  7.87 (s, 1H), 7.74 (d,  $J = 7.2$  Hz, 2H), 7.57 (s, 1H), 7.40 (t,  $J = 7.8$  Hz, 2H), 7.37-7.24 (m, 12H), 5.53 (s, 2H);  $^{13}\text{C-NMR}$  (150 MHz,  $\text{CDCl}_3$ )  $\delta$  138.1, 134.5, 131.6, 130.2, 129.1, 128.8, 128.7, 128.6, 128.5, 128.4, 128.0, 127.2, 126.0, 123.6, 65.5, 54.3; HRMS Calculated for  $\text{C}_{24}\text{H}_{21}\text{N}_6$   $[\text{M}+\text{H}]^+$ : 393.18277, Found: 393.18342.



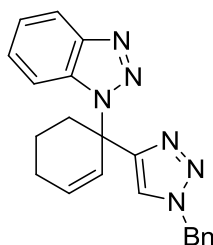
**1.5c**

**1-benzyl-4-(phenyl(4-phenyl-2H-1,2,3-triazol-2-yl)methyl)-1H-1,2,3-triazole (1.5c):**  $^1\text{H-NMR}$  (600 MHz,  $\text{CDCl}_3$ )  $\delta$  8.02 (s, 1H), 7.81 (d,  $J = 7.8$  Hz, 2H), 7.56 (s, 1H), 7.41-7.27 (m, 13H), 7.17 (s, 1H), 5.53 (s, 2H);  $^{13}\text{C-NMR}$  (150 MHz,  $\text{CDCl}_3$ )  $\delta$  137.3, 134.0, 130.5, 129.3, 129.1, 129.0, 128.8, 128.7, 128.4, 128.2, 127.5, 125.7, 123.4, 119.9, 60.7, 54.5; HRMS Calculated for  $\text{C}_{24}\text{H}_{21}\text{N}_6$   $[\text{M}+\text{H}]^+$ : 393.18277, Found: 393.18342.



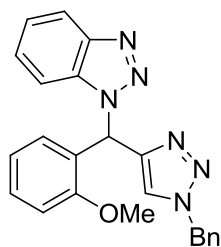
**1.5d**

**(E)-1-benzyl-4-(3-phenyl-1-(4-phenyl-2H-1,2,3-triazol-2-yl)allyl)-1H-1,2,3-triazole (1.5d):**  $^1\text{H-NMR}$  (600 MHz,  $\text{CDCl}_3$ )  $\delta$  7.87 (s, 1H), 7.78 (d,  $J = 7.2$  Hz, 2H), 7.50 (d,  $J = 9.0$  Hz, 1H), 7.45 (s, 1H), 7.43-7.39 (m, 4H), 7.37-7.26 (m, 9H), 6.67-6.60 (m, 2H), 5.51 (s, 2H);  $^{13}\text{C-NMR}$  (150 MHz,  $\text{CDCl}_3$ )  $\delta$  147.6, 139.3, 134.4, 131.1, 130.5, 129.1, 129.0, 128.8, 128.7, 128.6, 128.3, 128.1, 128.0, 127.0, 126.0, 122.8, 119.9, 66.2, 54.1; HRMS Calculated for  $\text{C}_{26}\text{H}_{23}\text{N}_6$   $[\text{M}+\text{H}]^+$ : 419.19842, Found: 419.19793.



**1.5e**

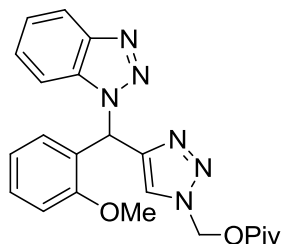
**1-(1-(1-benzyl-1H-1,2,3-triazol-4-yl)cyclohex-2-enyl)-1H-benzo[d][1,2,3]triazole (1.5e):**  $^1\text{H-NMR}$  (600 MHz,  $\text{CDCl}_3$ )  $\delta$  8.05 (d,  $J = 8.4$  Hz, 1H), 7.55 (d,  $J = 8.4$  Hz, 1H), 7.45 (s, 1H), 7.41-7.32 (m, 5H), 7.28-7.27 (m, 2H), 6.55 (s, 1H), 5.77-5.74 (m, 1H), 5.52 (s, 2H), 2.68-2.66 (m, 2H), 2.34-2.30 (m, 1H), 2.25-2.19 (m, 1H), 2.14-2.08 (m, 1H), 1.97-1.90 (m, 1H);  $^{13}\text{C-NMR}$  (150 MHz,  $\text{CDCl}_3$ )  $\delta$  148.1, 146.4, 134.5, 132.9, 132.2, 129.1, 128.8, 128.1, 127.0, 123.7, 121.4, 120.1, 119.5, 110.3, 56.3, 54.2, 29.4, 25.9, 20.4; HRMS Calculated for  $\text{C}_{21}\text{H}_{21}\text{N}_6$   $[\text{M}+\text{H}]^+$ : 357.18277, Found: 357.18226.



**1.5f**

**1-((1-benzyl-1H-1,2,3-triazol-4-yl)(2-methoxyphenyl)methyl)-1H-benzo[d][1,2,3]triazole**

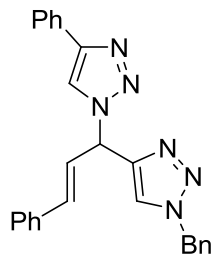
**(1.5f):**  $^1\text{H-NMR}$  (600 MHz,  $\text{CDCl}_3$ )  $\delta$  8.02 (d,  $J = 8.4$  Hz, 1H), 7.84 (s, 1H), 7.59 (s, 1H), 7.53 (d,  $J = 8.4$  Hz, 1H), 7.40 (t,  $J = 7.8$  Hz, 1H), 7.36-7.30 (m, 4H), 7.28-7.23 (m, 4H), 6.89-6.85 (m, 2H), 5.50 (s, 2H), 3.74 (s, 3H);  $^{13}\text{C-NMR}$  (150 MHz,  $\text{CDCl}_3$ )  $\delta$  156.5, 145.9, 145.6, 134.4, 132.9, 133.0, 129.1, 128.8, 128.7, 127.9, 127.2, 125.5, 123.8, 123.7, 120.8, 119.7, 110.8, 110.3, 55.5, 54.2, 53.2; HRMS Calculated for  $\text{C}_{23}\text{H}_{21}\text{N}_6\text{O}$   $[\text{M}+\text{H}]^+$ : 397.17768, Found: 397.17698.



**1.5g**

**(4-((1H-benzo[d][1,2,3]triazol-1-yl)(2-methoxyphenyl)methyl)-1H-1,2,3-triazol-1-yl)methyl**

**pivalate (1.5g):**  $^1\text{H-NMR}$  (600 MHz,  $\text{CDCl}_3$ )  $\delta$  8.04 (d,  $J = 8.4$  Hz, 1H), 7.84 (s, 2H), 7.49 (d,  $J = 8.4$  Hz, 1H), 7.40 (t,  $J = 7.2$  Hz, 1H), 7.31 (quintet,  $J = 7.2$  Hz, 2H), 7.22 (d,  $J = 7.8$  Hz, 1H), 6.92-6.89 (m, 2H), 6.22 (s, 2H), 3.78 (s, 3H), 1.17 (s, 9H);  $^{13}\text{C-NMR}$  (150 MHz,  $\text{CDCl}_3$ )  $\delta$  177.5, 156.5, 146.1, 145.8, 133.0, 130.2, 128.6, 127.3, 125.2, 125.1, 123.9, 120.9, 119.9, 110.9, 110.2, 69.8, 55.6, 53.2, 38.8, 26.7; HRMS Calculated for  $\text{C}_{22}\text{H}_{25}\text{N}_6\text{O}_3$   $[\text{M}+\text{H}]^+$ : 421.19881, Found: 421.19816.



**1.5h**

**(E)-1-benzyl-4-(3-phenyl-1-(4-phenyl-1H-1,2,3-triazol-1-yl)allyl)-1H-1,2,3-triazole (1.5h):**

$^1\text{H-NMR}$  (600 MHz,  $\text{CDCl}_3$ )  $\delta$  7.89 (s, 1H), 7.79 (d,  $J = 7.2$  Hz, 2H), 7.44 (s, 1H), 7.79 (t,  $J = 7.8$  Hz, 3H), 7.39-7.30 (m, 9H), 7.25 (d,  $J = 5.4$  Hz, 1H), 7.04 (dd,  $J = 15.6$  Hz, 5.4 Hz, 1H), 6.54 (d,  $J = 15.6$  Hz, 1H), 6.47 (d,  $J = 7.2$  Hz, 1H), 5.50 (s, 2H);  $^{13}\text{C-NMR}$  (150 MHz,  $\text{CDCl}_3$ )  $\delta$  147.9, 138.1, 134.4, 131.3, 130.3, 129.1, 129.0, 128.9, 128.8, 128.7, 128.6, 128.4, 128.3, 128.1, 127.4, 126.0, 122.4, 120.7, 70.5, 54.2; HRMS Calculated for  $\text{C}_{26}\text{H}_{23}\text{N}_6$   $[\text{M}+\text{H}]^+$ : 419.19842, Found: 419.19793

### III. ORTEP Drawing of the Crystal Structures.

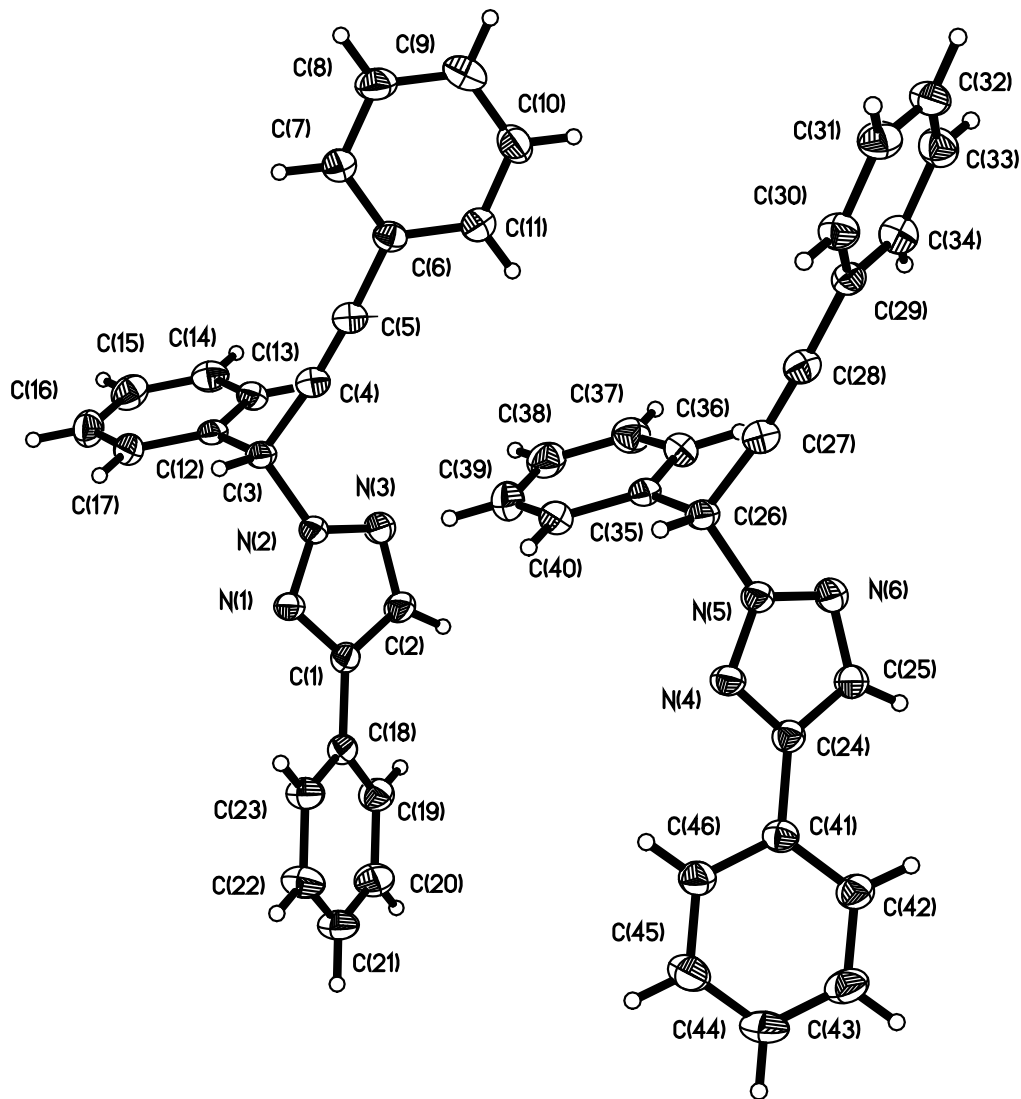


**Figure 1.** Perspective view of the molecular structure of  $C_{22}H_{24}N_6O_3$  (molecule 1) with the atom labeling scheme. The thermal ellipsoids are scaled to enclose 30% probability. CCDC number: 775267

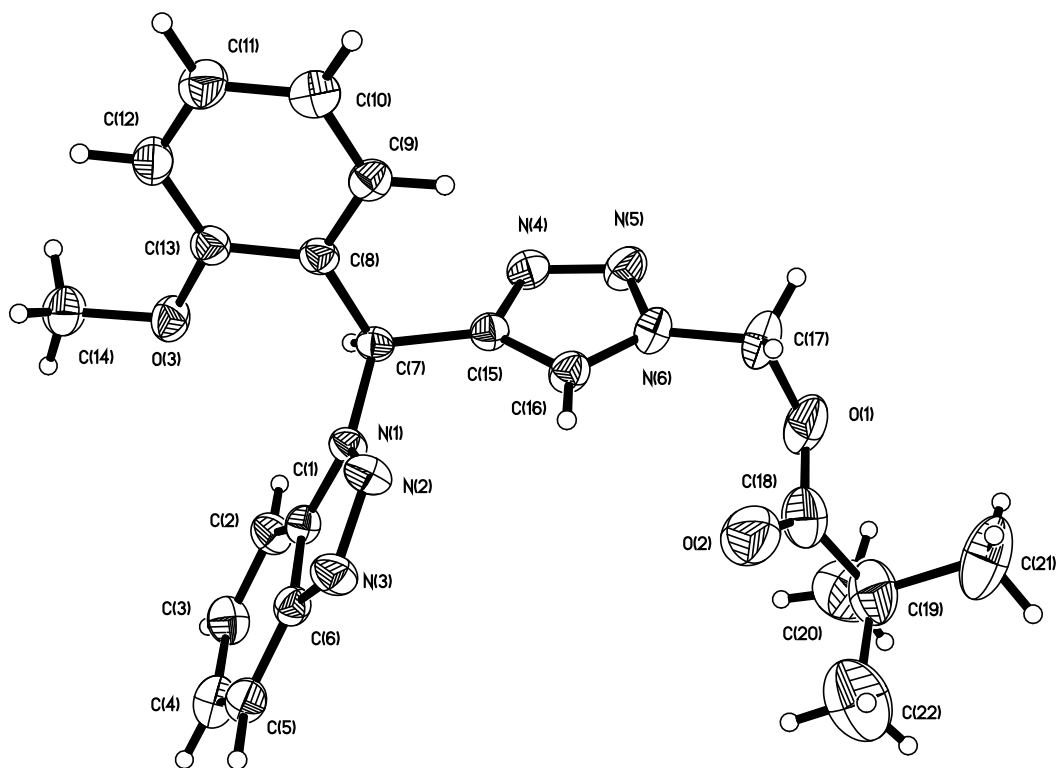


**Figure 2.** Perspective view of the molecular structure of C<sub>22</sub>H<sub>24</sub>N<sub>6</sub>O<sub>3</sub> (molecule 1) with the atom labeling scheme. The thermal ellipsoids are scaled to enclose 30% probability. CCDC number: 775268

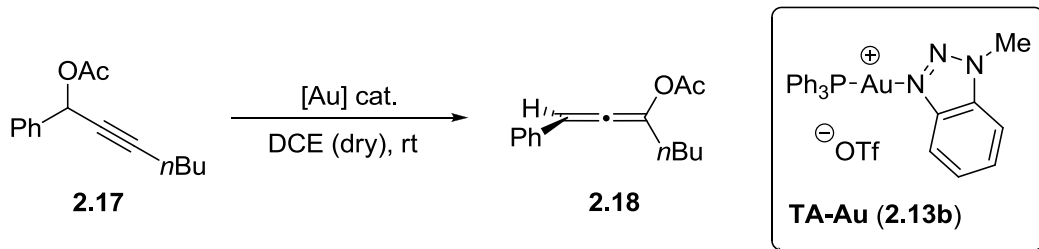


## Chapter Two: 1,2,3-triazoles work as X-factor to promote gold(I) complex in challenging chemical transformations - part I

### I. General Methods and Materials

All of the reactions dealing with air and/or moisture-sensitive reactions were carried out under an atmosphere of nitrogen using oven/flame-dried glassware. Unless otherwise noted, all commercial reagents and solvents were obtained from the commercial provider and used without further purification. <sup>1</sup>H NMR, <sup>13</sup>C NMR, and <sup>31</sup>P NMR, spectra were recorded on Agilent 400 MHz spectrometer. Chemical shifts were reported relative to internal tetramethylsilane ( $\delta$  0.00 ppm) or CDCl<sub>3</sub> ( $\delta$  7.26 ppm) for <sup>1</sup>H and CDCl<sub>3</sub> ( $\delta$  77.0 ppm) for <sup>13</sup>C. For the reaction monitoring, the reaction spectra were recorded using a ReactIR 15 from Mettler-Toledo AutoChem.

#### General procedure for the monitoring of [3,3]-rearrangement of propargyl ester <sup>1</sup>



The reaction was carried out as follows: a three-necked reaction vessel was fitted with a magnetic stirring bar. The IR probe was inserted through an adapter into the middle neck; the other two necks were capped by septa. The reaction vessel was charged with substrate **2.17** (29 mg, 0.125 mmol) in dry DCE (1.2 mL) followed by immediate initiation of data collection. TA-Au (**2.13b**) was then added and *in situ* IR spectra (2800-650cm<sup>-1</sup>) were recorded over the course of the reaction. The collected spectra were analyzed by iC IR 4.3 software and Origin 8.0. Peaks 1211 cm<sup>-1</sup> and 1757 cm<sup>-1</sup> were used to calculate the concentration. The substrate was synthesized according to Nolan's and our previous communications.<sup>2</sup>

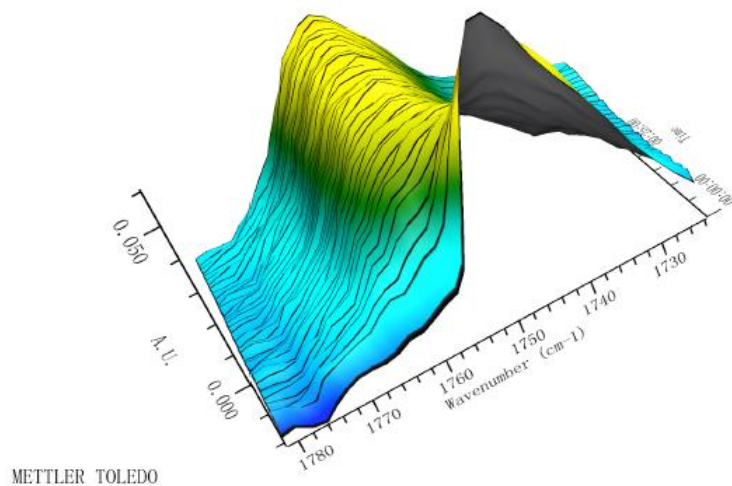


**Figure S1.** Kinetic profile of [3,3]-rearrangement of propargyl ester catalyzed by TA-Au (**2.13b**).

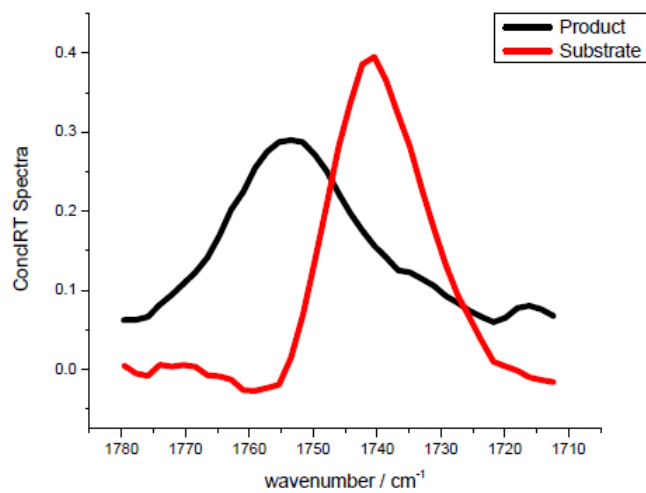


**Figure S2.** ConcIRT spectra of **2.17** (red) and **2.18** (black).

## II. Kinetic Profiles

### 1. Determination of kinetic order of [2.13b]

The reactions were monitored according to general procedure. Reaction conditions are: **2.17** (0.10 M in DCE, 1.2 mL), **2.13b** (0.002, 0.004, 0.006, 0.008 M in DCE), 30°C.

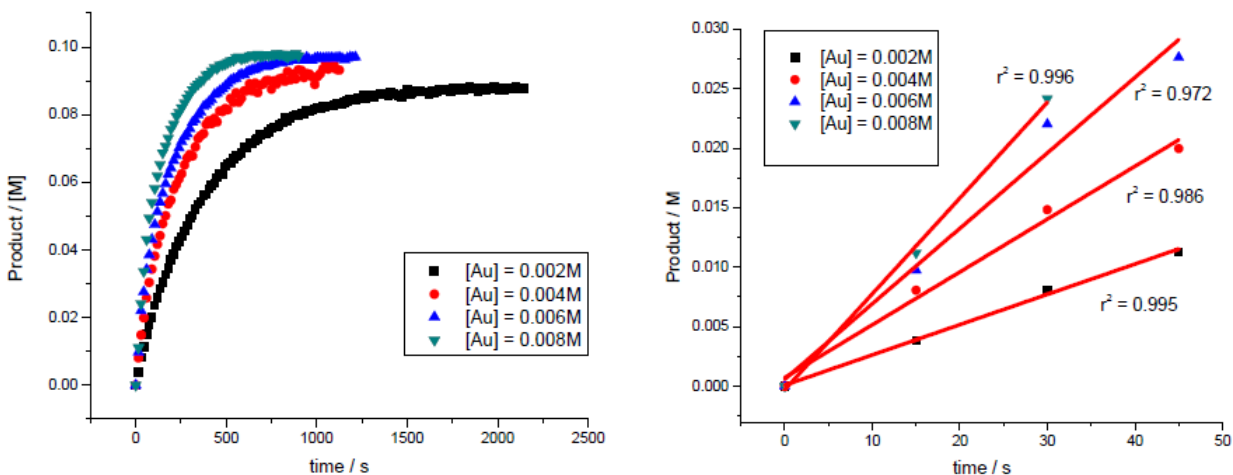


Figure S3. Determination of kinetic order of [2.13b].

### 2. Determination of kinetic order of [2.17]

The reactions were monitored according to general procedure. Reaction conditions are: **2.17** (0.10, 0.14, 0.17, 0.20 M in DCE, 1.2 mL), **2.13b** (0.003 M in DCE), 30°C.

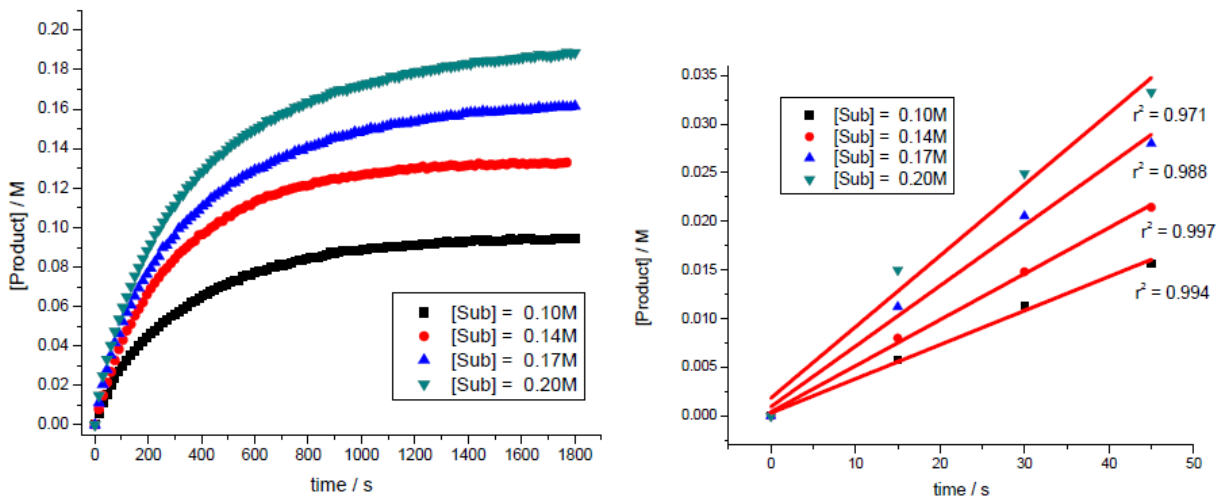


Figure S4. Determination of kinetic order of [2.17].

### 3. Variable temperature experiment

The reactions were monitored according to general procedure. Reaction conditions are: **2.17** (0.10 M in DCE, 1.2 mL), **2.13b** (0.003 M in DCE), at 22, 32, 38, and 46 °C.

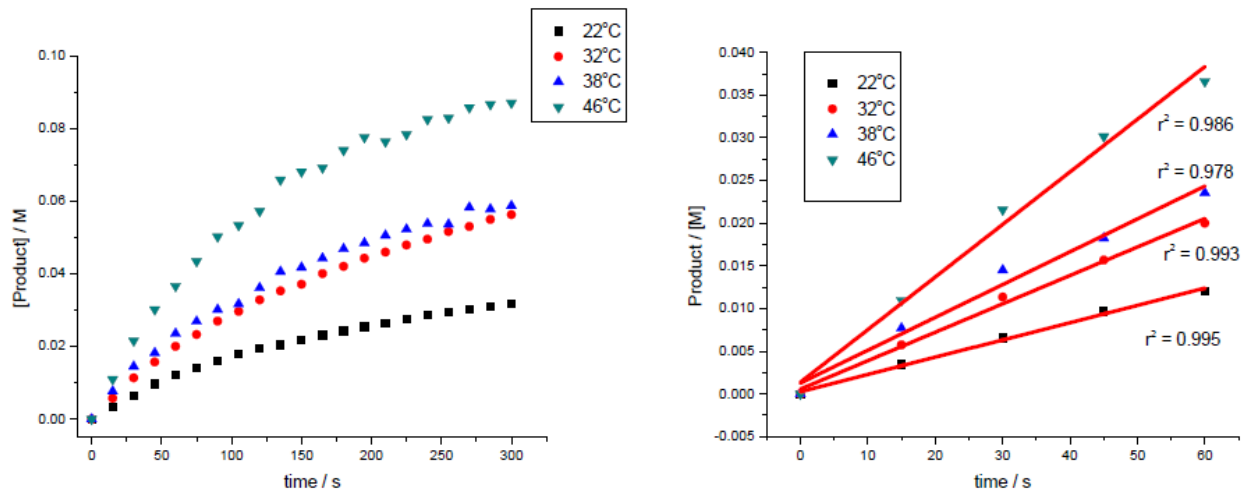


Figure S5. Kinetics profile at different temperatures.

### 4. Hammett plot with various modified TA-Au catalysts

The reactions were monitored according to general procedure. Reaction conditions are: **2.17** (0.10 M in DCE, 1.2 mL), **2.13b** (0.003 M in DCE), 26 °C.

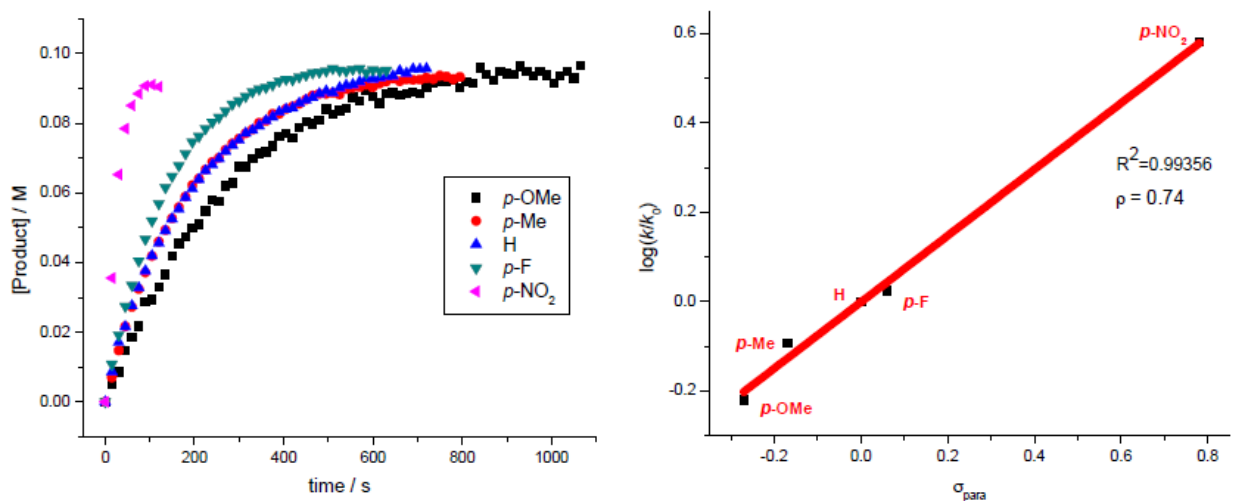
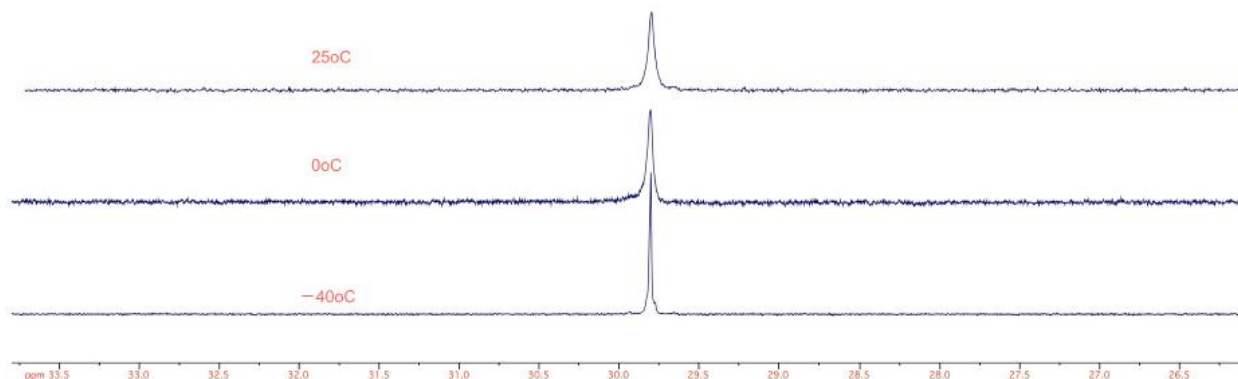


Figure S6. Kinetics profile using various TA-Au catalysts.

### III. $^{31}\text{P}$ NMR Experiments

#### Variable temperature experiment with catalyst 4

A NMR tube containing catalyst **2.13b** (0.025 M) in  $\text{CD}_2\text{Cl}_2$  (0.7 mL) was inserted in NMR machine.  $^{31}\text{P}$  NMR spectrum was recorded at 25 °C, 0 °C, and -40 °C.



**Figure S7.** Variable temperature experiment with catalyst **2.13b**.

#### $^{31}\text{P}$ NMR monitoring of the reaction progress

A NMR tube was charged with catalyst **2.13b** (2 mol %, 0.002 M) and **2.17** (1 equiv.) in  $\text{CD}_2\text{Cl}_2$  (0.6 mL). The tube was shaken periodically and NMR spectrum was taken at 0 min, 5 min, 15 min, and 60 min.

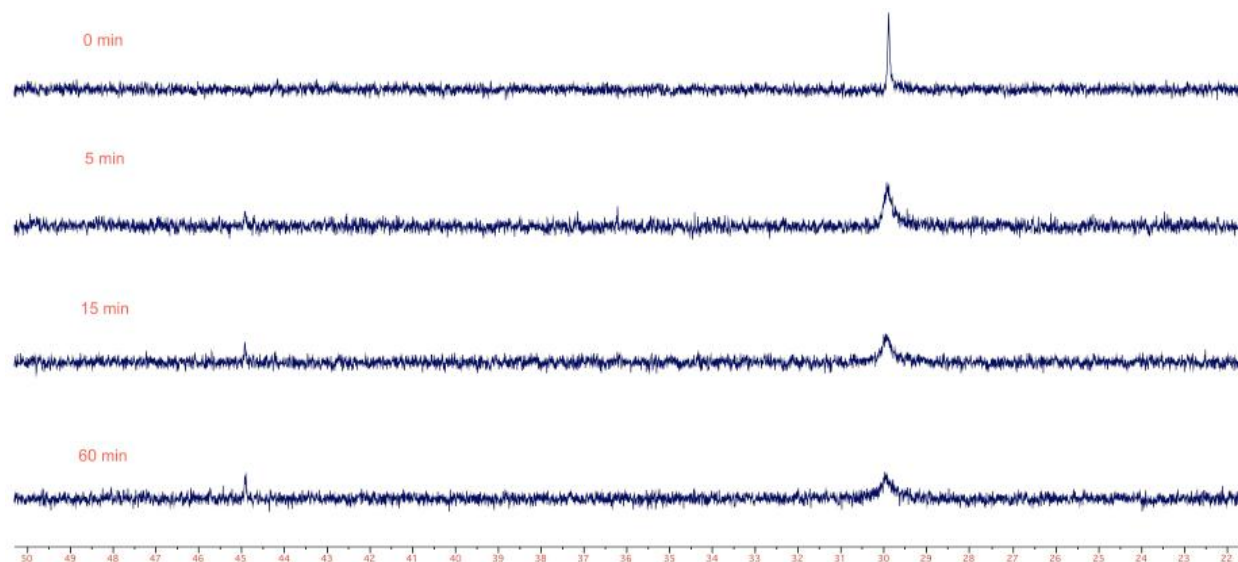
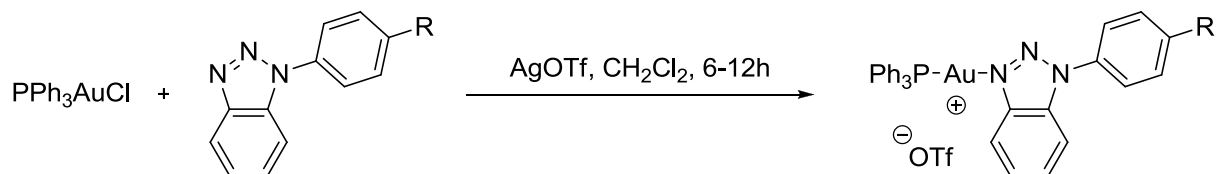


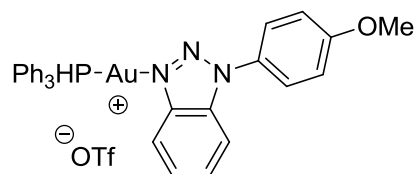
**Figure S8.**  $^{31}\text{P}$  NMR monitoring of the reaction progress.

#### IV. Catalyst Characterization

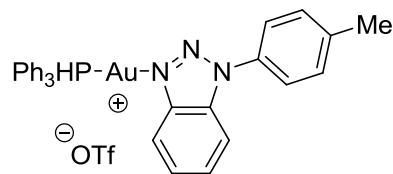
##### General procedure for TA-Au synthesis<sup>3</sup>



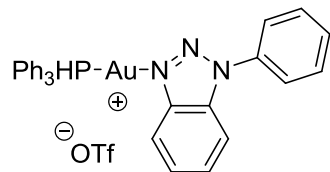
A 20 mL screw-cap vial was charged with  $\text{Ph}^3\text{PAuCl}$  (1 equiv.) and benzotriazole derivative (1 equiv.) in dry DCM (0.1 M), followed by the addition of  $\text{AgOTf}$  (1 equiv.). The vial was allowed to stir at ambient temperature for 6-12h, and concentrated *in vacuo* to give the product in >90% yield. Pure gold catalyst was obtained through diffusion of hexanes into DCM solution.



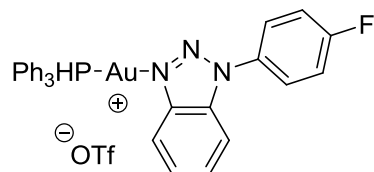
$^1\text{H-NMR}$  (400 MHz,  $\text{CDCl}_3$ )  $\delta$  8.25-8.22 (m, 1H), 7.95-7.93 (m, 1H), 7.84-7.80 (m, 2H), 7.76-7.74 (m, 2H), 7.68-7.51 (m, 15H), 7.22-7.20 (m, 2H), 3.93 (s, 3H).  $^{13}\text{C-NMR}$  (100 MHz,  $\text{CDCl}_3$ )  $\delta$  161.3, 143.4, 134.1, 133.9, 132.9, 129.8, 129.7, 129.0, 126.7, 126.1, 126.1, 125.2, 117.1, 115.5, 112.2, 55.8.  $^{31}\text{P-NMR}$  (162 MHz,  $\text{CDCl}_3$ )  $\delta$  31.9.



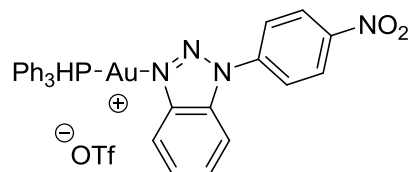
$^1\text{H-NMR}$  (400 MHz,  $\text{CDCl}_3$ )  $\delta$  8.28-8.26 (m, 1H), 7.98-7.95 (m, 1H), 7.87-7.81 (m, 2H), 7.73-7.71 (m, 2H), 7.68-7.58 (m, 15H), 7.53-7.51 (m, 2H), 2.51 (s, 3H).  $^{13}\text{C-NMR}$  (100 MHz,  $\text{CDCl}_3$ )  $\delta$  143.5, 141.6, 134.1, 134.0, 132.9, 131.1, 131.0, 129.9, 129.7, 129.2, 126.8, 126.1, 123.5, 119.2, 112.2, 21.3.  $^{31}\text{P-NMR}$  (162 MHz,  $\text{CDCl}_3$ )  $\delta$  30.7.



<sup>1</sup>H-NMR (400 MHz, CDCl<sub>3</sub>) δ 8.30-8.28 (m, 1H), 7.98-7.95 (m, 1H), 7.86-7.80 (m, 4H), 7.75-7.71 (m, 2H), 7.69-7.58 (m, 15H), 7.54-7.49 (m, 1H). <sup>13</sup>C-NMR (100 MHz, CDCl<sub>3</sub>) δ 135.1, 134.2, 134.1, 132.9, 131.1, 130.9, 130.5, 129.9, 129.8, 128.9, 126.8, 126.2, 123.7, 117.8, 112.0. <sup>31</sup>P-NMR (162 MHz, CDCl<sub>3</sub>) δ 30.4.



<sup>1</sup>H-NMR (400 MHz, CDCl<sub>3</sub>) δ 8.26-8.22 (m, 1H), 7.98-7.95 (m, 1H), 7.92-7.87 (m, 2H), 7.83-7.79 (m, 2H), 7.66-7.57 (m, 15H), 7.44-7.38 (m, 2H). <sup>13</sup>C-NMR (100 MHz, CDCl<sub>3</sub>) δ 143.8, 134.2, 134.1, 132.9, 131.2, 129.9, 129.9, 129.8, 128.9, 126.9, 126.2, 126.1, 126.0, 117.8, 112.1. <sup>31</sup>P-NMR (162 MHz, CDCl<sub>3</sub>) δ 30.3.



<sup>1</sup>H-NMR (400 MHz, CDCl<sub>3</sub>) δ 8.53 (d, *J* = 8.8 Hz, 2H), 8.25 (d, *J* = 8.4 Hz, 3H), 8.18 (d, *J* = 8.0 Hz, 1H), 7.90-7.81 (m, 2H), 7.66-7.53 (m, 15H). <sup>13</sup>C-NMR (100 MHz, CDCl<sub>3</sub>) δ 148.3, 143.7, 139.7, 134.1, 134.0, 132.8, 132.0, 129.8, 129.7, 126.8, 126.1, 125.8, 124.6, 117.3, 112.5. <sup>31</sup>P-NMR (162 MHz, CDCl<sub>3</sub>) δ 30.2.

## V. DFT Calculation

To examine the structural and energy aspects of this reaction, density function theory (DFT) theoretical calculations were carried out with the Gaussian 03 program. In brief, the geometrical optimizations and single point energy calculations were performed using Becke's three-parameter exchange functional and the nonlocal correlation functional of Lee, Yang and Parr (B3LYP) with the 6-311G basis set.

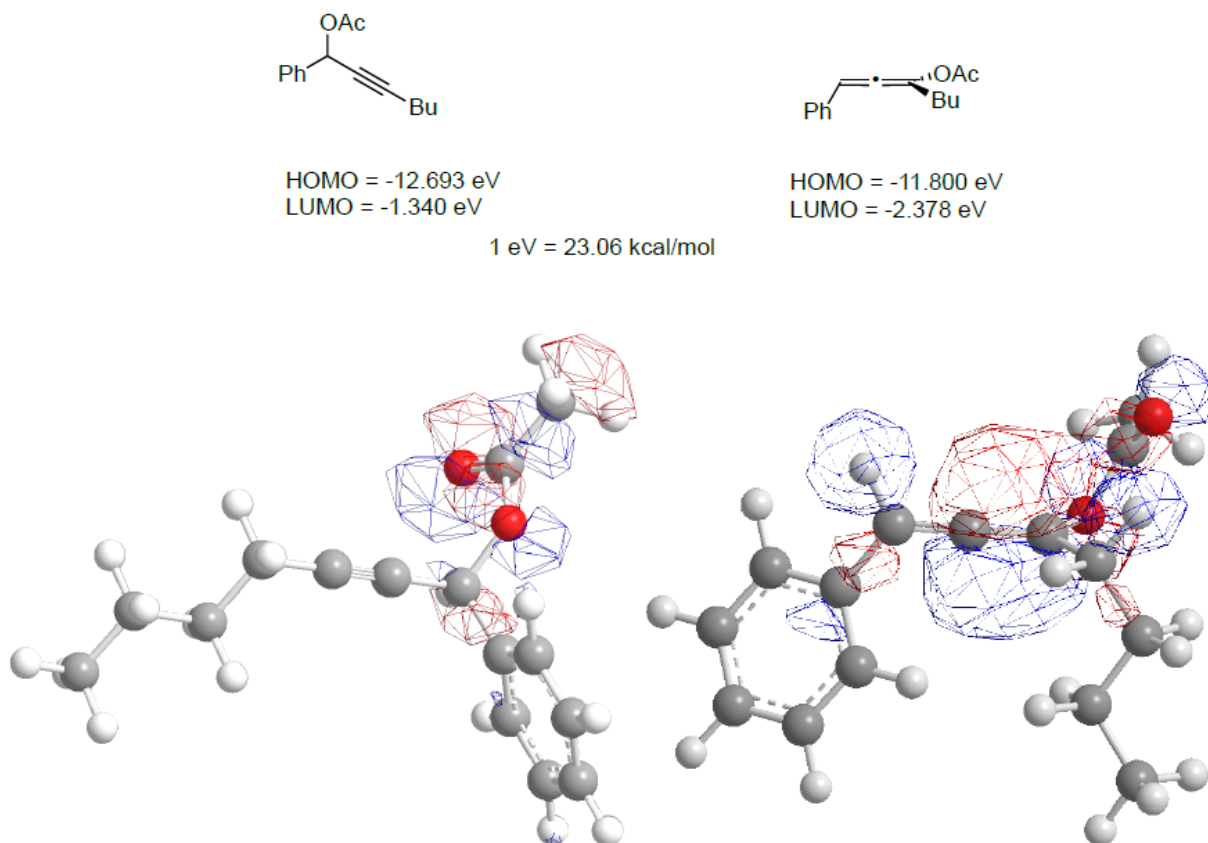
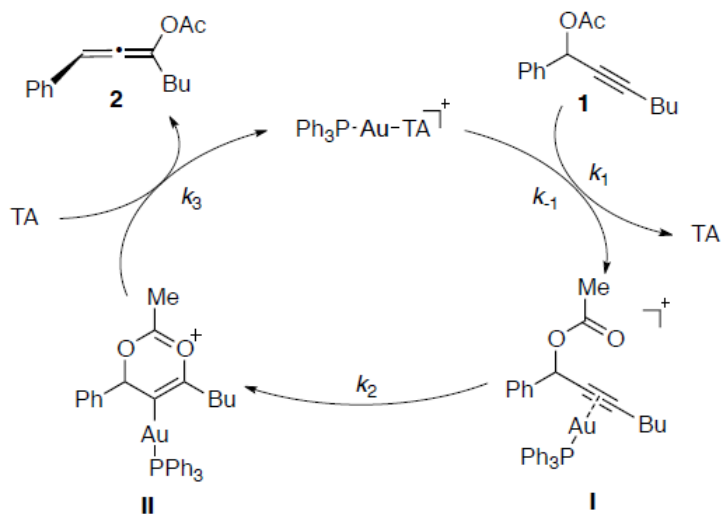


**Figure S9.** DFT calculation result.



## VI. Derivation of Rate Law



Overall rate equation:

$$r = k_3[\text{II}][\text{TA}]$$

Since the resting-state is  $\text{Ph}_3\text{PAuTA}$ , we can use steady-state approximation for I and II.

Steady-state for II:

$$k_1[\text{Ph}_3\text{PAuTA}][\text{I}] = k_{-1}[\text{I}][\text{TA}] + k_2[\text{I}]$$

Steady-state for III:

$$k_3[\text{II}][\text{TA}] = k_2[\text{I}]$$

Overall rate equation:

$$r = k_3[\text{II}][\text{TA}] = \frac{k_1 k_2}{k_{-1}[\text{TA}] + k_2} [\text{Ph}_3\text{PAuTA}][\text{I}]$$

## VII. Reference

1. C. He, J. Ke, H. Xu and A. Lei, *Angew. Chem. Int. Ed.*, 2013, **52**, 1527
2. D. Wang, L. N. S. Gautam, C. Bollinger, A. Harris, M. Li and X. Shi, *Org. Lett.*, 2011, **13**, 2618; N. Marion, S. Díez-Gonzalez, P. Fremont, A. R. Noble and S. P. Nolan, *Angew. Chem. Int. Ed.*, 2006, **45**, 3647.
3. K. Wang, M. Chen, Q. Wang, X. Shi and J. K. Lee, *J. Org. Chem.*, 2013, **78**, 7249.

## Chapter Three: 1,2,3-triazoles work as X-factor to promote gold(I) complex in challenging chemical transformations - part II

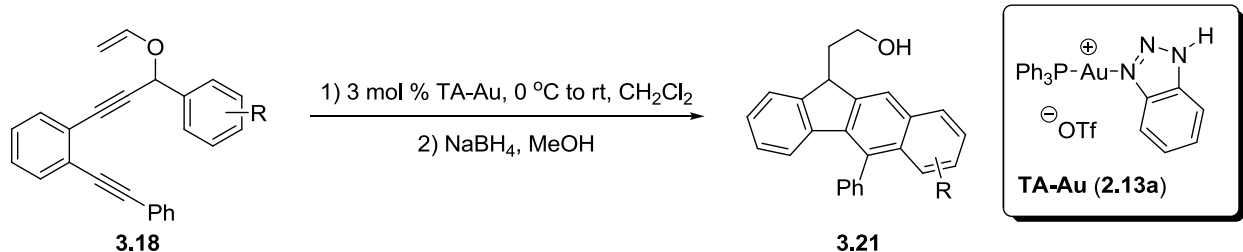
### I. General Methods and Materials

All of the reactions dealing with air and/or moisture-sensitive reactions were carried out under an atmosphere of nitrogen using oven/flame-dried glassware and standard syringe/septa techniques. Unless otherwise noted, all commercial reagents and solvents were obtained from the commercial provider and used without further purification.  $^1\text{H}$  NMR and  $^{13}\text{C}$  NMR spectra were recorded on Varian 600 MHz spectrometers. Chemical shifts were reported relative to internal tetramethylsilane ( $\delta$  0.00 ppm) or  $\text{CDCl}_3$  ( $\delta$  7.26 ppm) for  $^1\text{H}$  and  $\text{CDCl}_3$  ( $\delta$  77.0 ppm) for  $^{13}\text{C}$ . Flash column chromatography was performed on 230-430 mesh silica gel. Analytical thin layer chromatography was performed with precoated glass baked plates (250 $\mu$ ) and visualized by fluorescence and by charring after treatment with potassium permanganate stain. HRMS were recorded on LTQ-FTUHRA spectrometer.

Substrates **3.18** and **3.25** were synthesized according to the literature as below:

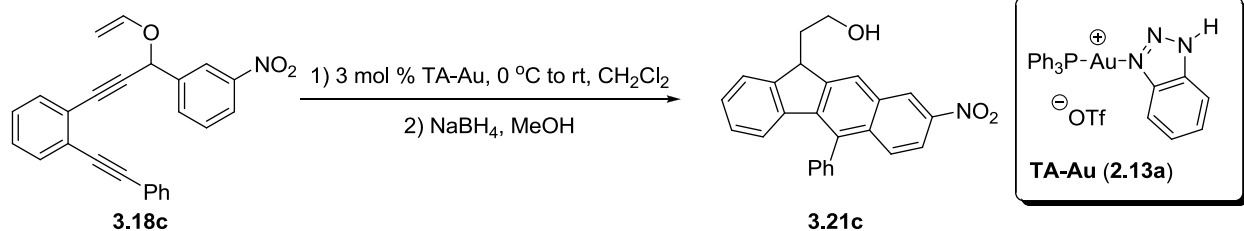
- (1). Li, H.; Petersen, J.; Wang, K. K. *J. Org. Chem.* **2001**, *66*, 7804-7810
- (2). Yu, M.; Zhang, G.; Zhang, L. *Org. Lett.* **2007**, *9*, 2147-2150.
- (3). Marion, N.; Carlqvist, P.; Gealageas, R.; Fremont, P.; Maseras, F.; Nolan, S. P. *Chem. Eur. J.* **2007**, *13*, 6437-6451.
- (4). Nonoshita, K.; Banno, H.; Maruoka, K.; Yamamoto, H. *J. Am. Chem. Soc.* **1990**, *112*, 316-322.
- (5). (a) Sherry, B. D.; Toste, F. D. *J. Am. Chem. Soc.* **2004**, *126*, 15978-15979. (b) Sherry, B. D.; Maus, L.; Laforteza, B. N.; Toste, F. D. *J. Am. Chem. Soc.* **2006**, *128*, 8132-8133. (c) Mauleon, P.; Krinsky, J. L.; Toste, F. D. *J. Am. Chem. Soc.* **2009**, *131*, 4513-4520.

### Procedure for the synthesis of fluorenyl ethanol 6a.



To a solution of **3.18a** (67 mg, 0.2 mmol) in dry CH<sub>2</sub>Cl<sub>2</sub> (2 mL, 0.1 M), was added Au(I) catalyst (4.4 mg, 0.006 mol, 3.0 mol%) at 0 °C. The reaction mixture was stirred at 0 °C for 4 hours. Temperature was slowly raised to RT, reaction mixture was stirred and monitored by TLC. After the reaction was completed (6-16 h), NaBH<sub>4</sub> and MeOH were treated. Upon completion, the solvent was removed under reduced pressure and the residue was purified by flash chromatography on silica gel (ethyl acetate/hexane = 1:8, V/V) to give **3.21a** (44% yield) as light yellow oil.

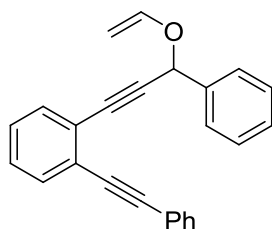
## II. Solvent Screening Data



Entry	conc. (M)	temp (°C)	time	conv. (%)	yield (%) <sup>a</sup>
1	0.1	rt	16 h	>99	47
2	0.1	rt	16 h	95	26
3	0.1	rt	16 h	97	21
4	0.1	rt	16 h	>99	32
5	0.1	rt	16 h	>99	15
6	0.1	rt	16 h	97	41
7	0.1	rt	16 h	32	0
8	0.1	rt	16 h	44	0
9	0.1	rt	16 h	>99	65

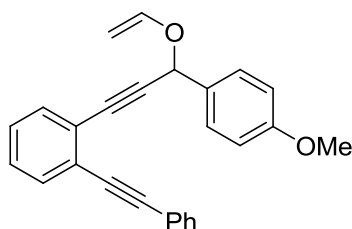
General reaction condition: **4e** (0.2 mmol), catalyst (3 mol%) in solvent (2 mL), the reactions were monitored by TLC, 0 °C to rt. <sup>a</sup> Conversion and yields were determined by NMR with 1,3,5-trimethoxybenzene as internal standard.

### III. Compounds Characterization



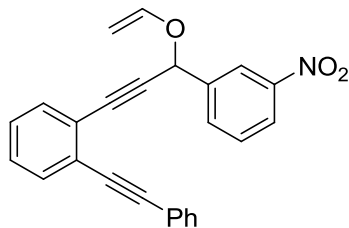
**3.18a**

**1-(3-(2-(2-phenylethynyl)phenyl)-1-(vinylloxy)prop-2-ynyl)benzene (3.18a)** was purified by flash chromatography (Hexane-EtOAc, v/v 15/1) as light yellow liquid;  $^1\text{H-NMR}$  (600 MHz,  $\text{CDCl}_3$ )  $\delta$  7.66 (dd,  $J = 4.8$  Hz, 2.4 Hz, 2H), 7.54 (dd,  $J = 12$  Hz, 6.6 Hz, 2H), 7.45 (dd,  $J = 7.8$  Hz, 1.8 Hz, 2H), 7.34-7.29 (m, 8H), 6.63 (dd,  $J = 13.8$  Hz, 6.6 Hz, 1H), 5.83 (s, 1H), 4.59 (dd,  $J = 13.8$  Hz, 1.8 Hz, 1H), 4.17 (dd,  $J = 6.6$  Hz, 2.4 Hz, 1H);  $^{13}\text{C-NMR}$  (150 MHz,  $\text{CDCl}_3$ )  $\delta$  149.4, 137.5, 132.3, 131.9, 131.8, 128.7, 128.6, 128.5, 128.4, 128.2, 127.9, 127.6, 126.0, 124.7, 123.0; HRMS Calculated for  $\text{C}_{25}\text{H}_{18}\text{O}$   $[\text{M}+\text{H}]^+$ : 335.1436, Found: 335.1431.



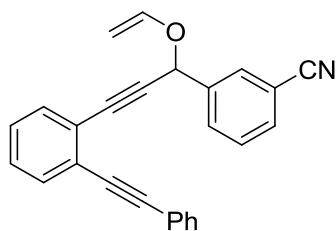
**3.18b**

**1-methoxy-4-(3-(2-(2-phenylethynyl)phenyl)-1-(vinylloxy)prop-2-ynyl)benzene (3.18b)** was purified by flash chromatography (Hexane- EtOAc, v/v 15/1) as light yellow liquid;  $^1\text{H-NMR}$  (600 MHz,  $\text{CDCl}_3$ )  $\delta$  7.57 (d,  $J = 9.0$  Hz, 2H), 7.53 (dd,  $J = 12.0$  Hz, 4.2 Hz, 2H), 7.45 (dd,  $J = 4.8$  Hz, 1.8 Hz, 2H), 7.34-7.29 (m, 5H), 6.78 (d,  $J = 9.0$  Hz, 2H), 6.60 (dd,  $J = 13.8$  Hz, 6.6 Hz, 1H), 5.76 (s, 1H), 4.56 (dd,  $J = 14.4$  Hz, 2.4 Hz, 1H), 4.14 (dd,  $J = 6.6$  Hz, 1.8 Hz, 1H), 3.75 (s, 3H);  $^{13}\text{C-NMR}$  (150 MHz,  $\text{CDCl}_3$ )  $\delta$  160.1, 149.6, 132.5, 132.1, 132.0, 129.9, 129.4, 128.7, 128.6, 128.5, 128.2, 126.3, 124.9, 123.3, 114.2, 93.7, 90.8, 90.2, 88.2, 87.1, 71.3; HRMS Calculated for  $\text{C}_{26}\text{H}_{20}\text{O}_2$   $[\text{M}+\text{H}]^+$ : 365.1542, Found: 365.1536.



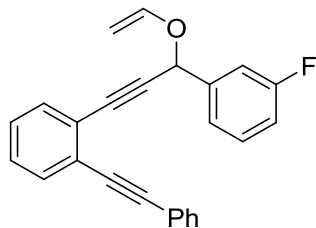
**3.18c**

**1-nitro-3-(3-(2-(2-phenylethynyl)phenyl)-1-(vinylloxy)prop-2-ynyl)benzene (3.18c)** was purified by flash chromatography (Hexane- EtOAc, v/v 15/1) as light yellow liquid;  $^1\text{H-NMR}$  (600 MHz,  $\text{CDCl}_3$ )  $\delta$  8.45 (s, 1H), 8.11 (dd,  $J = 7.8$  Hz, 2.4 Hz, 1H), 7.99 (d,  $J = 8.4$  Hz, 1H), 7.52 (dd,  $J = 13.2$  Hz, 7.8 Hz, 2H), 7.40 (d,  $J = 6.0$  Hz, 2H), 7.38-7.27 (m, 6H), 6.60 (dd,  $J = 13.8$  Hz, 6.6 Hz, 1H), 5.87 (s, 1H), 4.61 (dd,  $J = 14.4$  Hz, 2.4 Hz, 1H), 4.30 (dd,  $J = 6.6$  Hz, 2.4 Hz, 1H);  $^{13}\text{C-NMR}$  (150 MHz,  $\text{CDCl}_3$ )  $\delta$  149.0, 148.2, 139.7, 133.4, 132.2, 131.9, 131.6, 129.6, 128.9, 128.6, 128.3, 128.0, 126.2, 124.0, 123.5, 122.8, 122.4, 93.6, 91.6, 88.3, 87.9, 87.6, 69.9; HRMS Calculated for  $\text{C}_{25}\text{H}_{17}\text{NO}_3$   $[\text{M}+\text{H}]^+$ : 380.1287, Found: 380.1282.



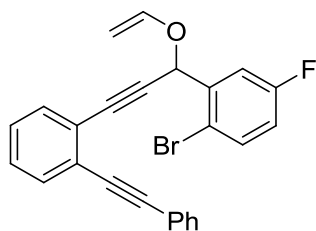
**3.18d**

**3-(3-(2-(2-phenylethynyl)phenyl)-1-(vinylloxy)prop-2-ynyl)benzonitrile (3.18d)** was purified by flash chromatography (Hexane- EtOAc, v/v 15/1) as light yellow liquid;  $^1\text{H-NMR}$  (600 MHz,  $\text{CDCl}_3$ )  $\delta$  7.91-7.89 (m, 2H), 7.56 (t,  $J = 7.8$  Hz, 2H), 7.52 (d,  $J = 6.6$  Hz, 1H), 7.43 (dd,  $J = 7.8$  Hz, 1.2 Hz, 2H), 7.37-7.30 (m, 6H), 6.58 (dd,  $J = 13.8$  Hz, 6.6 Hz, 1H), 5.82 (s, 1H), 4.60 (dd,  $J = 14.4$  Hz, 2.4 Hz, 1H), 4.23 (dd,  $J = 6.6$  Hz, 2.4 Hz, 1H);  $^{13}\text{C-NMR}$  (150 MHz,  $\text{CDCl}_3$ )  $\delta$  149.0, 139.2, 132.2, 132.0, 131.7, 131.6, 130.9, 129.4, 128.9, 128.6, 128.3, 128.0, 126.2, 124.0, 122.8, 118.4, 112.7, 93.6, 91.5, 88.4, 87.9, 87.7, 70.0; HRMS Calculated for  $\text{C}_{26}\text{H}_{17}\text{NO}$   $[\text{M}+\text{H}]^+$ : 360.1388, Found: 360.1383.



**3.18e**

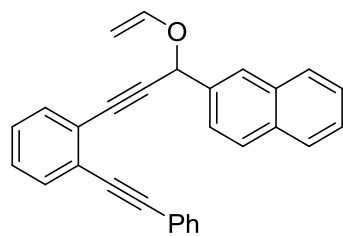
**1-fluoro-3-(3-(2-(2-phenylethynyl)phenyl)-1-(vinylloxy)prop-2-ynyl)benzene (3.18e)** was purified by flash chromatography (Hexane- EtOAc, v/v 8/1) as light yellow liquid;  $^1\text{H-NMR}$  (600 MHz,  $\text{CDCl}_3$ )  $\delta$  7.55 (dd,  $J = 16.2$  Hz, 7.2 Hz, 2H), 7.47-7.44 (m, 3H), 7.39-7.23 (m, 7H), 7.02 (td,  $J = 9.6$  Hz, 2.4 Hz, 1H), 6.62 (dd,  $J = 14.4$  Hz, 6.6 Hz, 1H), 5.82 (s, 1H), 4.61 (dd,  $J = 13.8$  Hz, 2.4 Hz, 1H), 4.20 (dd,  $J = 6.6$  Hz, 1.8 Hz, 1H);  $^{13}\text{C-NMR}$  (150 MHz,  $\text{CDCl}_3$ )  $\delta$  163.6, 162.0, 149.2, 140.0, 139.9, 132.3, 131.9, 131.7, 130.2, 130.1, 128.6, 128.5, 128.3, 127.9, 126.1, 124.4, 123.1, 123.0, 122.9, 115.6, 115.5, 114.5, 114.4, 93.6, 91.1, 89.1, 87.8, 87.3, 70.5; HRMS Calculated for  $\text{C}_{25}\text{H}_{17}\text{OF}$   $[\text{M}+\text{H}]^+$ : 353.1342, Found: 353.1336.



**3.18f**

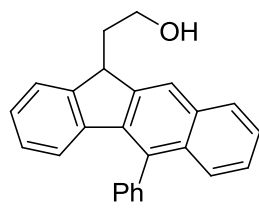
**1-bromo-4-fluoro-2-(3-(2-(2-phenylethynyl)phenyl)-1-(vinylloxy)prop-2-ynyl)benzene (3.18f)** was purified by flash chromatography (Hexane- EtOAc, v/v 8/1) as light yellow liquid;  $^1\text{H-NMR}$  (600 MHz,  $\text{CDCl}_3$ )  $\delta$  7.62 (dd,  $J = 9.0$  Hz, 3.0 Hz, 1H), 7.53 (t,  $J = 7.8$  Hz, 1H), 7.52-7.47 (m, 4H), 7.35-7.31 (m, 4H), 7.29 (td,  $J = 7.8$  Hz, 1.8 Hz, 1H), 6.92-6.89 (m, 1H), 6.59 (dd,  $J = 14.4$  Hz, 6.6 Hz, 1H), 6.06 (s, 1H), 4.57 (dd,  $J = 14.4$  Hz, 2.4 Hz, 1H), 4.21 (dd,  $J = 6.6$  Hz, 2.4 Hz, 1H);  $^{13}\text{C-NMR}$  (150 MHz,  $\text{CDCl}_3$ )  $\delta$  162.9, 161.3, 149.2, 139.1, 139.0, 134.1, 134.0, 132.2, 131.9, 131.7, 128.7, 128.6, 128.4, 128.2, 127.9, 126.2, 124.3, 122.9, 117.4, 117.3, 117.0, 116.7, 116.5, 93.7, 91.1, 88.3, 87.7, 87.1, 70.1; HRMS Calculated for  $\text{C}_{25}\text{H}_{16}\text{OFBr}$   $[\text{M}+\text{H}]^+$ : 431.0047, Found: 431.0042.





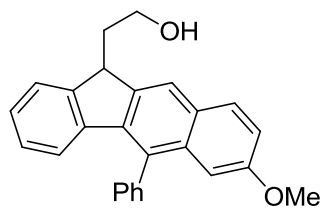
**3.18g**

**2-(3-(2-(2-phenylethynyl)phenyl)-1-(vinylloxy)prop-2-ynyl)naphthalene (3.18g)** was purified by flash chromatography (Hexane-EtOAc, v/v 8/1) as light yellow liquid;  $^1\text{H-NMR}$  (600 MHz,  $\text{CDCl}_3$ )  $\delta$  8.10 (s, 1H), 7.82 (d,  $J = 8.4$  Hz, 1H), 7.80-7.75 (m, 3H), 7.56 (d,  $J = 8.4$  Hz, 2H), 7.51-7.45 (m, 2H), 7.35-7.25 (m, 5H), 7.14 (t,  $J = 7.8$  Hz, 2H), 6.68 (dd,  $J = 14.4$  Hz, 6.6 Hz, 1H), 5.99 (s, 1H), 4.64 (dd,  $J = 13.8$  Hz, 2.4 Hz, 1H), 4.20 (dd,  $J = 6.6$  Hz, 1.8 Hz, 1H);  $^{13}\text{C-NMR}$  (150 MHz,  $\text{CDCl}_3$ )  $\delta$  149.4, 135.0, 133.4, 133.1, 132.3, 131.9, 128.7, 128.5, 128.3, 128.1, 127.9, 127.7, 126.7, 126.4, 126.2, 126.1, 125.1, 124.6, 122.9, 93.6, 90.9, 89.8, 87.9, 87.2, 71.6; HRMS Calculated for  $\text{C}_{29}\text{H}_{20}\text{O}$   $[\text{M}+\text{H}]^+$ : 385.1592, Found: 385.1587.



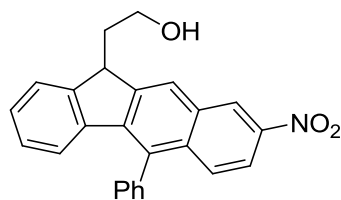
**3.21a**

**2-(5-phenyl-11H-benzo[b]fluoren-11-yl)ethanol (3.21a)** was purified by flash chromatography (Hexane- EtOAc, v/v 8/1) as yellow liquid;  $^1\text{H-NMR}$  (600 MHz,  $\text{CDCl}_3$ )  $\delta$  8.00 (s, 1H), 7.63-7.56 (m, 3H), 7.53 (dd,  $J = 7.2$  Hz, 6.6 Hz, 2H), 7.48-7.44 (m, 2H), 7.41-7.36 (m, 2H), 7.25 (t,  $J = 7.2$  Hz, 1H), 7.03 (t,  $J = 6.0$  Hz, 1H), 4.67 (d,  $J = 7.8$  Hz, 1H), 4.36 (t,  $J = 6.0$  Hz, 1H), 3.73-3.68 (m, 2H), 2.45-2.40 (m, 2H);  $^{13}\text{C-NMR}$  (150 MHz,  $\text{CDCl}_3$ )  $\delta$  147.7, 144.8, 140.6, 138.8, 136.8, 133.7, 132.8, 132.7, 130.1, 130.0, 129.1, 127.8, 127.7, 127.3, 126.9, 126.3, 125.5, 124.3, 123.7, 122.5, 60.2, 43.7, 36.9; HRMS Calculated for  $\text{C}_{25}\text{H}_{20}\text{O}$   $[\text{M}+\text{H}]^+$ : 337.1592, Found: 337.1587.



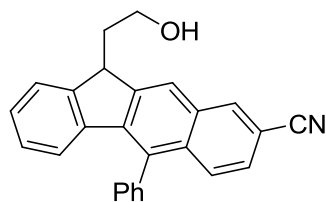
**3.21b**

**2-(7-methoxy-5-phenyl-11H-benzo[b]fluoren-11-yl)ethanol (3.21b)** was purified by flash chromatography (Hexane- EtOAc, v/v 8/1) as yellow liquid;  $^1\text{H-NMR}$  (600 MHz,  $\text{CDCl}_3$ )  $\delta$  7.54-7.53 (m, 1H), 7.48-7.45 (m, 3H), 7.41 (d,  $J = 9.0$  Hz, 2H), 7.33-7.30 (m, 3H), 7.28-7.25 (m, 2H), 6.76 (d,  $J = 9.0$  Hz, 2H), 4.11 (t,  $J = 7.2$  Hz, 1H), 3.96-3.92 (m, 1H), 3.80-3.75 (m, 4H), 2.10-2.04 (m, 1H);  $^{13}\text{C-NMR}$  (150 MHz,  $\text{CDCl}_3$ )  $\delta$  158.4, 133.5, 132.0, 131.9, 131.7, 128.5, 128.3, 128.0, 127.6, 125.9, 125.7, 123.2, 114.0, 95.4, 92.9, 88.4, 82.4, 60.8, 55.2, 41.2, 34.4; HRMS Calculated for  $\text{C}_{26}\text{H}_{22}\text{O}_2$   $[\text{M}+\text{H}]^+$ : 367.1698, Found: 367.1693.



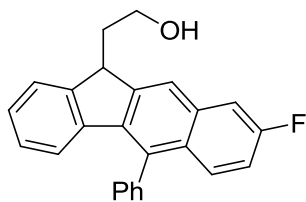
**3.21c**

**2-(8-nitro-5-phenyl-11H-benzo[b]fluoren-11-yl)ethanol (3.21c)** was purified by flash chromatography (Hexane- EtOAc, v/v 8/1) as yellow liquid;  $^1\text{H-NMR}$  (600 MHz,  $\text{CDCl}_3$ )  $\delta$  8.09 (s, 1H), 8.06 (d,  $J = 7.2$  Hz, 1H), 7.58-7.42 (m, 7H), 7.31 (d,  $J = 7.2$  Hz, 1H), 7.27 (t,  $J = 7.2$  Hz, 1H), 7.00 (t,  $J = 7.2$  Hz, 1H), 6.15 (d,  $J = 7.2$  Hz, 1H), 4.37 (t,  $J = 6.0$  Hz, 1H), 3.73 (t,  $J = 6.6$  Hz, 2H), 2.44-2.34 (m, 2H);  $^{13}\text{C-NMR}$  (150 MHz,  $\text{CDCl}_3$ )  $\delta$  149.6, 148.1, 146.7, 140.8, 139.8, 136.4, 131.8, 131.1, 130.6, 128.7, 128.6, 128.5, 127.2, 124.5, 124.3, 123.9, 123.3, 122.7, 122.2, 60.0, 43.5, 36.8; HRMS Calculated for  $\text{C}_{25}\text{H}_{19}\text{NO}_3$   $[\text{M}+\text{H}]^+$ : 382.1443, Found: 382.1438.



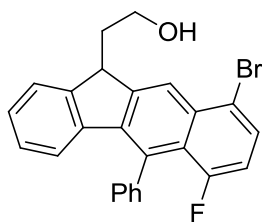
**3.21d**

**11-(2-hydroxyethyl)-5-phenyl-11H-benzo[b]fluorene-8-carbonitrile (3.21d)** was purified by flash chromatography (Hexane- EtOAc, v/v 8/1) as yellow liquid;  $^1\text{H-NMR}$  (600 MHz,  $\text{CDCl}_3$ )  $\delta$  8.14 (d,  $J = 7.8$  Hz, 1H), 8.07 (s, 1H), 7.92 (d,  $J = 8.4$  Hz, 1H), 7.68 (t,  $J = 7.2$  Hz, 1H), 7.62 (q,  $J = 7.2$  Hz, 2H), 7.52-7.48 (m, 3H), 7.44 (d,  $J = 6.0$  Hz, 1H), 7.28 (t,  $J = 7.2$  Hz, 1H), 7.03 (t,  $J = 7.2$  Hz, 1H), 6.29 (d,  $J = 7.8$  Hz, 1H), 4.37 (t,  $J = 6.0$  Hz, 1H), 3.73 (t,  $J = 6.6$  Hz, 2H), 2.44-2.36 (m, 2H);  $^{13}\text{C-NMR}$  (150 MHz,  $\text{CDCl}_3$ )  $\delta$  148.0, 146.2, 140.2, 139.9, 137.7, 136.8, 133.7, 133.0, 132.8, 131.0, 129.5, 129.2, 128.2, 127.3, 124.4, 123.7, 109.5, 102.9, 60.0, 43.5, 36.7; HRMS Calculated for  $\text{C}_{26}\text{H}_{19}\text{NO}$   $[\text{M}+\text{H}]^+$ : 362.1545, Found: 362.1539.



**3.21e**

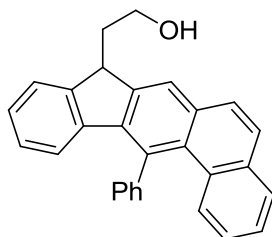
**2-(8-fluoro-5-phenyl-11H-benzo[b]fluoren-11-yl)ethanol (3.21e)** was purified by flash chromatography (Hexane-EtOAc, v/v 8/1) as yellow liquid;  $^1\text{H-NMR}$  (600 MHz,  $\text{CDCl}_3$ )  $\delta$  8.00 (s, 1H), 7.70 (d,  $J = 8.4$  Hz, 1H), 7.55-7.51 (m, 4H), 7.47-7.45 (m, 1H), 7.41-7.36 (m, 2H), 7.24 (t,  $J = 7.2$  Hz, 1H), 7.27-6.89 (m, 2H), 6.17 (d,  $J = 7.8$  Hz, 1H), 4.34 (t,  $J = 6.0$  Hz, 1H), 3.74-3.67 (m, 2H), 2.44-2.37 (m, 2H);  $^{13}\text{C-NMR}$  (150 MHz,  $\text{CDCl}_3$ )  $\delta$  175.8, 161.1, 159.4, 147.8, 145.8, 141.4, 140.5, 138.6, 135.1, 131.1, 128.7, 128.6, 127.7, 127.5, 127.2, 125.7, 124.4, 124.3, 124.2, 122.7, 111.4, 111.2, 60.2, 43.7, 37.0; HRMS Calculated for  $\text{C}_{25}\text{H}_{19}\text{OF}$   $[\text{M}+\text{H}]^+$ : 355.1498, Found: 355.1493.



**3.21f**

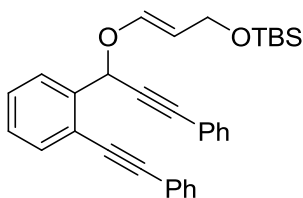
**2-(9-bromo-6-fluoro-5-phenyl-11H-benzo[b]fluoren-11-yl)ethanol (3.21f)** was purified by flash chromatography (Hexane-EtOAc, v/v 8/1) as yellow liquid;  $^1\text{H-NMR}$  (600 MHz,  $\text{CDCl}_3$ )  $\delta$  8.44 (s, 1H), 7.69 (dd,  $J = 8.4$  Hz, 4.2 Hz, 1H), 7.56-7.53 (m, 4H), 7.44-7.42 (m, 1H), 7.38-7.35 (m, 1H), 7.27 (t,  $J = 7.2$  Hz, 1H), 7.00 (t,  $J = 7.8$  Hz, 1H), 6.90 (dd,  $J = 12.6$  Hz, 8.4 Hz, 1H), 6.14 (d,  $J = 7.8$  Hz, 1H), 4.39 (t,  $J = 6.0$  Hz, 1H), 3.78-3.71 (m, 2H), 2.42 (q,  $J = 6.6$  Hz, 2H);

$^{13}\text{C}$ -NMR (150 MHz,  $\text{CDCl}_3$ )  $\delta$  160.6, 158.9, 147.9, 147.4, 140.7, 140.6, 139.9, 139.3, 132.6, 131.6, 129.3, 129.2, 128.7, 128.6, 128.5, 128.4, 128.0, 127.5, 127.1, 124.4, 124.3, 123.7, 123.6, 122.2, 117.3, 117.2, 111.7, 111.5, 60.1, 43.9, 36.9; HRMS Calculated for  $\text{C}_{25}\text{H}_{18}\text{OFBr}$   $[\text{M}+\text{H}]^+$ : 433.0603, Found: 433.0598.



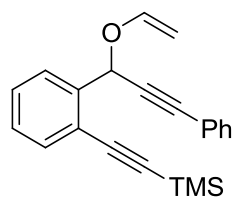
**3.21g**

**2-(13-phenyl-8H-indeno[2,1-b]phenanthren-8-yl)ethanol (3.21g)** was purified by flash chromatography (Hexane-EtOAc, v/v 8/1) as yellow liquid;  $^1\text{H}$ -NMR (600 MHz,  $\text{CDCl}_3$ )  $\delta$  7.93 (s, 1H), 7.79 (d,  $J = 7.2$  Hz, 1H), 7.74-7.72 (m, 2H), 7.62 (d,  $J = 8.4$  Hz, 1H), 7.55-7.54 (m, 1H), 7.51-7.49 (m, 1H), 7.46-7.42 (m, 2H), 7.36 (d,  $J = 8.4$  Hz, 2H), 7.31-7.24 (m, 4H), 7.16 (t,  $J = 7.8$  Hz, 1H), 4.34 (t,  $J = 7.2$  Hz, 1H), 4.01-3.97 (m, 1H), 3.83-3.79 (m, 1H), 2.19 (q,  $J = 6.0$  Hz, 2H);  $^{13}\text{C}$ -NMR (150 MHz,  $\text{CDCl}_3$ )  $\delta$  138.8, 133.5, 132.5, 132.0, 131.9, 131.6, 128.5, 128.3, 128.2, 128.0, 127.8, 127.7, 127.6, 126.1, 126.0, 125.9, 125.8, 125.7, 125.6, 123.1, 95.0, 93.0, 88.4, 82.7, 60.7, 40.9, 35.4; HRMS Calculated for  $\text{C}_{29}\text{H}_{22}\text{O}$   $[\text{M}+\text{H}]^+$ : 387.1749, Found: 387.1743.



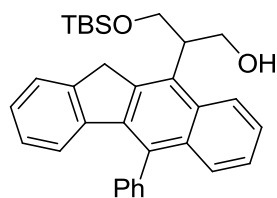
**3.25a**

**((E)-3-(3-phenyl-1-(2-(2-phenylethynyl)phenyl)prop-2-ynoxy)allyloxy)(tert-butyl)dimethylsilane (3.25a)** was purified by flash chromatography (Hexane-EtOAc, v/v 15/1) as light yellow liquid;  $^1\text{H}$ -NMR (600 MHz,  $\text{CDCl}_3$ )  $\delta$  7.74 (d,  $J = 7.8$  Hz, 1H), 7.50-7.47 (m, 3H), 7.37 (dd,  $J = 7.8$  Hz, 1.8 Hz, 1H), 7.33 (t,  $J = 7.8$  Hz, 1H), 7.28-7.25 (m, 4H), 7.23-7.19 (m, 3H), 6.54 (d,  $J = 12.6$  Hz, 1H), 6.15 (s, 1H), 5.22 (q,  $J = 12.6$  Hz, 1H), 4.05 (d,  $J = 6.6$  Hz, 2H), 0.87-0.66 (m, 9H), 0.09-0.05 (m, 6H);  $^{13}\text{C}$ -NMR (150 MHz,  $\text{CDCl}_3$ )  $\delta$  146.3, 139.3, 132.2, 131.8, 131.6, 128.8, 128.6, 128.5, 128.4, 128.2, 127.5, 123.0, 122.4, 122.3, 107.0, 94.9, 88.0, 86.5, 85.8, 70.0, 61.0, 26.2, 26.0, 18.3, -5.0; HRMS Calculated for  $\text{C}_{32}\text{H}_{34}\text{O}_2\text{Si}$   $[\text{M}+\text{H}]^+$ : 479.2406, Found: 479.2339.



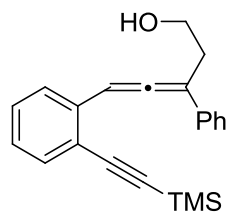
**3.25b**

**Trimethyl(2-(2-(3-phenyl-1-(vinylloxy)prop-2-ynyl)phenyl)ethynyl)silane (3.25b)** was purified by flash chromatography (Hexane- EtOAc, v/v 15/1) as light yellow liquid;  $^1\text{H-NMR}$  (600 MHz,  $\text{CDCl}_3$ )  $\delta$  7.83 (d,  $J = 7.8$  Hz, 1H), 7.52 (d,  $J = 7.8$  Hz, 1H), 7.50-7.48 (m, 2H), 7.41 (td,  $J = 7.2$  Hz, 1.8 Hz, 1H), 7.34-7.30 (m, 4H), 6.60 (dd,  $J = 13.8$  Hz, 6.6 Hz, 1H), 6.21 (s, 1H), 4.59 (dd,  $J = 13.8$  Hz, 2.4 Hz, 1H), 4.23 (dd,  $J = 6.6$  Hz, 2.4 Hz, 1H), 0.30-0.28 (m, 9H);  $^{13}\text{C-NMR}$  (150 MHz,  $\text{CDCl}_3$ )  $\delta$  150.1, 150.0, 139.7, 132.4, 131.8, 129.0, 128.6, 128.5, 128.2, 127.4, 122.4, 122.3, 101.9, 100.3, 90.0, 87.9, 85.7, 69.0, 68.9, -0.07; HRMS Calculated for  $\text{C}_{22}\text{H}_{22}\text{OSi}$   $[\text{M}+\text{H}]^+$ : 331.1518, Found: 331.1512.



**3.26a**

**3-(tert-butyldimethylsilyloxy)-2-(5-phenyl-11H-benzo[b]fluoren-10-yl)propan-1-ol (3.26a)** was purified by flash chromatography (Hexane-EtOAc, v/v 8/1) as yellow liquid;  $^1\text{H-NMR}$  (600 MHz,  $\text{CDCl}_3$ )  $\delta$  7.56-7.53 (m, 3H), 7.49-7.47 (m, 3H), 7.37-7.33 (m, 4H), 7.28-7.25 (m, 2H), 7.21 (t,  $J = 7.8$  Hz, 2H), 4.04 (dd,  $J = 9.6$  Hz, 4.2 Hz, 1H), 3.98-3.91 (m, 2H), 3.85 (t,  $J = 9.6$  Hz, 1H), 3.24-3.19 (m, 1H), 2.86 (br, 1H);  $^{13}\text{C-NMR}$  (150 MHz,  $\text{CDCl}_3$ )  $\delta$  135.2, 135.1, 132.7, 131.6, 128.7, 128.6, 128.4, 128.3, 127.5, 127.1, 126.4, 126.2, 123.1, 121.4, 108.3, 97.3, 94.5, 87.4, 66.4, 66.0, 43.9, 25.8, 18.2, -5.5; HRMS Calculated for  $\text{C}_{32}\text{H}_{36}\text{O}_2\text{Si}$   $[\text{M}+\text{H}]^+$ : 481.2563, Found: 481.2557.



**3.26b**

**5-(2-(2-(trimethylsilyl)ethynyl)phenyl)-3-phenylpenta-3,4-dien-1-ol (3.26b)** was purified by flash chromatography (Hexane-EtOAc, v/v 8/1) as yellow liquid;  $^1\text{H-NMR}$  (600 MHz,  $\text{CDCl}_3$ )  $\delta$  7.47 (q,  $J = 7.8$  Hz, 4H), 7.34 (t,  $J = 7.8$  Hz, 2H), 7.27-7.22 (m, 3H), 7.16-7.14 (m, 2H), 3.93 (t,  $J = 6.0$  Hz, 2H), 2.92-2.83 (m, 2H), 0.32-0.26 (m, 9H);  $^{13}\text{C-NMR}$  (150 MHz,  $\text{CDCl}_3$ )  $\delta$  207.0, 135.7, 135.3, 133.1, 128.9, 128.6, 127.4, 126.9, 126.2, 126.1, 121.2, 106.9, 103.0, 99.7, 96.6, 61.1, 33.3, 0.00; HRMS Calculated for  $\text{C}_{22}\text{H}_{24}\text{OSi}$   $[\text{M}+\text{H}]^+$ : 333.1675, Found: 333.1669.

## Chapter Four: 1,2,3-triazoles work as X-factor to promote gold(I) complex in challenging chemical transformations - part III

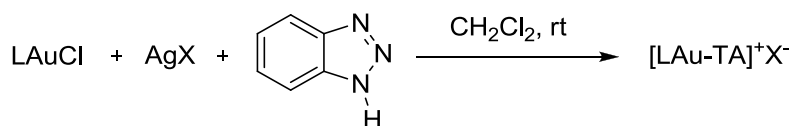
### I. General Methods and Materials

All of the reactions dealing with air and/or moisture-sensitive reagents were carried out under an atmosphere of nitrogen using oven/flame-dried glassware and standard syringe/septa techniques. Unless otherwise noted, all commercial reagents and solvents were obtained from the commercial provider and used without further purification.  $^1\text{H}$ ,  $^{13}\text{C}$ ,  $^{11}\text{B}$  and  $^{31}\text{P}$  NMR spectra were recorded on Agilent 400 MHz spectrometers, (400 MHz, 100 MHz, 128 MHz and 160 MHz) at a temperature of 300 K. NMR multiplicities are abbreviated as follows: s = singlet, d = doublet, m = multiplet. Chemical shifts ( $\delta$ ) and coupling constants (J) are expressed in ppm and Hz respectively. NMR chemical shifts were reported relative to internal tetramethylsilane ( $\delta$  0.00 ppm) or  $\text{CDCl}_3$  ( $\delta$  7.26 ppm) for  $^1\text{H}$  and  $\text{CDCl}_3$  ( $\delta$  77.0 ppm) or  $\text{CD}_3\text{CN}$  ( $\delta$  118.3 ppm) for  $^{13}\text{C}$ . Flash column chromatography was performed on 230-430 mesh silica gel. Analytical thin layer chromatography was performed with precoated glass baked plates (250 $\mu$ ) and visualized by fluorescence and by charring after treatment with potassium permanganate stain. HRMS were recorded on LTQ-FTUHRA spectrometer.

Substrates were synthesized according to the literature as below:

- [1]. L. N. Lee, A. S. C. Chan and F. Y. Kwong, *Eur. J. Org. Chem.* **2008**, 3403-3406.
- [2]. Sylvester, K. T.; Chirik, P. J. *J. Am. Chem. Soc.* **2009**, *131*, 8772-8774.
- [3]. W. Hess, J. W. Burton, *Chem. Eur. J.* **2010**, *16*, 12303-12306.
- [4]. J. C. Sheehan, W. A. Bolhofer, *J. Am. Chem. Soc.* **1950**, *72*, 2786-2788.

#### Procedure for the synthesis of $\text{LAu}(\text{TA})^+\text{X}^-$ .

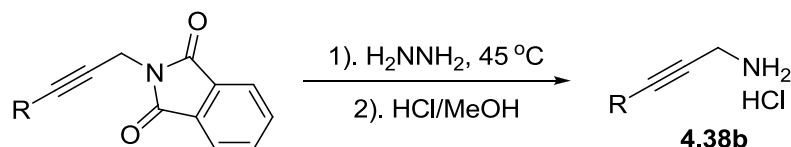


To freshly distilled dichloromethane (3 ml) was successively added LAuCl, 0.3 mmol 1.0 eq., L = PPh<sub>3</sub> (Triphenylphosphine), IPr (1,3-bis(2,6-diisopropylphenyl)imidazol-2-ylidene), XPhos (2-Dicyclohexylphosphino-2',4',6'-triisopropylbiphenyl), 1H-benzo[d][1,2,3]triazole (35.7 mg, 0.3 mmol, 1.0 eq.), AgX (79.4 mg, 0.310 mmol, 1.1 eq., X = TfO<sup>-</sup>, F<sub>6</sub>Sb<sup>-</sup>). The reaction mixture was stirred at room temperature for 6 hours and was slowly filtered through celite pad twice to remove the AgCl and excess amount of the AgX. The clear solution was concentrated under reduced pressure. The resulting crude product was purified by recrystallization from dichloromethane and hexane to afford LAu(TA)<sup>+</sup>X<sup>-</sup> as white solid.

### 31P NMR sample preparation

To a NMR sample tube with a sealed capillary tube containing H<sub>3</sub>PO<sub>4</sub>/D<sub>2</sub>O (1M) solution as internal standard for chemical shift ( $\delta$  0.00 ppm) and integration (value = 100), was successively added gold(I) complex/CDCl<sub>3</sub> solution (0.052 M, 0.5 mL), and **4.38b**/CDCl<sub>3</sub> solution (0.39 M, 0.2 mL). Then the tube was sealed and shaken.

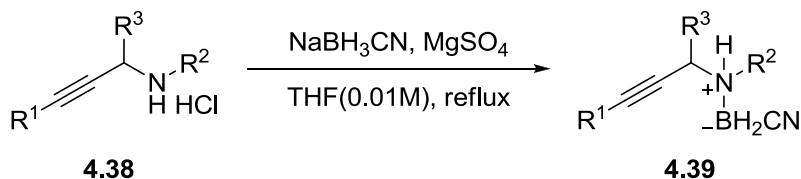
### Procedure for the synthesis of propargyl amine deprotection.



To 31.5 mL hydrazine monohydrate was added 2-(3-phenylprop-2-ynyl)isindoline-1,3-dione (1.044 g, 4 mol). The reaction mixture was stirred at 45 °C. The reaction was monitored by TLC. After the reaction was completed (25 min) the mixture was cooled to room temperature and was poured to a vessel containing dichloromethane (15 mL). The mixture was extracted with dichloromethane (3 × 10mL) and the combined organic phase was washed with brine (2 × 10mL), dried over Na<sub>2</sub>SO<sub>4</sub> and was concentrated under rotary vacuum evaporator. The resulting crude product was added dropwise into a HCl (1M) solution in EtOH and stir for 15 min at RT. Solvent was removed under reduced pressure and the residue was triturated from dichloromethane/hexane solution (1/2 = V/V) to give 3-phenylprop-2-yn-1-amine hydrochloride **4.38b** (97% yield) as white solid.

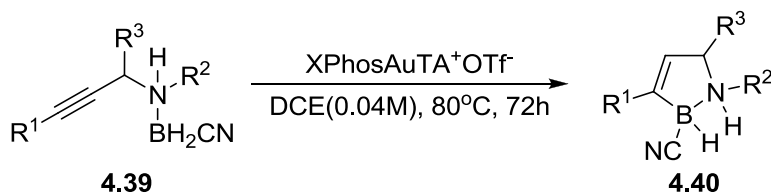


### Procedure for the synthesis of propargyl amine boranecarbonitrile 2.



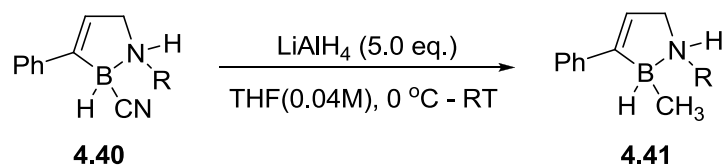
To a solution of propargyl amine hydrochloride **4.38** (50.0 mmol, 1.0 eq.) in tetrahydrofuran (250 mL, 0.2 M), was successively added  $\text{MgSO}_4$  (10.0 g),  $\text{NaBH}_3\text{CN}$  (250.0 mmol, 5.0 eq.). The reaction mixture was stirred at refluxing for 24 hours. The reaction mixture was monitored by TLC. Upon completion, the solid precipitates was removed by filtration and washed with diethyl ether ( $3 \times 10\text{mL}$ ). The combined mixture was washed with brine ( $2 \times 10\text{mL}$ ) and solvent was removed under reduced pressure. The residue was purified by flash chromatography on silica gel (ethyl acetate/hexane = 1/2, V/V) to give **4.39** as white solid or colorless liquid.

### Procedure for the Au(I) catalyzed alkyne hydroboration 3.



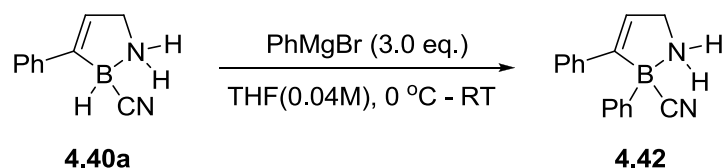
To a solution of **4.39** (0.2 mmol, 1.0 eq.) in 1,2-dichloroethane (5 mL, 0.04 M), was added  $\text{XPhosAu(TA)OTf}$  (9.3 mg, 5 mol %). The reaction mixture was stirred at  $80^\circ\text{C}$  for 72 hours and monitored by TLC. Upon completion, solvent was removed under reduced pressure and the residue was purified by flash chromatography on silica gel (ethyl acetate/hexane = 1/2, V/V) to give **4.40** as white solid or colorless liquid.

### Procedure for lithium aluminium hydride ( $\text{LiAlH}_4$ ) reduction of 4.



To a solution of **4.40** (0.5 mmol, 1.0 eq.) in tetrahydrofuran (12 mL, 0.04 M) at 0 °C, LiAlH<sub>4</sub> was added (19 mg, 0.5 mmol, 1.0 eq.). The reaction mixture was stirred at 0 °C for 15 min and warmed to RT and stirred for 30 min, then the second portion of LiAlH<sub>4</sub> was added (38 mg, 1.0 mmol, 2.0 eq.). The reaction was monitored by TLC. Upon completion, solvent was removed under reduced pressure and the residue was purified by flash chromatography on silica gel (ethyl acetate/hexane = 1/2, V/V) to give **4.41a** as white solid or **4.41b** as colorless liquid.

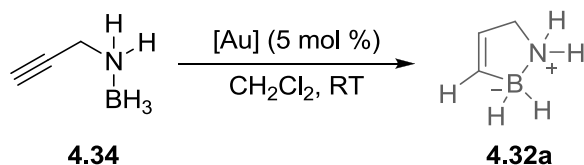
#### Procedure for phenyl substitution on boron center of 4a.



To a solution of **4.40a** (85 mg, 0.5 mmol, 1.0 eq.) in tetrahydrofuran (12 mL, 0.04 M) at 0 °C, PhMgBr (2.8 M solution in diethyl ether) was added (0.18 mL, 0.5 mmol, 1.0 eq.). The reaction mixture was stirred at 0 °C for 15 min and warmed to RT and stirred for 30 min, then the second portion of PhMgBr (2.8 M solution in diethyl ether) was added (0.36 mL, 1.0 mmol, 2.0 eq.) and stirred at RT. Reaction was monitored by TLC. Upon completion, solvent was removed under reduced pressure and the residue was purified by flash chromatography on silica gel (ethyl acetate/hexane = 1/2, V/V) to give **4.42** as white solid.

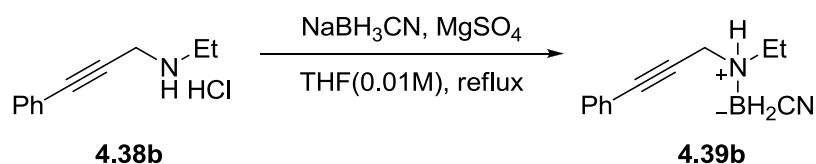
## II. Condition Screening Data

**Table 1. Condition screening of amine borane **1** with typical and classic gold catalysts.**



entry	Au catalyst	time	conv. (%)	yield (%)
1	PPh <sub>3</sub> AuCl/AgOTf	1 hr or 24 hr	<5	n.d.
2	IPrAuCl/AgOTf	1 hr or 24 hr	<5	n.d.
3	XPhosAuCl/AgOTf	1 hr or 24 hr	<5	n.d.
4	P(OMe) <sub>3</sub> AuCl/AgOTf	1 hr or 24 hr	<5	n.d.
5	[PPh <sub>3</sub> Au] <sup>+</sup> Tf <sub>2</sub> N <sup>-</sup>	1 hr or 24 hr	<5	n.d.
6	[XPhosAu] <sup>+</sup> Tf <sub>2</sub> N <sup>-</sup>	1 hr or 24 hr	<5	n.d.
7	[PPh <sub>3</sub> Au-TA] <sup>+</sup> TfO <sup>-</sup>	1 hr or 24 hr	<5	n.d.
8	[PPh <sub>3</sub> Au-TA] <sup>+</sup> F <sub>6</sub> Sb <sup>-</sup>	1 hr or 24 hr	<5	n.d.
9	[IPrAu-TA] <sup>+</sup> TfO <sup>-</sup>	1 hr or 24 hr	<5	n.d.
10	[IPrAu-TA] <sup>+</sup> F <sub>6</sub> Sb <sup>-</sup>	1 hr or 24 hr	<5	n.d.
11	[XPhosAu-TA] <sup>+</sup> TfO <sup>-</sup>	1 hr or 24 hr	<5	n.d.
12	[XPhosAu-TA] <sup>+</sup> F <sub>6</sub> Sb <sup>-</sup>	1 hr or 24 hr	<5	n.d.

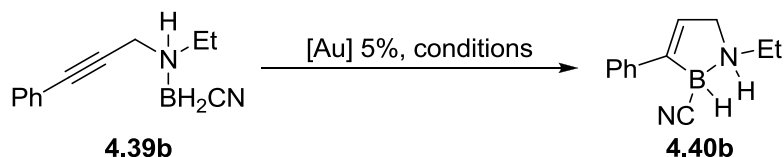
General reaction conditions: entry 1-4, all Au catalyst was generated by mixing corresponding LAuCl (L = PPh<sub>3</sub>, IPr, XPhos, P(OMe)<sub>3</sub>) complexes with AgOTf (1.1 eq.) in CH<sub>2</sub>Cl<sub>2</sub> (1 mL), the mixture was stirred for 5 minutes then filtered through cotton pad and added to a solution of **1** in CH<sub>2</sub>Cl<sub>2</sub>. RT = room temperature, n.d. = not determined. Conversion and yields were determined by NMR with *p*-xylene as internal standard. TA = 1H-benzo[d][1,2,3]triazole.

**Table 2. Condition Screening of the formation of propargyl amine boranecarbonitrile 3b.**

entry	solvent	temp. (°C)	eq. of NaBH <sub>3</sub> CN	conv. (%) <sup>a</sup>	yield (%) <sup>a</sup>
1	CH <sub>2</sub> Cl <sub>2</sub>	rt	3	<5	n.d.
2	CHCl <sub>3</sub>	rt	3	<5	n.d.
3	MeOH	rt	3	<5	n.d.
4	DMF	rt	3	<5	n.d.
5	MeCN	rt	3	<5	n.d.
6	Et <sub>2</sub> O	rt	1	<5	n.d.
7	Et <sub>2</sub> O	rt	3	47	25
8	Et <sub>2</sub> O	rt	5	92	43
9	THF	rt	1	<5	n.d.
10	THF	rt	5	11	trace
11	THF	reflux	1	23	9
12	THF	reflux	5	<b>&gt;99</b>	<b>87</b>

General reaction conditions: NaBH<sub>3</sub>CN, MgSO<sub>4</sub> (600mg, 5 mmol 5.0 eq.) was suspended in solution and stirring at room temperature, **4.38b** (195mg, 1 mmol, 1.0 eq.) was added slowly and the reaction mixture was let stirred at the indicated conditions. rt = room temperature, n.d. = not determined. Conversion and yields were determined by NMR with *p*-xylene as internal standard.

**Table 3. Condition Screening of alkyne hydroboration.**



entry	Au catalyst (5%)	solvent	T (°C)	Time	conv. (%)	yield (%)
1	PPh <sub>3</sub> AuCl	CH <sub>2</sub> Cl <sub>2</sub>	rt	72 hr	<5	n.d.
2	PPh <sub>3</sub> AuCl/AgOTf	CH <sub>2</sub> Cl <sub>2</sub>	rt	30 min or 72 hr	19	17
3	IPrAuCl/AgOTf	CH <sub>2</sub> Cl <sub>2</sub>	rt	30 min or 72 hr	15	11
4	XPhosAuCl/AgOTf	CH <sub>2</sub> Cl <sub>2</sub>	rt	30 min or 72 hr	<5	n.d.
5	P(OMe) <sub>3</sub> AuCl/AgOTf	CH <sub>2</sub> Cl <sub>2</sub>	rt	30 min or 72 hr	<5	n.d.
6	[PPh <sub>3</sub> Au-TA] <sup>+</sup> TfO <sup>-</sup>	CH <sub>2</sub> Cl <sub>2</sub>	rt	72 hr	<5	n.d.
7	[PPh <sub>3</sub> Au] <sup>+</sup> Tf <sub>2</sub> N <sup>-</sup>	CH <sub>2</sub> Cl <sub>2</sub>	rt	72 hr	32	21
8	[XPhosAu] <sup>+</sup> Tf <sub>2</sub> N <sup>-</sup>	CH <sub>2</sub> Cl <sub>2</sub>	rt	72 hr	>99	71
9	[XPhosAu-NCMe] <sup>+</sup> F <sub>6</sub> Sb <sup>-</sup>	CH <sub>2</sub> Cl <sub>2</sub>	rt	30 min or 72 hr	16	2
10	PPh <sub>3</sub> AuCl	DCE	80	72 hr	<5	n.d.
11	XPhosAuCl/AgOTf	DCE	80	30 min or 72 hr	10	5
12	IPrAuCl/AgOTf	DCE	80	30 min or 72 hr	<5	n.d.
13	[PPh <sub>3</sub> Au-TA] <sup>+</sup> TfO <sup>-</sup>	DCE	80	24 hr or 72hr	35	24
14	[PPh <sub>3</sub> Au] <sup>+</sup> Tf <sub>2</sub> N <sup>-</sup>	DCE	80	24 hr or 72hr	47	34
15	[XPhosAu-TA] <sup>+</sup> TfO <sup>-</sup>	DCE	80	72 hr	<b>99</b>	<b>93</b>
16	[XPhosAu-TA] <sup>+</sup> F <sub>6</sub> Sb <sup>-</sup>	DCE	80	72 hr	73	59

17	[XPhosAu] <sup>+</sup> Tf <sub>2</sub> N <sup>-</sup>	DCE	80	72 hr	82	72
18	[XPhosAu-TA] <sup>+</sup> TfO <sup>-</sup>	THF	65	72 hr	85	73
19	[XPhosAu-TA] <sup>+</sup> TfO <sup>-</sup>	DMF	80	72 hr	84	63
20	[XPhosAu-TA] <sup>+</sup> TfO <sup>-</sup>	Toluene	90	72 hr	39	36
21	[XPhosAu-TA] <sup>+</sup> TfO <sup>-</sup>	MeCN	80	72 hr	88	65

General reaction conditions: **4.39b** (39 mg, 0.2 mmol 1.0 eq.), solvent (5 mL) and Au catalyst (0.01 mmol, 5 mol %) was successively added into 20 mL reaction vial and stirred at corresponding temperature. rt = room temperature, n.d. = not determined, TA = 1H-benzo[d][1,2,3]triazole. Conversion and yields were determined by NMR with *p*-xylene as internal standard.

**Table 4. Catalyst Decomposition Monitoring by  $^{31}\text{P}$  NMR.**

entry	Au catalyst	time	per-catalyst (%)
1	$\text{PPh}_3\text{AuCl}/\text{AgOTf}$	0	100
		5 min	0
2	$[\text{PPh}_3\text{Au}]^+\text{Tf}_2\text{N}^-$	0	100
		5 min	0
3	$[\text{PPh}_3\text{Au-TA}]^+\text{TfO}^-$	0	<b>100</b>
		1 hr	<b>90</b>
		20 hr	<b>55</b>
4	$\text{XPhosAuCl}/\text{AgOTf}$	0	100
		5 min	0
5	$[\text{XPhosAu}]^+\text{Tf}_2\text{N}^-$	0	100
		5 min	0
6	$[\text{XPhosAu-NCMe}]^+\text{F}_6\text{Sb}^-$	0	100
		5 min	0
7	$[\text{XPhosAu-TA}]^+\text{TfO}^-$	0	<b>100</b>
		1 hr	<b>90</b>
		20 hr	<b>85</b>

A sealed capillary tube containing  $\text{H}_3\text{PO}_4/\text{D}_2\text{O}$  (1M) solution was used as internal standard for chemical shift ( $\delta = 0.00$  ppm) and integration (value = 100). For detailed experimental data, please see.

### III. ORTEP Drawing of the Crystal Structure

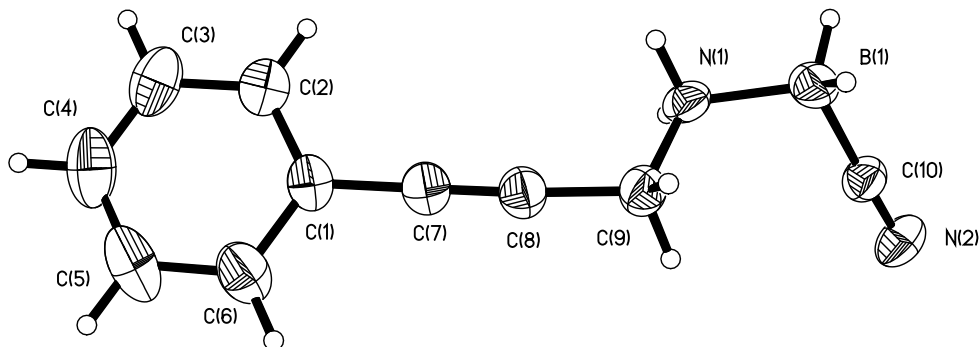


Figure 1. Perspective view of the molecular structure of **4.39a** ( $C_{10}H_{11}BN_2$ ) with the atom labeling scheme provided for the non-hydrogen atoms. The thermal ellipsoids are scaled to enclose 30% probability for purposes of clarity. CCDC number: 954118.

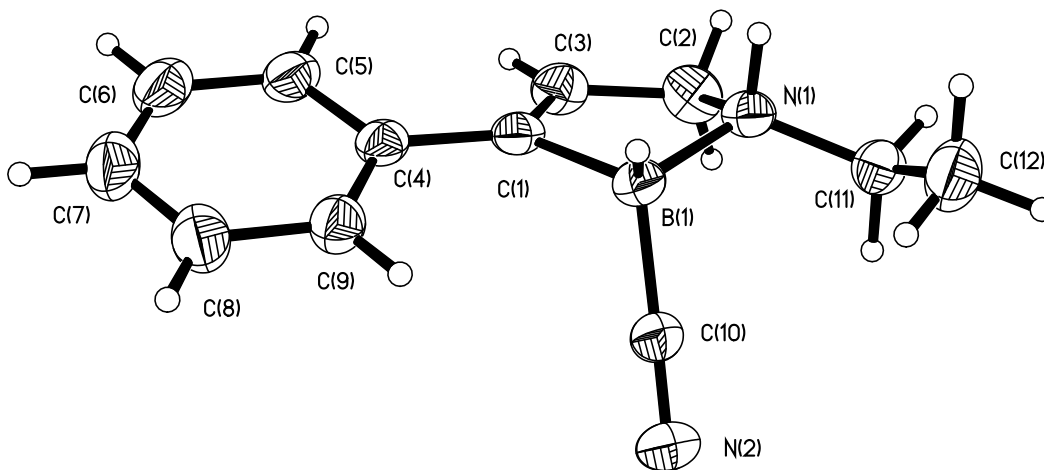


Figure 2. Perspective view of the molecular structure of **4.40b** ( $C_{12}H_{15}BN_2$ ) with the atom labeling scheme. The thermal ellipsoids are scaled to enclose 30% probability. CCDC number: 954119.



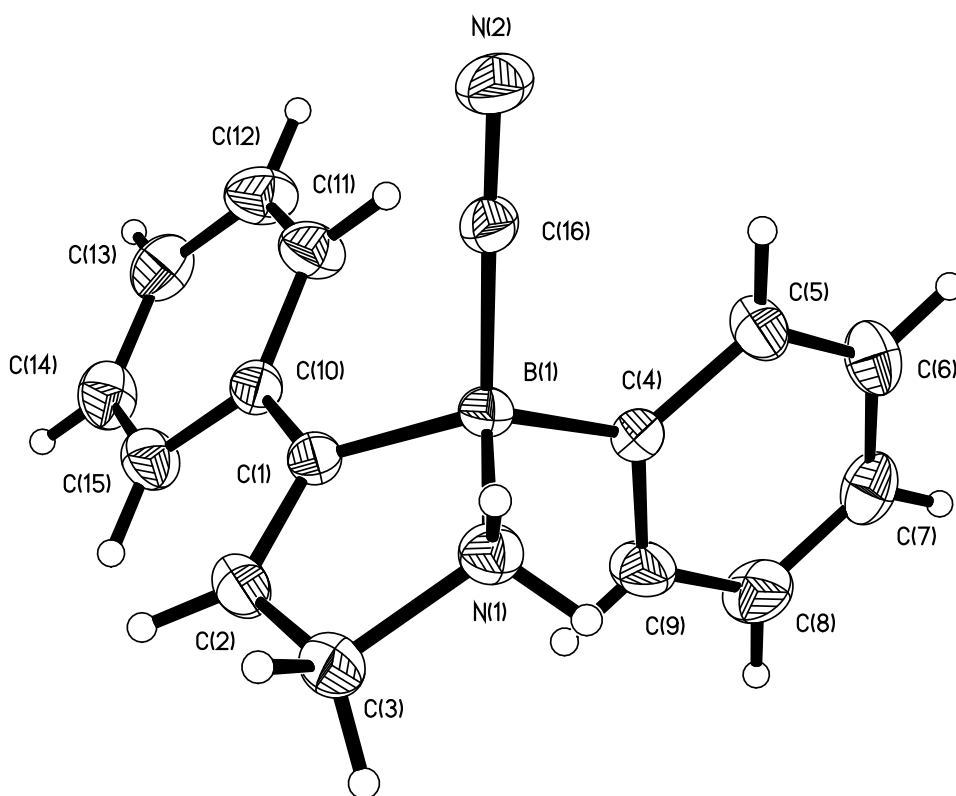
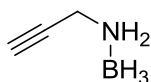


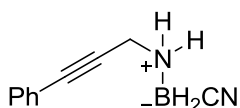
Figure 3. Perspective view of the molecular structure of **4.42** (C<sub>16</sub>H<sub>15</sub>BN<sub>2</sub>) with the atom labeling scheme. The thermal ellipsoids are scaled to enclose 30% probability. CCDC number: 965653.

## IV. Compounds Characterization



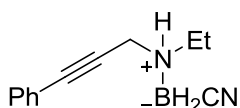
**4.34**

**4.34** was purified by flash chromatography (Hexane/EtOAc, v/v 2/1) as light yellow liquid; <sup>1</sup>H-NMR (400 MHz, CDCl<sub>3</sub>) δ 4.15 (b, 3H), 3.56 (ddd, J = 9.2 Hz, 5.2 Hz, 2.4 Hz, 2H), 2.46 (t, J = 2.0 Hz, 1H), 1.83-1.09 (b, 3H); <sup>13</sup>C-NMR (100 MHz, CDCl<sub>3</sub>) δ 77.5, 75.1, 37.6; <sup>11</sup>B-NMR (128 MHz, CDCl<sub>3</sub>) -18.76; HRMS Calculated for C<sub>3</sub>H<sub>8</sub>BN [M+Na]<sup>+</sup>: 92.0647, Found: 92.0644.



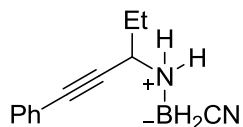
**4.39a**

**4.39a** was purified by flash chromatography (Hexane/EtOAc, v/v 2/1) as white solid with 97% yield; <sup>1</sup>H-NMR (400 MHz, CD<sub>3</sub>CN) δ 7.47-7.44 (m, 2H), 7.41-7.36 (m, 3H), 5.03 (b, 2H), 3.69 (t, J = 6.8 Hz, 2H), 2.15-1.24 (b, 2H); <sup>13</sup>C-NMR (100 MHz, CD<sub>3</sub>CN) δ 136.8, 134.3, 133.9, 127.2, 90.9, 87.8, 41.2; <sup>11</sup>B-NMR (128 MHz, CD<sub>3</sub>CN) -18.20; HRMS Calculated for C<sub>10</sub>H<sub>11</sub>BN<sub>2</sub> [M+Na]<sup>+</sup>: 193.0907, Found: 193.0909.



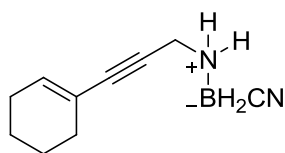
**4.39b**

**4.39b** was purified by flash chromatography (Hexane/EtOAc, v/v 2/1) as yellow liquid with 87%; <sup>1</sup>H-NMR (400 MHz, CDCl<sub>3</sub>) δ 7.46-7.44 (m, 2H), 7.37-7.31 (m, 3H), 5.25 (b, 1H), 3.99 (dd, J = 11.2 Hz, 2.4 Hz, 1H), 3.72 (dd, J = 11.2 Hz, 5.2 Hz, 1H), 3.25-3.19 (m, 1H), 3.09-3.02 (m, 1H), 2.23-1.56 (b, 2H), 1.32 (t, J = 4.8 Hz, 3H); <sup>13</sup>C-NMR (100 MHz, CDCl<sub>3</sub>) δ 131.8, 129.1, 128.4, 121.6, 87.9, 80.0, 46.9, 42.7, 10.8; <sup>11</sup>B-NMR (128 MHz, CDCl<sub>3</sub>) -20.45; HRMS Calculated for C<sub>12</sub>H<sub>15</sub>BN<sub>2</sub> [M+Na]<sup>+</sup>: 221.1225, Found: 221.1220.



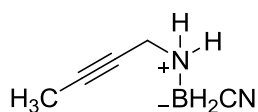
**4.39c**

**4.39c** was purified by flash chromatography (Hexane/EtOAc, v/v 2/1) as white solid with 89%; <sup>1</sup>H-NMR (400 MHz, CDCl<sub>3</sub>) δ 7.47-7.44 (m, 2H), 7.32-7.24 (m, 3H), 5.03 (b, 1H), 4.87 (b, 1H), 3.83-3.76 (m, 1H), 1.99-1.90 (m, 1H), 1.83-1.74 (m, 1H), 1.05 (t, J = 7.2 Hz, 3H); <sup>13</sup>C-NMR (100 MHz, CD<sub>3</sub>CN) δ 131.7, 128.7, 128.2, 121.8, 87.2, 84.6, 51.0, 26.9, 9.6; <sup>11</sup>B-NMR (128 MHz, CD<sub>3</sub>CN) -21.38; HRMS Calculated for C<sub>12</sub>H<sub>15</sub>BN<sub>2</sub> [M+Na]<sup>+</sup>: 221.1225, Found: 221.1220.



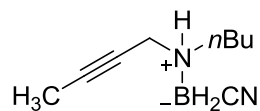
**4.39d**

**4.39d** was purified by flash chromatography (Hexane/EtOAc, v/v 2/1) as light yellow liquid with 81% yield; <sup>1</sup>H-NMR (400 MHz, CDCl<sub>3</sub>) δ 6.16 (t, J = 2.0 Hz, 1H), 4.75 (b, 2H), 3.69 (t, J = 6.4 Hz, 2H), 2.10-2.07 (m, 4H), 1.66-1.55 (m, 4H); <sup>13</sup>C-NMR (100 MHz, CDCl<sub>3</sub>) δ 137.0, 119.4, 78.7, 60.5, 37.0, 28.7, 25.6, 22.0, 21.3; <sup>11</sup>B-NMR (128 MHz, CDCl<sub>3</sub>) -22.68; HRMS Calculated for C<sub>10</sub>H<sub>15</sub>BN<sub>2</sub> [M+Na]<sup>+</sup>: 197.1221, Found: 197.1218.



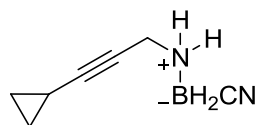
**4.39e**

**4.39e** was purified by flash chromatography (Hexane/EtOAc, v/v 2/1) as light yellow liquid with 73% yield; <sup>1</sup>H-NMR (400 MHz, CDCl<sub>3</sub>) δ 4.86 (b, 2H), 3.55-3.50 (m, 2H), 2.79-1.17 (b, 2H), 1.85 (t, J = 2.4 Hz, 3H); <sup>13</sup>C-NMR (100 MHz, CDCl<sub>3</sub>) δ 83.9, 72.0, 36.5, 3.5; <sup>11</sup>B-NMR (128 MHz, CDCl<sub>3</sub>) -25.65; HRMS Calculated for C<sub>5</sub>H<sub>9</sub>BN<sub>2</sub> [M+Na]<sup>+</sup>: 131.0751, Found: 131.0755.



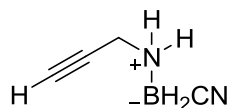
**4.39f**

**4.39f** was purified by flash chromatography (Hexane/EtOAc, v/v 2/1) as light yellow liquid with 91% yield; <sup>1</sup>H-NMR (400 MHz, CDCl<sub>3</sub>) δ 4.83 (b, 1H), 3.72 (dt, J = 16.4 Hz, 2.8 Hz, 1H), 3.42 (ddd, J = 16.4 Hz, 4.8 Hz, 2.0 Hz, 1H), 3.05-3.00 (m, 1H), 2.87-2.79 (m, 1H), 1.84 (t, J = 2.4 Hz, 3H), 1.69-1.61 (m, 2H), 1.38-1.29 (m, 2H), 0.94 (t, J = 7.6 Hz, 3H); <sup>13</sup>C-NMR (100 MHz, CDCl<sub>3</sub>) δ 84.6, 70.3, 51.8, 43.1, 27.4, 19.9, 13.5, 3.5; <sup>11</sup>B-NMR (128 MHz, CDCl<sub>3</sub>) -20.29; HRMS Calculated for C<sub>9</sub>H<sub>17</sub>BN<sub>2</sub> [M+Na]<sup>+</sup>: 187.1377, Found: 187.1379.



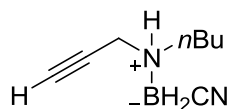
**4.39g**

**4.39g** was purified by flash chromatography (Hexane/EtOAc, v/v 2/1) as light yellow liquid with 83% yield; <sup>1</sup>H-NMR (400 MHz, CDCl<sub>3</sub>) δ 4.81 (b, 2H), 3.49 (td, J = 7.2 Hz, 2.0 Hz, 2H), 2.28-1.31 (b, 2H), 1.27-1.20 (m, 1H), 0.84-0.73 (m, 2H), 0.72-0.67 (m, 2H); <sup>13</sup>C-NMR (100 MHz, CDCl<sub>3</sub>) δ 91.3, 68.0, 36.6, 8.2, -0.8; <sup>11</sup>B-NMR (128 MHz, CDCl<sub>3</sub>) -25.77; HRMS Calculated for C<sub>7</sub>H<sub>11</sub>BN<sub>2</sub> [M+Na]<sup>+</sup>: 157.0912, Found: 157.0908.



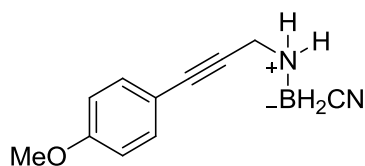
**4.39h**

**4.39h** was purified by flash chromatography (Hexane/EtOAc, v/v 2/1) as light yellow liquid with 66% yield; <sup>1</sup>H-NMR (400 MHz, CDCl<sub>3</sub>) δ 5.02 (b, 2H), 3.47 (ddd, J = 13.6 Hz, 6.8 Hz, 2.8 Hz, 2H), 2.72 (t, J = 2.8 Hz, 1H), 2.03-1.05 (b, 2H); <sup>13</sup>C-NMR (100 MHz, CDCl<sub>3</sub>) δ 82.3, 80.3, 40.3; <sup>11</sup>B-NMR (128 MHz, CDCl<sub>3</sub>) -18.23; HRMS Calculated for C<sub>4</sub>H<sub>7</sub>BN<sub>2</sub> [M+Na]<sup>+</sup>: 117.0594, Found: 117.0587.



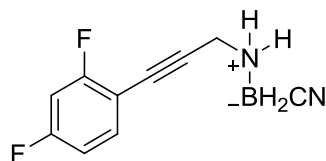
**4.39i**

**4.39i** was purified by flash chromatography (Hexane/EtOAc, v/v 2/1) as light yellow liquid with 85% yield; <sup>1</sup>H-NMR (400 MHz, CDCl<sub>3</sub>) δ 5.47 (b, 1H), 3.70 (dt, J = 17.2 Hz, 3.6 Hz, 1H), 3.46 (ddd, J = 16.8 Hz, 7.2 Hz, 2.4 Hz, 1H), 3.03-2.95 (m, 1H), 2.86-2.79 (m, 1H), 2.45 (t, J = 2.4 Hz, 1H), 1.84 (t, J = 2.4 Hz, 3H), 1.66-1.58 (m, 2H), 1.34-1.27 (m, 2H), 0.91 (t, J = 7.2 Hz, 3H); <sup>13</sup>C-NMR (100 MHz, CDCl<sub>3</sub>) δ 76.4, 74.6, 51.7, 42.0, 27.1, 19.8, 13.4; <sup>11</sup>B-NMR (128 MHz, CDCl<sub>3</sub>) -20.29; HRMS Calculated for C<sub>8</sub>H<sub>15</sub>BN<sub>2</sub> [M+Na]<sup>+</sup>: 173.1221, Found: 173.1227.



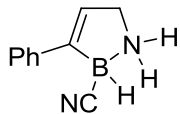
**4.39j**

**4.39j** was purified by flash chromatography (Hexane/EtOAc, v/v 2/1) as light yellow solid with 89% yield; <sup>1</sup>H-NMR (400 MHz, CDCl<sub>3</sub>) δ 7.36 (d, J = 8.8 Hz, 2H), 6.83 (d, J = 8.8 Hz, 2H), 4.86 (b, 2H), 3.79 (s, 3H), 3.74 (t, J = 6.4 Hz, 2H), 2.33-1.46 (b, 2H); <sup>13</sup>C-NMR (100 MHz, CDCl<sub>3</sub>) δ 160.2, 133.4, 114.0, 113.4, 87.3, 80.2, 55.3, 37.1; <sup>11</sup>B-NMR (128 MHz, CDCl<sub>3</sub>) -23.72; HRMS Calculated for C<sub>11</sub>H<sub>13</sub>BN<sub>2</sub>O [M+Na]<sup>+</sup>: 223.1018, Found: 223.1025.



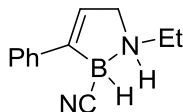
**4.39k**

**4.39k** was purified by flash chromatography (Hexane/EtOAc, v/v 2/1) as light yellow solid with 90% yield; <sup>1</sup>H-NMR (400 MHz, CD<sub>3</sub>CN) δ 7.55-7.49 (m, 1H), 7.05-6.97 (m, 2H), 5.13 (b, 2H), 3.74 (t, J = 6.8 Hz, 2H), 2.20-1.23 (b, 2H); <sup>13</sup>C-NMR (100 MHz, CD<sub>3</sub>CN) δ 169.7, 169.6, 167.2, 167.0, 140.3, 140.2, 117.5, 117.4, 117.2, 112.1, 111.9, 109.9, 109.8, 109.7, 109.6, 109.4, 109.3, 92.9, 83.4, 41.2; <sup>11</sup>B-NMR (128 MHz, CD<sub>3</sub>CN) -23.47; HRMS Calculated for C<sub>10</sub>H<sub>9</sub>BF<sub>2</sub>N<sub>2</sub> [M+Na]<sup>+</sup>: 229.0724, Found: 229.0719.



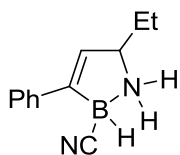
**4.40a**

**4.40a** was purified by flash chromatography (Hexane/EtOAc, v/v 2/1) as white solid with 93% yield; <sup>1</sup>H-NMR (400 MHz, CDCl<sub>3</sub>) δ 7.49-7.47 (m, 2H), 7.32 (t, J = 7.2 Hz, 2H), 7.23 (t, J = 7.2 Hz, 1H), 6.06 (s, 1H), 5.80 (b, 1H), 4.22 (b, 1H), 3.96 (d, J = 14.8 Hz, 1H), 3.83-3.78 (m, 1H), 3.57-2.41 (b, 1H); <sup>13</sup>C-NMR (100 MHz, CDCl<sub>3</sub>) δ 137.9, 128.4, 127.2, 127.0, 122.2, 51.6; <sup>11</sup>B-NMR (128 MHz, CDCl<sub>3</sub>) -13.85; HRMS Calculated for C<sub>10</sub>H<sub>11</sub>BN<sub>2</sub> [M+Na]<sup>+</sup>: 193.0907, Found: 193.0909.



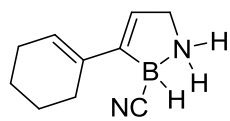
**4.40b**

**4.40b** was purified by flash chromatography (Hexane/EtOAc, v/v 2/1) as white solid with 89% yield; <sup>1</sup>H-NMR (400 MHz, CDCl<sub>3</sub>) δ 7.47 (d, J = 5.6 Hz, 2H), 7.31 (t, J = 5.2 Hz, 2H), 7.22 (t, J = 4.8 Hz, 1H), 6.10 (s, 1H), 4.33 (b, 1H), 3.97 (ddd, J = 9.6 Hz, 4.0 Hz, 1.6 Hz, 1H), 3.70 (dd, J = 9.6 Hz, 5.6 Hz, 1H), 3.37-3.32 (m, 1H), 3.15-3.09 (m, 1H), 1.36 (t, J = 5.2 Hz, 3H); <sup>13</sup>C-NMR (100 MHz, CDCl<sub>3</sub>) δ 137.9, 128.3, 127.3, 126.9, 121.3, 58.5, 46.5, 13.1; <sup>11</sup>B-NMR (128 MHz, CDCl<sub>3</sub>) -12.75; dr = 3:1; HRMS Calculated for C<sub>12</sub>H<sub>15</sub>BN<sub>2</sub> [M+Na]<sup>+</sup>: 221.1225, Found: 221.1220.



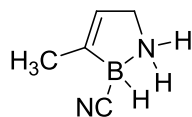
**4.40c**

**4.40c** was purified by flash chromatography (Hexane/EtOAc, v/v 2/1) as white solid with 85% yield; <sup>1</sup>H-NMR (400 MHz, CDCl<sub>3</sub>) δ 7.48 (d, J = 8.0 Hz, 2H), 7.31 (t, J = 7.2 Hz, 2H), 7.23 (t, J = 7.2 Hz, 1H), 6.10 (s, 0.5H), 6.05 (s, 1H), 4.92 (s, 0.5H), 4.64 (s, 0.5H), 4.14 (q, J = 6.4 Hz, 0.5H), 3.94 (q, J = 6.0 Hz, 0.5H), 3.56 (s, 0.5H), 3.37-2.43 (b, 1H), 1.75-1.51 (m, 3H), 0.98 (t, J = 7.2 Hz, 1.5H), 0.92 (t, J = 7.6 Hz, 1.5H); <sup>13</sup>C-NMR (100 MHz, CDCl<sub>3</sub>) δ 138.1, 138.0, 128.3, 127.2, 127.1, 127.0, 126.9, 126.8, 126.7, 66.6, 65.9, 27.9, 27.8, 10.3, 9.9; <sup>11</sup>B-NMR (128 MHz, CDCl<sub>3</sub>) -6.54; dr = 1:1; HRMS Calculated for C<sub>12</sub>H<sub>15</sub>BN<sub>2</sub> [M+Na]<sup>+</sup>: 221.1225, Found: 221.1220.



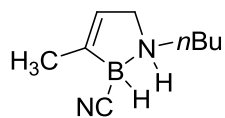
**4d**

**4.40d** was purified by flash chromatography (Hexane/EtOAc, v/v 2/1) as light yellow liquid with 77% yield; <sup>1</sup>H-NMR (400 MHz, CD<sub>3</sub>CN) δ 5.80 (t, J = 4.0 Hz, 1H), 5.58 (s, 1H), 4.95 (b, 2H), 3.81-3.76 (m, 1H), 3.69-3.67 (m, 1H), 2.20-2.11 (m, 4H), 1.69-1.64 (m, 2H), 1.61-1.56 (m, 2H); <sup>13</sup>C-NMR (100 MHz, CD<sub>3</sub>CN) δ 140.7, 133.6, 125.5, 55.8, 31.1, 30.9, 27.9, 27.6; <sup>11</sup>B-NMR (128 MHz, CD<sub>3</sub>CN) -12.15; HRMS Calculated for C<sub>10</sub>H<sub>15</sub>BN<sub>2</sub> [M+Na]<sup>+</sup>: 197.1221, Found: 197.1218.



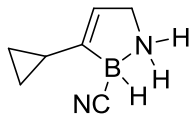
**4.40e**

**4.40e** was purified by flash chromatography (Hexane/EtOAc, v/v 2/1) as light yellow liquid with 63% yield; <sup>1</sup>H-NMR (400 MHz, CDCl<sub>3</sub>) δ 5.55 (b, 1H), 5.41 (s, 1H), 4.23 (b, 1H), 3.85-3.77 (m, 1H), 3.70-3.63 (m, 1H), 3.01-2.07 (b, 1H), 1.83 (t, J = 2.4 Hz, 3H); <sup>13</sup>C-NMR (100 MHz, CDCl<sub>3</sub>) δ 121.8, 51.1, 16.7; <sup>11</sup>B-NMR (128 MHz, CDCl<sub>3</sub>) -15.86; HRMS Calculated for C<sub>5</sub>H<sub>9</sub>BN<sub>2</sub> [M+Na]<sup>+</sup>: 131.0751, Found: 131.0755.



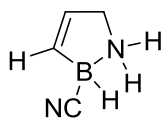
**4.40f**

**4.40f** was purified by flash chromatography (Hexane/EtOAc, v/v 2/1) as light yellow liquid with 81% yield; <sup>1</sup>H-NMR (400 MHz, CDCl<sub>3</sub>) δ 5.39 (s, 1H), 4.37 (s, 1H), 3.79-3.74 (m, 1H), 3.50-3.43 (m, 1H), 3.21-3.12 (m, 1H), 2.99-2.91 (m, 1H), 1.78 (s, 3H), 1.74-1.62 (m, 2H), 1.38 (q, J = 7.2 Hz, 2H), 0.97 (t, J = 6.0 Hz, 3H); <sup>13</sup>C-NMR (100 MHz, CDCl<sub>3</sub>) δ 121.3, 58.5, 54.4, 51.5, 29.5, 19.8, 13.6; <sup>11</sup>B-NMR (128 MHz, CDCl<sub>3</sub>) -11.22; dr = 3:1; HRMS Calculated for C<sub>9</sub>H<sub>17</sub>BN<sub>2</sub> [M+Na]<sup>+</sup>: 187.1377, Found: 187.1379.



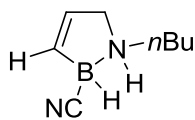
**4.40g**

**4.40g** was purified by flash chromatography (Hexane/EtOAc, v/v 2/1) as light yellow liquid with 73% yield; <sup>1</sup>H-NMR (400 MHz, CDCl<sub>3</sub>) δ 5.59 (b, 1H), 5.50 (s, 1H), 4.19 (b, 1H), 3.88-3.81 (m, 1H), 3.70-3.65 (m, 1H), 2.91-1.97 (b, 1H) 1.63-1.57 (m, 1H), 0.75-0.57 (m, 4H); <sup>13</sup>C-NMR (100 MHz, CDCl<sub>3</sub>) δ 119.8, 51.0, 13.8, 6.3; <sup>11</sup>B-NMR (128 MHz, CDCl<sub>3</sub>) -14.84; HRMS Calculated for C<sub>7</sub>H<sub>11</sub>BN<sub>2</sub> [M+Na]<sup>+</sup>: 157.0912, Found: 157.0908.



**4.40h**

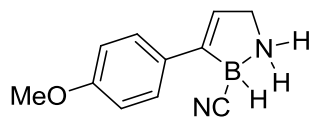
**4.40h** was purified by flash chromatography (Hexane/EtOAc, v/v 2/1) as light yellow liquid with 89% yield; <sup>1</sup>H-NMR (400 MHz, CDCl<sub>3</sub>) δ 6.01 (d, J = 8.0 Hz, 1H), 5.85 (d, J = 8.0 Hz, 1H), 5.56 (b, 1H), 4.15 (b, 1H), 3.91-3.75 (m, 1H), 3.75-3.68 (m, 1H), 3.19-2.20 (b, 1H); <sup>13</sup>C-NMR (100 MHz, CDCl<sub>3</sub>) δ 128.9, 51.6; <sup>11</sup>B-NMR (128 MHz, CDCl<sub>3</sub>) -13.42; HRMS Calculated for C<sub>4</sub>H<sub>7</sub>BN<sub>2</sub> [M+Na]<sup>+</sup>: 117.0594, Found: 117.0587.



**4.40i**

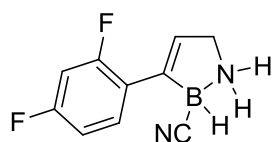
**4.40i** was purified by flash chromatography (Hexane/EtOAc, v/v 2/1) as light yellow liquid with 90% yield; <sup>1</sup>H-NMR (400 MHz, CDCl<sub>3</sub>) δ 6.08 (d, J = 7.6 Hz, 1H), 5.85 (d, J = 7.6 Hz, 1H), 4.22 (s, 1H), 3.82 (dd, J = 14.0 Hz, 6.4 Hz, 1H), 3.54-3.48 (m, 1H), 3.26-3.17 (m, 1H), 3.05-2.95 (m, 1H), 1.79-1.62 (m, 2H), 1.45-1.35 (m, 2H), 0.98 (t, J = 7.2 Hz, 3H); <sup>13</sup>C-NMR (100 MHz, CDCl<sub>3</sub>) δ 128.6, 58.6, 51.4, 29.7, 19.8, 13.6; <sup>11</sup>B-NMR (128 MHz, CDCl<sub>3</sub>) -11.70; dr = 2:1; HRMS Calculated for C<sub>8</sub>H<sub>15</sub>BN<sub>2</sub> [M+Na]<sup>+</sup>: 173.1221, Found: 173.1227.





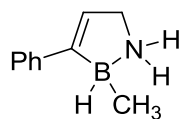
**4.40j**

**4.40j** was purified by flash chromatography (Hexane/EtOAc, v/v 2/1) as white solid with 43% yield; <sup>1</sup>H-NMR (400 MHz, CD<sub>3</sub>CN) δ 7.40 (dd, J = 6.8 Hz, 2.4 Hz, 2H), 6.87 (dd, J = 9.6 Hz, 2.4 Hz, 2H), 6.00 (s, 1H), 5.17-4.94 (b, 2H), 3.85-3.77 (m, 5H), 3.37-2.27 (b, 1H); <sup>13</sup>C-NMR (100 MHz, CD<sub>3</sub>CN) δ 128.9, 121.9, 118.3, 114.6, 111.0, 55.9, 55.3; <sup>11</sup>B-NMR (128 MHz, CD<sub>3</sub>CN) -13.90; HRMS Calculated for C<sub>11</sub>H<sub>13</sub>BN<sub>2</sub>O [M+Na]<sup>+</sup>: 223.1018, Found: 223.1025.



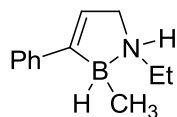
**4.40k**

**4.40k** was purified by flash chromatography (Hexane/EtOAc, v/v 2/1) as white solid with 80% yield; <sup>1</sup>H-NMR (400 MHz, CDCl<sub>3</sub>) δ 7.52-7.37 (m, 1H), 6.87-6.77 (m, 2H), 6.30 (s, 1H), 5.59 (s, 1H), 4.28 (s, 1H), 4.10-4.04 (m, 1H), 3.94-3.89 (m, 1H), 3.57-2.23 (b, 1H); <sup>13</sup>C-NMR (100 MHz, CDCl<sub>3</sub>) δ 131.6, 126.4, 126.3, 111.2, 111.1, 110.9, 110.8, 104.3, 104.0, 103.7, 51.8; <sup>11</sup>B-NMR (128 MHz, CDCl<sub>3</sub>) -9.00; HRMS Calculated for C<sub>10</sub>H<sub>9</sub>BF<sub>2</sub>N<sub>2</sub> [M+Na]<sup>+</sup>: 229.0724, Found: 229.0719.



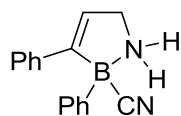
**4.41a**

**4.41a** was purified by flash chromatography (Hexane/EtOAc, v/v 2/1) as white solid with 73% yield; <sup>1</sup>H-NMR (400 MHz, CDCl<sub>3</sub>) δ 7.47 (dd, J = 8.4 Hz, 1.2 Hz, 2H), 7.29 (tt, J = 7.6 Hz, 2.0 Hz, 2H), 7.19 (tt, J = 7.6 Hz, 1.2 Hz, 1H), 5.98 (s, 1H), 4.08 (b, 2H), 3.86-3.81 (m, 2H), 3.23-2.15 (b, 2H); <sup>13</sup>C-NMR (100 MHz, CDCl<sub>3</sub>) δ 139.7, 128.2, 126.9, 126.6, 118.2, 51.9; <sup>11</sup>B-NMR (128 MHz, CDCl<sub>3</sub>) -2.90; HRMS Calculated for C<sub>9</sub>H<sub>12</sub>BN [M+Na]<sup>+</sup>: 168.0960, Found: 168.0956.



**4.41b**

**4.41b** was purified by flash chromatography (Hexane/EtOAc, v/v 2/1) as colorless liquid with 81% yield; <sup>1</sup>H-NMR (400 MHz, CDCl<sub>3</sub>) δ 7.48 (dd, J = 8.8 Hz, 1.6 Hz, 2H), 7.29 (t, J = 7.2 Hz, 2H), 7.18 (t, J = 7.6 Hz, 1H), 5.92 (s, 1H), 4.07 (b, 1H), 3.89 (dd, J = 14.8 Hz, 6.4 Hz, 1H), 3.47 (ddd, J = 12.0 Hz, 7.6 Hz, 2.4 Hz, 1H), 3.05-2.95 (m, 1H), 2.88-2.80 (m, 1H), 1.83 (t, J = 7.2 Hz, 3H); <sup>13</sup>C-NMR (100 MHz, CDCl<sub>3</sub>) δ 139.8, 128.1, 126.8, 126.5, 117.7, 58.8, 48.7, 13.0; <sup>11</sup>B-NMR (128 MHz, CDCl<sub>3</sub>) -5.08; HRMS Calculated for C<sub>11</sub>H<sub>16</sub>BN [M+Na]<sup>+</sup>: 196.1273, Found: 196.1279.



**4.42**

**4.42** was purified by flash chromatography (Hexane/EtOAc, v/v 2/1) as white solid with 67% yield; <sup>1</sup>H-NMR (400 MHz, CD<sub>3</sub>CN) δ 7.46 (dd, J = 8.4 Hz, 1.6 Hz, 2H), 7.35 (dt, J = 8.0 Hz, 1.6 Hz, 2H), 7.25 (tt, J = 6.4 Hz, 1.6 Hz, 2H), 7.19 (tt, J = 8.4 Hz, 1.6 Hz, 3H), 7.12 (tt, J = 6.8 Hz, 1.6 Hz, 1H), 6.36 (s, 1H), 5.55 (b, 1H), 4.82 (b, 1H), 3.94-3.80 (m, 2H), 2.20 (s, 3H); <sup>13</sup>C-NMR (100 MHz, CDCl<sub>3</sub>) δ 139.7, 133.7, 129.0, 128.6, 127.9, 127.8, 127.6, 126.4, 50.8; <sup>11</sup>B-NMR (128 MHz, CDCl<sub>3</sub>) -6.22; HRMS Calculated for C<sub>10</sub>H<sub>11</sub>BN<sub>2</sub> [M+Na]<sup>+</sup>: 193.0913, Found: 193.0917.